THE COLLOIDAL STABILITY AND SURFACE CHEMISTRY OF STÖBER SILICA

By

HOWARD ALLEN KETELSON. B.Sc. Hon., M.Sc.A.

A Thesis

Submitted to the School of Graduate Studies

in Partial Fulfillment of the Requirements

for the Degree

Doctor of Philosophy

McMaster University

© Copyright by Howard Allen Ketelson, September 1996

THE COLLOIDAL STABILITY AND SURFACE CHEMISTRY OF STÖBER SILICA

DOCTOR OF PHILOSOPHY (1996) McMaster University
Hamilton Ontario

TITLE: The Colloidal Stability and Surface Chemistry of Stöber Silica

AUTHOR: Howard Allen Ketelson, B.Sc. (McMaster University), M.Sc.A. (McGill University)

SUPERVISORS: Professors Mike A. Brook and Robert Pelton

NUMBER OF PAGES: xxxii, 287

ABSTRACT

Colloidal silica was prepared by the Stöber method to give particles having a narrow size distribution and spherical geometry. The electrokinetic and coagulation behavior of the particles were investigated in water, acetone, and acetone-water mixtures and the experimental data were compared to simple theoretical models. The relative permittivity, ε_r, of the dispersion medium was varied between 21 and 79 by controlling the acetone:water ratio. For $\varepsilon_r > 33$, the particles could not be coagulated using NaI concentrations up to 0.5 M. The critical coagulation concentration (c_c) values could not be predicted by calculations based on using standard DLVO theory. In the absence of salt, the zeta-potentials (ζ-potentials) remained constant at approximately -50 mV when $24.3 < \varepsilon_r < 78.5$ but increased to -80 mV for $\varepsilon_r < 24.3$. A single-site dissociation model predicted that the ζ-potentials should decrease with increasing acetone content. The inability of the theoretical models to predict the colloidal stability behavior of silica in acetone and acetone - water mixtures, especially when $\varepsilon_r > 33$, was believed to be due to the presence of a silica gel surface layer which acted as a steric barrier at short-range interparticle distances.

The colloidal stability and surface properties of Stöber silica modified with triethoxysilane (TES) ($HSi(OEt)_3$) was studied (polyTES). The polyTES particles were reacted with vinylnaphthalene, styrene, and vinyl-terminated poly(dimethylsiloxanes) using the platinum-catalyzed hydrosilation reaction. These reactions demonstrated that Stöber silica modified with TES can lead to a variety of colloidally stable dispersions in solvents ranging in polarity from water to hexane. It was also shown that bis(1,3-divinyl,1,1,3,3-tetramethyldisiloxane)Pt^0 could be hydrosilated on the polyTES surface to give catalytically active, surface-bound platinum nanoparticles with an average diameter of 2 nm. The polyTES layer grafted to the silica surface was believed to be critical in controlling the ultimate size of the supported platinum nanoparticles. The surface properties of the polyTES particles were studied and it was shown that the polyTES chains had a high surface density of 2.22 nm^{-2} and they expanded when solvated by aqueous alkaline solutions.

PREFACE

This thesis contains research work carried out by the author during the period beginning September 1992 to August 1996. The field of colloid and surface science is broad and encourages the studies to be multi-disciplinary. In the following chapters of this thesis, a multi-disciplinary approach was taken to investigate the surface chemistry, chemical modification, and colloidal stability of silica particles. Chapters 2, 3, 4, 5, and 7 have been published in the literature. Although their content has been kept intact, certain modifications have been done to the main text in order to make this thesis reflect one continuous body of work. Appendices, which contain information not included in the published papers, have been added after some of the Chapters. This thesis also contains several transmission electron micrograph images and many of them are displayed on full pages to give them the attention they deserve. The captions for the micrograph images are displayed on the opposite page to the photographs.

ACKNOWLEDGMENT

This Ph.D. work was unique in that there were two main supervisors (Dr. Robert Pelton - Chemical Engineering and Dr. Mike Brook - Chemistry) with widely different backgrounds. In most cases this difference would have led to discontinuities in the research but in fact it enhanced the work presented herein. I must first thank both of my supervisors for allowing me to pursue my research interests and giving me ALL the tools necessary to successfully carry out my work. Their encouragement and trust for my work will never be forgotten. Nor will their time spent teaching me about writing scientific papers and leading me to paths I would have never crossed on my own.

In September 1992 the word "colloid" was not part of my vocabulary. I am grateful to Dr. Pelton for leading me into the "world of small dimensions" over the past 4 years and for sharing with me his in-depth knowledge of colloid and polymer properties he has gained during his industrial and academic careers. I must also say a few words about Dr. Brook who instilled "millions" of ideas into my mind. His creativity, knowledge and enthusiasm pertaining to the "world of silicon chemistry" is "untouchable" and it rubbed off on me. If there were "model" supervisors to have then both Robert Pelton and Mike Brook would fit the

criteria. I thank them both for giving me some of the most interesting times I have encountered during my life.

I must also extend my appreciation to Professor Alex Bain and Professor Archie E. Hamielec for serving on my Ph.D. committee and reading this thesis during a short time.

One of the most interesting and valuable contacts I made during the past 4 years was that with Yew M. Heng of the Electron Microscopy Facility, Health Science Centre. His timeless patience and technical skill's in obtaining the TEM's of at least a thousand silica samples will be on my mind forever. I owe him a great deal as this thesis is also part of him. Most notably, I will miss his friendship and the discussions we had about what else we could do to characterize my "silica balls". I hope we get to work together again someday.

I must also give thanks to the staff at the Electron Microscopy Facility for their kindness. I thank Dr. G. T. Simon and Dr. L. Arsenault for allowing me to visit the facility and take valuable time away from Yew Heng's "normal" work load. Also, I must thank Ernie Spitzer of the E.M. facility for laughing at my "silica balls"! On a serious note, I thank Ernie for always making his time

available for me. I consider him a friend and I hope one day Yew Meng will learn the proper way of getting that "right" gray tone.

The following people are also acknowledged for their support during the course of this thesis and convenience to access the research facilities:

Brian Sayer for his help in both liquid and solid-state NMR spectroscopy and George Timmins for help with all the fluorescence and IR instruments.

Doug Keller, the Lab Manager for Dr. Pelton, helped me out countless of times when materials or instruments were needed.

Justina Derkach is acknowledged for the several hundred times I needed something in the Chemical Engineering Department and always found the time and patience to help me.

Dr. Glen Facey (University of Ottawa, Department of Chemistry) obtained and helped interpret several of the important solid-state NMR spectra in the latter stages of my work. I must thank him for taking a few week-ends in order to help me out in times of desperation.

Carol Jennings (Xerox Research, Sheridan Research Park) introduced me to DRIFTS and obtained several spectra of my silica materials.

Claude Azran must be thanked for his time and skill in drawing some of the pictures in this thesis. I would have spent another year on this thesis trying to equal the technical skill he put into these drawings.

Support and funding for this research work was gratefully provided by the Natural Science and Engineering Research Council and the Department of Chemistry at McMaster University. Also, Drs. Pelton and Brook are thanked for their financial support to alleviate my T.A. duties starting from September 1994.

I made several friends during my time spent in JHE 139 who should also be acknowledged yet there are too many to list all of them. I should acknowledge Mike Ajersch, Beverly Wasmund, Debnath De, and H. Xiao who were in JHE 139 when I began my thesis and made things more comfortable. Ian McLennan, who came to our lab during my final year, was a source of inspiration and laughter. I must thank him for teaching me about NMR, surfactants, and almost everything else there is to know in this world.

Finally, there are three people who have made this thesis possible. First, I cannot find any words which could express my thanks and love for Nathalie Jette who was with me throughout my M.Sc. and Ph.D. research work. Our times spent together at McMaster made life bearable at the university and kept me going when I needed a push. Her mind, soul, and love kept me in touch with reality and has made me a better person. I will never forget her. Last but not least, this thesis is for my parents. I could write a thesis on how my parents have supported me during my education. They have instilled confidence in me and

have been a scurce of inspiration during difficult and good times. This thesis would not have been written if not for them, hence, in my opinion, they deserve the Ph.D. as much as I do. God bless my mother and father for their love and devotion to me. This thesis is devoted to you both.

Table of Contents

LIST OF FIGURES

Chapter 3

Chapter 4

Chapter 5

Chapter 6

Chapter 7

Chapter 8

LIST OF SCHEMES

LIST OF TABLES

LIST OF ABBREVIATIONS

a	particle radius
A_{12}	combined Hamaker constant
c_c	critical coagulation concentrations
C	electrolyte concentration
d_H	hydrodynamic diameter
D	diffusion coefficient of particles
e_0	electronic charge
F	Faraday's constant
k_b	Boltzmann's constant
k_f	Smoluchowski diffusion-limited fast rate constant
k_s	rate constant for slow aggregation
n	refractive index of light
N_0	initial particle number concentration
N_A	Avogadro's number
N_s	number of SiOH sites per area
pK_a	ionization constant
q	scattering vector
R	ideal gas constant
$s(z)$	Shedlovsky crowding factor

T	absolute temperature
W	stability ratio
x	distance between surface and plane of shear
z	valence of ion
α	optical factor
Λ	equivalent conductance
Λ_0	molar conductivity at infinite dilution
ε_0	vacuum permittivity
ε_r	dielectric permittivity of solvent
κ^{-1}	Debye-Hückel (electrical double layer) length
λ	wavelength of light
μ_E	electrophoretic mobility
η	viscosity
θ	light scattering angle
σ_0	surface charge density
Γ_r	relaxation rate
τ_R	relative turbidity
Ψ_0	surface potential
ζ	zeta-potential

LIST OF PUBLICATIONS

1. Ketelson, H. A.; Brook, M. A.; Pelton, R. H. "Sterically Stabilized Silica Colloids: Radical Grafting of Poly(methylmethacrylate) and Hydrosilylative Grafting of Silicones to Functionalized Silica", *Polymers for Advanced Technologies* **1995**, *6*, 335.
2. Ketelson, H. A.; Brook, M. A.; Pelton, R. H. "Colloidal Silica-Bearing Hydrosilane Groups" *Chemistry of Materials* **1995**, *7*, 1376.
3. Ketelson, H. A.; Pelton, R. H.; Brook, M. A. "Colloidal Stability of Stöber Silica in Acetone" *Langmuir* **1996**, *12*, 1134.
4. Ketelson, H. A.; Pelton, R. H.; Brook, M. A. "Colloidal Stability of Stöber Silica in Acetone-Water Mixtures" *Journal of Colloid and Interface Science* **1996**, *179*, 600.
5. Ketelson, H. A.; Brook, M. A.; Pelton, R. H. "Hydridosilsesquioxane Silica Supported Platinum Nanoparticles" *Chemistry of Materials* **1996**, *8*, 2195.
6. Ketelson, H. A.; Pelton, R. H.; Brook, M. A. "Surface and Colloidal Properties of Hydrosilane Modified Silica Dispersions" submitted to *Colloids and Surfaces.*

7. Brook, M.A.; Ketelson, H.A.; Pelton, R.H. "The Controlled Formation of Pt(0) Clusters in a Silsesquioxane Gel" to be submitted to *Inorg. Chim. Acta.* (invited manuscript).
8. United States Patent Pending- Inventors: Howard A. Ketelson, Michael A. Brook, and Robert Pelton. Title: *Platinum Catalyst, Method of Making, and Uses of Thereof.* Filed in the United States Patent and Trademark Office on September 6, 1996.

Chapter 1

Introduction

1.1. General.

One of the most studied aspects of particles suspended in a medium is their colloidal stability. The understanding and the control of the colloidal stability of particle dispersions is of great technological interest in complex formulations such as paint, ink, detergents, catalysts, etc. Particle suspensions are considered to be colloidal when the dimensions of the particles fall in the size range of 1 nm ≤ radius ≤ 500 nm. In this size range, the particle motion (*i.e.*, diffusion) is dominated by Brownian motion (Robert Brown: 1773-1858) which results from the kinetic energy gained by the particles by particle-particle and particle-solvent (continuous phase) molecule collisions.[1] The lower size limit (*i.e.*, 1 nm) indicates the colloid is much larger (*i.e.*, by at least 10x) compared to the molecules of the continuous phase. On the other hand, for colloids with dimensions larger than 500 nm, Brownian motion becomes dominated by gravitation and/or convection.

One of the most important features of colloids, which results from their small dimensions, is the high interfacial area compared with the bulk phase.[2] Henceforth, surface effects at the interfacial region (i.e., the solid/liquid interface) dominate their colloidal behavior. From a thermodynamic viewpoint, the work, *dw*, required to create a new surface is proportional to the area, *dA*, of the new surface (i.e., $w \propto dA$). Due to the high surface area of colloids, the work needed to create the new surface will increase; hence, *dw* is positive for an increase in area (*i.e., dG*, the Gibbs free energy is positive). Henceforth, it becomes energetically favorable to minimize the surface area (which could be achieved by the aggregation small colloid particles into a larger one).[3]

An important factor related to the stability of colloids is that they are attracted to one another due to van der Waals forces which persist over large interparticle distances. The energy of attraction between two spherical colloid particles varies as their separation with the following dependance as $1 / D^2$ where D is the distance between two sphere centres.[4] In order to achieve colloidal stability, repulsive forces are needed which have a longer range than the those given given by the van der Waals attractive forces.

The two most recognized forces which stabilize colloids are known as electrostatic and steric forces. The most recognized theory in colloid science which models the interparticle interactions between charged (electrostatic)

colloidal particles was first derived by Derjaguin, Landau, Verwey and Overbeek (commonly referred to as the DLVO theory).[5] In the DLVO theory, the interparticle (spherical particles are assumed) interactions are modelled as the total pair interaction potential V(r) as a function of the interparticle distance. V(r) is described by an electrostatic repulsive force originating from the formation of a net charge on the surface (*e.g., viz.* the dissociation of surface groups) and an attractive force (*i.e,* the Van der Waal forces) resulting from fluctuating dipoles. Colloidal stability is achieved when the particles are separated by electrostatic repulsions which originate from the overlap of the electrical double layers surrounding the charged particles. The length of the electrical double layer, given by the reciprocal Debye-Hückel length, depends on the dielectric permittivity of the surrounding medium and the salt concentration. For dilute dispersions at low ionic strength the double layer length is large whereas at high ionic strengths the charges are screened out which collapses the double layer.

The second most generally recognized stabilizing force is based on steric effects which originate from the interaction between particles bearing macromolecules on the particle surface (i.e., steric stabilization).[6] In this case the repulsion results from the overlap of the polymer segments which pushes them apart. The repulsion is caused by an increase in the osmotic pressure at close interparticle distances in the region where the polymer segments overlap.

In order to test colloid stabilization theories a number of model colloid systems have been used. For example, the early studies (pre-1930's) focused on using solids such as AgI, HgS, Ag, and α - FeOOH. However, particles characterized by a narrow size distribution and by a spherical geometry were difficult to prepare.[7] In the 1940's, the technique of emulsion polymerization was used to produce well-defined polystyrene latexes and these particles are still used today in many of the fundamental colloid studies published in the literature.[8]

Mineral oxide systems such as silica have also been widely studied due in part to their ease of preparation in the laboratory and their commercial use in industrial applications. For example, the surface and interfacial properties of silica have been exploited in a wide variety of industrial applications for materials such as polymer fillers, chromatographic packings, catalysts, and optical and electronic materials. In this respect, a variety of studies have been performed using silica to investigate its wetting, adhesion, colloidal stability and reactivity properties.[9,10] An excellent review of silica chemistry by Iler is available which includes data on the factors influencing the macroscopic properties (density, particle size, porosity, etc) of silica such as pH and temperature, and experimental data is also given on the colloidal stability of silica dispersions in water.[9]

In the past few decades non-invasive characterization techniques such as light scattering, microelectrophoresis, atomic force microscopy, and neutron scattering have been developed. Essential to using these techniques in the silica colloid field is the use of a well-defined silica particle system since information about the surface properties and colloidal behavior can be readily gained. For example, it would be advantageous to have a silica system which has the following "model" properties: narrow particle size distribution, flexible control of particle size, spherical geometry, and smooth surface with well-defined surface groups.

1.2 Silica Colloids.

Silica was first produced on a commercial scale from water glass in the 1850's and since this period a variety of chemical and physical methods have been developed to produce silica materials of varying surface areas and porosity.[9] In spite of the many variations of silica particles available, few offer the "model" properties described above. Fortunately, one particular process, that developed by Stöber, Fink, and Bohn, has been studied over the last decade and its synthesis is well now established to produce "model" silica dispersions.[11] In the Stöber method, spherical particles with a narrow size distribution are conveniently prepared by the hydrolysis and condensation of tetraethylorthosilicate using a mixture of water, alcohol (the cosolvent), and ammonia. Silica particles with "model" properties can be synthesized in the

size range of ~50 nm to 1000 nm. The resulting particles are electrostatically stabilized by negative surface charges arising from the dissociated silanol groups in the alkaline medium (the potential determining ions on the silica particles are H^+ and OH^-). The most commonly invoked model to describe the electrical double layer on mineral oxide solids such as silica is the triple layer model.[12]

1.3 The scope of this thesis.

The work described in this thesis is based on using Stöber silica as a "model" colloid system to study the colloidal stability of silica in media of varying polarity and also to perform selective chemical modifications to the silica surface to control its surface properties.

Although there are many studies dealing with the surface chemistry and colloidal stability of silica in water, few of them have addressed the role of changing the dielectric permittivity of the dispersion medium using polar organic solvents. In Part I of this thesis, Stöber silica was used as a "model" colloid system and experimental data were obtained to provide insight into their colloidal stability and surface properties in acetone and acetone-water mixtures. Stöber silica has also attracted attention in the material science and ceramic fields.[10] In Part II of the thesis, the colloidal and surface properties of silica are examined after surface treatment with organosilanes and polymers.

1.4 Outline of thesis.

Part I: Colloidal Properties of Silica Dispersions in Polar Organic Media

In Chapter 2, results were obtained from coagulation and microelectrophoresis experiments for Stöber silica dispersed in acetone and water. Attempts were made to explain the observed properties in acetone in terms of generally accepted models of aqueous silica dispersions. In Chapter 3, the investigation of the colloidal properties of Stöber silica was extended to acetone-water mixtures. Experimental electrokinetic and coagulation results were compared with theoretical predictions using standard colloid theory.

Part II: Chemical Transformations at the Silica Interface: Preparation and Surface Properties

In Chapter 4, Stöber silica was modified with hydrosilane groups (Si-H) and these were used to carry out hydrosilation reactions with organic molecules having vinyl groups. This procedure offered a convenient route to prepare surface modified silica colloids bearing a variety of chemical groups (*i.e.*, styrene, anthracene, dimethylsiloxane).

In Chapter 5, the hydrosilane modified silica was reacted with Karstedt's catalyst, bis(1,3-divinyl,1,1,3,3-tetramethyldisiloxane)Pt^0, to give catalytically

active surface bound platinum nanoparticles with an average diameter of 2 nm. The supported platinum nanoparticles were recycled through at least three consecutive hydrosilation reactions while maintaining their catalytic activity. It was postulated that the microstructure of the grafted hydrosilane polymer surface layer supports and protects the supported platinum nanoparticles from aggregating into macrosize platininum aggregates.

In Chapter 6, the investigation of the colloidal and surface properties of hydrosilane modified Stöber silica was continued. Information such as the polymer thickness, grafting density, and surface dynamics in the interfacial region were obtained to provide a molecular picture of the TES polymer bound to the silica surface.

In Chapter 7, Stöber silica particles were used to prepare sterically stabilized dispersions using PMMA and PDMS. Their preparation, characterization, and colloidal properties were examined.

In Chapter 8, cationic silica was prepared using a variety of amine precursors and characterized, and it was found that the surface charge properties could be influenced to generate positively charged colloidal particles in alkaline media.

References

1 Hunter, R.J. *Introduction to Modern Colloid Science*; Oxford University Press: Oxford, 1993, pp. 33.

2 Adamson, W. *Physical Chemistry of Surfaces* (3rd ed.); Wiley: New York, 1979.

3 Atkins, P.W. *Physical Chemistry* (3rd ed.); W.H. Freeman and Company: New York, 1986, pp.627.

4 Israelachvili, J. *Intermolecular and Surface Forces*; Academic Press: London, 1992.

5 Verwey, E.J.W.; Overbeek, J. Th.G. *Theory of the Stability of Lyophobic Colloids*; Elsevier: Amsterdam, 1948.

6 Napper, D.H. *Polymeric Stabilisation of Colloidal Dispersions*; Academic Press: London, 1983.

7 de Rooy, N.; de Bruyn, P.L.; Overbeek, J.Th.G. *J. Colloid Interface Sci.* **1980**, *75*, 542 and references cited therein.

8 Harkins, W.D. *J. Am. Chem. Soc.* **1947**, *69*, 1428.

9 Iler, R.K. *The Chemistry of Silica*; Wiley: New York, 1979.

10 Vansant, E.F.; van der Voort, P.; Vrancken, K.C. *Characterization and Chemical Modification of the Silica Surface*; Elsevier: Amsterdam, 1995.

11 Stöber, W.; Fink, A.; Bohn, E. *J. Colloid Interface Sci.* **1968**, *26*, 62.

12 Yates, D.E.; Levine, S.; Healy, T.W. *Trans. Faraday Soc.*, **1974**, *70*, 1807.

PART I

Colloidal Properties of Stöber Silica Dispersions in Polar Organic Media

Chapter 2

Colloidal Stability of Stöber Silica in Acetone

Abstract

The colloidal stability of Stöber silica dispersed in acetone (99.7 wt%) was investigated and compared to the results obtained in water using electrophoresis and coagulation experiments with NaI, CaI_2, and Bu_4NI. A critical coagulation concentration (c_c) of 19.6 mM NaI in acetone was observed whereas Bu_4NI acetone solutions up to 145 mM had no effect on the stability of the silica organosols. In NaI and Bu_4NI acetone solutions, the magnitude of the electrophoretic mobilities of the silica organosols decreased with increasing electrolyte concentration. From 0.11 to 13.5 mM NaI the electrophoretic mobilities decreased from -3.3×10^{-8} $m^2 V^{-1} s^{-1}$ to -0.39×10^{-8} $m^2 V^{-1} s^{-1}$; from 3.9 to 39 mM Bu_4NI the mobilities decreased from -2.8×10^{-8} $m^2 V^{-1} s^{-1}$ to -0.91×10^{-8} $m^2 V^{-1} s^{-1}$. Results using a single - site dissociation model were compared with

experimental ζ-potentials for silica in NaI acetone solutions and showed adequate agreement when ΔpH was assumed to be 2. Experimental coagulation concentrations for NaI and Bu_4NI did not agree with simple DLVO theory. The discrepancy was believed to be due to the presence of a steric barrier consisting of a silicic acid gel network. CaI_2 additions to the silica acetone solutions influenced the electrostatic potential of the particles and caused coagulation. At 0.06 and 1 mM CaI_2, the electrophoretic mobilities of the particles were -2.9×10^{-8} $m^2 V^{-1} s^{-1}$ and $+2.3 \times 10^{-8}$ $m^2 V^{-1} s^{-1}$, respectively. The charge reversal led to the re-stabilization of the particles as evidenced by two c_c values 0.045 mM (c_{c1}) and 2.75 mM (c_{c2}).

2.1 Introduction

Colloidal silica has been widely used in industrial products[1] (e.g., catalyst supports, polymer fillers, optical and electronic materials) and also in the laboratory as a model system in catalysis[2], colloid science[3] and materials science[4]. Although commercial silica sols are available, including for example, Dupont Ludox® silica, Stöber silica[5] is particularly appropriate for model colloidal studies since spherical particles can be prepared of various sizes with a narrow size distribution. Reported studies involving Stöber silica include mechanisms of particle nucleation and growth processes, particle microstructure,[6] and surface modification reactions using silane coupling agents[7] and polymers.[8]

The preparation of Stöber silica involves the ammonia catalyzed hydrolysis and condensation of tetraethylorthosilicate (TEOS) in an aqueous alcohol (usually ethanol) solution. The particles are electrostatically stabilized which originates from the ionization of surface silanol groups in the ammonia mixture

There are many publications dealing with the surface chemistry and colloidal stability of silica in water.[9] A number of workers have characterized and modeled the surface electrochemical properties of silica.

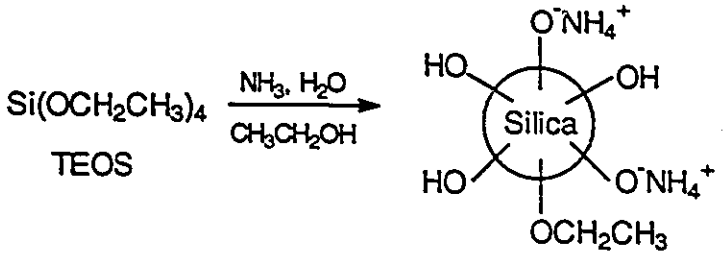

Scheme 2.1. Stöber silica preparation.

A key feature of silica is that the surface charge density (σ_o) determined by potentiometric titration is much larger than that predicted by models using the ζ - potential.[10] The discrepancy has been attributed to the adsorption of counterions within the surface of shear; models accounting for this effect have been proposed.[11, 12,13]

Aqueous silica sols have been shown to be colloidally stable in the isoelectric region (iep) at pH=2-3 and at pH's >6.[1] The silica sol stability at the iep, in spite of the low ζ - potentials, has been explained due to repulsive hydration forces at the silica - water interface.[14] In the presence of coagulating ions, Allen and Matijevic[14c] have proposed the silica hydrosols become destabilized by an ion exchange process. For every coagulating counterion adsorbed onto the silica surface, a silanol group becomes blocked from

hydrogen-bonding with water molecules and this process dehydrates the hydroxylated silica surface.

More recently, it has been shown by several groups that the forces measured between silica surfaces using the surface force apparatus deviate from classic DLVO theory.[15] An additional non-DLVO short-range monotonic repulsive force has been measured at small surface separations in the range of 1-5 nm. This behavior has been explained by the presence of a structured layer of water (10 to 20 molecular layers thick) at the silica interface which gives rise to a short - range repulsive hydration force.[15] On the basis of adhesion, friction, contact angle and surface force measurements, Vigil *et al.*[16] proposed that the additional short range repulsion was due to a short - range steric repulsive force originating from a surface gel layer composed of oligomeric silicic acid groups. The work by Vigil *et al.*[16] gives more support for the original gel layer model proposed by Tadros and Lyklema.[17]

Despite the interest in Stöber silica, few systematic studies have been directed towards understanding its colloidal stability in organic media.[18] Kosmulski and Matijevic[18d] have studied the electrokinetic behavior of Stöber silica sols as a function of pH in dioxane-water mixtures. The ζ - potentials were low and approached zero in mixtures containing 97.5 wt% dioxane and 1 mM KCl. Using mixtures having 90-95 wt% dioxane, the ζ - potentials changed from

negative to positive with increasing electrolyte (KCl, RbCl, and CsCl) concentrations which was attributed to the formation and adsorption of ion-dioxane complexes within the Stern layer. In another study by the same authors,[18b] the ζ - potentials for silica in water-alcohol (up to 30 wt%) mixtures were studied as a function of pH and it was observed that the ζ - potentials decreased with increasing additions of alcohol and KCl content.

Other colloidal systems including silver, silver iodide and α-goethite have also been investigated in polar organic media.[19] For example, de Rooy *et al.*[19b] showed that the ζ - potentials of negatively charged Ag and AgI sols in 99.5 % ethanol decreased with increasing $LiNO_3$ concentration and that the colloidal stability of the sols in mixtures rich in organic content (ethanol or acetone) were sensitive to small coagulant concentrations.[19b]

Reported in this paper are the results obtained from coagulation and microelectrophoresis experiments for Stöber silica dispersed in acetone (99.7 wt%) and water. Attempts are made to explain the observed properties in acetone in terms of generally accepted models of aqueous silica sols.

2.2 Experimental

Materials. Acetone (99.5 wt%, glass distilled, Caledon), sodium iodide (99+%, Aldrich), calcium iodide hydrate, CaI_2•4-6 H_2O (98%, Aldrich), tetrabutylammonium iodide (98%, Aldrich), ammonia in ethanol (2.0 M, Aldrich), and absolute ethanol (RDL) were used as received. Tetraethylorthosilicate (99.999+%, Aldrich) was distilled in vacuo prior to use.

Stöber Silica Synthesis. H_2O (4.3 mL, 0.24 mol), NH_3 (50.7 mL, 0.1 mol) and absolute ethanol (73 mL) were mixed in a glass vessel inserted in a 30°C water bath fitted with a submerged magnetic stirrer. The mixture was stirred for 30 min to allow the liquids to come to thermal equilibrium. TEOS (6 mL, 27 mmol) was quickly added. A sonicating probe was inserted through a specially fitted hole through the top of the vessel and positioned 5 cm below the liquid level.[20] The mixture turned cloudy after approximately 20 min and was left stirring with sonication for 10 h. At that time, TEOS (12 mL, 54 mmol) and H_2O (1.9 mL, 0.1 mol) were added to the alcosol mixture. Following a further 10 h mixing period, a third addition of TEOS (12 mL, 54 mmol) and water (1.9 mL, 0.1 mol) were added to the dispersion. Centrifugation and redispersion cycles with 5 x EtOH followed by 5 x fresh acetone (glass distilled) were employed to clean the products of unreacted material. The sedimented solids were redispersed in

fresh solvent using a sonicator following each centrifugation cycle. Using this procedure, about 7 wt% solid content was obtained. Centrifugation and redispersion cycles were used to clean the silica free of ammonia using 5 x EtOH followed by 5 x acetone. For silica dispersions in water, the particles were washed with Milli-Q treated distilled water until the conductivity of the suspension approached 18 $m\Omega\ cm^{-1}$.

^{13}C NMR (CP-MAS) δ 60.59, 17.24.

^{29}Si NMR (MAS) δ -103, -110, -96.

Elemental analysis: %C 3.40; %H 1.07; %Si 45.86.

Water content measurements of the silica / acetone dispersions by Karl Fischer titrations were performed by Galbraith Laboratories, Inc., Knoxville, TN. Analysis of the acetone (in the absence of silica) without further purification showed 0.30% water. For a 0.5 wt% silica dispersion in acetone (aged for 1 week), the analysis showed 0.31% water content. Assuming a silica surface concentration of 7-8 SiOH / nm^2, and all the water from the acetone adsorbs on the surface, we estimate a 0.3 wt% water content in bulk solution would correspond to approximately 4 H_2O monolayers on the silica surface.

Electron microscopy. The transmission electron micrographs (TEM) of the colloids were acquired using a JEOL JEM-1200EX microscope. Carbon coated Formvar grids were used.

Dynamic light scattering (DLS). Dust free silica dispersions were prepared by successively rinsing all glassware with acetone, Mill-Q water, a 2% HF solution followed by several washings using Milli-Q water. All the solvents and salt solutions used to prepare the particle dispersions were filtered through 0.2 μm Millipore filters.

Particle size measurements were carried out at 25±0.5°C using a Brookhaven Instruments (Holtsville, NY) photon correlation spectrometer fitted with a Brookhaven Model BI - 9000AT digital correlator and a Lexel (Fremont, CA) Model 95 Ar ion laser operating at a power of 150 mW. The experiments were carried out using a wavelength of 514.5 nm and a scattering angle of 90°. The mean diffusion coefficient of the particles (D), was determined from the relaxation rate Γ_r (see Appendix A2.3).

The mean D was used to calculate the mean hydrodynamic particle diameter, d_H, based on the Stokes-Einstein equation. The data were fitted by the method of cumulants in terms of the first moment using Version 4.0 of the

Brookhaven BI-2P software..[21] Data were collected for 500 seconds and a minimum of 10 measurements were made.

Microelectrophoresis. The electrophoretic mobilities of silica dispersions in water and acetone with or without salt were measured using a Coulter DELSA 440. Particle velocities were determined at seven positions across the cell and the stationary mobility values were calculated by fitting the data to a linearized form of the Komagata equation. Details of the experimental procedure have been published elsewhere.[22] Electrophoretic mobilities were converted to ζ - potentials using the O'Brien and White computer program.[23] The equivalent conductances for Na^+ and I^- in acetone were taken from the literature.[24]

Conductivity. The conductivities of the acetone and water electrolyte solutions were obtained at 25°C using a Copenhagen Radiometer CDM 83 meter equipped with a silver glass electrode (Copenhagen, Type CDC 304). The conductivities of the silica dispersions containing salt were measured using the Coulter DELSA microelectrophoresis apparatus at 25°C and the data agreed with those obtained for the salt solutions using the conductivity meter.

Coagulation Experiments. The coagulation experiments were carried out by adding a series of freshly prepared electrolyte solutions of increasing

concentration to silica dispersions consisting of 0.75 wt% silica in a quartz cuvette. After a 30 min period, the silica suspension was gently mixed and the percent transmittance of the silica sol, $\%T_S$ was recorded at 60 min. The $\%T_S$ was obtained at $\lambda = 500$ nm using a Hewlett Packard 8452A UV/VIS Diode Array Spectrophotometer. During the 60 min period, several control readings (i.e., no added electrolyte, $\%T_C$) were recorded. All experiments were performed at 25°C.

The relative turbidity of a silica dispersion was calculated using

$$\tau_R = \frac{\log\left(100/\%T_s\right)}{\log\left(100/\%T_c\right)} \qquad [2.1]$$

In Eq. [2.1], $\tau_R \approx 1$ indicates a colloidally stable suspension whereas τ_R values > 1 indicate the onset of particle coagulation where most of the flocs remained suspended during the timescale of the experiment. $\tau_R < 1$ indicates that silica flocs have formed and settled. The concentration of the electrolyte added to the silica dispersion, which corresponded to the point at which the particles settled leaving a clear supernatant, was taken to be the coagulation concentration c_c. The reported electrolyte concentrations added to the silica sols are corrected for the dilution factor when the electrolyte solution of known

concentration was added to an equal volume of the particle suspension without any salt.

Disk Centrifuge Particle (DCP) Size Analysis. The particle size distributions in water were measured using DCP as a function of CaI_2 to confirm the sensitivity of the relative turbidity experiments. Sedimentation experiments were performed at 25°C with a Brookhaven BI-DCP Particle Sizer equipped with a polycarbonate disk. Analyses of the particle size distributions were carried out in the Homogeneous Start mode. Samples were prepared by using a stock dispersion having about 0.5 wt% silica content. Samples were accelerated at 3000 rpm for silica in water and at 2000 rpm when using acetone as the continuous phase. The data collected from experiments was analyzed using Brookhaven Software Version 5.02 which gives diameters as the geometric mean moments and the distribution of particle sizes was expressed as the differential mass distribution. More information about the disk centrifuge using the homogeneous mode is given in the literature references.[25]

Particle size distributions for aqueous silica dispersions in 2, 5, and 10mM CaI_2 were measured with a disk centrifuge and the data are plotted in Figure 2.1. The particle size distributions between 2 mM and 5 mM CaI_2 were narrow with an average diameter of 0.20 μm which is close to 0.155 μm obtained in the absence of CaI_2. The silica sol was coagulated in 10 mM CaI_2 as

evidenced by the broad polydisperse distribution from which the average diameter was 0.8 μm.

Figure 2.1. Differential volume-average particle distributions as a function of CaI_2 concentration for unmodified silica dispersions in water (pH=8) using the disk centrifuge particle sizer. Density of silica used to calculate particle sizes from DCP data was 2000 kg/m^3. Average diameter of silica in water from DLS was 180 nm.

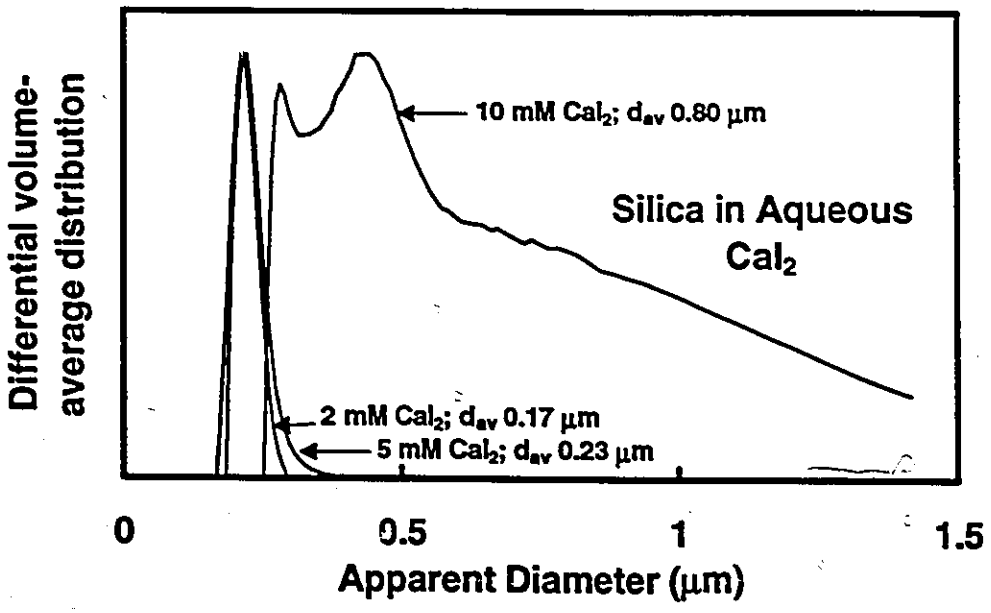

2.3 Results

Stöber Silica Size and Morphology

TEM examination (a representative example is shown in Figure 2.2a) of the silica dispersion prepared by the Stöber method showed that the particles were spherical with a narrow size distribution. The average particle diameter obtained from electron microscopy was 155 nm with a relative standard deviation of 10% as determined from counting and measuring 280 particles by image analysis. The size distribution bar graph is given in Figure 2.2b.

An average particle diameter of 177 ± 1 nm in acetone with a standard deviation of the distribution of 10% was determined by dynamic light scattering (DLS) which measures the hydrodynamic diameter (d_H) based on the Stokes-Einstein relation. The smaller particle sizes obtained by electron microscopy as compared to the DLS results have been previously reported and are considered to result from particle shrinkage under the electron beam.[26]

The particle size distributions of silica in acetone were also determined with a disk centrifuge particle size (DCP) apparatus which measures the volume average particle diameters at a constant velocity. Stöber silica particle densities

Figure 2.2. Top: (a) Transmission electron micrograph of silica particles dried from acetone (Scale bar = 1 μm). **Bottom:** (b) Size distribution bar graph of silica particles dried from acetone.

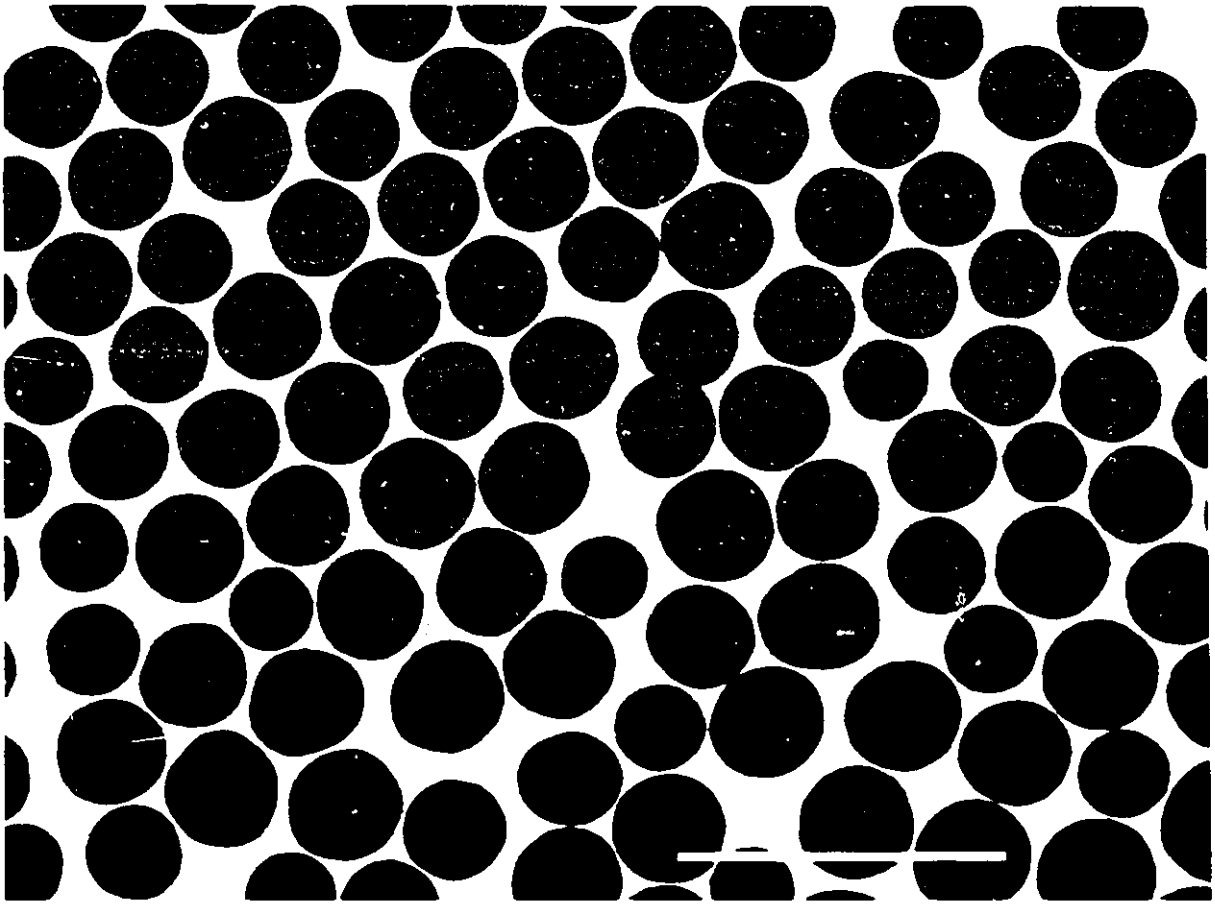

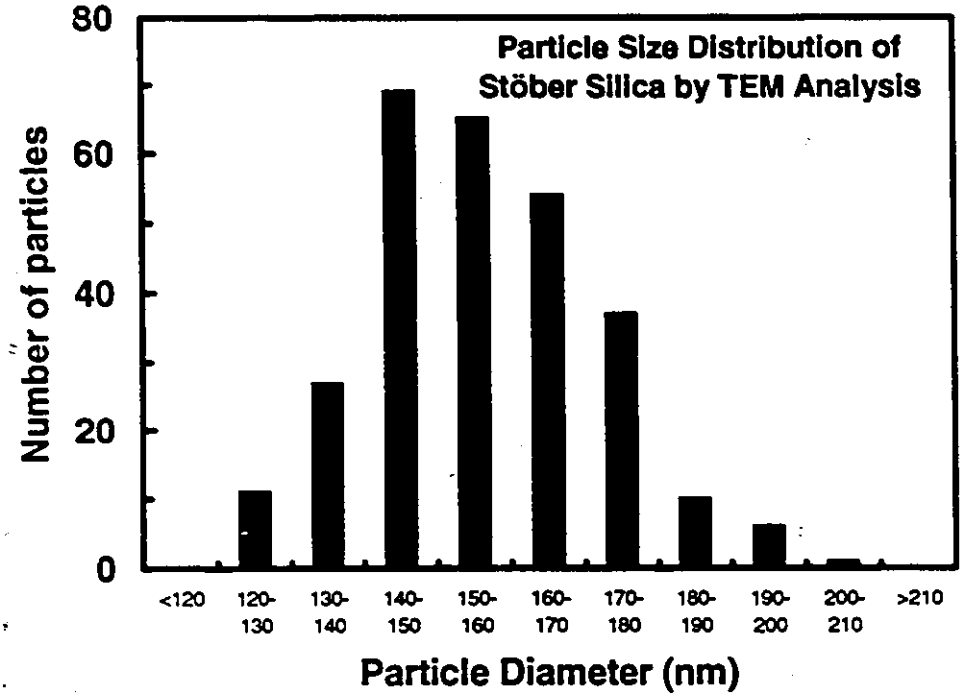
Particle Size Distribution of
Stöber Silica by TEM Analysis
Number of particles
0
20
40
60
80
<120
120-130
130-140
140-150
150-160
160-170
170-180
180-190
190-200
200-210
>210
Particle Diameter (nm)

of 2000-2100 kg/m^3 have been reported for particles with average diameters of 70 to 900 nm using helium pycnometry and by measuring the mass of silica using a known volume of the suspension.[6b,7b,c] Assuming a particle density of 2000 kg/m^3, the average particle diameter in acetone obtained by DCP analysis was 156 ± 4 nm.

The difference in particle diameters obtained by DLS (177 nm) and by DCP analysis was believed to be due to the particle porosity, since pores open to the solvent (acetone) would influence the centrifugal force on a particle in the DCP experiment. If the average particle density was chosen to be 1730 kg/m^3, the DCP data gave the same particle diameter (177 nm) as that obtained by DLS. Similar results were obtained by Bogush *et al.*[6f] with silica particles esterified with stearyl alcohol; the calculated Stöber particle densities were in the range of 1780 to 1860 kg/m^3 assuming that the stearyl alcohol molecules plug all the pores.

Assuming the density of pure silica is 2000 kg/m^3 and the apparent particle density is 1730 kg/m^3, a simple calculation shows that the particle porosity is 15% which is consistent with previous investigations where Stöber silica was shown to have a microporosity of 10 - 15%.[6f] DCP measurements were also carried out with silica dispersed in ethanol and water and similar porosity results were obtained as with pure acetone. These results indicated

that solvent within the particle pores was not trapped, hence the pores were believed to be open. See Appendix A2.1 for further discussion about the silica porosity.

Dissociation of Electrolytes

The solubility of electrolytes in non-aqueous media and the degree of electrolyte dissociation are much lower than in water. Figure 2.3 shows the equivalent conductances, Λ, for NaI, Bu_4NI and CaI_2 as a function of electrolyte concentration. In all cases the equivalent conductivity decreased with electrolyte concentration, which is typical for the behavior of weak electrolytes and is indicative of ion-pair formation.[27] The conductances for NaI - acetone solutions obtained by Krumgal'z and Gerzhberg[28] are plotted in Figure 2.3 and showed similar behavior to the conductances obtained in the present study.

The degree of dissociation of NaI and Bu_4NI in 99.7 wt% acetone was estimated from conductivity measurements according to the method proposed by Fuoss and Shedlovsky.[29] See Appendix A2.2 for further details on the calculations. The limiting conductance's for NaI (Λ_o=182.5 S cm^2 mol^{-1}) and Bu_4NI (Λ_o=184.1 S cm^2 mol^{-1}) needed to calculate the degree of dissociation were obtained from the literature.[28,30] The concentrations of dissociated ions, c_{diss}, calculated for NaI and Bu_4NI in acetone are given in Table 2.1. According

to the calculations, approximately 70% of the ions are expected to be dissociated in acetone using concentrations as high as 20 mM NaI or Bu_4NI.

Figure 2.3. Equivalent conductance data plotted as a function of electrolyte concentration for NaI, CaI_2, and Bu_4NI (tetrabutylammonium iodide) in 99.7 wt% acetone. The dashed line corresponds to the equivalent conductance data reported by Krumgal'z and Gerzhberg[28] for NaI in acetone.

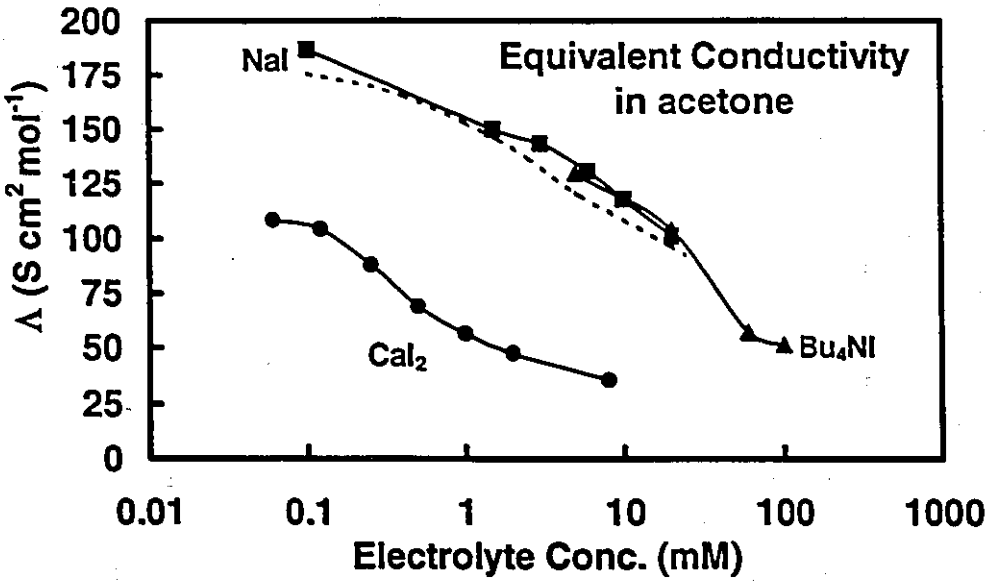

In the case of the CaI_2 acetone solutions, the situation is complicated since several types of dissociation processes are possible. The simplest ones are represented by the following dissociation equilibria reactions;

$$CaI_2 \rightleftharpoons CaI^+ + I^- \rightleftharpoons Ca^{++} + I^- + I^-$$

Scheme 2.2. Possible dissociation pathways for partially dissociated CaI_2.

Since concentrations of intermediate ions such as CaI^+ were not known, the concentration of dissociated ions for CaI_2 could not be estimated with accuracy. On this basis the CaI_2 concentrations were reported in the present work by not taking ion-pair formation into account.

The κa values corrected for ion-pair formation for NaI and Bu_4NI in acetone are shown in Table 2.1 where κ is the reciprocal Debye-Hückel length given by Eq. [2.2] and *a* is the particle radius.

$$\kappa = \left(\frac{2e_o^2 N_A C}{\varepsilon_o \varepsilon_r k_b T} \right)^{0.5} \qquad [2.2]$$

The data in Table 2.1 shows that κa varied from 6.94 to 111 for the NaI and Bu_4NI acetone solutions used to study the colloidal stability of silica.

Table 2.1. A comparison of the total concentration of electrolyte (NaI and Bu_4NI) in 99.7 wt% acetone, c_{tot}, with the concentration of the dissociated electrolyte, c_{diss}, estimated from conductivity data. Also shown are the corresponding estimated κa (see Eq. [2.2]) values based on the particle radius, a=88.5 nm.

NaI (mM)			Bu_4NI (mM)		
c_{tot}	c_{diss}	κa	c_{tot}	c_{diss}	κa
0.15	0.15	6.94	5.0	3.94	35.5
1.50	1.32	20.6	20.0	13.9	66.7
3.0	2.58	28.7	60.0	24.2	88.2
6.0	4.85	39.5	100	38.8	111
10.0	7.50	49.1			
20.0	13.5	65.8			

Electrophoresis. Electrophoretic mobilities, determined by microelectrophoresis, of the silica particles in 0.15 mM NaI aqueous solution as a function of pH are shown in Figure 2.4. From pH 2 to 6 the mobilities decreased from +0.51 x 10^{-8} $m^2 V^{-1} s^{-1}$ to -3.0 x 10^{-8} $m^2 V^{-1} s^{-1}$. This data indicates that the isoelectric point (iep) for the Stöber silica hydrosols was pH 2.7. Previous investigations of the effect of pH on the electrokinetic behavior of silica hydrosols show the iep to be between 2 and 3.5.[31,32,33] The mobilities of silica hydrosols from pH 7-10 remained at about -4.5 x 10^{-8} $m^2 V^{-1} s^{-1}$ indicating nearly complete dissociation of the silanol groups in the alkaline pH region.

The effect of NaI, CaI_2, and Bu_4NI additions on the electrophoretic mobility of the silica particles in 99.7 wt% acetone are plotted in Figure 2.5. With NaI and Bu_4NI, the mobilities became less negative with increasing electrolyte concentration. For example, the mobilities changed from -2.8 x 10^{-8} $m^2 V^{-1} s^{-1}$ to -1.5 x 10^{-8} $m^2 V^{-1} s^{-1}$ as the NaI concentration was raised from 1.3 to 4.85 mM.

In the presence of the bulky Bu_4NI, much higher salt concentrations (c.f. NaI) were needed to lower the electrophoretic mobility of the silica organosols. For example, in the Bu_4NI concentration range 3.9- 38.8 mM, the mobilities decreased from only -2.8 x 10^{-8} $m^2 V^{-1} s^{-1}$ to -0.90 x 10^{-8} $m^2 V^{-1} s^{-1}$. A smaller effect of Bu_4NI on the electrophoretic mobility of silica was observed as

compared to that using NaI. For example, using concentrations of 13.5 mM NaI and 13.9 mM Bu_4NI where their degree of dissociation was similar (see Table 2.1), the mobilities were -0.39 x 10^{-8} $m^2 V^{-1} s^{-1}$ using NaI and -1.7 x 10^{-8} $m^2 V^{-1} s^{-1}$ using Bu_4NI.

A different trend was observed for the effect CaI_2 additions on the electrophoretic mobility of silica in acetone. The CaI_2 concentrations in the acetone solutions were not corrected for ion-pair formation since the nature of the ions in their dissociated form was not known (*vide supra*). Figure 2.5 shows the electrophoretic mobilities changed from -2.9 x 10^{-8} $m^2 V^{-1} s^{-1}$ to 0 as the concentration of CaI_2 was raised from 0.06 mM to 0.25 mM. In 1 mM CaI_2, the electrophoretic mobility was +2.3 x 10^{-8} $m^2 V^{-1} s^{-1}$.

The electrophoretic mobilities of the silica hydrosols (pH=8) in the presence of NaI and CaI_2 were examined and the results are shown in Figure 2.5 for comparison with the silica organosols. With aqueous NaI additions from 15 to 250 mM, the mobilities ranged between -3.7 x 10^{-8} $m^2 V^{-1} s^{-1}$ and -1.2 x 10^{-8} $m^2 V^{-1} s^{-1}$.

In the presence of aqueous CaI_2 solutions, Figure 2.5 shows the mobilities decreased regularly from -2.1 x 10^{-8} $m^2 V^{-1} s^{-1}$ to -0.12 x 10^{-8} $m^2 V^{-1} s^{-1}$

as the concentration was raised from 4 mM to 80 mM. Therefore, the charge reversal observed for silica in CaI_2 - acetone solutions at about 0.25 mM did not take place using CaI_2 concentrations up to 80 mM for the hydrosols.

Figure 2.4. Electrophoretic mobilities of silica hydrosols in 0.15 mM NaI as a function of pH.

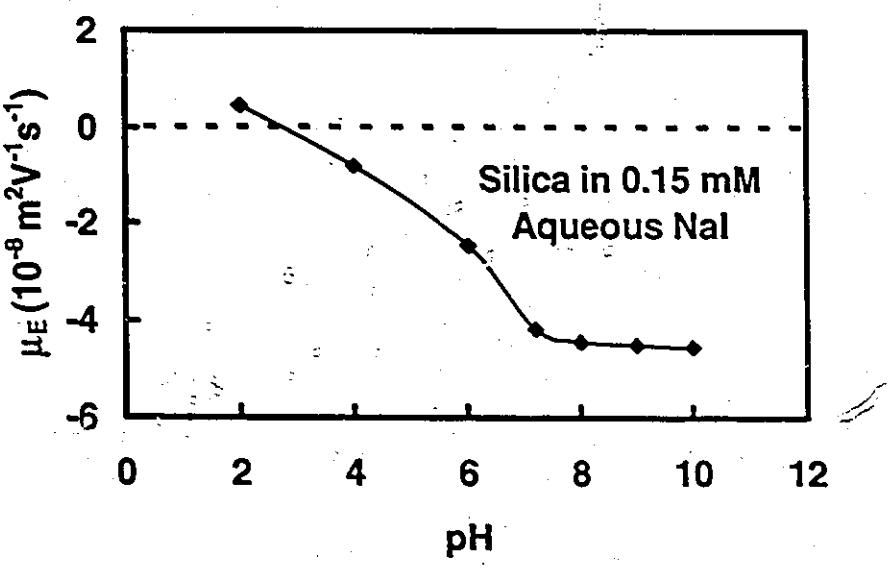

Figure 2.5. The variation of the electrophoretic mobility of colloidal silica in 99.7 wt% acetone (AC) and water (pH=8 for aqueous solutions) as a function of NaI, CaI_2, and Bu_4NI concentrations. NaI and Bu_4NI concentrations in acetone shown in graph are the concentrations of dissociated ions shown in Table 2.1.

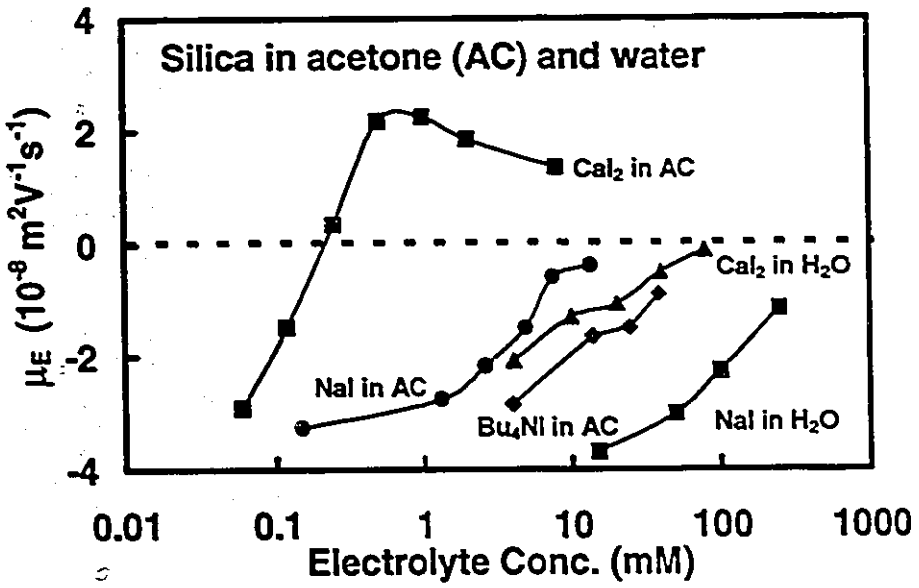

Coagulation Experiments. The colloidal stability of the silica sols was measured as a function of electrolyte concentration using turbidity measurements. Figure 2.6 and Figure 2.7 show the variation of the relative turbidities (τ_R) as a function of electrolyte concentrations for silica in acetone and water respectively. τ_R (Eq. [2.1]) was obtained from measurements of the percent transmittance of the silica dispersions in the presence of electrolyte. $\tau_R \approx 1$ indicates a colloidally stable dispersion, $\tau_R > 1$ indicates the onset of particle agglomeration, and $\tau_R < 1$ indicates that silica flocs have formed and settled. Coagulation concentration values, c_c, were assigned to electrolyte concentrations corresponding to the point where the flocs settled leaving a clear supernatant as indicated when $\tau_R < 1$.

Figure 2.6 shows the relative turbidity curves obtained for the silica particles in the presence of CaI_2, NaI and Bu_4NI acetone solutions. The c_c observed with NaI was 19.6 mM whereas the silica organosol was insensitive towards Bu_4NI concentrations up to 145 mM. On the other hand, silica in CaI_2 acetone solutions had two c_c values, 0.045 and 2.75 mM.

Figure 2.6. Variation of the relative turbidity with electrolyte concentration of unmodified silica dispersions in 99.7 wt% acetone upon addition of NaI, CaI_2, and Bu_4NI. NaI and Bu_4NI concentrations shown in graph are the concentrations of dissociated ions shown in Table 2.1.

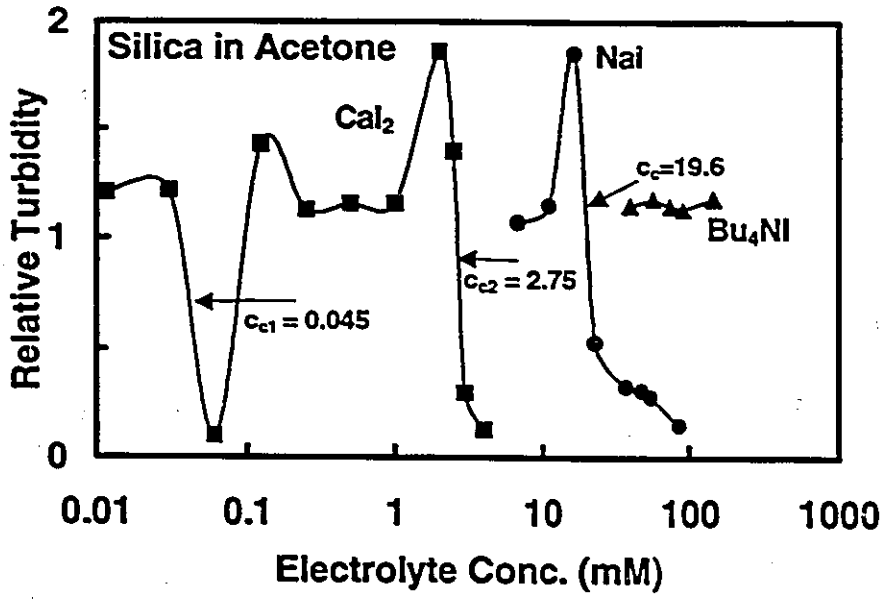

Figure 2.7. Variation of the relative turbidity with electrolyte concentration for unmodified silica dispersions in aqueous NaI and CaI_2 solutions (pH=8). c_c=7.5 mM.

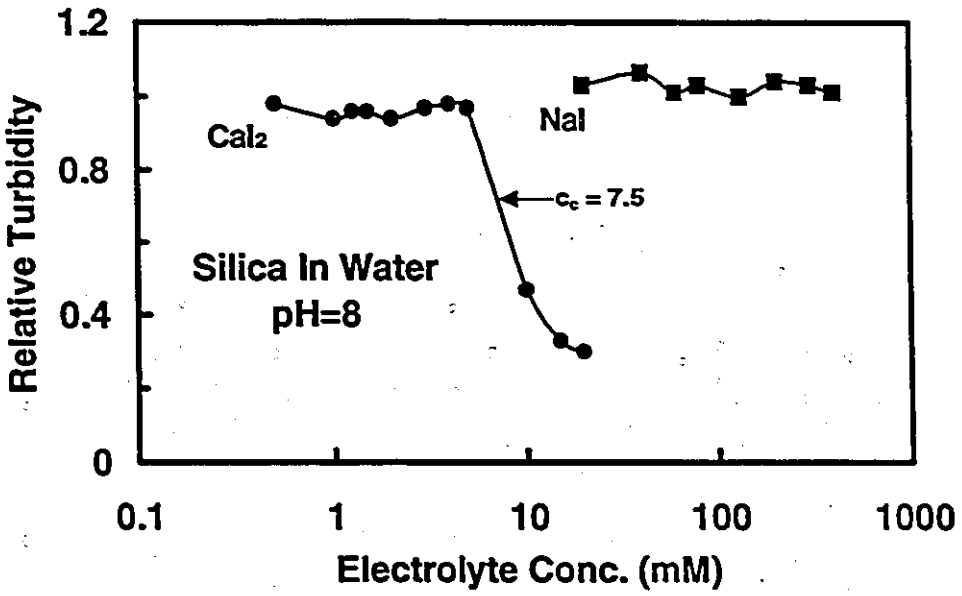

In comparison to the silica organosols, aqueous silica dispersions (pH=8) were less sensitive towards electrolyte addition. Comparison of Figure 2.6 with Figure 2.7 shows that NaI concentrations up to 0.8 mM did not coagulate the aqueous sol. These results are in good agreement with those reported by Allen and Matijevic.[14c] For example, c_c concentrations for Ludox® AM silica ranged from about 2.5 to 1.1 M NaI as the pH was raised from 6 to 8 indicating saturated 1:1 salt solutions were needed to coagulate the hydrosols.

Coagulation experiments for Stöber silica hydrosols were also performed in the presence of CaI_2 and the results in Figure 2.7 show that the $\tau_R \approx 1$ between 0.5 to 5 mM CaI_2. Further increases in CaI_2 concentration led to decreases in τ_R to 0.4 indicating particle coagulation. Figure 2.7 shows the c_c was 7.5 mM for the silica hydrosols as compared to 0.045 mM CaI_2 for silica in acetone (Figure 2.6). The coagulation results in aqueous CaI_2 were supported by the DCP experiments shown in Figure 2.1 where the silica sol coagulated in 10 mM CaI_2 as evidenced by the broad polydisperse distribution from which the average diameter was 800 nm. Coagulation experiments performed by Allen and Matijevic[14c] using Ludox® silica hydrosols and $CaCl_2$ as the coagulant showed the critical coagulation concentration to be 25 mM at pH=8. The higher magnitude of this c_c compared to our observed c_c reflects the smaller size (15 nm) of the Ludox® silica. See Appendix A2.3 for c_c. data obtained from DLS measurements using CaI_2, $CaCl_2$, and $Ca(NO_3)_2$.

2.4 Discussion

Three features of results obtained in the present study parallel those in the literature. First, the colloidal stability of the silica in acetone solutions was sensitive to small concentrations of NaI but remained insensitive towards the same coagulant in water. Similar observations have been reported for goethite (α-FeOOH) in acetone-water mixtures where the sensitivity of the organosols towards additions of $LiNO_3$ increased as the dielectric permittivity was decreased.[19b]

Second, the effect of multi-valent electrolytes on the stability of silver sols in 99.5 wt% ethanol has been studied and the results follow the charge reversal trend obtained in the present work for the silica acetone solutions in the presence of CaI_2.

Third, the silica hydrosols at intermediate pH's were observed to be remarkably stable in the presence of high concentrations of NaI and Bu_4NI which is similar to the properties of Ludox® silica in aqueous NaI solutions.[14c] In the following paragraphs our electrokinetic and stability results for silica in acetone are examined in terms of conventional colloid theory.

Site - dissociation - site - binding models, as presented by Yates *et al.*[12], are frequently used to quantitatively describe the double layer properties of the oxide / liquid interface. In the present work we were unable to measure variables such as the surface charge density of the particles in acetone as a function of pH. Therefore, we used the simpler single site-dissociation model described by Hunter.[34] The single-site model accounts only for the dissociation of silanols. The assumption that no counterion adsorption (ion exchange with surface silanols) occurs at the silica surface is incorrect (also, see Appendix A2.1) based on previous work which has shown ion-binding at the silica/water interface to take place for silica hydrosols in the presence of electrolytes.[35]

The following expressions from the single-site model give the theoretical ζ -potentials:

$$\zeta = 4\frac{a\tanh\left[\tanh\left[\frac{1}{4}\psi_o\frac{e_o}{k_bT}\right]\exp(-\kappa x)\right]}{e_o}k_bT \qquad [2.3]$$

where x represents the distance between the surface and the plane of shear, κ is the recripocal Debye-Hückel parameter (Eq. [2.2]), e_o is the electronic charge, k_b is the Boltzmann constant, T is the absolute temperature and ψ_o gives the surface potential as calculated from the Gouy-Chapman theory:

$$\psi_o = 59.8\,(\Delta pH) - 59.8\,\log\left(\frac{\dfrac{-N_S\kappa}{4N_AC}}{\sinh\left(\dfrac{e_o\psi_o}{2k_bT}\right)} - 1\right) \qquad [2.4]$$

where N_s refers to the total number of ionizable silanol sites per cm^2; N_A and C correspond to Avogadro's number and the bulk electrolyte concentration respectively; and, $\Delta pH = pK_a - pH$

Figure 2.8 shows theoretical ζ-potentials as a function of κ*a* plots for ΔpH = 2, 1, and -0.7. N_s was assumed to be 7.9×10^{14} sites cm^{-2} based on previous studies using silica,[18b] and a value of 0.5 nm was used for x The best agreement between theory and the experimental results was obtained using ΔpH = 2.

Although the dissociation constant for silanols in acetone is not known, some insight concerning its magnitude can be obtained from other sources. For example, Nowak *et al.*[36] studied the dissociation behavior of several substituted phenols in acetone-water mixtures using a potentiometic titration method. The pK_a for 2,6 dichlorophenol in water was found to be 6.79 which is similar to that reported for silica silanols in water[37]. The corresponding pK_a for 2,6

dichlorophenol was 10.98 in 94 wt% acetone (ε_r=21.5). By analogy, this suggests that the pK_a for silanols may be of similar magnitude.

Figure 2.8. Comparison of experimental ζ - potentials calculated using the O'Brien and White program with those predicted from the single - site dissociation model as a function of κa for NaI acetone solutions. The theoretical curves were calculated with Eq's. [2.3] and [2.4] assuming x=0.5 nm and N_s = 7.9 x 10^{14} cm^{-2}. κ was calculated using NaI concentrations corrected for ion-pair formation (see Table 2.1) and a = 88.5 nm.

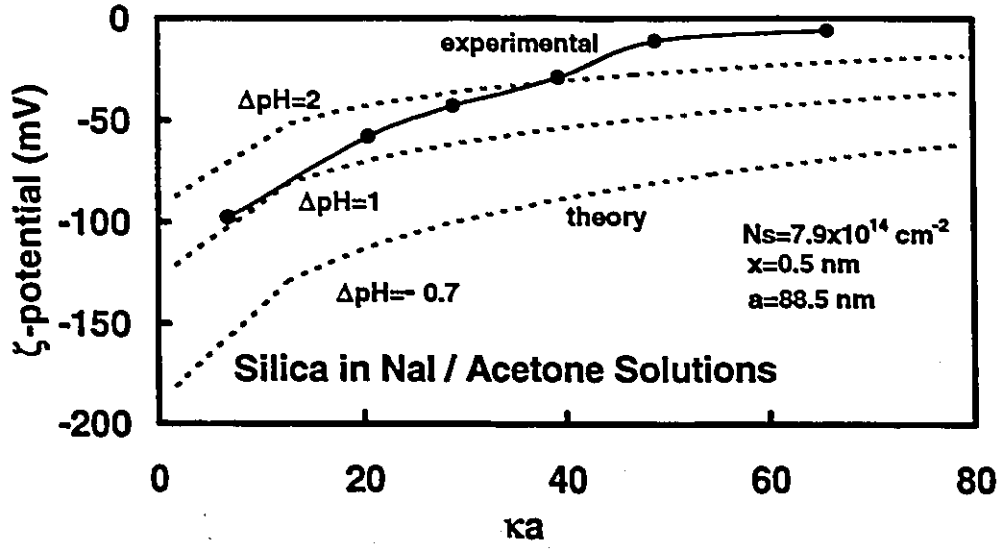

Assuming the pK_a for silanols in acetone is about 11, the corresponding pH value is 9 based on $\Delta pH = 2$.

The single-site dissociation model appeared to predict the ζ-potential of silica as a function of κa for NaI in acetone. On the other hand, the colloidal stability results showed some unexpected trends. This is illustrated by comparing the observed c_c values with those predicted by DLVO theory.

For low surface potentials the following expression for c_c is given by Hunter:[38]

$$c_c = 7.09 \times 10^{-41} \left(\frac{\varepsilon_r^2 \psi_d^4}{A_{12}^2 z^2} \right) \qquad [2.5]$$

where ψ_d is the electrostatic potential at the beginning of the diffuse double layer. The observed ζ-potentials of the silica samples were assumed to be equal to ψ_d.

A_{12}, the combined Hamaker constant, was estimated by the relation:

$$A_{12} \approx \left(\sqrt{A_{11}} - \sqrt{A_{22}} \right)^2 \qquad [2.6]$$

where A_{11} and A_{22} refers to the non-retarded Hamaker constants for the particle silica and the medium (acetone=4.1×10^{-20} J or water=3.7×10^{-20} J) interacting across vacuum.

Since the silica particles were shown to have a porosity of 15%, this must be taken into account when calculating A_{11}. The Hamaker constant for a particle filled with a medium interacting with an alike particle across a vacuum, A_{11}^{p}, can be estimated using the following expression;[39]

$$A_{11}^{p} = A_{11}\phi_p + A_{22}(1-\phi_p) \qquad [2.7]$$

where $\phi_p = 0.87$ corresponds to the internal solids volume fraction of the particle.

Figure 2.9 shows c_c values calculated from Eq. [2.5] as a function of ζ-potentials. According to theory, the c_c's for silica in aqueous 1:1 electrolyte solutions are expected to decrease from 61 to 1 mM when the ζ - potentials are -50 and -18 mV, respectively. The open triangle shows the experimental ζ-potential at 800 mM, the highest concentration measured, and no coagulation was observed. Clearly, the experiments did not follow the predictions based on the simple theory.

According to theory, the c_c values using NaI and Bu_4NI in acetone were much lower than the experimental values. At the experimental c_c of 19.6 mM NaI in acetone (shown in Figure 2.9), the ζ-potential was -5 mV which indicated NaI concentrations at least 100 times greater were needed to coagulate the silica as compared to that expected from theory. In the case of Bu_4NI acetone solutions,

Figure 2.9. Comparison of experimental and theoretical critical coagulation (c_c) concentrations for silica in acetone (AC) and water (WA, pH=8) as a function of ζ - potential. The theoretical c_c's were computed assuming the silica surface potential was low (≈ less than -50 mV) according to Eq. [2.5]. Parameters for calculations were T=25°C; ε_r=20.7 and A_{12}= 0.18 x 10^{-20} J for acetone; ε_r=78.5, A_{12}= 0.27 x 10^{-20} J for water. The observed c_c values with their respective ζ - potentials are shown in the plot for silica in NaI / AC and CaI_2 / WA solutions. c_c's were not observed for silica in Bu_4NI / AC and NaI / WA solutions hence the dashed arrows shown next to these data points indicate higher concentrations are needed to coagulate the sols.

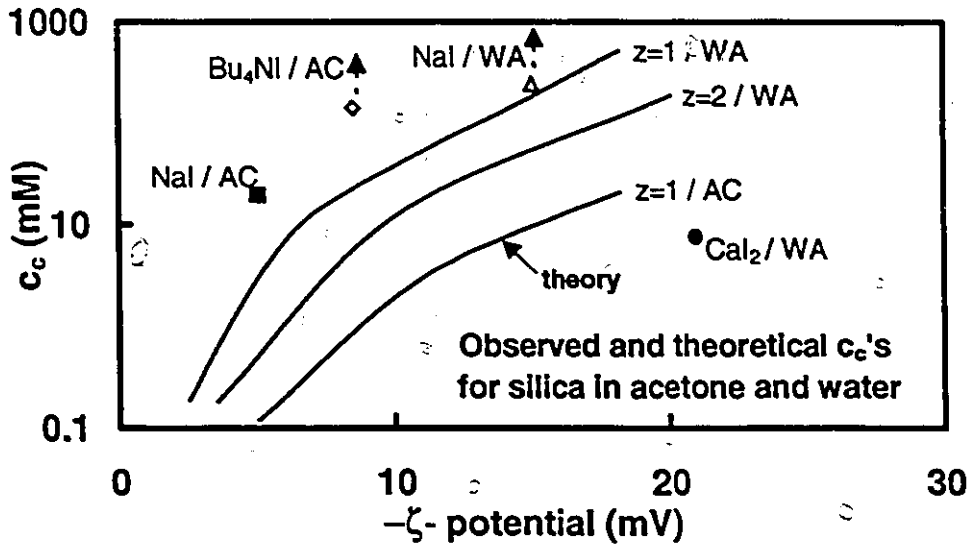

the silica was insensitive towards concentrations up to 146 mM although the observed ζ - potential of -16 mV was low.

The theory used to generate the curves in Figure 2.8 and Figure 2.9 were based on many approximations and simplifications. Nevertheless, we have confidence in the conclusion that the colloidal stability of Stöber silica in acetone cannot be explained by simple DLVO theory. Similar conclusions have been reached about silica and water.[14,15,16] In fact, a recent article by Vigil *et al.*[16] makes a convincing case for the presence of a short steric barrier at the silica / water interface. If so, our results suggest that the barrier can be collapsed by high NaI concentrations in acetone but not in water whereas the solubility of the steric chains is not influenced by Bu_4NI in acetone.

The CaI_2 results in acetone were not modeled because little is known about the dissociation behavior. Although a low degree of dissociation for CaI_2 in acetone (Table 2.1) was expected, the silica organosols were observed to be sensitive towards small changes in CaI_2 concentrations (Figure 2.6). It seems reasonable to propose that the charge reversal of the particles induced by CaI_2 in acetone reflects the specific adsorption of charged cationic chemical complexes at the silica / acetone interface; CaI^+ is one possibility, see Scheme 2.2.

Charge reversal has been reported by de Rooy *et al.*[19b] using Ag sols dispersed in 99.5% ethanol containing $Ca(NO_3)_2$ and $La(NO_3)_3$. CaI_2 additions caused charge reversal and stabilization in acetone whereas in water the ζ - potential decreased and flocculation was observed (*c.f.* Figure 2.6 with Figure 2.7). From Figure 2.9 it can be seen that for z=2 in water the theoretical c_c's were 19.5 mM and 4 mM using ψ_d of -20 and -7.7 mV, respectively. The experimentally determined c_c was 7.5 mM at which the ζ - potential was about -25 mV. The lower c_c as compared to theory using aqueous CaI_2 solutions is in line with previous investigations which showed multi-valent metal ions are effective coagulants due to specific adsorption effects.[40]

2.5 Conclusion

(1) Stöber silica particles had large negative ζ-potentials in 99.7 wt% acetone and the dependency on NaI concentration could be modeled by a single - site dissociation model to give a reasonable description of the experimental ζ-potentials assuming ΔpH=2, N_s=7.9 x 10^{14} sites cm^{-2}, and that the plane of shear was 0.5 nm away from the particle. There was insufficient experimental data to justify the use of more elaborate models.

(2) The colloidal stability of Stöber silica in acetone could not be explained by only electrostatic stabilization according to simple DLVO theory. A thin steric barrier, proposed by Vigil *et al.*[16] for silica in water, seems to explain qualitatively the results in acetone.

(3) CaI_2 induced charge reversal of Stöber silica in acetone as well as restabilization at intermediate concentrations. The specific adsorption of CaI^+ is proposed with no direct evidence.

Appendix A2.1 Porosity of Stöber silica.

There are many studies in the literature which use "model" colloid systems. Polymer based latices, such as polystyrene, and inorganic oxide particles such as colloidal silica are often treated as being good model systems to carry out experiments for both industrial and scientific purposes. The "model" particle systems are expected to be monodisperse, spherical, and to have rigid smooth surfaces supporting well-defined chemical groups. Stöber silica is a commonly used model colloid system and its "model" properties have been discussed (see 2.1 Introduction). With the increased use of Stöber silica over the past decade there has been several studies investigating it's growth mechanism and matrix microstructure.[2,3,6,41] Both of these issues still remain unresolved and are becoming increasingly important due to the increased interest of using Stöber silica as "model" oxide supports in the ceramic and coating areas.[42]

In Chapter 2, we postulated that the Stöber silica matrix has a porosity of 15% based on DCP and DLS measurements of the particle size. While some studies claim the silica matrix has a porous nature,[6b,c,7f] others claim it is a non-porous species.[7c] Evidence is provided below to address the silica porosity issue. This note describes the characterization of Stöber silica by electron

microscopy and titration experiments after mixing the silica with aqueous Ca^{++} solutions.

Stöber silica (1 wt%) was mixed with an aqueous 40 mM CaI_2 solution at pH=6.8 (protected from light) for 24 hours and subsequently prepared for characterization by TEM as described previously.[43]

Figure A2.1-1a (see opposite page) shows the X-ray image maps obtained from TEM analysis of the sectioned particle pieces. In Figure A2.1-1a, the image map on the left corresponds to an X-ray mapping image of a 50 nm silica section probed for silicon (red signals) whereas the X-ray map on the right shows the same section probed for Ca^{++}. The green signals arising from detected Ca^{++} are visible throughout the silica section (shown by the higher concentration of green signals in the center of the image). The X-ray map image in Figure A2.1-1a provides visual evidence that silica has a porous matrix capable of allowing Ca^{++} ions to diffuse into its interior. The X-ray spectrum for the 50 nm sectioned piece is given in Figure A2.1-1b (bottom spectrum) showing the presence of silicon and calcium signals within the particle interior.

Figure A2.1-1 **Top Image:** *Left* - TEM scan image of X-ray map taken for a 50 nm silica particle section (center of photo) probed for silicon (red color signals); *Right* - X-ray calcium map (green color signals) of same silica particle. Other calcium or silicon signals shown in the images arise from smaller microtomed silica pieces or X-ray beam backscattering. **Bottom Image:** X-ray spectrum of 50 nm silica particle section.


SI
CA
MAG:2000000X
95 16 nm
MAG:2000000X
95 16 nm

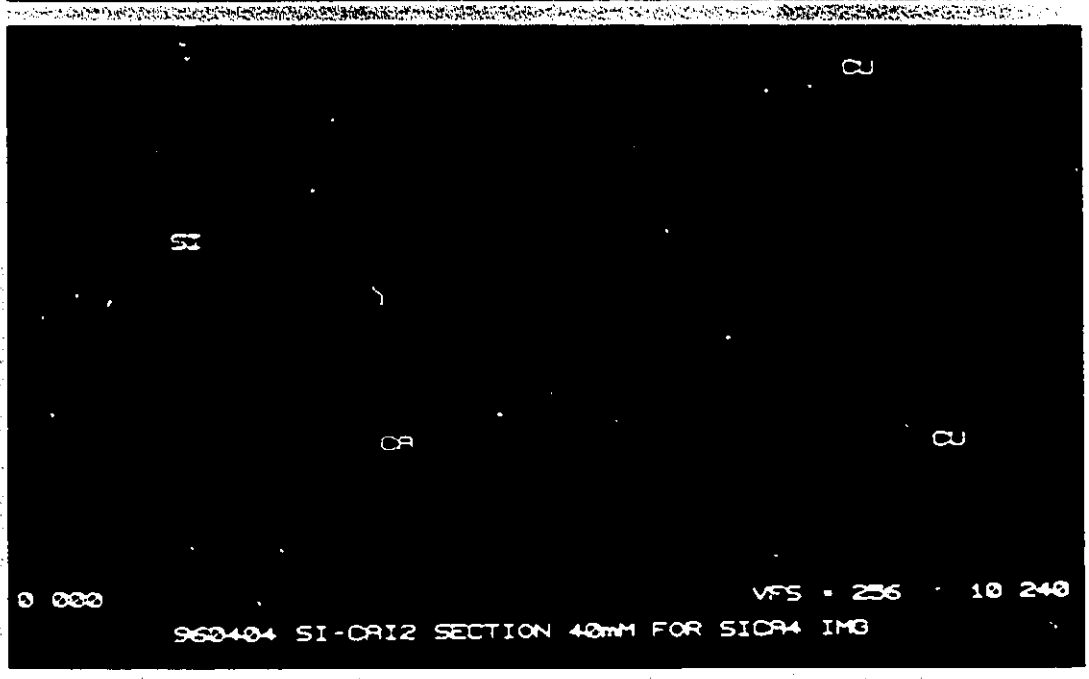
CU
SI
CA
CU
0 000
VFS = 256 10 240
960404 SI-CA12 SECTION 40mM FOR SICA4 IMG

Further analysis of the Ca^{++} adsorption onto the silica sample was carried out using a potentiometric titration apparatus equipped with a Ca^{++} ion selective electrode.[44] Two binding isotherms were obtained for the silica where CaI_2 was added to "wet" silica and to silica that was initially dried at 120°C.

Figure A2.1-2. Adsorption of Ca^{++} on silica by titration using aqueous CaI_2 solutions at pH=6.8 as a function of the equilibrium CaI_2 concentration. "Wet" silica refers to silica which remained in water whereas the "dry" silica corresponds to silica which underwent heat treatment at 120°C before CaI_2 was added.

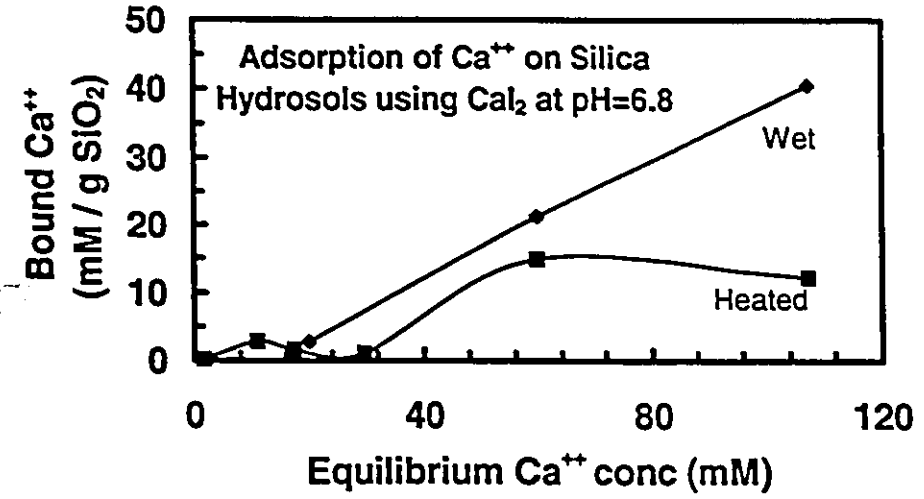

Figure A2.1-2 shows the "wet" silica displays a linear dependence for adsorbed Ca^{++} as a function of the equilibrium CaI_2 concentration. By contrast,

the "dry" silica has a Langmuir type adsorption pattern which displays a maximum sorption capacity around 12 mM Ca^{++} per gram SiO_2. Taking the density of silica to be 1700 kg m^{-3} a simple calculation shows there would be 2 x 10^{-18} C m^{-3}. If all the Ca^{++} counterions are considered to occupy a surface layer thickness of 0.2 nm, we expect there to be 0.4 C m^{-2} or 2.5 charges per nm^2 in the 0.2 nm thick layer. We can compare this result to a fully ionized surface in water. Assuming a high surface charge density, a typical value would correspond to σ_0 = 0.3 C m^{-2} which is one charge per 0.5 nm^2.[45] Since this surface charge density is lower than the counterion (Ca^{++}) density calculated based on the Stöber silica data it is likely that this difference reflects the porosity of the Stöber silica. We also believe the difference between the two Ca^{++} adsorption profiles (as shown in Figure A2.1-2) is due to the porous nature of the "wet" silica. After heat-treatment the pores of the "dry" silica sample may be collapsing and this process would be expected to limit the sorption capacity of the silica for Ca^{++}.

One of the important features of the above porosity discussion is that related to the growth mechanism of Stöber silica. Bailey and Mecartney have used cryogenic transmission electron microscopy to follow the genesis and formation of Stöber silica particles.[41] The results that during the initial stages of the particle growth mechanism, the TEOS monomers polymerized to form silica microgel seed clusters. Although these microgel clusters will collapse with

further growth *viz.* condensation reactions, these microgel microstructure may reflect the porosity of the Stöber silica observed in our results. Further support for a microgel Stöber silica matrix based on elemental analysis results has also been reported by Jelinek *et al.* in which the particle microstructure was described as having a "poly(silicic acid) skeleton with micropores enclosing a water/ammonia mixture".[6b]

Appendix A2.2 Ion dissociation calculations.

In non-aqueous media, the solubility of electrolytes and the degree of electrolyte dissociation is much lower compared to using water as the solvent. To adequately describe the electrical double layer behavior of the silica organosols, the extent of ion association in acetone needs to be addressed.

The degree of dissociation, α, was estimated using conductivity data according to the following equation proposed by Fuoss and Shedlovsky:[46]

$$\alpha = s(z)\frac{\Lambda}{\Lambda_o} \qquad [A1]$$

where Λ is the molar conductivity, Λ_o is the molar conductivity at infinite dilution, and s(z) is the Shedlovsky crowding factor defined by

$$s(z) = \left[\frac{z}{2} + \left(1 + \left(\frac{z}{2}\right)^2\right)^{0.5}\right]^2 \qquad [A2]$$

where

$$z = (a\Lambda_o + b)\Lambda_0^{-1/2}(c_o\Lambda)^{1/2} \qquad [A3]$$

and a and b correspond to the Debye-Hückel ion interaction parameters which are represented as follows

$$a = q\left(\frac{z^3 eF^2}{24\pi\varepsilon\varepsilon_o RT}\right)\left(\frac{2}{\pi\varepsilon_r\varepsilon_o RT}\right)^{0.5} \qquad [A4]$$

and

$$b = \left(\frac{z^2 eF^2}{3\pi\eta}\right)\left(\frac{2}{\varepsilon_r\varepsilon_o RT}\right)^{0.5} \qquad [A5]$$

where q=0.50 for a 1:1 electrolyte, z is charge valence, F is Faraday's constant, R is the gas constant, T is the absolute temperature, ε_o is the vacuum permittivity, and ε_r and η correspond to the dielectric permittivity and viscosity of the continuous phase, respectively.

For example, the molar conductivity, Λ, was measured to be 33.5 S cm^2 mol^{-1} for a 0.5 mM NaI acetone solution. The Shedlovsky crowding factor, $s(z)$ was calculated to be 1.75 based on using the Debye-Hückel ion interaction parameters of a=1.69 and b=3.32x10^{-5}, and z=0.51. The molar conductivity at infinite dilution, Λ_o, for NaI in acetone was obtained from published data and it was determined to be 182.5 Scm^2 mol^{-1}. From these data the degree of dissociation, α, for a 0.5 mM NaI acetone solution is calculated to be 0.32 hence only 32% of the ions are expected to be dissociated as Na^+ and I^-

Appendix A2.3 Critical coagulation concentrations of Stöber silica using aqueous Ca^{++} solutions based on DLS measurements.

The mean diffusion coefficient of the particles (D), was determined from the relaxation rate Γ_r of the autocorrelation function given by

$$\Gamma_r = Dq^2 \qquad [A6]$$

where q is the scattering vector given by

$$q = \left(\frac{4\pi n}{\lambda}\right)\sin\left(\frac{\theta}{2}\right) \qquad [A7]$$

where n is the refractive index of the scattering medium (acetone or water), λ is the wavelength of incident light, and θ corresponds to the scattering angle.

The mean D was used to calculate the mean hydrodynamic particle diameter, d_H, based on the Stokes-Einstein equation. The data were fitted by the method of cumulants in terms of the first moment using the Brookhaven software (version # BI9).[47] Data were collected for 500 seconds and a minimum of 10 measurements were made.

c_c's for silica dispersions using CaI_2 solutions at pH=6.8 ± 0.2 were determined from plots of the stability ratio (W) as a function of salt concentration (c).[48] *W* is defined by the following expression which gives the ratio of rate constants for doublet formation:

$$W = \frac{k_f}{k_s} \qquad \text{[A8]}$$

where k_s is the rate constant for the slow aggregation regime where not every particle collision will result in permanent contact and k_f is the Smoluchowski diffusion-limited fast aggregation constant given by the following equation:[49]

$$k_f = \frac{8k_BT}{3\eta} \qquad \text{[A9]}$$

where k_B is Boltzmann's constant, T is the temperature, and η refers to the viscosity of the continuous phase.

Experimental stability ratios (*W*) were calculated by obtaining k_s according to the following expression developed by Virden and Berg:[50]

$$k_s = \frac{1}{r_{H_0}(\alpha)N_0}\left[\frac{dr_H}{dt}\right]_{t=0} \qquad \text{[A10]}$$

where r_{H_0} corresponds to the initial hydrodynamic radius at t=0, α is an optical factor, N_0 is the initial particle number concentration, and $\frac{dr_H}{dt}$ is the measured initial slope extrapolated to t=0. The silica particle number concentration used in the kinetic experiments was 6.3×10^8 particles cm^{-3} and α was 0.35.

Figure A2.3-1. Stability ratio as a function of aqueous CaI_2, $CaCl_2$, and $Ca(NO_3)_2$ solutions for Stöber silica at pH=6.8.

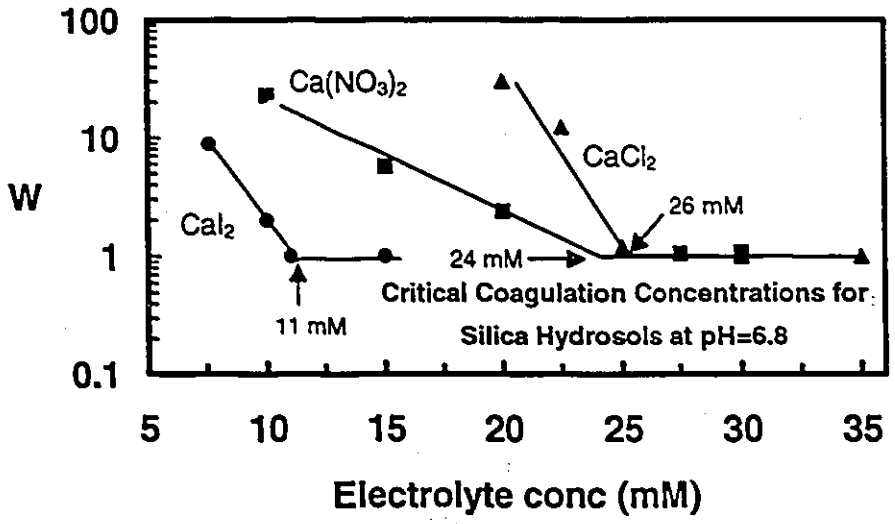

Figure A2.3-1 shows the c_c's obtained for silica in the presence of Ca^{++} solutions containing iodide, chloride, and nitrate. The c_c's were determined to be 11 mM, 24 mM, and 26 mM, for the iodide, chloride, and nitrate solutions, respectively. The differences between the c_c's was believed to be reflected in

the nature of the counter-ion. The coagulation of sols has been previously studied as a function of the differences in the counter-ion for electrolytes of the same valency.[14c51] Differences in the coagulation behavior of aqueous sols in the presence of electrolytes having different counter-ions have been shown to be reflected in the hydration energies, size, and polarizabilities of the counter-ion. This is based on the well-known Hofmeister series of ions where the order of adsorbability of anions from aqueous solutions is $I^- > Br^- > Cl^- > F^- > NO_3^-$.[52] The c_c's shown in Figure A2.3-1 follow the Hofmeister trend.

Appendix A2.4 Colloidal Glass.

In the past 10 years there have been several papers reporting on the phase behavior of spherical colloidal particles.[53] In particular, order formation of colloidal particles has received special attention since their properties may be useful indicators of the fundamental chemical and physical characteristics (*e.g.*, crystallization, hard sphere models, and coulombic interactions) displayed by atomic liquids and solids.

A dilute ethanol suspension consisting of spherical colloidal silica particles containing 1 mM CaI_2 was stored for a 6 month period at room temperature. Following this time frame, several glassy pieces of solid matter (referred to as colloidal glass herein) were observed at the bottom of the glass vessel. The colloidal glass displayed glittering iridescent colors as they were rotated towards a conventional light source. A drop of the colloidal glass suspension was placed on a glass slide and analyzed using a light microscope (magnification 10X). Several irregular shaped glassy pieces ranging in size from 1 mm to 2000 mm were initially observed. The most interesting effect occurred during the time when the ethanol was evaporating (took about 1-2 min) in that an ordered arrangement of vertical and horizontal planes developed for a few seconds in some pieces but then quickly disappeared. The appearance of this ordering effect was captured by fitting a camera on the light microscope. Figure

A2.4.1 shows two large colloidal glass pieces (scale bar=100 μm) photographed at the instant the ordered pattern emerged. Figure A2.4.1 shows dark vertical bands streaming across the larger glass piece situated on the left. The dark bands have a width of approximately 20 μm each with an average spacing between them of 10 μm. The colloidal glass piece situated at the bottom left in Figure A2.4.1 showed both vertical and horizontal bands having a width of about 25 μm which appeared to overlap one another. The silica particle size in the sample was on the order of 200 nm hence they are much below the resolution capable for light microscopy. As mentioned above, this ordered pattern only occurred during the evaporation of the ethanol. For this reason, electron microscopy or X-ray diffraction was unsuccessful and could not be used to visualize the packing arrangement of the silica particles.

Figure A2.4-1. Light microscope photograph taken of "colloidal glass" formed by suspending spherical silica (average diameter was approximately 200 nm) particles in an ethanol solution containing 1 mM CaI_2 for 6 months. The two arrows are pointing towards one of the repeating dark bands (width = 20 μm) observed only at some instance whilst the ethanol was evaporating from the glass slide used as a support. Scale bar = 100 μm.

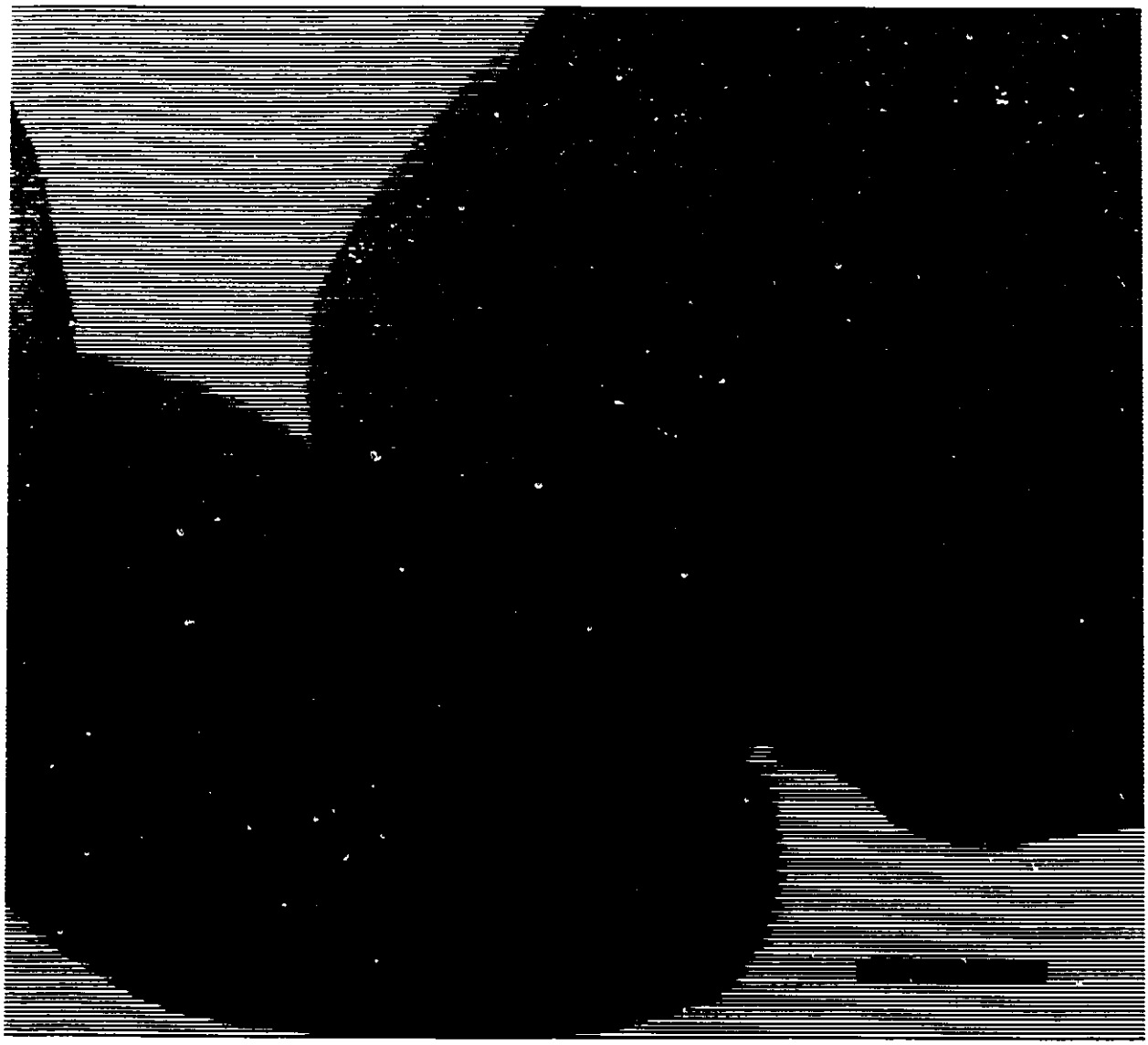

2.6 References

[1] Iler, R.K. *The Chemistry of Silica*; Wiley: New York, 1979; pp 528-599 and references cited therein.

[2] Badley, R.D.; Ford, W.T. *J. Org. Chem.* **1989**, *54*, 5437.

[3] (a) van Helden, A.K. Ph.D. Thesis, 1980, University of Utrecht. (b) van Blaaderen, A. Ph.D. Thesis, 1992, University of Utrecht.

[4] Brinker, C.J.; Scherer, G.W. *J. Non-Cryst. Solids* **1985**, *70*, 301.

[5] Stöber, W.; Fink, A.; Bohn, E. *J. Colloid Interface Sci.* **1968**, *26*, 62.

[6] (a) van Blaaderen, A.; Van Geest, J.; Vrij, A. *J. Colloid Interface Sci.* **1992**, *154*, 481. (b) Jelinek, L.; Dong, P.; Rojas-Pazos, C.; Taïbi, H.; Kováts, E. sz. *Langmuir* **1992**, *8*, 2152. (c) Bogush, G.H.; Zukoski IV, C.F. *J. Colloid Interface Sci.* **1991**, *142*, 1. (d) Look, J.; Bogush, G.H.; Zukoski, C.F. *Faraday Discuss. Chem. Soc.* **1990**, *90*, 345. (e) Philipse, A.P. *Colloid Polym. Sci.* **1988**, *266*, 1174. (f) Bogush, G.H.; Tracy, M.A.; Zukoski, C.F IV *J. Non-Cryst. Solids* **1988**, *104*, 95. (g) Vrij, A.; Jensen, J.W.; Dhont, J.K.G.; Pathmamanoharan, C.; Kops-Werkhoven, M.M.; Fijnaut,H.M. *Faraday Discuss. Chem. Soc.*, **1983**, *76*, 19.

[7] (a) Ketelson, H.A.; Brook, M.A.; Pelton, R.H. *Chem. Mater.* **1995**, *7*, 1370. (b) van Blaaderen, A.; Vrij, A.. *J. Colloid Interface Sci.* **1993**, *156*, 1. (c) Badley, R.D.; Ford, W.T.; McEnroe, F.J.; Assink, R.A. *Langmuir*, **1990**, *6*, 792. (d) Goodwin, J.W.; Harbron, R.S.; Reynolds, P.A. *Colloid Polym. Sci.* **1990**, *268*, 766.(e) Philipse, A.P.; Vrij, A. *J. Colloid Interface Sci.* **1989**, *128*, 121. (f) van Helden, A.K.; Jansen, J.W.; Vrij, A. *J. Colloid Interface Sci.* **1981**, *81*, 354.

[8] (a) Ketelson, H.A.; Brook, M.A.; Pelton, R.H. *Polymers. Adv. Tech.*, **1995**, *6*, 335.. (b) Auroy, P.; Auvray, L.; Léger, L. *J. Colloid Interface Sci.*, **1992**, *150*, 187. (c) Pathmamanoharan, C. *Colloids Surf.* **1990**, *50*, 1. (d) *ACS Symp. Ser.*, #240; Edwards, J.; Lenon, S.; Toussaint, A.F.; Vincent, B, 1984, pp 281. (e) Clarke, J.; Vincent, B. J. Colloid Interface Sci. **1981**, *82*, 208.

[9] Iler, R.K. *The Chemistry of Silica*; Wiley: New York, 1979.

[10] Hunter, R.J. *Zeta Potential in Colloid Science*; Academic Press: London, 1981; pp 278-282.

[11] For general reviews see, for example: (a) Westall, J.; Hohl, H. *Adv. Colloid Interface Sci.* 1980, *12*, 265. (b) Healy, T.W.; White, L.R. *Adv. Colloid Interface Sci.* 1978, *9*, 303. (c) *Surface and Colloid Science*; Wiley: New York, 1973; E. Matijevic, ed., James, R.O.;Parks, pp 119.

[12] Yates, D.E.; Levine, S.; Healy, T.W. *Trans. Faraday Soc.*, 1974, *70*, 1807.

[13] Davis, J.A.; James, R.O.; Leckie, J.O. *J. Colloid Interface Sci.* 1978, *63*, 480.

[14] (a) Sasaki, S.; Maeda, H. *J. Colloid Interface Sci.* 1994, *167*, 146. (b) Frolov, Y.G.; Shabanova, N.A. *Langmuir*, 1987, *3*, 640. (c) Allen, L.H.; Matijevic, E. *J. Colloid Interface Sci.*, 1969, *31*, 287. (d) Depasse, J.; Watillon, A. *J. Colloid Interface Sci.*, 1970, *33*, 430. (e) Vold, M.J. *J. Colloid Sci.* 1961, *16*, 1.

[15] (a) Grabbe, A.; Horn, R.G. *J. Colloid Interface Sci.* 1993, *157*, 375. (b) Meagher, L. *J. Colloid Interface Sci.* 1992, *152*, 293. (c) Ducker, W.A.; Senden, T.J.; Pashley, R.M. *Nature*, 1991, *353*, 239. (d) Elimelech, M. *J. Chem. Soc. Faraday Trans.*, 1990, *86*, 1623. (e) Horn, R.G.; Smith, D.T.; Haller, W. *Chem. Phys. Lett.* 1989, *162*, 404,. (f) Peshel, G.; Belouschek, P.; Müller, M.M.; Müller, M.R.; Kõnig, R. *Colloid Polymer Sci.* 1982, *260*, 444.

[16] Vigil, G.; Zhenghe, X.; Steinberg, S.; Israelachvili, J. *J. Colloid Interface Sci.* 1994, *165*, 367.

[17] (a) For a general discussion see: Hunter, R.J. *Zeta Potential in Colloid Science*; Academic Press: New York, 1981; pp 284-285.(b) Tadros, Th.F.; Lyklema, J. *J. Electroanal. Chem.*, 1968, *17*, 267. (c) Lyklema, J. *J. Electroanal. Chem.* 1968, *18*, 341. (d) Abendroth, R.P. *J. Colloid Interface Sci.* 1970, *34*, 591. (e) Perram, J. *J. Chem. Soc., Faraday 2*, 1973, 993.

[18] (a) Kosmulski, M. *Colloids Surf.* 1995, *95*, 81. (b) Kosmulski, M.; Matijevic, E. *Langmuir* 1992, *8*, 1060. (c) Kosmulski, M.; Matijevic, E. *Colloid Polym. Sci.* 1992, *270*, 1046.(d) Kosmulski, M.; Matijevic, E. *Langmuir* 1991, *7*, 2066.

[19] (a) Kitahara, A. *Adv. Colloid Interface Sci.* 1992, *38*, 1. (b) de Rooy, N.; de Bruyn, P.L.; Overbeek, J. T. G. *J Colloid Interface Sci.* 1980, *75*, 542. (c) Baran, A.A.; Chekhovaya, I.N.; Vdovenko, L.I.; Korsunskaya, A.I. *Kolloidn. Zh.* 1976, *39*, 419. (d) Baran, A.A.; Chekhovaya, I.N. *Kolloidn. Zh.* 1976, *39*, 426. (e) Vincent, B.; Bijsterbosch, B.H.; Lyklema, J. *J Colloid Interface Sci.* 1971, *37*, 171. (f) Kratohvil, J.P.; Orhanovic, M.; Matijevic, E. *J. Phys. Chem.* 1960, *64*, 1216 and references cited therein. (g) Mackor,

E.L. *Recueil*, **1951**, *70*, 841. (h)Verwey, E.J. *Rec. Trav. Chim.* **1941**, *60*, 625. (I) Weiser, H.B.; Mack, G.L. *J. Phys. Chem.* **1930**, *34*, 86, 101.

20 Although sonication is not necessary for the particle synthesis, we have found that in some samples a small amount of silica gel precipitated at bottom of reaction vessel due to mixing problems. It was observed that a sonicating probe helped to reduce this gel formation.

21 Berne, B.J.; Pecora, R. Dynamic Light Scattering with Applications to Chemistry, Biology, and Physics; John Wiley & Sons, Inc.; NY, 1976.

22 Pelton, R.; Miller, P.; McPhee, W.; Rajaram, S. *Colloids Surf.*, **1993**, *80*, 181.

23 Mangelsdorf, C.; Chan, D.; White, L. *WinMobil*, Version 2.10, **1993**. See O'Brien, R.W.; White, L.R. *J. Chem. Soc., Faraday Trans.* 2 **1978**, *74*, 1607.

24 Evans, D.F.; Thomas, J.; Nadas, J.A. *J. Phys. Chem.* **1971**, *75*, 1714.

25 (a) Murley, R.D. *Nature*, **1965**, *207*, 1089. (b) Langer, G. *Colloid Polym. Sci.*, **1979**, *257*, 522.

26 van Blaaderen, A.; van Geest, J.; Vrij, A. *J. Colloid Interface Sci.* **1986**, *110*, 591.

27 Robinson, R.A., Stokes, R.H. *Electrolyte Solutions*, Butterworths Scientific: London, 1959; pp 392.

28 Krumgal'z, B.S.; Gerzhberg, Yu.I. *Zh., Obs. Khim.*, **1973**, *43*, 462. Kitahara, A.; Karasawa, S.; Yamada, H. *J. Colloid Interface Sci.* **1967**, *25*, 490.

29 Fuoss, R.M.; Shedlovsky, Th. J. *J. Am. Chem. Soc.* **1949**, *71*, 1496.

30 Gill, D.S.; Sharma, A.N.; Schneider, H., *J. Chem. Soc., Faraday Trans.1.* **1982**, *78*, 465.

31 Zurita, L, Carrique, F., and Delgado, A.V., Colloids Surf., **92**, *23* (1994).

32 Rutland, M.W., and Pashley, R.M., J. Colloid Interface Sci., **130**, *448* (1989).

33 Iler, R.K. *The Chemistry of Silica*; Wiley: New York, 1979; pp 660.

34 Hunter, R.J. *Zeta Potential in Colloid Science*; Academic Press: London, 1981; pp 270.

35 Iler, R.K. *The Chemistry of Silica*; Wiley: New York, 1979; pp 664-667.

36 Nowak, B.; Pawlak, Z., *J. Chem. Soc., Faraday Trans. 1*, **1982**, *78*, 2693.

37 Schindler, P.; Kamber, H.R. *Helv. Chim. Acta* **1968**, *51*, 1781.

38 Hunter, R.J. *Foundations of Colloid Science (Volume 1)*; Academic Press: London, **1989**; pp 420.

39 van der Hoeven, Ph.C.; Lyklema, J. *Adv. Colloid Interface Sci.* **1992**, *42*, 205.

40 Matijevic, E. J. *Colloid Interface Sci.* **1973**, *43*, 217.

41 Bailey, J.K.; Mecartney, M.L. *Colloids Surf.* **1992**, *63*, 151.

[42] Hansprasopwattana, A.; Srinivasan, S.; Sault, A.G.; Datye. A.K. *Langmuir* **1996**, *12*, 3173.

[43] The particles were washed 3 x centrifugation/redispersion cycles using Milli-Q water. A drop of the dispersion was placed on a grid and then dried under vacuum to remove water. The dried particles were embedded in Spurr's epoxy resin and polymerized at 60°C overnight. Sections of the embedded sample were cut at about 50 nm on a Reichert Ultracut E ultramicrotome using a diamond knife. Transmission electron microscopy images were recorded at the magnification of 80, 000 X on a JEOL 1200 EX electron microscope. The TEMSCAN was equipped with a Noran conventional Be window, Si(Li) X-ray detector and a Noran TN 5502 mult-channel analyzer (Madison, WI). Images were recorded at 64x 64 pixel (1.0 sec/pixel) x 200, 000.

[44] The concentration of free calcium in solution was analysed using a Radiometer ABU 93 autotitrator equipped with a calcium specific electrode (Orion Research). EDTA was used as the titrant. Data acquisition and analysis was carried out using a Radiometer ABU triburette fitted with 5 mL syringes for reagent additions and the software ALIQUOT (R. Pelton McMaster University).

[45] Israelachvili, J. *Intermolecular and Surface Forces*; Academic Press: London, 1992, pp.217.

[46] Fuoss, R.M.; Shedlovsky, Th. *J. Am. Chem. Soc.*, 1949, 71, 1496.

[47] Berne, B.J.; Pecora, R. Dynamic Light Scattering with Appplications to Chemistry, Biology, and Physics; John Wiley & Sons, Inc.; NY, 1976.

[48] (a) Reerink, H.; Overbeek, J.T.G. *Discuss. Faraday Soc.*, 1954, *18*, 74. (b) Ottewill, R.H.; Shaw, J.N. *Discuss. Faraday Soc.*, 1966, *42*, 154.

[49] Overbeek, J.T.G., in "Kinetics of Flocculation", H.R. Kruyt, Ed., p.278. Elsevier, Amsterdam, 1952.

[50] (a) Virden, J.W.; Berg, J.C. *J. Colloid Interface Sci.* 1992, *149*, 528; (b) Einarson, M.B.; Berg, J.C. *J. Colloid Interface Sci.* 1993, *155*, 165.

[51] Milonjic, S.K. *Colloids Surfaces* 1992, *63*, 113.

[52] Hunter, R.J. *Introduction to Modern Colloid Science*; Oxford Science: New York, 1993; pp 289.

[53] (a) Kose, A.; Hachisu, S. *J. Colloid Interface Sci.* 1974, *46*, 460. (b) Pusey, P.N. van Megen, W. *Nature* 1986, *320*, 340. (c) Okubo, T. *Langmuir* 1994, *10*, 1695.

Chapter 3

Colloidal Stability of Stöber Silica in Acetone - Water Mixtures

Abstract

The colloidal stability and electrokinetic properties of Stöber silica dispersed in acetone - water mixtures containing NaI and CaI_2 were investigated. The relative permittivity, ε_r, of the dispersion medium was varied between 21 and 79 by controlling the acetone:water ratio. In the presence of NaI, the coagulation concentrations (c_c) increased from 19.6 to 125 mM as ε_r of the mixtures was raised from 20.7 to 33. However, for $\varepsilon_r > 33$, the particles could not be coagulated using NaI concentrations up to 0.5 M. The silica was sensitive towards CaI_2 additions when $\varepsilon_r < 24.3$ as indicated by the observation of two c_c values at 0.045 and 2.5 mM when ε_r was 20.7. As ε_r was raised from 24.3 to 78, only relatively small changes in the c_c were observed from 3 to 7.5 mM CaI_2, respectively. The experimental c_c results could not be predicted by calculations using classic DLVO theory. Zeta potentials (ζ-potentials) for the silica were between -45 and -50 mV throughout the entire ε_r range using 1.5 mM NaI

solutions. In the absence of salt, the ζ-potentials remained constant at approximately -50 mV when 24.3 < ε_r < 78.5 but increased to -80 mV for ε_r < 24.3. The ζ-potentials using 1 mM CaI_2 solutions remained at about -20 mV from ε_r 78.5 to 33 but changed from -3 mV to +20 mV as ε_r decreased from 24.3 to 20.7. Theoretical ζ-potentials calculated using the single site dissociation model were compared with the experimental data. The model predicted the ζ-potentials should decrease with increasing acetone content (decreasing ε_r). The inability of the theoretical models to predict the colloidal stability of silica in acetone-water mixtures, especially when ε_r > 33, was believed to be due to the presence of a silica gel surface layer which acted as a steric barrier at short-range interparticle distances.

3.1 Introduction

The paint and coating industries are undergoing a conversion from organic to aqueous based - containing delivery systems.[1] In some cases, mixtures of water or polar organic solvents are required. A survey of the literature shows there have been few experimental studies reporting on the surface properties of model colloidal systems (spherical particles having a narrow size distribution) in mixed (e.g. organic + water) solvent systems.[2,3] The need for reliable data using model colloids stabilized by electric charge in polar organic media to interpret their electrokinetic and coagulation properties has recently been emphasized.[4,5]

Stöber silica has been used as a model colloid system in several areas of research (e.g., ceramics, catalysis, colloid stability) since spherical particles can be prepared of various sizes with a narrow size distribution.[6] Previous work in our laboratory has shown that aqueous dispersions of Stöber silica can be solvent - exchanged with acetone and reacted with silanes[7] and polymers[8] to prepare silica stabilized non-aqueous dispersions. An interesting aspect of these transformations was that the colloidal stability was maintained throughout the preparation procedure. In the present work the colloidal stability of unmodified silica was investigated as water was replaced with acetone. This corresponds to the first step in the synthetic transformations previously reported.[7,8]

A comparison of the colloidal stability and electrokinetic properties of Stöber silica in pure acetone with those in water has been reported.[9] The key findings were that in both water and acetone, NaI and Bu_4NI salts were less effective as coagulants than predicted by DLVO theory. For example, the critical coagulation concentration (c_c) observed using NaI acetone solutions was one hundred times greater than that predicted by theory. Also, the particles were observed to be insensitive towards Bu_4NI acetone additions up to 145 mM in acetone. The discrepancy between the experimental results and theory was believed to be due to the presence of a steric barrier on the silica surface consisting of a silicic acid gel network which has been recently proposed by Vigil *et al.*[10] for silica interactions in water. Past interpretation of the electrokinetic and coagulation properties of silica particles in water and mixed solvents has indicated the influence of water[11] (hydration forces) and solvent adsorption effects[2] at the silica / liquid interface. Besides the work of the Israelachvili group[10] there has been few experimental studies supporting the silica gel hypothesis since the work of Tadros and Lyklema.[12]

This paper contains the first report of the properties of colloidal silica in acetone - water mixtures. Experimental electrokinetic and coagulation results are compared with predictions using a single site-dissociation model and classical electrical double layer theory.

3.2 Experimental

Acetone (99.5 wt%, glass distilled, Caledon), *N,N* - dimethylformamide (99.9+%, HPLC grade, Aldrich - Sigma), sodium iodide (99+%, Aldrich), and calcium iodide hydrate, CaI_2•4-6 H_2O (98%, Aldrich) were used as received. All water was obtained from Milli-Q treatment of distilled water.

Silica particles were prepared using the Stöber method as described in Chapter 2-Experimental 2.2. Dynamic light scattering showed the particles had an average diameter of 179 nm in acetone with a standard deviation of the distribution of 10%. The relative permittivities,[13] viscosities,[14] and refractive indices[15] of the acetone - water mixtures used in the present study were obtained from published data at 25°C and are given in Table 3.1. The viscosity of DMF - water mixtures and that for pure DMF at 25°C was taken from the literature.[16]

Water content measurements of the silica dispersions in acetone by Karl Fischer titrations were performed by Galbraith Laboratories, Inc., Knoxville, TN. Analysis of the acetone (in the absence of silica) without further purification showed 0.30% water. For a 0.5 wt% silica dispersion in acetone (aged for 1 week), the analysis showed 0.31% water content.

Table 3.1. Values of the relative permittivity (ε_r),[13] viscosity (η),[14] and refractive indices[15] for compositions of the acetone - water mixtures.

Acetone (wt%)	Relative Permittivity, ε_r	Viscosity (cp), η	Refractive Index
99.7	20.7	0.32	1.355
89.6	24.3	0.45	1.361
74.6	32.9	0.72	1.363
49.8	48.6	1.24	1.360
24.9	64	1.33	1.350
9.9	73.2	1.09	1.340
0	78.5	0.89	1.332

The electrophoretic mobilities of the particles were measured using a Coulter DELSA 440. The details of the experimental procedure have been discussed in Chapter 2-Experimental 2.2. The ζ-potentials for silica in acetone - water mixtures containing NaI were calculated using the computer program Mobility^{c}.[17]

The coagulation experiments were carried out as described in Chapter 2-Experimental 2.2.

The conductivities of the acetone, acetone-water and water electrolyte solutions were obtained at 25°C using a Copenhagen Radiometer CDM 83 meter equipped with a silver glass electrode (Copenhagen, Type CDC 304). The conductivities of the silica dispersions containing salt were measured using the Coulter DELSA microelectrophoresis apparatus at 25°C and the data agreed with those obtained for the salt solutions using the conductivity meter.

3.3 Results

Dissociation of Electrolytes

Conductivity experiments were carried out to probe the extent of salt dissociation in acetone-water mixtures. Conductance values in acetone - water mixtures having 1.5 mM and 1 mM NaI are plotted in Figure 3.1 as a function of ε_r, the relative permittivity. Solvent compositions corresponding to the ε_r values are given in Table 3.1.

The conductivities for the mixtures containing NaI and CaI_2 were lowered with small additions of acetone in the regions between ε_r of 78.5 to 60. For example, in 1.5 mM NaI solutions the conductivities were 0.18 and 0.11 mS cm^{-1} for mixtures having ε_r values 78.5 and 64, respectively. For the mixtures having ε_r values ranging from 60 to 40, the conductivities were about 0.11 mS cm^{-1} for both the CaI_2 and NaI solutions. At high acetone concentrations ($20.7 < \varepsilon_r < 33$) the NaI and CaI_2 solutions behaved differently. The conductivity of NaI in 99.7 wt% acetone was higher than in water whereas the conductivity of CaI_2 was low and not a strong function of acetone composition.

Figure 3.1. Variation of the conductivity, Λ, and the viscosity, η, as a function of the relative permittivity (ε_r) of acetone - water mixtures at 25°C. Plots of the conductivity were obtained using 1.5 mM NaI and 1 mM CaI_2. ε_r values for the mixtures were obtained from the data reported by Åkerlöf.[13] Viscosity data for the acetone - water mixtures were taken from the literature.[14]

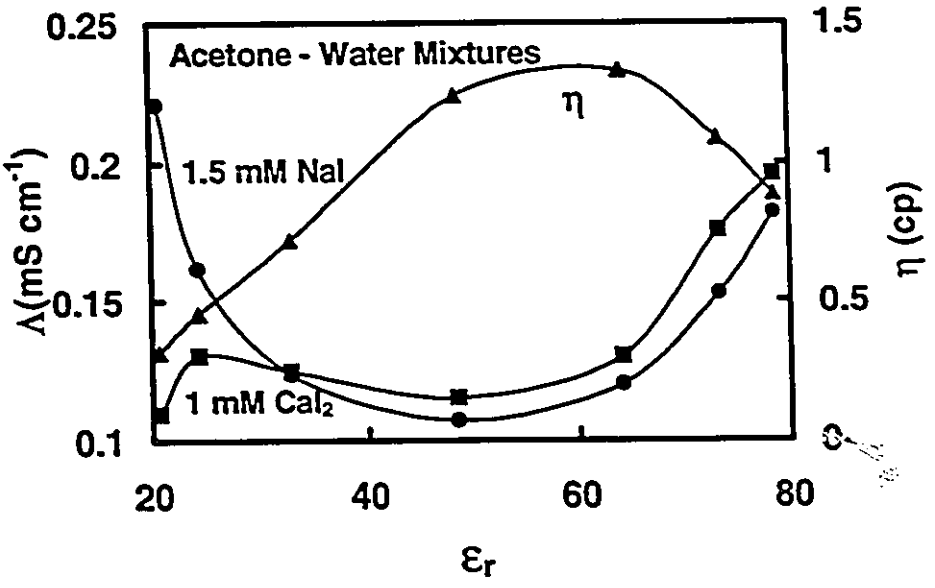

The dissociation of NaI and CaI_2 in 99.7 wt % acetone was examined using conductivity measurements in a previous study.[9] The concentration dependence on the conductivity data for NaI and CaI_2 acetone solutions was found to be typical for the behavior of weak electrolytes. For example, the degree of ion dissociation in acetone changed from 88% to 68% as the NaI concentration was raised from 1.5 to 20 mM. For CaI_2 solutions the degree of

dissociation was low. However, since at least two equilibrium reactions are required to describe the behavior of CaI_2,[18] it is difficult to predict the detailed ionic composition from the conductivity data.

Ionic mobilities reflect the balance of viscous drag and electrostatic forces in a conductivity experiment. The influence of solvent composition on the solution viscosity for the acetone-water mixtures is shown in Figure 3.1. The viscosity curve showed a flat maximum at about 1.3 cp for mixtures near ε_r of 60, and as the relative permittivities of the pure solvents were approached, lower viscosity values were observed. Therefore, the solvent viscosity behavior may be an explanation for the observed NaI conductivity changes shown in Figure 3.1.

Electrophoresis. Plots of the electrophoretic mobilities obtained for silica as a function of ε_r in acetone - water mixtures having 1.5 mM NaI and 1 mM CaI_2 are given in Figure 3.2. Large negative mobility values were observed for all solvent combinations containing 1.5 mM NaI. The smallest mobility values were observed in mixtures having intermediate ε_r values which roughly corresponded to the maxima in the viscosity data, whereas the two highest mobility values were observed in water and 99.7 wt% acetone.

Figure 3.2. Electrophoretic mobilities for silica as a function of the relative permittivities (ε_r) for acetone - water mixtures containing 1.5 mM NaI at 25°C. Viscosity data as a function of ε_r for the mixtures are also plotted.[14]

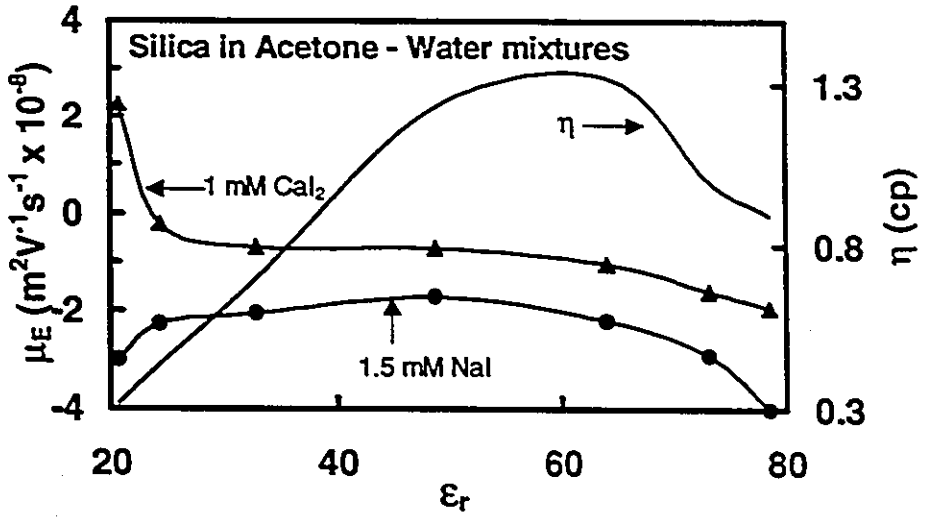

The electrophoretic mobility data for silica as a function of ε_r in the presence of 1 mM CaI_2 are also plotted in Figure 3.2. In acetone (ε_r = 20.7) the mobility value was positive (+2.25 x 10^{-8} m^2 V^{-1} s^{-1}). For the mixtures where ε_r ranged from 24.3 to 73.2 the mobilities were negative and increased from -0.22 x 10^{-8} m^2 V^{-1} s^{-1} to -1.95 x 10^{-8} m^2 V^{-1} s^{-1}. Presumably, the positive mobility reflects the specific adsorption of calcium ions on the silica surface.[9]

A few electrophoresis measurements were also carried out with silica dispersed in DMF - water mixtures containing 1.5 mM NaI to examine the influence of viscosity on the electrophoretic mobilities. Figure 3.3 shows the plot of the viscosity as a function of ε_r for DMF - water mixtures. The parabolic shape of the viscosity plot, where the values change from about 0.8 cp for the pure DMF and water to a maximum of 2.3 cp at intermediate ε_r values, follows a similar trend to that observed for the acetone-water mixtures (Figure 3.2). The high viscosities at intermediate ε_r values for the DMF - water mixtures have been attributed to structured solvated complexes between DMF and water forming $DMF{\cdot}3H_20$.[16]

Also shown in Figure 3.3 are the electrophoretic mobilities for silica dispersed in DMF - water mixtures as a function of ε_r. The lowest mobility values were observed at intermediate ε_r values. Thus, the variation of the electrophoretic mobilities observed for the silica particles in NaI solutions of water - acetone and water - DMF reflect the viscosity behaviour of the solvent mixtures. Similar results have been reported by Baran *et al.*[3 c] for antimony sulfide particles in aqueous organic (alcohols, acetone and dioxane) mixtures.

Figure 3.3. Variation of the electrophoretic mobilities for silica dispersions as a function of the relative permittivities (ε_r) for DMF - water mixtures at 25°C containing 1.5 mM NaI. The ε_r values and viscosities (η) for the mixtures were taken from the literature.[16]

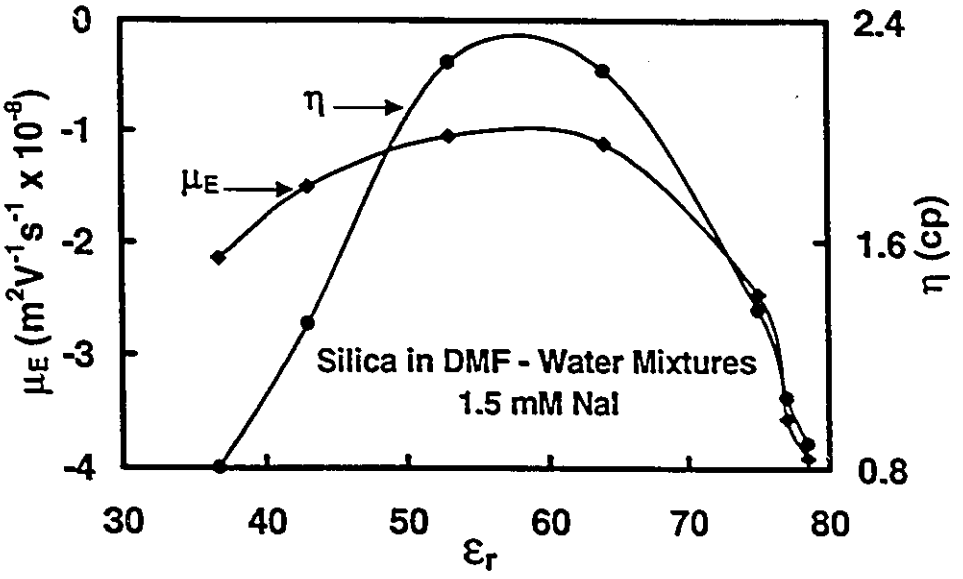

The electrophoretic mobilities obtained for silica in acetone - water mixtures were converted to ζ-potentials using the Smoluchowski equation[19] and the results are plotted in Figure 3.4 as a function of ε_r. The ζ-potential results using 1.5 mM NaI showed that they remained relatively constant at about -55 mV throughout the entire range of the mixtures. ζ-potentials for the 1.5 mM NaI acetone solutions were also calculated using the Mobility© program into account

retardation and relaxation effects.[17] The data plotted in Figure 3.4 from this calculation show a similar trend to that calculated using the Smoluchowski equation. However, the ζ-potentials were about -10 mV higher.

Comparatively, the ζ-potentials for siiica dispersed in 1 mM CaI_2 solutions remained constant between -17 to - 20 mV from ε_r 78.5 to 24.3. When $\varepsilon_r < 24.3$ the ζ-potentials of the silica reversed charge.[9] ζ-potentials were also obtained for silica in acetone - water mixtures containing no salt and the results in Figure 3.4 show that the values remained constant at about -45 mV from ε_r 78.5 to 24.3 but subsequently increased to -85 mV when $\varepsilon_r < 24.3$.

Coagulation Experiments. Relative turbidities for silica in acetone - water mixtures were measured as a function of NaI and CaI_2 concentration to obtain c_c (coagulation concentrations) values as a function of ε_r. τ_R (see Eq. [2.1] in Chapter 2-Experimental 2.2) was obtained from measurements of the percent transmittance of the silica dispersions in the presence of electrolyte. $\tau_R \approx 1$ indicates a colloidally stable dispersion, $\tau_R > 1$ indicates the onset of particle agglomeration, and $\tau_R < 1$ indicates that silica flocs have formed and settled. Coagulation concentration values, c_c, were assigned to electrolyte concentrations corresponding to the point where the flocs settled leaving a clear supernatant as indicated when $\tau_R < 1$.

Figure 3.4. Variation of the ζ-potentials as a function of the relative permittivities (ε_r) for silica in acetone - water mixtures at 25°C. Data was obtained for mixtures containing 1.5 mM NaI and 1 mM CaI_2 (not corrected for ion pair formation), and also for mixtures in the absence of salt. Electrophoretic mobilities were converted to ζ-potentials using the Smoluchowski equation and the Mobility[c] program.[17]

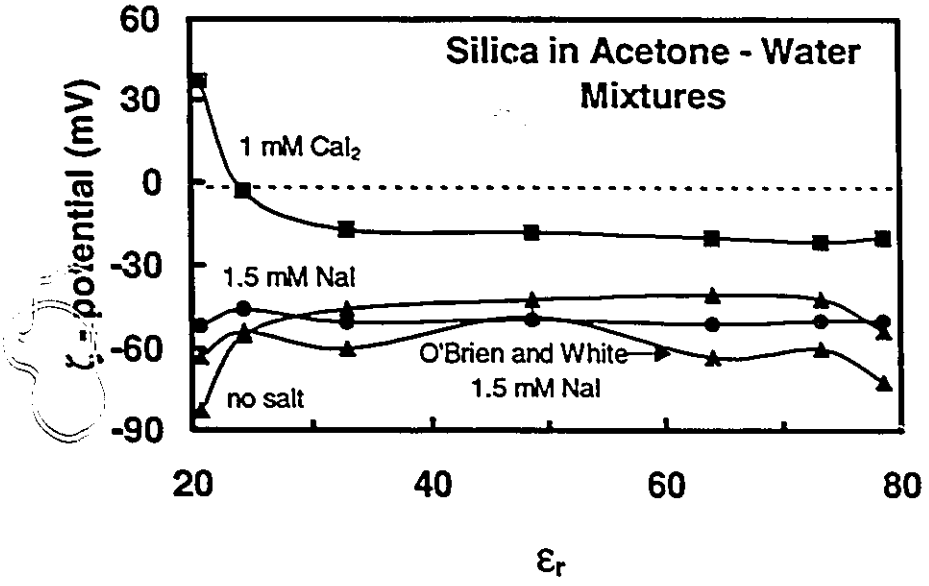

Figure 3.5 shows the c_c values of the silica sols as a function of ε_r using NaI solutions. The c_c's increased linearly from 19.6 to 125 mM NaI as ε_r was changed from 20.7 to 33. For ε_r values greater than 33 the silica sol was insensitive towards coagulant concentrations up to 250 mM. This result was

surprising since the colloidal stability of sols in organic - water mixtures have been shown to be very sensitive towards small ε_r changes.[3] For example, de Rooy *et al.*[3b] showed that the coagulation concentrations for α-FeOOH sols in acetone-water mixtures using $LiNO_3$ were raised from 3.6 to 60 mM as ε_r changed from 20.7 to approximately 50.

Figure 3.6 shows that the c_c results obtained from the relative turbidity experiments using CaI_2 acetone - water solutions. The c_c's gradually decreased from 7.5 to 3 mM using mixtures having ε_r 78.5 and 24.3, respectively. In comparison, the silica sol stability was sensitive towards CaI_2 additions when ε_r was 20.7 as evidenced by the observation of two c_c values, 0.045 and 2.75 mM.[9] The two c_c values were due to the charge reversal of Stöber silica in acetone CaI_2 solutions which led to restabilization of the particles at intermediate concentrations. The specific adsorption of CaI^+ was proposed with no direct evidence.[9]

Figure 3.5. Variation of the coagulation concentrations (c_c) for silica in the presence of NaI as a function of the relative permittivities (ε_r) for the acetone - water mixtures. ε_r values at 25°C for the mixtures were obtained from the data reported by Åkerlöf.[13] The c_c values are not corrected for ion-pair formation except that for ε_r 20.7. The dashed line shows the theoretical predictions calculated from DLVO theory based on Eq. [3.5] assuming a low diffuse layer potential ($\psi_d \approx \zeta$) of -15 mV.

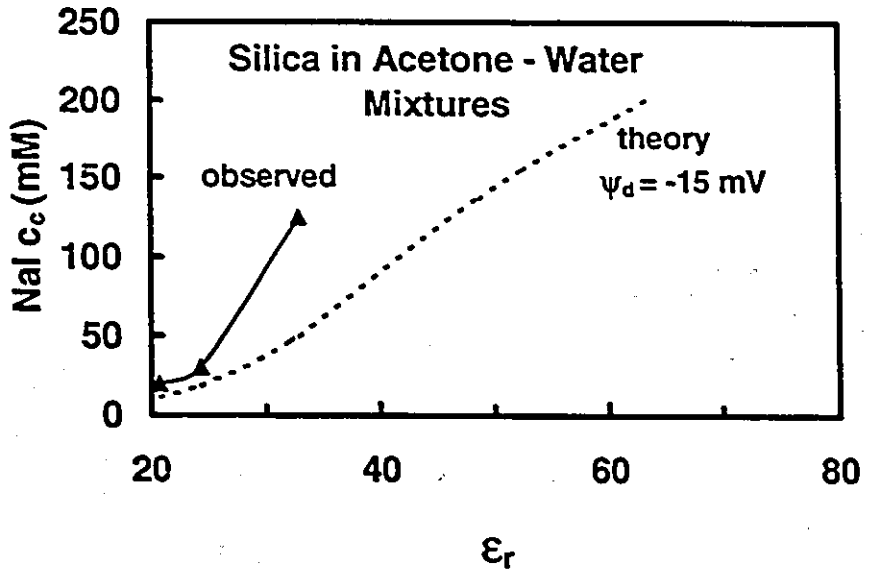

Figure 3.6. Coagulation concentrations (c_c) of silica in the presence of CaI_2 as a function of the relative permittivities (ε_r) for the acetone -water mixtures. ε_r values for the mixtures at 25°C were estimated from the data reported by Åkerlöf.[13] The c_c values are not corrected for ion-pair formation. The dashed line shows theoretical predictions calculated from DLVO theory based on Eq. [3.5] assuming a low diffuse layer potential ($\psi_d \approx \zeta$) of -15 mV.

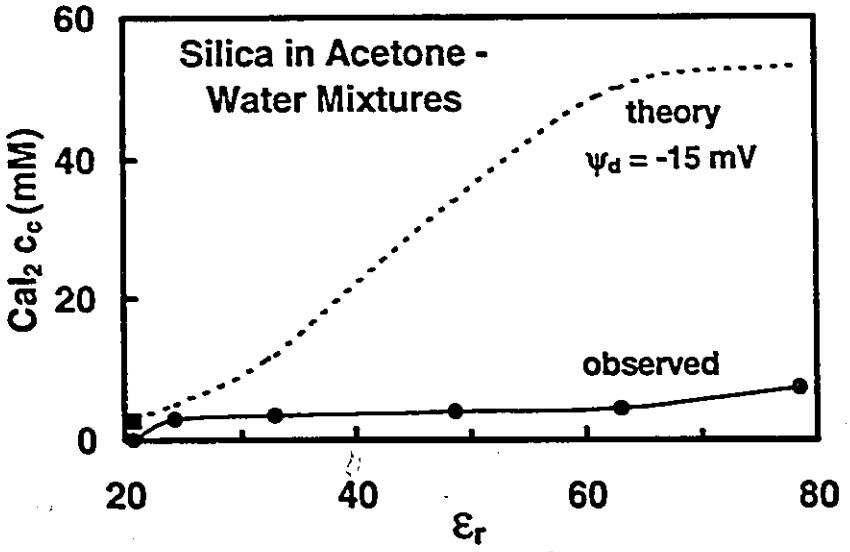

3.4 Discussion

The colloidal stability of Stöber silica dispersed in acetone - water mixtures is easily accessed experimentally. By contrast, fundamental physical parameters, including pH and the pK_a of silanols (Si-OH) could not be measured in organic media. Nevertheless, in the following sections we attempt to use standard models to compare the electrokinetic and coagulation results reported herein. To carry out the analysis, an estimate of the variation of the pK_a of the silanols as a function of ε_r of the acetone - water mixtures is needed in order to model the ζ-potential and coagulation concentration (c_c) values.

Two approaches were used to estimate the pK_a of SiOH as a function of ε_r. First, Nowak *et al.*[20] showed that the pK_a values for 2,6 - dichlorophenol in acetone - water mixtures increased from 8.3 to 11 as ε_r of the mixture decreased from approximately 50 to 20. Since the pK_a of 2,6 - dichlorophenol in water is 6.79, which is the same as that reported for SiOH,[21] the effect of ε_r on the pK_a for 2,6 - dichlorophenol appears to be a useful approximation for the pK_a of SiOH in acetone - water mixtures.[22]

The second approach to determine the effect of ε_r on the pK_a for SiOH was based on the Born equation[23] in which the Gibbs free energy change of transfer

of an ion (1:1 electrolyte) from solvent (s) to water (w) can be described as follows:

$$\Delta G_i = -\frac{1}{2}\left(\frac{z_i^2 e^2 N_A}{4\pi\varepsilon_o r_i}\right)\left(\frac{1}{\varepsilon_S} - \frac{1}{\varepsilon_W}\right) \qquad [3.1]$$

where r_i is the radius of the ion, and ε_S and ε_W represent the relative permittivities of the solvent medium and water, respectively.

From Eq. [3.1] the following expression can be used to relate the dissociation constant to the relative permittivity of the medium.[24]

$$\Delta G_i(diss) = pK_a^{solvent} - pK_a^{water} = 122\left(\frac{1}{\varepsilon_S} - 0.0128\right)\left(\frac{1}{r_{H^+}} - \frac{1}{r_{SiO^-}}\right) \qquad [3.2]$$

where ε_S is the dielectric constant of the medium, r_{H^+} and r_{SiO^-} refer to the hydrated radii for the H_3O^+ and the SiO^- ion respectively.

The pK_a's for SiOH as a function of the ε_r's for the acetone - water mixtures are plotted in Figure 3.7 based on Eq. [3.2] and the pK_a results reported for 2,6 - dichlorophenol in acetone - water mixtures.[20] The pK_a's using Eq. [3.2] were obtained by assuming r_{H^+} = 2.8 Å and r_{SiO^-} = 3.0 Å (radius of a hydrated OH^- ion).

Figure 3.7. Effect of the relative permittivity (ε_r) on the pK_a of silica silanols (SiOH) in acetone-water mixtures (dashed line) computed using the Born energy expression (see Eq.'s [3.1] and [3.2]). For comparison the variation of the pK_a for 2,6 - dichlorcphenol in acetone - water mixtures as determined by Nowak *et al.* are also plotted.[20]

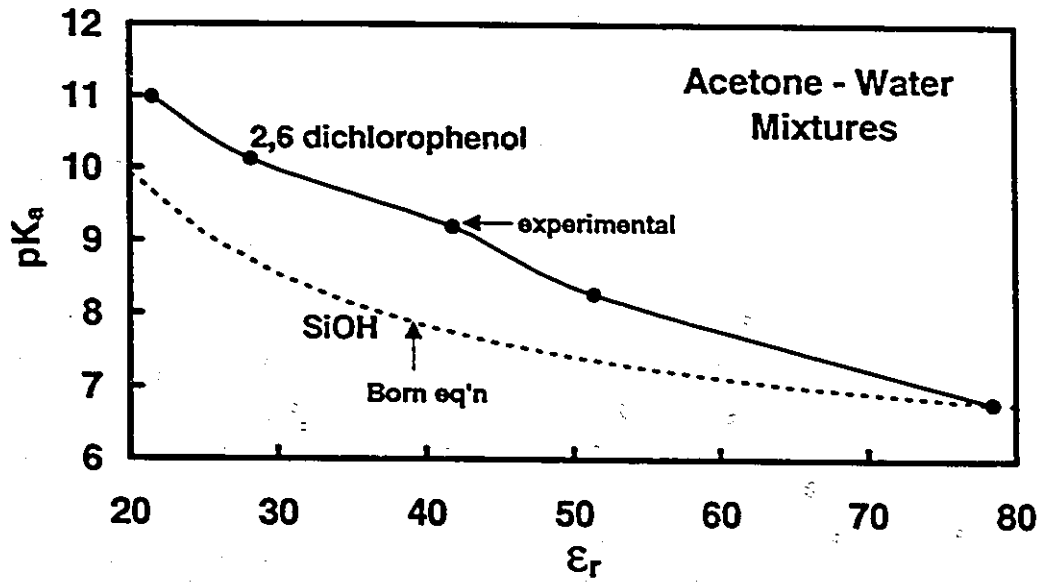

Comparison of the two curves in Figure 3.7 shows that the pK_a's increase as the concentration of acetone in the mixture increases. The Born equation assumes only electrostatic effects are important however non-electrostatic or chemical effects also influence dissociation as the composition of a mixture changes.[24] Therefore, we used the 2,6 - dichlorophenol data from Nowak *et al.*[20] for modeling the ζ-potentials.

The single site-dissociation model as given by Hunter was used to model the electrokinetic properties of the silica dispersions.[25] The following expression can be used to compute the theoretical ζ-potentials:

$$\zeta = 4\frac{a\tanh\left[\tanh\left[\frac{1}{4}\psi_o\frac{e_o}{k_bT}\right]\exp(-\kappa x)\right]}{e_o}k_bT \qquad [3.3]$$

where e_o is the unit of electronic charge, k_b is the Boltzmann constant, x represents the distance between the surface and the plane of shear, κ is the reciprocal Debye length, and ψ_o gives the surface potential as calculated from the Gouy-Chapman theory:

$$\psi_o = 59.8(pK_a - pH) - 59.8\log\left[\frac{\frac{N_S\kappa}{4N_AC}}{\sinh\left(\frac{\psi_o e_o}{2k_bT}\right)} - 1\right] \qquad [3.4]$$

where N_S refers to the total number of ionizable silanol sites and C corresponds to the bulk electrolyte concentration. The pK_a and N_s for silanols in water have been previously reported to be 6.8 and 7.9×10^{14} sites cm^{-2}, respectively.[5,21]

Theoretical ζ-potentials (dashed lines) in Figure 3.8 for silica as a function of ε_r in acetone - water mixtures were obtained by applying the single site - dissociation model (Eq.'s [3.3] and [3.4]) using the pK_a values reported for 2,6 - dichlorophenol in acetone - water mixtures assuming the pH of the solutions was constant at either 7.5 or 8.5. Figure 3.8 shows the model predicts a decrease in the ζ-potentials as ε_r is lowered (increasing acetone composition). Comparatively, the experimental ζ-potentials also shown in Figure 3.8, show little dependence on ε_r of the mixtures. Although the model is simple, more complicated models, such as a site- dissociation site- binding model,[26] would not change the general features of the plot and the conclusions.

The following expression was used to calculate theoretical c_c's assuming low particle surface potentials:[27]

$$c_c = 7.09 \times 10^{-41} \left(\frac{\varepsilon_r^2 \psi_d^4}{A_{12}^2 z^2} \right) \qquad [3.5]$$

where ψ_d is the diffuse layer potential. The ζ-potentials of the silica samples were assumed to be equal to ψ_d.

Figure 3.8. Variation of the theoretical ζ-potentials (dashed curves calculated using Eq.'s [3.3] and [3.4]) and experimental ζ-potentials with the relative permittivities (ε_r) for silica dispersed in acetone - water mixtures containing 1.5 mM NaI. Experimental ζ-potentials were calculated using the Mobility© program.[17] For the theoretical curves, the pK_a values were varied (10.98 to 6.79) as a function of the relative permittivities ($21 < \varepsilon_r < 80$) using the literature pK_a data for 2,6 - dichlorophenol in acetone-water mixtures.[20]

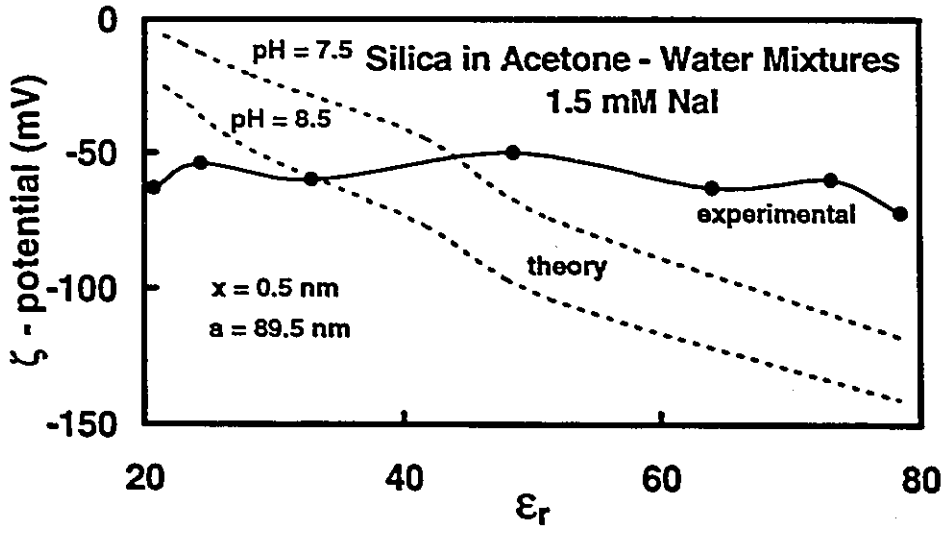

The Hamaker constant for the silica dispersions in acetone - water mixtures can be approximated by:[28]

$$A_{1(2)} = \left(A_{11}^{1/2} - A_{22}^{1/2} \right)^2 \qquad [3.6]$$

where A_{11} and A_{22} represent the Hamaker constants for silica and the acetone - water mixtures, respectively.

The Hamaker constants for acetone - water mixtures, A_{22}, were approximated using the following expression:[29]

$$A_{22} = \frac{3}{4} k_b T \frac{(\varepsilon_r - 1)^2}{(\varepsilon_r + 2)^2} + \frac{3 h \nu_e}{16\sqrt{2}} \frac{\left(n_m^2 - 1 \right)^2}{\left(n_m^2 + 1 \right)^{3/2}} \qquad [3.7]$$

where h is Planck's constant, $\nu_e = 2.9 \times 10^{15}$ s^{-1} corresponds to the absorption frequency, and n_m corresponds to the refractive indices of the mixtures (Table 3.1) which were obtained from published data.[15]

The theoretical c_c curves as a function of ε_r are shown in Figure 3.5 (z=1) and Figure 3.6 (z=2). Assuming a ζ-potential of -15 mV, Eq. [3.5] predicts that increases in the acetone concentration ($\varepsilon_r < 78.5$) should be accompanied by a decrease in the coagulation concentrations of the silica sols in the presence of

NaI and CaI_2. Although the experimental c_c's using NaI (Figure 3.5) decreased as ε_r of the mixture was lowered from 33 to 20.7, the silica was insensitive towards high NaI concentrations when $\varepsilon_r > 33$. Furthermore, the addition of CaI_2 to the acetone - water mixtures (Figure 3.6) only caused small changes in the c_c's from 7.5 to 3 mM as ε_r decreased from 78.5 to 24.3. On this basis, the observed behavior of the silica in acetone - water mixtures when $\varepsilon_r > 33$ did not follow the theoretical predictions assuming only electrostatic forces stabilize the particles.

To account for the discrepancy between the theory and the colloidal stability behavior of silica in water mixtures, a common explanation postulates the presence of a structured water layer several angstroms thick (hydration forces) at the silica / liquid interface.[11,30] In the present study it was believed that if hydration forces were responsible for the enhanced colloidal stability of silica in water, the effect of increasing the acetone composition would dehydrate the water layer. The removal of the water layer by acetone would therefore be expected to make the particles more sensitive towards electrolyte additions. Based on the c_c and ζ-potential experiments it appears that acetone had no effect on the electrical double layer and coagulation properties of silica dispersed in mixtures where $33 < \varepsilon_r < 78.5$.

An alternative explanation is the presence of a thin gel layer on the surface which could act as a steric barrier (See Appendix A3.1 for further details). Convincing evidence for this was recently published by the Vigil *et al.*.[10] If the presence of a steric layer is accepted, the present results show under the conditions under which the steric layer collapses (See Appendix A3.2). That is, when silica is exposed to mixtures having high acetone concentrations ($\varepsilon_r < 33$). Comparison between theory and experiment for the coagulation (Figure 3.5 and Figure 3.6) and electrokinetic (Figure 3.4 and Figure 3.8) data shows that simple DLVO behavior may be obeyed at ε_r values less than 24. For silica dispersed in acetone - water mixtures where $\varepsilon_r < 24$, we speculate that steric interactions are not significant. Future attempts to directly measure force distance curves between silica surfaces in aqueous acetone mixtures may clarify the observed colloidal stability behavior.

3.5 Conclusion

(1) Contrary to single site - dissociation model predictions, the ζ-potentials of Stöber silica in dilute NaI, were nearly independent of the ratio of acetone to water when ε_r of the mixtures ranged from 33 to 78.5.

(2) In 99.7 wt% acetone, silica displayed two coagulation concentrations reflecting the transition from a negative to a positively charged sol. By contrast, the coagulation concentration values for CaI_2 was nearly independent of solvent composition for the acetone-water mixtures.

(3) The concentration of NaI required for coagulation of the silica particles throughout most of the range of acetone - water mixtures was much greater than predictions from classical electrical double layer theory. This was explained by the presence of a silica gel layer on the particle surface which acted as a steric barrier. However, it was proposed that the steric layer collapsed when the acetone content was greater than 90 wt%.

Appendix A3.1

Figure A3.1-1. Influence of dielectric constant, ε_r, from acetone-water mixtures on the hydrodynamic diameter (nm) of colloidal silica as measured by dynamic light scattering. Error bars represent the standard deviation of the mean distribution. Particle diameters were obtained by the cumulant method using the linear moments analysis. For each mixture, data was collected over a period of three days to confirm the colloidal stability and reproducibility of the results. On average, at least 20 data collections were obtained for each sample.

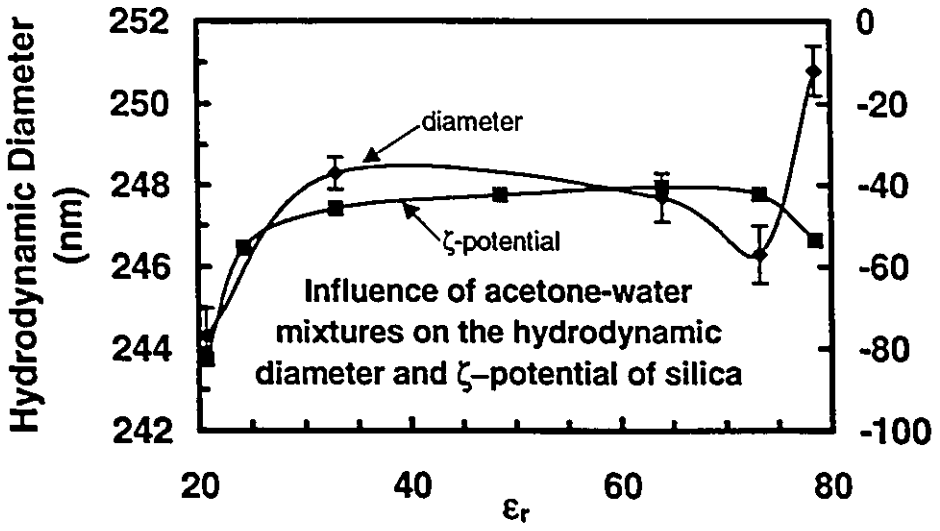

The plot in Figure A3.1-1 shows the hydrodynamic particle diameters were 246.3 ± 0.7 nm, 247.7 ± 0.6 nm, and 248.3 ± 0.4 nm for ε_r values of 73.2, 64, and 32.9, respectively. Hence, the hydrodynamic diameters did not change by more

than 1 nm within the ε_r range of 73.2 to 32.9. By contrast, the hydrodynamic particle diameter in acetone (ε_r 20.7) was determined to be 244.3 ± 0.7 nm. This represents a decrease of 4 nm as the ε_r of the medium was changed from 32.9 to 20.7. Evidence has been given by swelling and surface force measurements for "wet" silica surfaces that there exists a dynamic 1 - 2 nm thick silica gel layer on the surface.[10] The magnitude of the hydrodynamic particle diameter change in Figure A3.1-1 (~ 4 nm from ε_r 32.9 to 20.7) may also reflect the collapse of the silica gel layer. The higher value obtained by the light scattering measurements, compared to the published data, was expected since the hydrodynamic diameter also takes into account the thickness of a thin solvent sheath intimately associated with the particle surface.

Figure A3.1-2 shows the hydrodynamic particle diameter changes as a function of κa using aqueous NaI the electrolyte solution. The most significant particle size change occurred when κa ranged from 5.4 to 8.5 where the particle diameter decreased by 2.6 nm ± 0.5 nm. The magnitude of this change may reflect the collapse of the gel layer on the silica surface due to neutralization of the silicic acid groups (*c.f.*, charge-charge repulsion results in swelling) occupying the gel layer.

Figure A3.1-2 Influence of aqueous NaI salt concentrations on the hydrodynamic particle diameters for Stöber silica in water at pH=7.5.

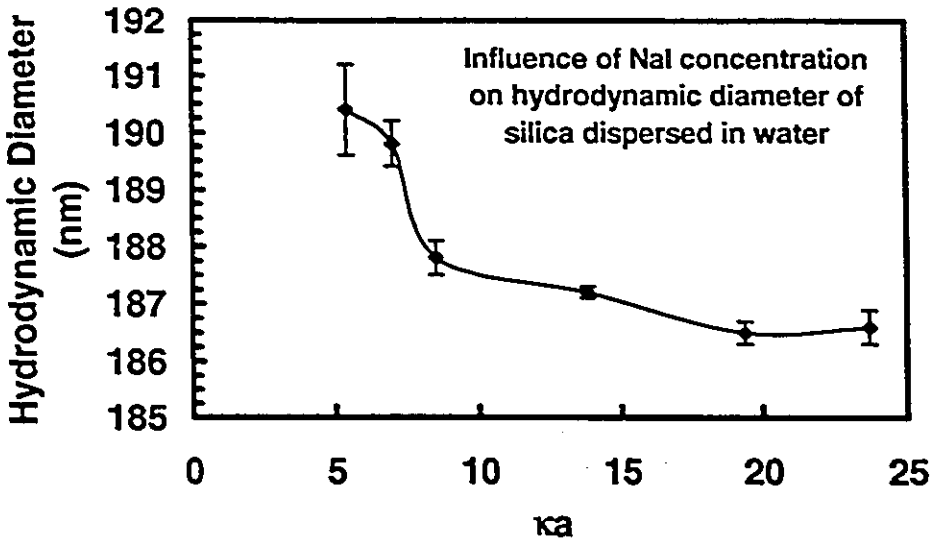

Another factor which could also cause the particle diameter changes shown in figure A3.1-2 is the primary electroviscous effect. Electroviscous effects affect the hydrodynamic behavior of colloidal suspensions.[31] The primary electroviscous effect is the result the distortion of the electrical double layers around the particles caused by shear stresses. This phenomenon causes an increase in the viscous drag forces on the particle, hence the viscosity of the suspension increases. It has been shown that the primary electroviscous effect is proportional to the square of the particle volume fraction. If the primary electroviscous effect was important, the viscosity used to calculate the diffusion coefficient would be incorrect and the particle diameter would be wrong. In our

experiments, the Debye length, κ^{-1}, was chosen to be much smaller (ranged from 17.6 nm to 11.0 nm for κa of 5.4 to 8.5, respectively) than the particle size and therefore the primary electroviscous effect should be negligible.[32]

Changes in the hydrodynamic diameters as a function of salt concentration may also reflect the reduction of the electrical double layer length (i.e., κ^{-1}). Hence we cannot rule out that the size change observed in Figure A3.1-2 may be the result of a changes in κ^{-1}. More advanced techniques such as surface force measurements would be needed to clarify this issue.

Appendix A3.2

Figure A3.2-1 Cartoon of silica gel layer on silica surface. (a) Silica gel layer exposed to water or acetone-water mixtures ($\varepsilon_r > 24.3$). In this case the medium acts as a good solvent and the silica gel is swollen. A repulsive steric force would be expected at short-range interparticle distances. (b) In acetone water mixtures where $\varepsilon_r < 24.3$, the silica gel collapses. Under these conditions, the electrostatic force is expected to dominate over the steric force.

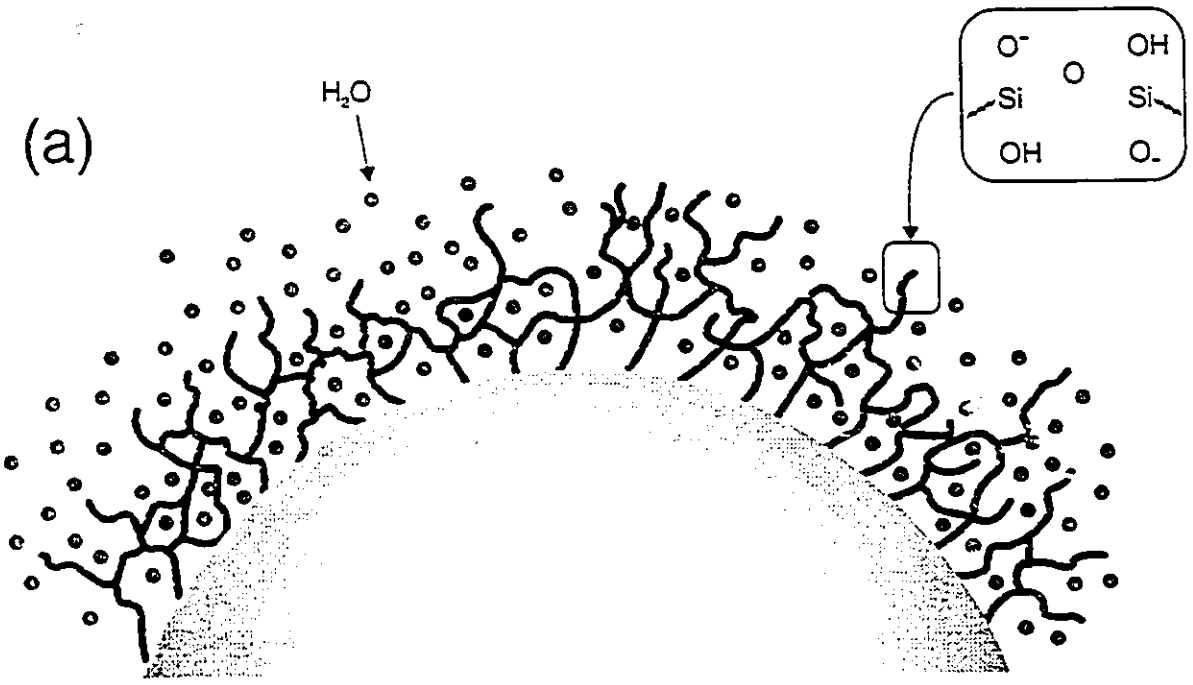

Silica-Water
Interface

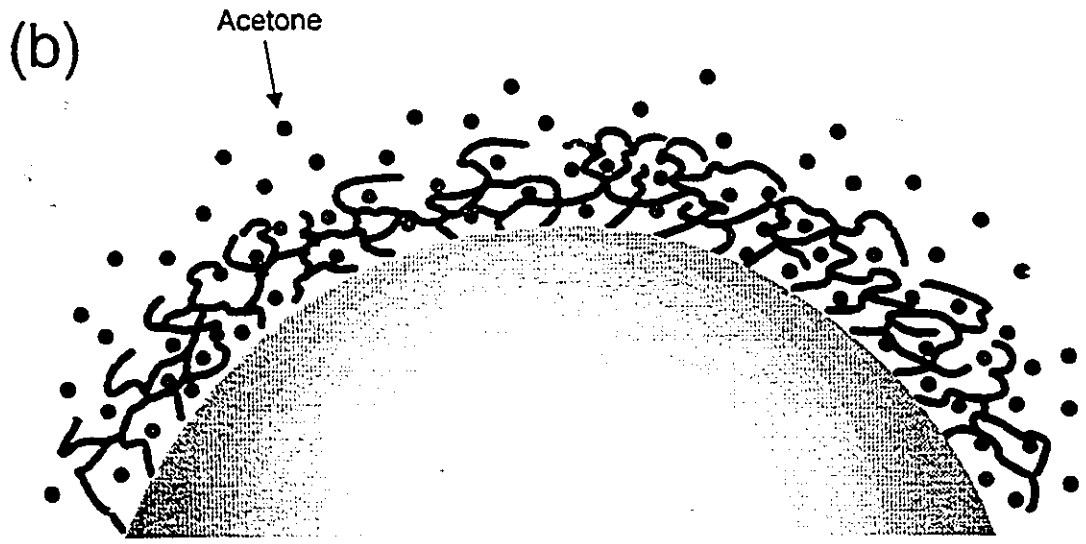

Silica-Acetone/Water
Interface

3.6 References

[1] Wicks, Z.W., Jones, F.N., and Pappas, S.P. *Organic Coatings: Science and Technology - Vol. 2*; Wiley: New York, 1994.

[2] See Kosmulski, M. *Colloids Surf.* **1995**, *95*, 81 for a review on the surface properties of inorganic oxide particles dispersed in mixed polar media.

[3] For earlier work on colloid stabilization in polar media see (a) Kitahara, A. *Adv. Colloid Interface Sci.* **1992**, *38*, 1. (b) de Rooy, N.; de Bruyn, P.L.; Overbeek, J. T. G. *J Colloid Interface Sci.* **1980**, *75*, 542. (c) Baran, A.A.; Chekhovaya, I.N.; Vdovenko, L.I.; Korsunskaya, A.I. *Kolloidn. Zh.* **1976**, *39*, 419. (d) Baran, A.A.; Chekhovaya, I.N. *Kolloidn. Zh.* **1976**, *39*, 426. (e) Vincent, B.; Bijsterbosch, B.H.; Lyklema, J. *J Colloid Interface Sci.* **1971**, *37*, 171. (f) Kratohvil, J.P.; Orhanovic, M.; Matijevic, E. *J. Phys. Chem.* **1960**, *64*, 1216 and references cited therein. (g) Mackor, E.L. *Recueil* **1951**, *70*, 841. (h) Verwey, E.J. *Rec. Trav. Chim.* **1941**, *60*, 625. (i) Weiser, H.B.; Mack, G.L. *J. Phys. Chem.* **1930**, *34*, 101.

[4] Kosmulski, M.; Matijevic, E. *Langmuir* **1991**, *7*, 2066.

[5] Kosmulski, M.; Matijevic, E. *Langmuir* **1992**, *8*, 1060.

[6] Stöber, W.; Fink, A.; Bohn, E. *J. Colloid Interface Sci.* **1968**, *26*, 62.

[7] Ketelson, H.A.; Brook, M.A.; Pelton, R. *Chem. Mater.* **1995**, *7*, 1376.

[8] Ketelson, H.A.; Brook, M.A.; Pelton, R. *Polym. Adv. Tech.* **1995**, *6*, 335.

[9] Ketelson, H.A.; Pelton, R.; Brook, M.A. *Langmuir*, **1996**, *12*, 1134.

[10] Vigil, G.; Zhenghe, X.; Steinberg, S.; and Israelachvili, J. *J. Colloid Interface Sci.* **1994**, *165*, 367.

[11] Allen, L.H.; Matijevic, E. *J. Colloid Interface Sci.* **1969**, *31*, 287.

[12] Tadros, Th.F.; Lyklema, J. *J. Electroanal. Chem.* **1968**, *17*, 267.

[13] Åkerlöf, G.; *J. Am. Chem. Soc.* **1932**, *54*, 4125.

[14] *International Critical Tables of Numerical data, Physics, Chemistry and Technology (Volume VII)*, E.W. Washburn,. Ed: McGraw-Hill: New York, 1930, pp 21.

[15] *International Critical Tables of Numerical data, Physics, Chemistry and Technology (Volume VII)*, E.W. Washburn,. Ed: McGraw-Hill: New York, 1930, pp 68.

[16] Bahadur, L.; Ramanamurti, M.V. *Can. J. Chem.* **1984**, *62*, 1051.

[17] White, L.R.; Mangelsdorf, C.S.; Chan, D. Y. *Mobility*© computer program, Department of Mathematics, University of Melbourne, 1989. See O'Brien, R.W.; White L.R. *J. Chem. Soc., Faraday Trans.* 2 **1978**, *74*, 1607.

[18] Robinson, R.A.; Stokes, R.H. *Electrolyte Solutions*; Butterworths Scientific: London, 1959, pp 392.

[19] Hunter, R.J. *Introduction to Modern Colloid Science*; Oxford University Press: New York, 1993, pp 239.

[20] Nowak, B.; Pawlak, Z. *J. Chem. Soc., Faraday Trans. 1* 1982, *78*, 2693.

[21] Schindler, P.; Kamber, H.R. *Helv. Chim. Acta* **1968**, *51*, 1781.

[22] It is important to note that the pK_a's for 2,6 dichlorophenol in acetone - water mixtures (reference 21) were obtained up to ε_r 21.5 (94 wt% acetone). We have applied the single site - dissociation model (see reference 9) for silica where ε_r is 21 (99.7 wt% acetone) and found the best fit for the ζ-potentials using $\Delta pH \approx 2$ which corresponds to pKa's of 10-12 using pH values of 8.5-9. pK_a values ≈ 12 have been assumed to represent the dissociation of SiOH where ε_r is 21 for the model calculations in the present paper. Studies (see reference 25) have shown, however, that the pK_a's of alcohols can be very sensitive towards traces of water as observed by their significant increase in mixtures containing high organic concentrations.

[23] Born, M. *Z. Physik* **1920**, *1*, *45*, 221.

[24] (a) Sager, E.E.; Robinson, R.A.; Bates, R.G.,*J. Res. Natl Bur. Stand., Sect. A* **1964**, *68*, 305. (b) Bates, R. G. in *Hydrogen-Bonded Solvent Systems*, (A.K. Covington, and P. Jones, Ed.); Taylor & Francis: London, 1968, pp 54-55..

[25] Hunter, R.J. *Zeta Potential in Colloid Science*; Academic Press: London, 1981, pp 270.

[26] Yates, D.E.; Levine, S.; Healy, T.W. *J. Chem. Soc., Faraday Trans. 1* **1974**, *70*, 1807.

[27] Hunter, R.J. *Zeta Potential in Colloid Science*; Academic Press: London, 1981, pp 240.

[28] Israelachvili, J. *Intermolecular and Surface Forces*; Academic Press: London, 1992, pp 200.

[29] van der Hoeven, Ph.C.; Lyklema, J. *Adv. Colloid Interface Sci.* **1992**, *42*, 205.

[30] (a) Vold, M.J. *J. Colloid Sci.* **1961**, *16*, 1. (b) Grabbe, A.; Horn, R.G. *J. Colloid Interface Sci.* **1993**, *157*, 375. (c) Meagher, L. *J. Colloid Interface Sci.* **1992**, *152*, 293. (d) Ducker, W.A.; Senden, T.J.; Pashley, R.M. *Nature* **1991**, *353*, 239. (e) Elimelech, M. *J. Chem. Soc. Faraday Trans.* **1990**, *86*, 1623. (f) Horn, R.G.; Smith, D.T.; Haller, W. *Chem. Phys. Lett.* **1989**, *162*, 404.

[31] Van de Ven, T.G.M. *Colloidal Hydrodynamics*; Academic Press: London, 1989.

[32] Honig, E.P.; Punt, W.F.J.; Offermans, P.H.G. *J. Colloid Interface Sci.* **1990**, *134*, 169.

PART II

Chemical Transformations at the Silica Interface:

Preparation and Surface Properties

Chapter 4

Colloidal Silica Bearing Hydrosilane Groups

Abstract

Stöber silica was functionalized with three silyl coupling agents: triethoxysilane (TES), dimethylethoxysilane (DMES) and vinyltrimethoxysilane (VTM). Microelectrophoresis, dynamic light scattering, and elemental analysis were used to study the degree of interaction between the silyl coupling agents and the silica surface. Small changes in the electrophoretic mobilities and particle diameters between the unmodified (Si-OH) and DMES silica (Si-DMES) indicated that Si-DMES coupled to the surface through a single point of attachment. In contrast, the surface coupling reaction with TES (Si-TES) led to multilayered, oligomeric species bound to the surface. The mobilities for Si-OH and Si-TES in acetone decreased from -4.77 x 10^{-8} to -3.87 x 10^{-8} m^2 V^{-1} s^{-1} and the particle diameter of Si-TES was 13 nm larger than the bare silica. Although VTM has three alkoxy groups capable forming large oligomeric species, the mobility of the VTM modified silica (Si-VTM) decreased to only -4.41 x 10^{-8} m^2 V^{-1} and the particle diameter increased by only 4 nm. The surface reaction with VTM showed that the nature of the functional group

on the silyl coupling agent played an important role in determining the reactivity of alkoxy groups with the silica surface. Using the Pt-catalyzed hydrosilation reaction, Si-TES was reacted with vinylnaphthalene (Si-TES-VN), styrene (Si-TES-ST), and vinyl-terminated polydimethylsiloxanes (Si-TES-PDMS). These reactions demonstrated that Stöber silica modified with TES can lead to a variety of colloidally stable model dispersions in solvents varying in polarity from water to hexane. The modified silica systems were characterized by ^{13}C and ^{29}Si solid-state NMR, diffuse reflectance infra-red spectroscopy (DRIFTS), elemental analysis, transmission electron microscopy, fluorescence and UV-Vis absorption spectroscopy.

4.1 Introduction

The study of colloidal materials is motivated by the remarkably interesting properties that they possess. It is further driven by the wide variety of industrial applications which exploit these species in fields including sol-gel science, adhesion and lubrication technology, chromatography, colloid science and catalysis.[1] In order to better understand these materials, there remains the need for well-defined model colloidal systems. It would be of particular interest to develop model systems which are colloidally stable in a variety of solvents of differing polarity and whose stability could originate from electrostatic, steric or electrosteric forces.

The ideal model colloid would be: monodisperse; have a regular surface with functional groups that can be freely interconverted between charged and non-polar species; have a surface to which other moieties can be attached; have a core with no, or at least known, porosity; and be readily prepared and modified. There are very few chemical systems that can satisfy all of these requirements. We have begun a general exploration of the use of silica particles in this context because they possess many of the necessary properties.

One well-studied colloidal system, which has found widespread use as a model system in several areas, is silica prepared by the Stöber process.[2] The silica synthesis involves the ammonia catalyzed hydrolysis and condensation of tetraethyl

orthosilicate (TEOS). There are several characteristic features of this process: (i) the particles can conveniently be grown to diameters in the colloidal range between 20 nm to 1 μm,[3] (ii) colloidally stable spherical particles having a narrow size distribution can be readily prepared for particle diameters greater than 50 nm, (iii) the silica particles are non-porous, and, iv) the surface properties of the particles can be chemically modified.[4]

Stöber silica prepared in the manner just described is electrostatically stabilized by the electrical double layer formed from the ionization of silanol groups, a process facilitated by the presence of the aqueous NH_3 mixture.[4] A series of centrifugation / redispersion cycles allows one to change the solvent while maintaining colloidal stability, providing that the permittivity of the continuous medium is sufficiently high.[5]

For investigations in non-polar media, colloidal particles are usually stabilized with polymers.[6] Although many techniques have been developed to prepare sterically stabilized dispersions, problems such as; swelling of the polymer lattices, irreproducibility in the synthesis, particularly if the process involves dry stages,[7] and controlling the nature of the polymer attachment at the liquid/solid interface have been encountered.[8]

In the case of silica, problems associated with the particle core, such as swelling, do not arise. The modification of the surface is facilitated by the presence of reactive silanol groups. One approach towards mineral surface modification, developed to permit the use of mineral fillers in polymers, utilizes the strength of the Si-O bond. Organosilanes ($RSi(OR')_3$, coupling agents) are grafted to the mineral rendering the inorganic surface much more hydrophobic (Si-OSiR', Scheme 4.1).[9] Examples of this approach have already been reported for Stöber silica. For example, condensation reactions between colloidal silica and conventional alkoxy bearing silane coupling agents having aminopropyl (Silica-O-$SiCH_2CH_2CH_2NH_2$), mercaptopropyl (Silica-O-$SiCH_2CH_2CH_2SH$), chloropropyl (Silica-O-$SiCH_2CH_2CH_2Cl$) or methacryloxypropyl (Silica-O-$SiCH_2CH_2CH_2OCO$-$CH(Me)=CH_2$) functionalities have been described.[5,10] Stöber silica has also been coated with fluorescent dyes.[11,12]

There are several other methods by which polymers can be grafted onto a particle surface. As one example, the coupling process just described has been utilized to attach radical initiators to the surface. Upon radical initiation in the presence of a reactive monomer, steric groups are attached to the surface.[13] Poly(stearic acid), poly(isobutene) derivatives[14] and hydroxy-terminated poly(dimethylsiloxanes) (PDMS) have been grafted to the surfaces of the particles using condensation reactions.[7,15] Finally, vinyl and methacrylate modified silica spheres have been used to carry out the radical grafting of PMMA onto particle

surfaces or the attachment of a hydrosilane terminated silicone ($HMe_2Si(OSiMe_2)_nOSiMe_2H$) through a hydrosilation reaction.[16]

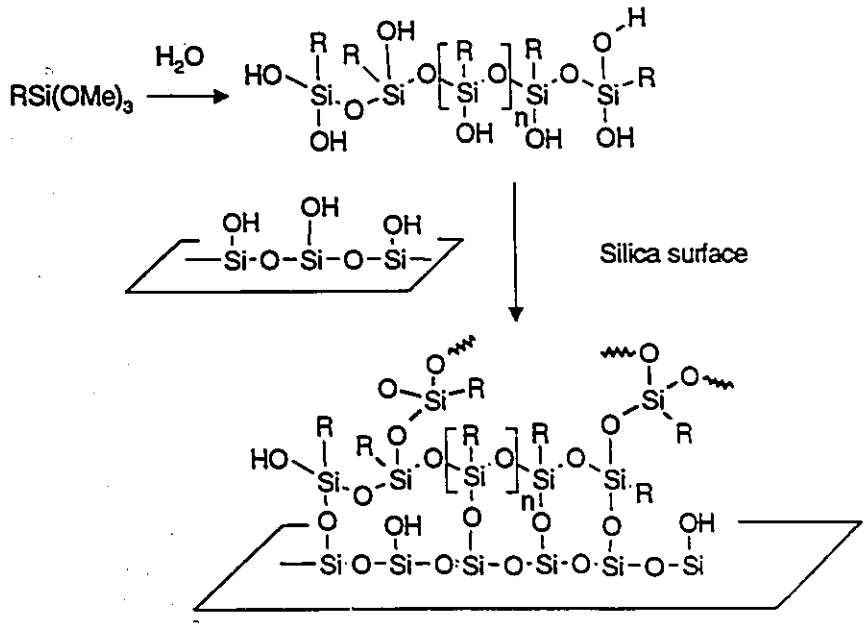

Scheme 4.1. Reaction of trialkoxysilane with silica under aqueous conditions.

Preparing a model colloidal system requires a generic, surface functional group that will allow the attachment of a wide variety of groups under ionic, transition metal-catalyzed or radical conditions.[17] None of the systems described above is generic in this sense. Hydrosilane functionalities (Si-H), however, are remarkably versatile in that they serve as convenient precursors for the introduction of organic moieties under a wide range of conditions, taking advantage of the relatively weak Si-H bond (Scheme 4.2).[17]

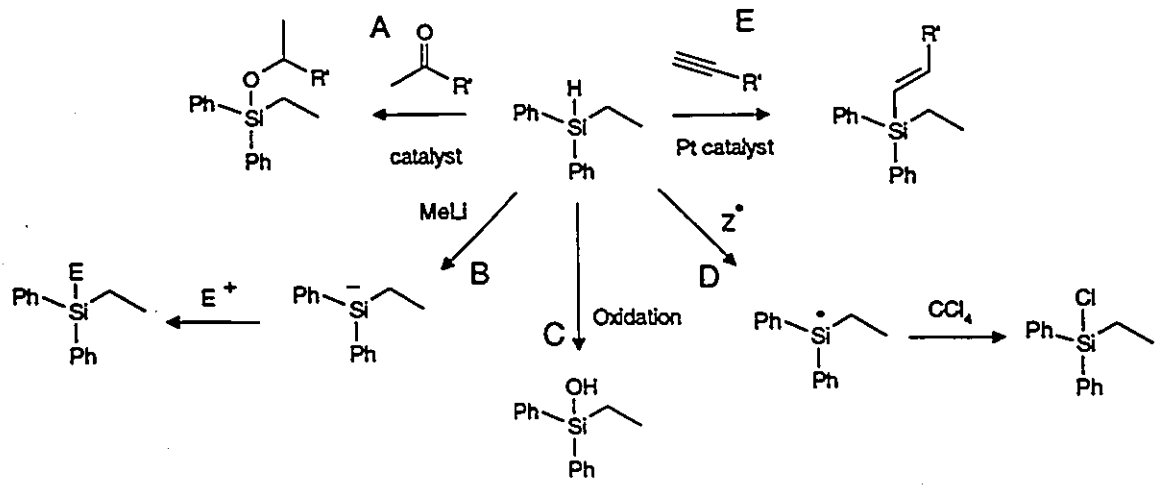

Scheme 4.2. Some examples of reactions using hydrosilanes; A: Carbonyl reduction; B: Nucleophilic addition; C: Oxidation; D: Free-radical; E: Hydrosilation.

Given the beneficial properties of silica already alluded to, we were interested in determining if Si-H modification of the silica surface would provide a general route to well-defined colloidal systems that could be readily modified in analogy to the reactions shown in Scheme 4.2. Although the modification of Stöber silica with Si-H groups has not been reported in the literature, there are a few studies which have attached Si-H groups to high surface area porous silica for applications in biomaterials,[18] chromatography[19] and catalysis.[20]

Our exploration to date of the use of hydrosilanes as surface functional groups for model colloidal systems is given below. We have examined the preparation of silica particles modified with Si-H groups derived from triethoxysilane and

dimethylethoxysilane, characterized the materials spectroscopically and physically, and used them in the preparation of derivatized materials through the hydrosilation reaction.

4.2 Experimental Section

Instrumentation and Analytical Procedures.

Solid-state ^{13}C and ^{29}Si Nuclear Magnetic Resonance Spectroscopy: A Bruker MSL-100 spectrometer operating at 25.2 MHz for carbon was used to obtain ^{13}C cross polarization (CP) / magic angle spinning (MAS) solid state spectra. Direct polarization ^{29}Si spectra were obtained using a Bruker AM 500 spectrometer equipped with a solid state accessory operating at 99.3 MHz for silicon. Adamantane was used as the internal reference in the ^{13}C CP-MAS experiments, $SiMe_4$ was used as an internal standard for ^{29}Si NMR MAS experiments. The MAS spectra were run with long delay times (18 s) to allow essentially complete relaxation of the T and Q units.

Electron microscopy, dynamic light scattering (DLS), and microelectrophoresis were carried out as described in Chapter 2-Experimental 2.2.

Diffuse reflectance FTIR (DRIFTS): DRIFTS spectra were recorded on a Nicolet 20DX spectrometer using a Spectra Tech diffuse reflectance accessory. All spectra were measured from approximately 4000 to 400 cm^{-1} and the number of scans was typically 100 with a resolution of 4 cm^{-1}. The samples were analyzed after; washing

with absolute ethanol and acetone, respectively, followed by precipitation of the particles in diethyl ether and drying in a vacuum oven at 60 °C / 0.01 mmHg for 24 hours. All samples were run neat and fine KBr (FTIR grade, Aldrich) was used as the background file. The solids were approximately 2 mm deep in the sample (cup) holder.

UV-VIS spectroscopy. The UV-VIS spectra were recorded using using a Hewlett Packard 8452A UV/VIS Diode Array Spectrophotometer at 25°C equipped with a quartz cuvette.

Elemental analyses: Combustion analyses (C, H, N and Si) of the unmodified and modified silica products were performed by Guelph Chemical Laboratories Ltd., Guelph, Ontario, Canada.

General Procedures.

The glassware used for the silica synthesis and surface modifications was cleaned by rinsing several times with acetone, followed by a 2% HF solution and finally with several rinses using Milli Q water once again to remove traces of HF. The glassware was subsequently dried and stored in a vaccum oven for 24 hours before each use. A Lauda Series RMS-6 Refrigerating Circulator bath was used to control reaction temperatures. A Beckman L7-55 Ultra Centrifuge with a type 60Ti

rotor operating at 3500 rpm and at 25°C was used to carry out all the sedimentation / redispersion cycles on the unmodified and modified silica samples.

Materials.

A 2.0 M NH_3 in ethanol solution (Aldrich), toluene (Caledon, reagent grade), carbon tetrachloride (BDH, reagent grade), chloroform (BDH, reagent grade), diethyl ether (BDH, reagent grade), hexane (Fisher Scientific, HPLC grade), acetone (Caledon, dried (95.5 wt%) and glass distilled), potassium iodide (Aldrich, 99%), sodium thiosulfate, volumetric standard solution in water (Aldrich, 0.0998N), *N*-bromosuccinimide (Aldrich, 99%), vinyl-terminated poly(dimethylsiloxane) (PDMS-Vi, United Chemicals, Mw=62 700), Karstedt's Pt catalyst[21] (2-3 wt% Pt concentration in xylene, $[(Pt)_2(H_2C{=}CH\text{-}SiMe_2OSiMe_2CH{=}CH_2)_4]$, United Chemicals), and 2-vinylnaphthalene (Aldrich, 98%) were used as received. Tetraethyl orthosilicate (TEOS, Aldrich, 99.999+%), triethoxysilane (TES) (Aldrich, 95%), dimethylethoxysilane (DMES) (United Chemical Technologies, 98%), and vinyltrimethoxysilane (VTM) (Aldrich, 98%) were distilled prior to use.

Syntheses.

Stöber Silica Si-OH

For the preparation of Stöber Silica Si-OH see Chapter 2-Experimental 2.2.

$HSi(OEt)_3$ Modified Silica Si-TES

To a clean and colloidally stable acetone/silica dispersion containing 0.5 g solid / 200 mL solvent was added TES (1.4 mL, 7.5 mmol). The mixture was stirred under reflux and a stream of nitrogen under positive pressure for 36 h. The silica Si-TES was subsequently cleaned free of unreacted silane coupling agent using centrifugation/redispersion cycles, 5 x acetone.

IR (DRIFTS) ν:Si-H 2251 cm^{-1} v strong; this peak was not observed in Si-OH. This peak is found at 2225 cm^{-1} in TES. (see Chapter 6 for a more complete characterization of Si-TES).

HMe_2SiOEt Modified silica Si-DMES

As above, but with DMES (1.0 mL, 7.5 mmol).

IR (DRIFTS) ν: Si-H 2147 cm^{-1} v strong; this peak was not observed in Si-OH. This peak is found at 2147 cm^{-1} in DMES.

Oxidative titration

The procedure of Harzdorf was used to determine the number of Si-H groups attached to the TES- or DMES-modified silica surface Si-TES and Si-DMES,

respectively.[23] A general description follows: the modified particles (at least 0.5 g) were introduced into a 250 mL flask followed by carbon tetrachloride (25 mL) and a freshly prepared *N*-bromosuccinimide solution (15 mL, 0.1M in acetic acid, 1.5 mmol). The mixture was sonicated at room temperature for 30 min. Immediately following this period, KI (2 g, 12 mmol) dissolved in water (50 mL) was added to the dispersion giving a reddish brown color. Titration with 0.0998 N sodium thiosulphate led to a violet color which became a clear, colorless solution at the endpoint. Blank titrations were done in the same manner except that the solids were excluded from the titration vessel and the mixture was not left to stand for 30 min. Two blanks were titrated for each analysis of a modified silica sample. The concentration of Si-H surface groups was determined from the difference in volumes of $Na_2S_2O_3$ needed to obtain the end point between the blank and silica compounds. See Table 4.1.

H_2C=CHSi(OMe)$_3$ (VTM) Modified silica Si-VTM

As above, but with H_2C=$CHMe_2SiOEt$ (1.0 mL, 7.5 mmol).

^{13}C NMR (CP-MAS) δ 137.14, 128.16, 51.41, 17.79.

Grafting to Surface Functional Silica

Hydrosilation of TES Particles With Vinylnaphthalene (VN) Si-TES-VN

To a colloidal dispersion of Si-TES containing 0.2 g solid/ 10 mL THF was added vinylnaphthalene (VN, 0.95 g, 6.2 mmol). After stirring for 30 min at room

temperature, Karstedt's catalyst (100 µL) was injected into the reaction mixture. The mixture was stirred at reflux for 24 h. The mixture was cleaned free of unreacted VN by washing with THF using 3 x centrifugation/redispersion cycles.

UV-vis: The superposition of the starting material and Si-TES-VN is shown in Figure 4.2.

IR (DRIFTS): An attenuation of the peak at 2251 cm^{-1} could clearly be seen to that shown in Figure 4.1.

Hydrosilation of TES Particles With Styrene (ST) Si-TES-ST

As above: (0.2g solid/ 10 mL THF); ST (0.95 g, 6.2 mmol).

UV-Vis: The superposition of the starting material and Si-TES-ST is shown in Figure 4.2.

IR (DRIFTS): An attenuation of the peak at 2251 cm^{-1} could clearly be seen similar to that shown in Figure 4.1 (Top spectrum).

Hydrosilation of TES Particles With Vinyl-Terminated Silicones (VT-PDMS) Si-TES-PDMS

Si-TES (*ca.* 1 g) was transferred to acetone (60 mL) and added to VT-PDMS (Mw=62 700, 10 g) dissolved in hexane (60 mL). The reaction vessel was charged with Karstedt's catalyst (100 µL). The mixture was stirred under an open atmosphere for 10 h at 80°C. The silica was cleaned of unreacted PDMS with fresh hexane using at least 5 x centrifugation/redispersion cycles at 7000 rpm for 30 min.

IR (DRIFTS): v:attenuation of the Si-H peak at 2251 cm^{-1}, 1259 cm^{-1}.

^{29}Si NMR (MAS) δ -111, -101, -92, -22.

4.3 Results and Discussion

Particle Surface Properties

DLS measurements

The particle sizes as measured by DLS for Stöber silica (Si-OH) in acetone before and after the chemical modification reactions are given in Table 4.1. In the case of DMES surface functionalization, no significant differences were observed between the diameters obtained for the unfunctionalized and DMES functionalized spheres. For example, the average particle diameters obtained for Si-OH and Si-DMES in acetone were 179 and 178 nm, respectively. By contrast, the thickness of the surface layer of TES on the particles was different. For example, the particle diameter of Si-TES was 192 nm which is 13 nm greater than that observed for Si-OH.

Since Si-DMES bears only one alkoxy group that can participate in a surface reaction, it is expected that the maximum surface coverage would be a monolayer assuming the DMES molecules are not physically adsorbed onto the particle surface. In contrast, Si-TES may oligomerize prior to or following condensation with the silica surface silanols. These oligomers could extend away from the surface or lie flat on it and could, furthermore, be linear or network polymers. These possibilities are shown in Scheme 4.3.

For comparison with Si-TES, another trifunctional silane $H_2C=CHSi(OMe)_3$ (VTM) which can also oligomerize was examined. Under the same reaction conditions used to make Si-TES, Si-VTM was prepared. The particle size of Si-VTM in acetone was only 4 nm larger (Table 4.1) than the Si-OH from which it was prepared (Scheme 4.3).

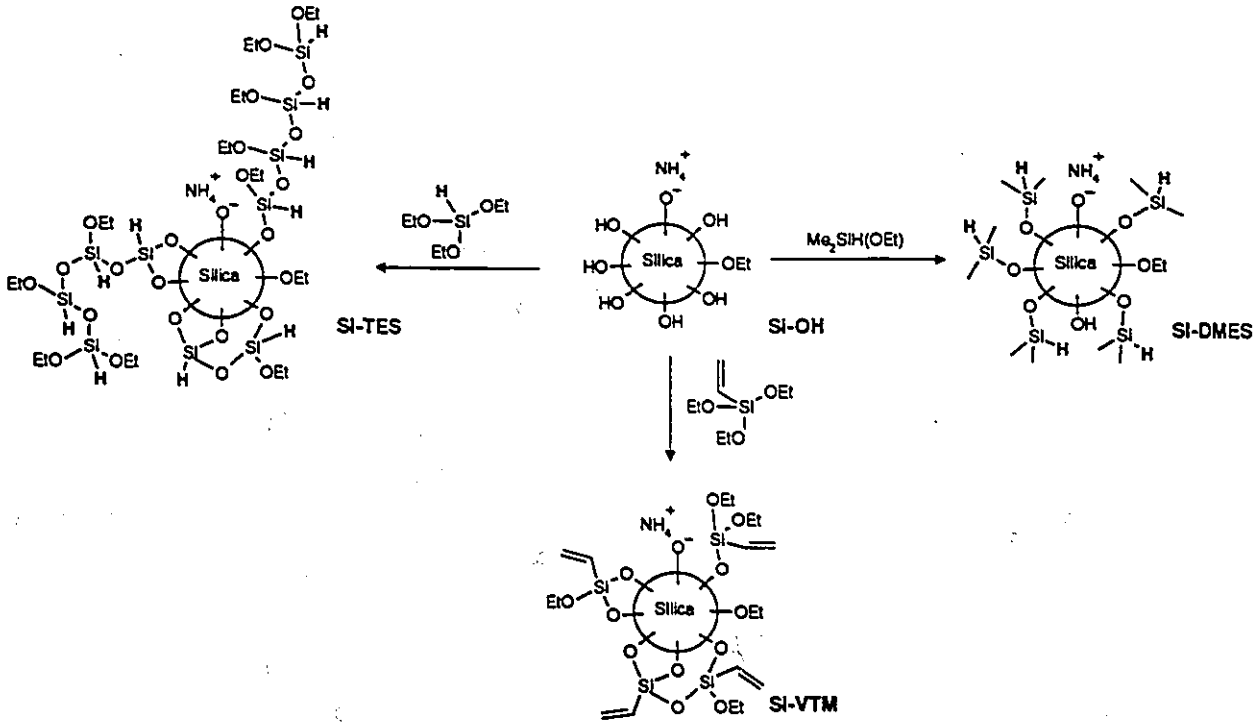

Scheme 4.3. Surface treatment of silica with organosilanes.

Electrophoresis and Colloidal Stability

Stöber silica is electrostatically stabilized through dissociation of the surface silanols in the presence of ammonia. Investigations on the electrokinetic properties

of silica hydrosols have shown that at pH's above the isoelectric point (~2.2 for silica), the negative charge of the silica surface increases due to an increase in the degree of dissociation of the silanol groups.[4] We wished to synthesize modified silica particles which required the use of organic solvents. It was of interest, therefore, to know how Stöber silica would behave, in a colloidal sense, in such solvents. Unfortunately there is limited data in the literature on the electrokinetic properties and colloidal stability of silica in organic media; hence, electrophoretic mobility measurements in acetone for the unmodified and modified silica dispersions were carried out. Microelectrophoresis in acetone (see Table 4.1) showed that the unmodified and functionalized particles were negatively charged. For example, the mobility of Si-OH was -4.79×10^{-8} m^2 V^{-1} s^{-1}.[22]

Following the surface modification of Si-OH with TES, the particle mobility in acetone (of Si-TES) decreased to -3.87×10^{-8} m^2 $V^{-1}s^{-1}$. In contrast, the electrophoretic mobilities of Si-DMES and Si-VTM were observed to be similar to the unmodified silica. For example, the mobilities for Si-DMES and Si-VTM were -5.35×10^{-8} m^2 $V^{-1}s^{-1}$ and -4.41×10^{-8} m^2 $V^{-1}s^{-1}$, respectively. The mobilities observed for Si-DMES and Si-VTM were comparable to Si-OH and are consistent with the particle diameter results obtained by DLS (*vide supra*, Table 4.1). Similarly, the mobility of Si-TES was lower than Si-OH consistent with the larger particle diameter found by DLS. The changes in electrokinetic behavior and colloidal stability behavior between Si-TES and Si-DMES are examined in more detail elsewhere.[22]

FT-IR Surface Characterization

The presence of Si-H groups on the silica particles was evident from DRIFTS; the most apparent difference between the spectra obtained for Si-OH and Si-TES was the presence of the Si-H peak at 2251 cm^{-1} (Figure 4.1). The grafting process only occurred to a significant degree at elevated temperatures (~60 °C); no spectroscopic evidence for the Si-H group was observed when the modification reaction was carried out at room temperature. In the case of Si-DMES, the Si-H peak was observed to shift to 2147 cm^{-1} from 2225 cm^{-1} in TES.

Surface yield for Si-TES and Si-DMES Functionalization

An oxidative titration method was employed to determine the number of Si-H groups attached to the particle surface.[23] The coverage was found to be 6-8 Si-H groups/nm^2 for Si-TES and 2-3 Si-H groups/nm^2 for Si-DMES.[23]

The degree of silane monomer coverage of the silica surface was also determined from the carbon content difference (see elemental analysis results in Table 4.1) between Si-OH, Si-TES, and Si-DMES. In the case of Si-OH, the carbon and hydrogen weight % content were 2.04 and 1.25 respectively. Badley *et al.*[10] have reported carbon contents of 2.25 - 2.53 wt% C for Stöber silica.

Figure 4.1. DRIFT spectra of Stöber silica: Top spectrum: (a) Silica modified with TES (Si-TES); and Bottom spectrum: (b) Silica modified with silicone using the Pt-catalyzed hydrosilation between Si-TES and VT-PDMS (MW=62 700) (Si-TES-PDMS).

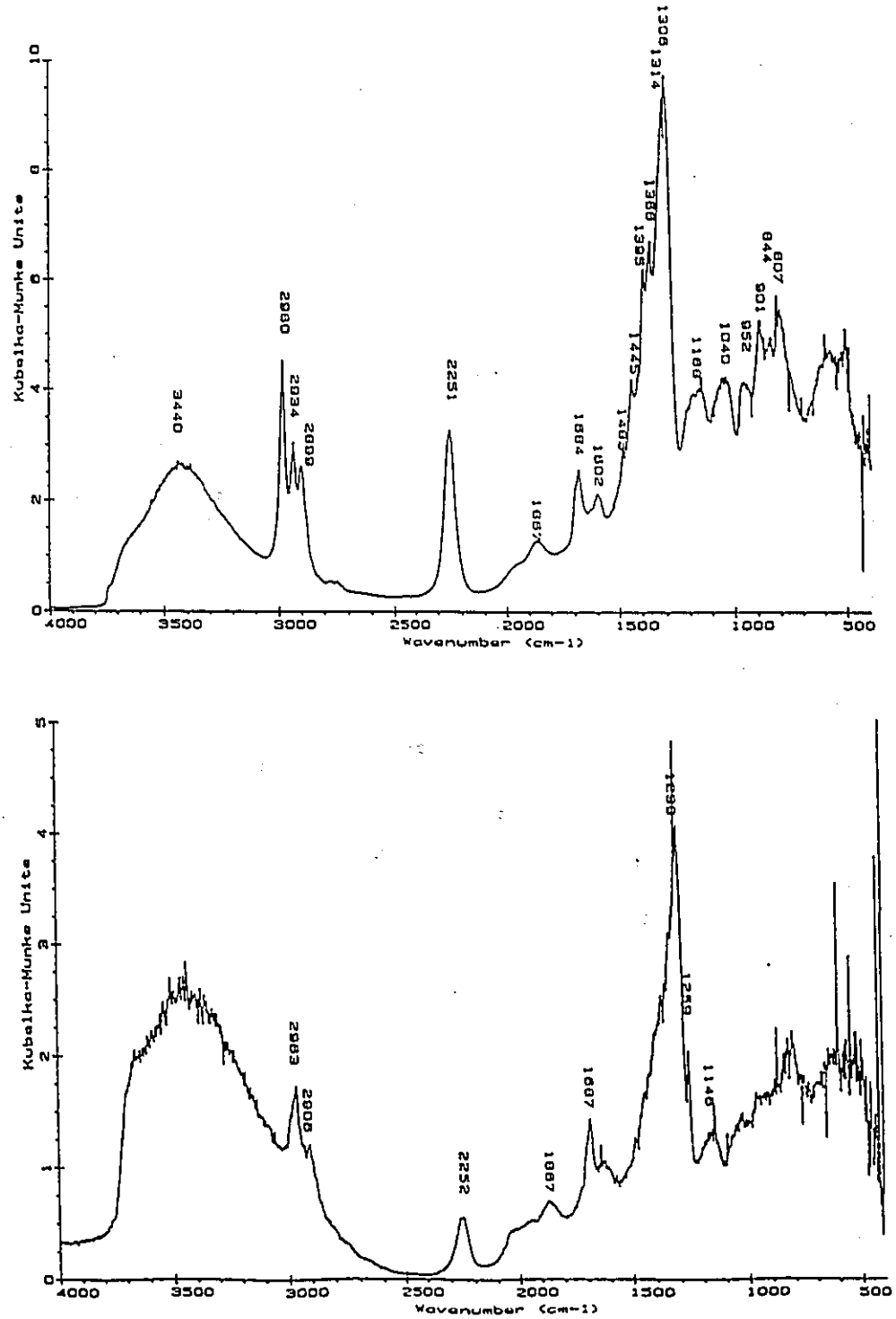

It is noteworthy that Stöber silica has been shown to have high concentrations of unhydrolyzed ethoxy groups (within the particle core and on the surface) consistent with the high carbon contents observed in this work.[10,11,24] The results in Table 4.1 show that the carbon content for both Si-TES and Si-DMES are higher than Si-OH. For Si-TES and Si-DMES, the carbon contents were 4.12 and 2.14 wt%, respectively. The higher carbon content observed for Si-TES indicates the presence of unhydrolyzed Si-OEt and that TES multi-layers are grafted to the particle surface.

Investigations of silylated surfaces have shown that multi-layers having thicknesses up to 30 nm can be incorporated on the particle surface.[9] Factors which can affect the degree of silane coverage include the water content, pH, reactivity and availability of surface groups and the nature of the organosilane agent. A further factor which affects the silane coverage is the porosity of the silica particle. It has been shown that Stöber silica has a microporosity of 10-15%[3] and that residual concentrations of ammonia and water remain trapped inside the particle matrix.[25] Although elemental analysis of Si-OH (Figure 4.1) detected no nitrogen, the possibility of ammonia leaching out over time should not be ruled out. One major problem associated with the presence of ammonia on the particle surface is its effect on the hydrosilation surface reactions. For example, amines have been observed to act as poisons towards platinum catalysts when added to hydrosilation reaction

mixtures.[26] Thus, the efficacy of the surface hydrosilation will be modulated by the degree of catalyst poisoning.

Unmodified silica dispersions aged in acetone for a few months were observed in some cases to develop a yellow discoloration which was presumed to arise from chemical complexes of ammonia and acetone leaching out of the particle interior. However, characterisation of the Si-TES and Si-DMES dispersions in acetone using DLS, electrophoresis, and DRIFTS following a 1 year ageing period showed similar results to those obtained with the freshly prepared modified samples. No discoloration or change in colloidal stability was observed during this time period. It is believed that the surface modification reaction blocks the pores with the organosilanes which effectively traps any residual ammonia within the particle interior. Further experiments are currently in progress to study the silica particle porosity.

Surface Modification by Hydrosilation

The Si-H bond is an extremely useful functional group. Its reactivity can be exploited through hydrosilation under very mild conditions in the presence of a variety of catalysts, the most efficacious of which are platinum-based (Scheme 4.2A,E). Because of the importance of this reaction to the silicone industry, a great deal is known about the reaction mechanism and the types of reagents susceptible to the reaction.[27]

Table 4.1. Characterization of Silica Particles Before and After Treatment with Silanes.

	Si-OH	Si-TES	Si-DMES	Si-VTM	Si-TES-PDMS
DLS (nm)[a]	179 ± 2	192 ± 3	178 ± 2	173 ± 2[b]	242 ± 5
Electrophoretic Mobility ($m^2 V^{-1} s^{-1} \times 10^{-8}$)	-4.79±0.12	-3.70±0.10	-5.35±0.29	-4.41±0.11	0
weight %	2.04	4.12	2.14	4.83	-
weight % Si	40.53	-	-	-	-
weight % H	1.25	1.55	1.36	1.37	-
Titration Si-H wt%	-	0.5 - 0.7	0.15-0.2	-	-
# Si-H / nm^2	-	6-8	2-3	-	-

[a]The relative particle size changes upon functionalization were similar irrespective of whether TEM or DLS was used. The absolute sizes of the particles were somewhat smaller by TEM.

[b] New particle batch; d_H=169 ± 1 nm.

[c] No nitrogen was detected by combustion analysis in this sample; detection limit = 0.01%.

The synthetic value of this method lies in the ability of the Si-H group to add to most π-bonds forming stable covalent bonds (Si-X, X = C, O, N, etc.), particularly

with terminal π-bonds such as $H_2C{=}CR_2$, HC≡CR and $O{=}CR_2$. The hydrosilation reaction occurs with high yields, typically > 90%, under mild conditions and is simple to perform. Thus, one can use the silica surface bound Si-H group for grafting a wide selection of organic moieties containing the functional groups listed above to the silica surface.

This synthetic approach was utilized to prepare the model silica systems and is illustrated by the examples shown in Scheme 4.4. Both small organic molecules and polymeric chains were grafted to the particle surface. Following the reaction of Si-TES with vinylnaphthalene and styrene, respectively, the presence of the naphthalene and styrene moieties on the silica surface were qualitatively detected by ultraviolet (UV) absorption. In the case of Si-TES-VN, the fluorescence spectrum showed a maximum at about 350 nm which corresponded to that obtained with vinylnaphthalene dissolved in CH_2Cl_2. Figure 4.2 compares the UV-VIS spectra obtained for Si-TES, Si-TES-VN, and vinylnaphthalene in 2-propanol. For Si-TES-VN, an absorption band occurred at approximately 280 nm which corresponds to the excitation wavelength for the naphthalene group. In the case of the UV absorption spectra of Si-TES in 2-propanol, a significant shift occurred at approximately 300 nm.

Figure 4.2. UV-VIS absorption spectra for Si-TES-VN and Si-TES-ST following hydrosilation reaction using Si-TES particles.

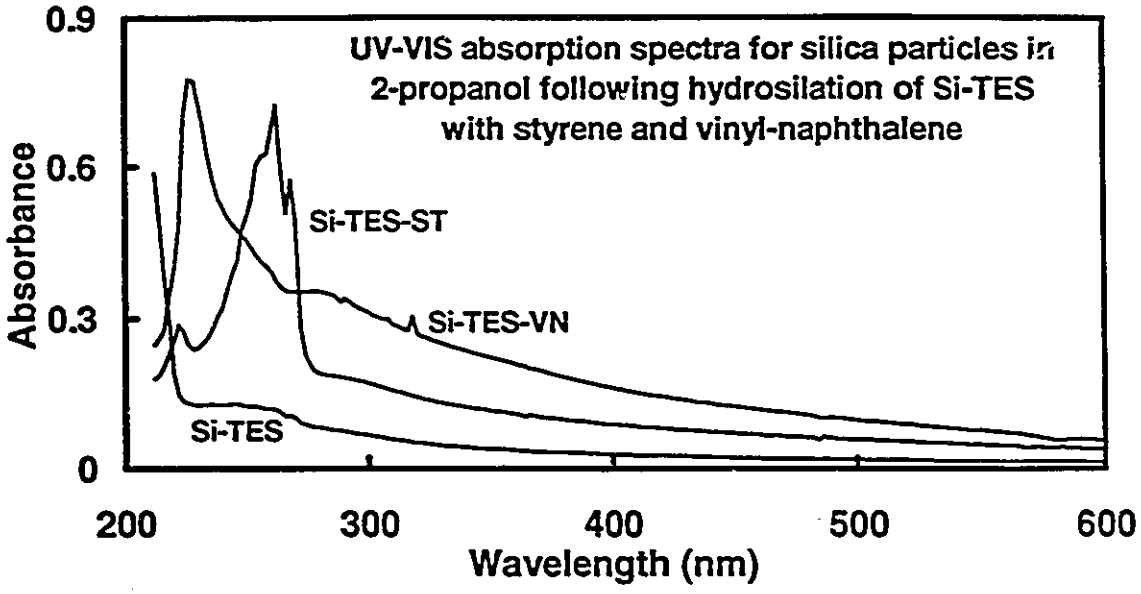

In comparison to Si-TES, intense absorption bands occurred between 220-250 nm for Si-Styrene which corresponds to the typical adsorption absorption bands associated with aromatic rings. If any of the vinyl groups of styrene remained unreacted, the absorption band in the Si-styrene spectrum would be expected to shift towards 280 nm. An estimation of the degree of grafting of the vinyl precursors was obtained by combustion analysis. For example, the carbon content increased from 4.12 for Si-TES to 4.85 and 4.47 for Si-TES-VN and Si-TES-ST, respectively. The number of groups grafted to Si-TES can be estimated using the carbon content differences (see Table 4.1) before and after the hydrosilation reaction. For example,

for Si-TES-VN and Si-TES-ST the carbon wt% differences were 0.73% and 0.35%, respectively. For silica having a diameter of 177 nm and a density of 2.0 g cm^{-3}, the specific surface area is about 20 m^2 g^{-1}. On this basis, the number of naphthalene and styrene groups hydrosilated to the silica surface corresponds roughly to 1.5 and 2.0 groups nm^{-2}, respectively. Since 6-8 Si-H groups nm^{-2} were estimated from the titration results to be present on the surface of Si-TES, only a small fraction of the available Si-H groups appear to participate in the hydrosilation surface reaction. Residual Si-H groups were observed in the IR spectra for Si-TES-VN and Si-TES-ST. Further work is needed to confirm whether these low grafting yields are due to steric factors, particle porosity, the reaction conditions or a combination of these and other factors.

Vinylsilicones (H_2C=$CHSiMe_2[OSiMe_2]_nSiMe_2CH$=$CH_2$) (where MW ≈ 28 000 and 62 700, respectively) were also reacted with Si-TES using the hydrosilation reaction in a mixture of acetone and *n*-hexane (Scheme 4.4C). The ^{29}Si MAS solid state NMR spectrum of the silicone modified silica shown in Figure 4.3, shows a signal at -22 ppm which was consistent with the presence of D units $(Me_2SiO)_n$ on the particle surface. The other peaks in the spectrum at -110, -102 and -93 ppm corresponded to the $Si(OSi)_4$ (Q_4), $Si(OSi)_3OH$ (Q_3), and $Si(OSi)_2(OH)_2$ (Q_2) environments, respectively, in colloidal silica.[10,11] Figure 4.1b shows the spectra obtained using DRIFTS. The intensity of the Si-H peak at 2251 cm^{-1} was found to decrease significantly following the hydrosilation reaction. Moreover, the sharp

absorption signal at 1259 cm^{-1} in the DRIFTS spectrum confirmed the presence of the silicone D units. Residual Si-H groups can also be seen in the IR spectra indicating several of the Si-H groups remained unreacted. From the DLS measurements of the latex, the particle diameter increased from 192 (Si-TES) to 242 nm (Si-TES-PDMS) following the hydrosilation reaction with silicone (MW ≈ 62, 700).

Figure 4.3. Top spectrum: ^{29}Si MAS NMR of Stöber silica modified with silicone by the Pt-catalyzed hydrosilation reaction between Si-TES and VT-PDMS (MW=62 700). Bottom spectrum: ^{29}Si MAS NMR of untreated Stöber silica.

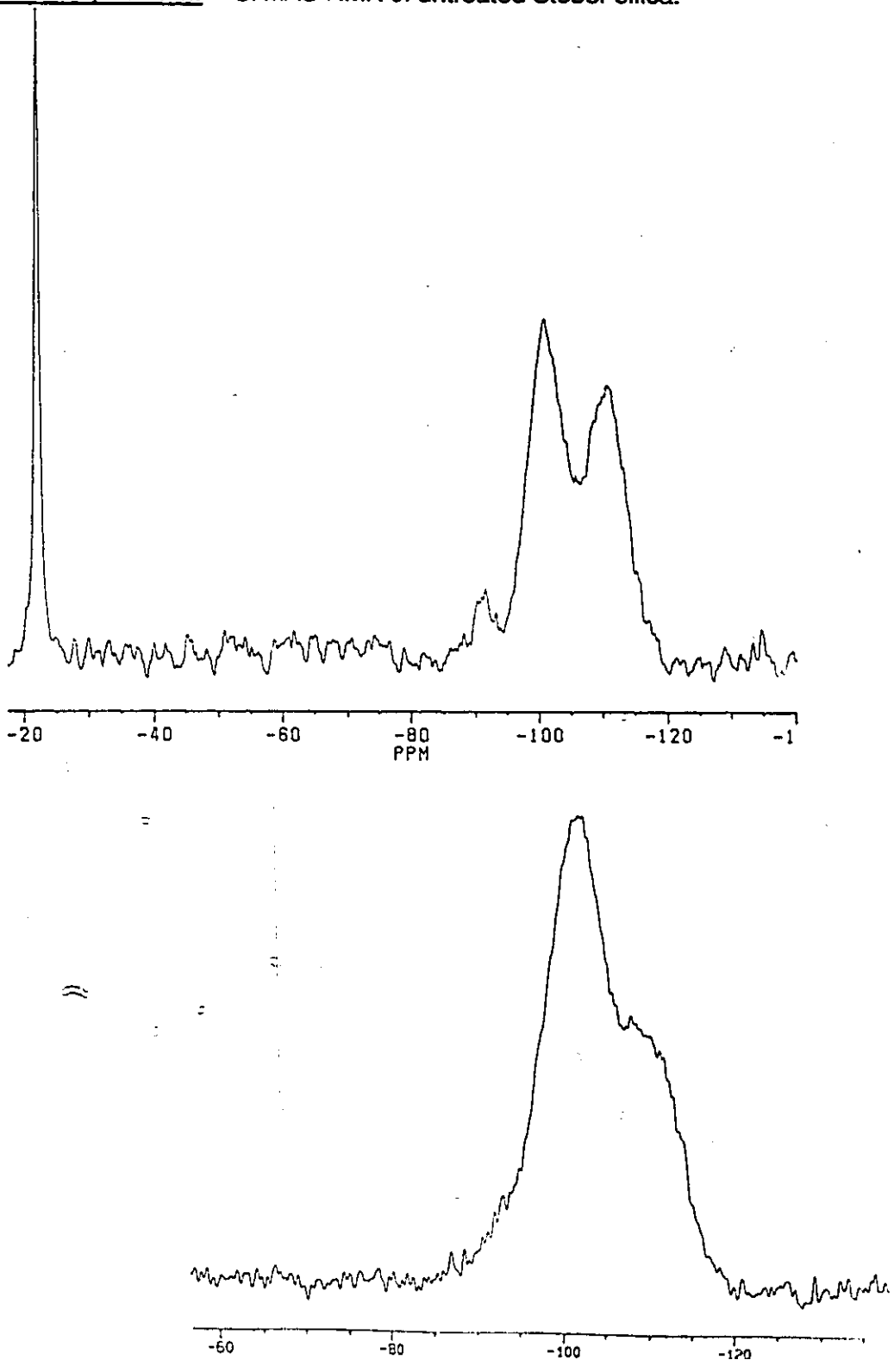

Figure 4.4 shows the TEM of the Si-TES-PDMS particles dried from *n*-hexane. Note the ordered packing arrangements of the particles and the migration of the small particles towards the boundaries.[28] The interstitial space between the particles is approximately 20-25 nm. This separation may result from the thickness of surface polymer layers on adjacent particles. For comparison, the TEM of the precursor Si-OH particle shown in Figure 4.5 in which the particles are clearly making contact.

In order to ensure that all of the silicone was grafted to the particle surface, several qualitative tests were carried out. Si-TES-PDMS remained stable upon transfer to $CHCl_3$ or heptane but flocculated in polar solvents such as acetone, DMF or water. If the hydrosilation reaction was attempted using Si-OH, the silica coagulated. Further research will be carried out in the future that is directed towards obtaining quantitative information on the surface concentration of silicone necessary to sterically stabilize silica using the hydrosilation reaction.

Figure 4.4 TEM of Stöber silica modified with poly(dimethylsiloxane) (MW=62 700). The particle diameter as measured by DLS was 242 nm (Scale bar = 1000 nm). The hydrodynamic thickness of the PDMS layer corresponded to 50 nm.

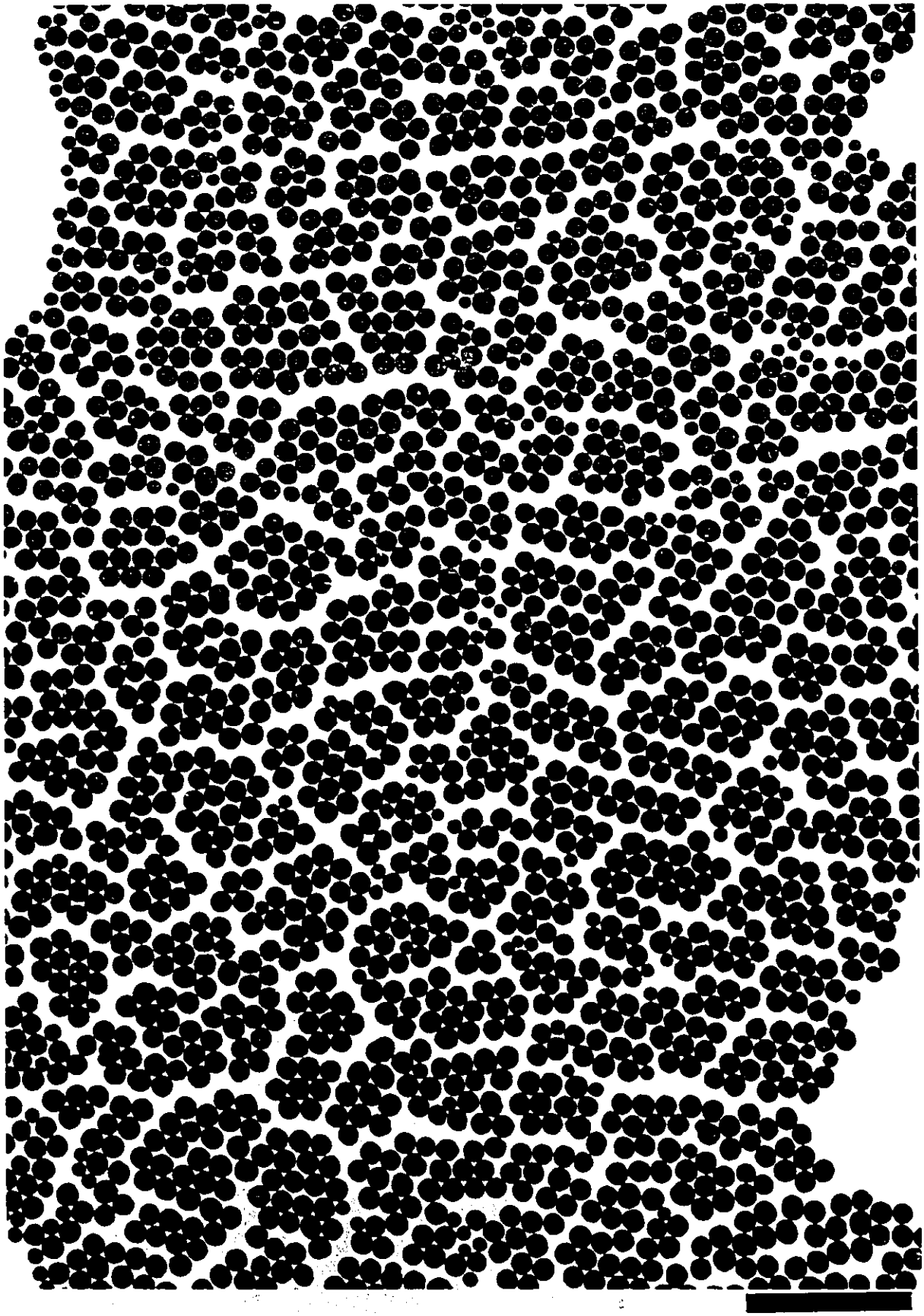

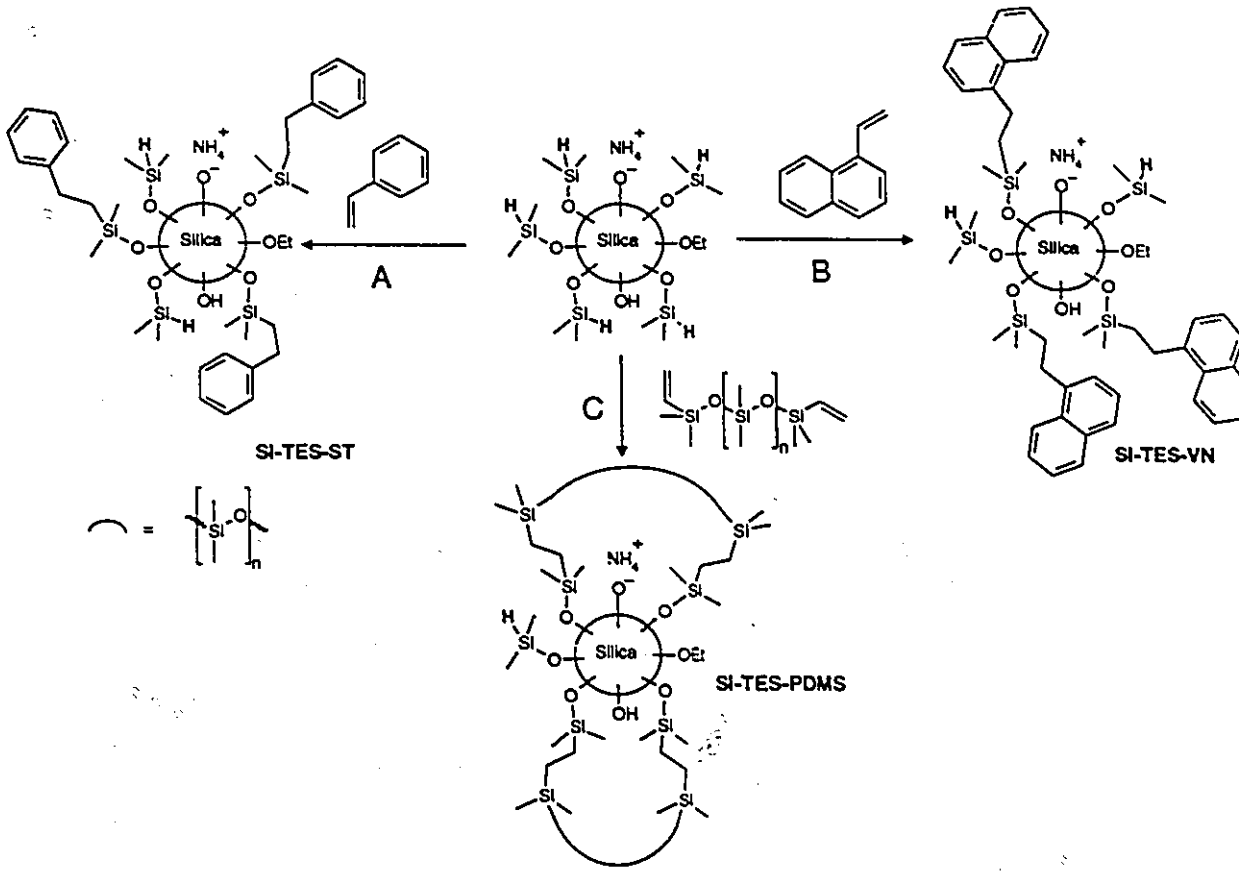

Scheme 4.4 Hydrosilation reactions using silica modified with TES ($HSi(OEt)_3$).

Figure 4.5: TEM of Stöber silica (Si-OH) (Scale bar = 1000 nm).

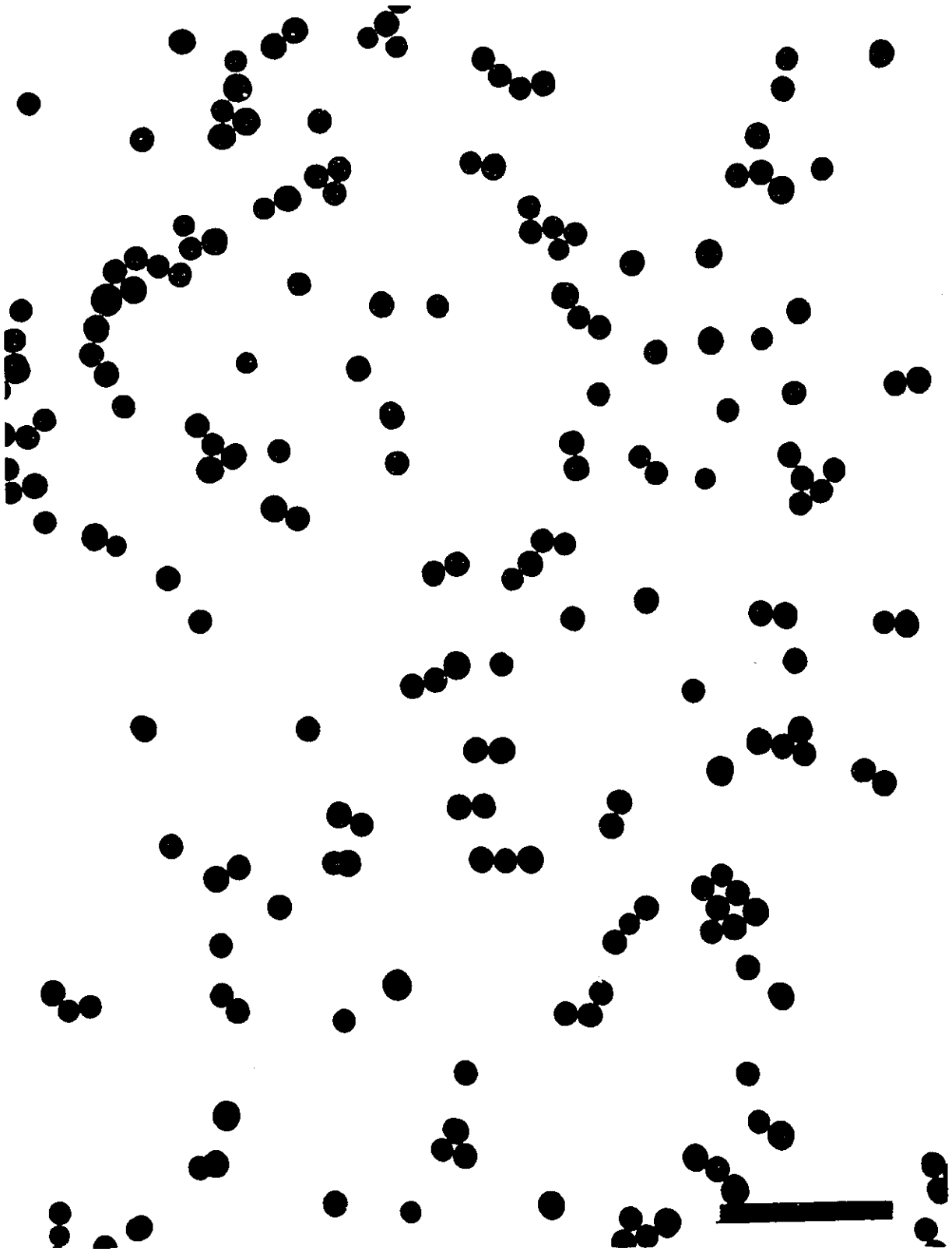

4.4 Conclusion

(1) The Si-H-containing alkoxysilane reagent TES was found to be a useful silyl coupling agent. Stöber silica may be surface functionalized with TES and the resulting Si-H modified particles can be used to carry out Pt-catalyzed hydrosilation surface reactions with organic molecules such as vinylnaphthalene, styrene or polymers such as vinyl-terminated silicones. This general procedure should be equally applicable to many other interesting moieties which can lead to the preparation of novel model inorganic-organic systems.

(2) A significant difference in the degree of silane surface coverage was observed using TES and VTM. Although TES and VTM can both oligomerize to a network polymer (silsesquioxane) through three functional sites, TES formed a dense, 13 nm layer on the silica surface, whereas a surface layer of only 4 nm resulted with VTM. The origin of this difference, which could involve the relative size of H *versus* $CH{=}CH_2$ groups, needs to be clarified .

Appendix A4.1. Hydridosilsesquioxane Gel

Silica based xerogels using sol-gel chemistry have increasingly attracted attention in material and ceramic science due to their high surface areas and ability to form monolithic gels at room temperature.[29] One particular xerogel which has made significant contributions to the family of inorganic-organic hybrid materials is that corresponding to silica gels with Si-H functionalities (commonly referred to as hydridosilsesquioxanes).[30] The gels can be prepared *via* hydrolysis -condensation reactions using triethoxysilane (TES) ($HSi(OEt)_3$) in the presence of water/polar organic mixtures (typically ethanol or acetone). In order to retain a high percentage of Si-H groups, alkaline conditions must be avoided due to their displacement in the presence of OH-.

In this note, hydridosilsesquioxane gels were prepared *via* hydrolysis-condensation reactions using TES in the presence of acetone - water mixtures. The product was characterized by NMR and TEM microscopy. Table A4.1 gives the experimental conditions used to qualitatively investigate the formation of the gel products. All samples were initially shaken a few times to mix all the components homogeneously and then they were left open to the atmosphere (without stirring) at 25°C for 10 hours before any characterization was performed.

Table A4.1-1. Conditions used to prepare hydridosilsesquioxane gels.

Sample#	mmol TES	mmol Acetone	mmol H_2O	Observations
1	3.6	-	22	forms white precipitates within 2 min, viscous sol'n turns to gel after 30 min
2	3.5	8.4	-	no change
3	4.2	4.5	27	firm optically clear gel forms after 2.5 hrs
4	3.5	6.3	5.6*	firm optically clear gel forms after 2.5 hrs

The data in Table A4.1-1 shows that only samples 4 and 5 gave clear gel materials. TES was unreactive in the presence of only acetone (containing 0.3 wt% water). Sample 3 was placed in an oven and heated for 24 h at 120°C. The ^{29}Si NMR CP-MAS NMR (1 msec contact time) of sample 3 showed two major signals; one at -101.3 ppm which corresponds to the Q_3 silicon environment and the other at -84.6 ppm which is assigned to the T^{H1} silicon unit.

The microstructure of the gel was also characterized by TEM analysis. Small pieces of a dried sample were embedded in Spurr's epoxy resin and polymerized at 60°C overnight. Sections from the embedded sample were cut at 50 nm on a Reichert Ultracut E ultramicrotome using a diamond knife. TEM images were recorded at the magnification of 80,000X on a JEOL 1200EX electron microscope and a sample image of the sectioned sample is given in Figure A4.1-2. The gel sample was observed to be porous as evidenced by the varying shades of white and gray patches existing throughout the section. The porosity profile was analysed by

digitising the TEM negatives using a CCD video camera interfaced with a KONTRON Image Analysis System equipped with the VIDAS software package (version#5.2). Each image of 49,046 nm^2 was digitised in 512 x 512 pixels format. Grey level discrimination was performed on each of the binary images created such that the pore structure could be analysed with respect to the area, diameter, and perimeter of the pore regions. A total of 17 261 pores were counted and the mean diameter of the pores was 4.92 nm (the minimum and maximum pore diameter corresponded to 1.05 nm and 37.80 nm, respectively).

Figure A4.1-1. ^{29}Si NMR CP-MAS solid state NMR of hydridosilsesquioxane gel (sample#3).

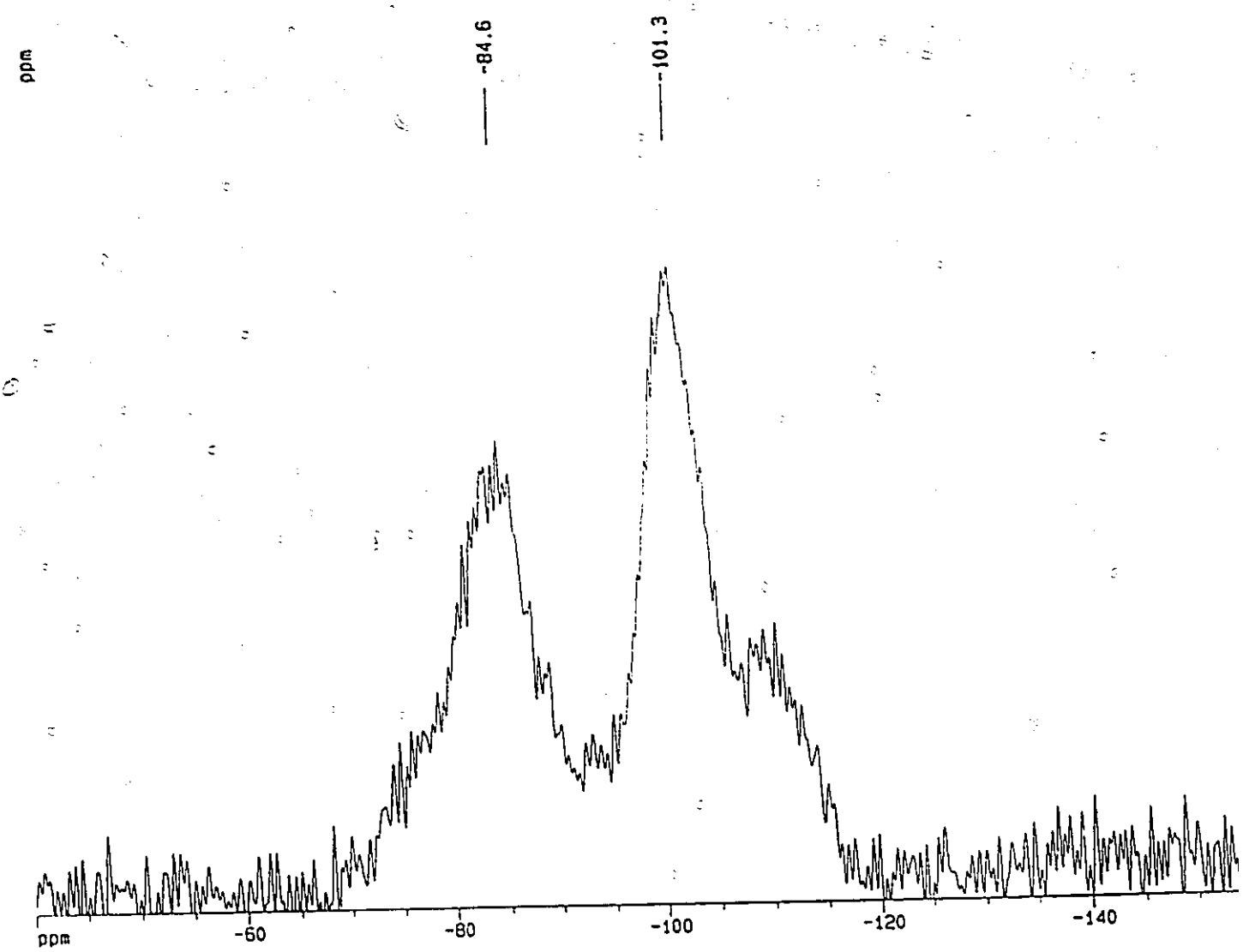

Figure A4.1-2. TEM image of a piece of hydridosilsesquioxane gel which was sectioned by ultramicrotomy (Scale bar = 100 nm).

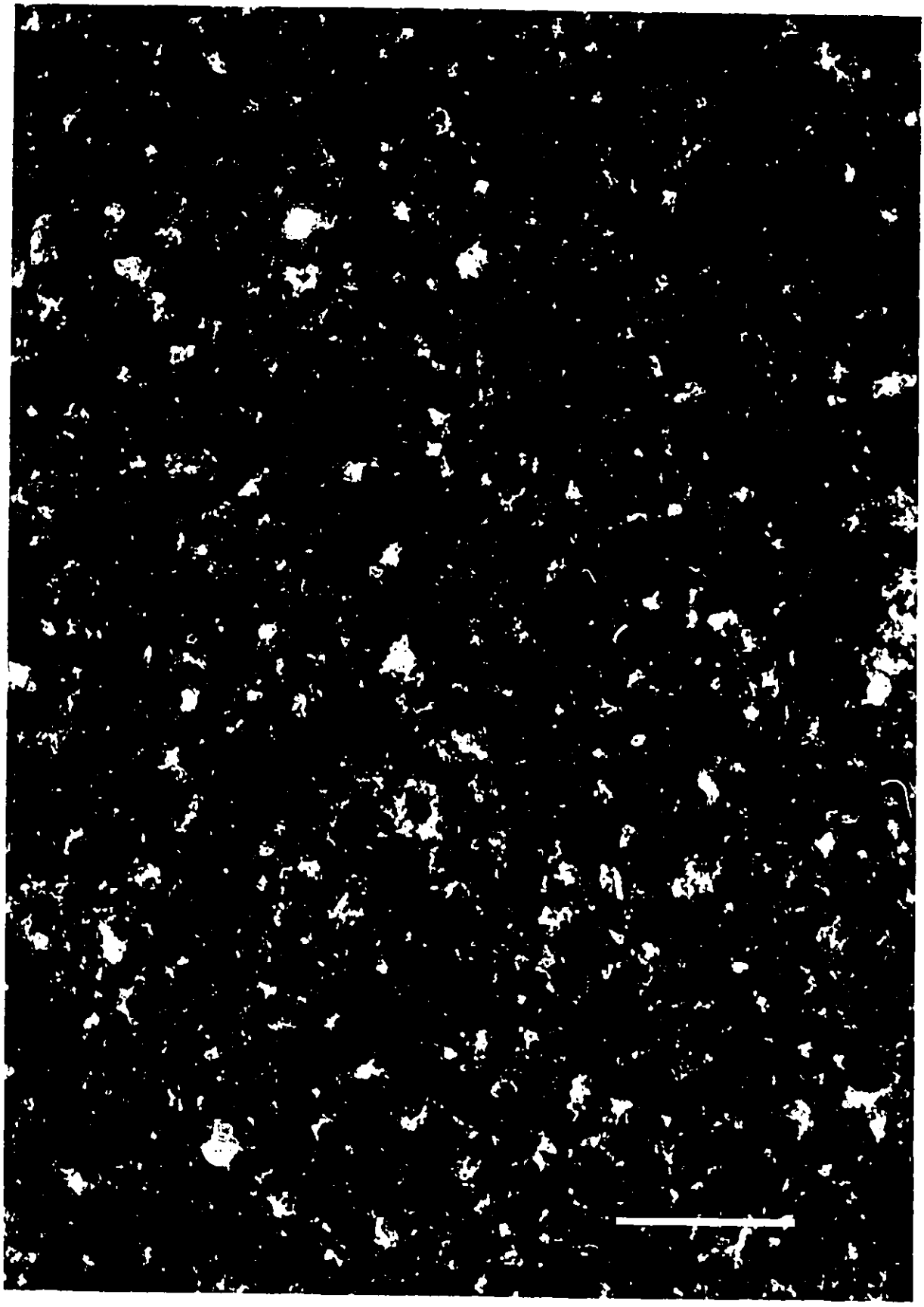

4.5 References

[1] Brinker, C.J.; Scherer, G.W. *Sol-Gel Science*, Academic Press, Boston, pp 839-870, 1990.

[2] Stöber, W.; Fink, A.; Bohn, E. *J. Colloid Interface Sci.* **1968**, *26*, 62.

[3] Bogush, G.H.; Tracy, M.A.; Zukoski IV, C.F. *J. Non-Cryst. Solids*, **1988**, *104*, 95.

[4] Iler, R.K. *The Chemistry of Silica*, Wiley, New York, 1979.

[5] Philipse, A.P.; Vrij, A.J. *J. Colloid Interface Sci.*, **1989**, *128*, 121.

[6] Napper, D.H. *Polymeric Stabilisation of Colloidal Dispersions*, London, Academic Press, 1983.

[7] Edwards, J.; Lenon, S.; Toussaint, A.F.; Vincent, B. *ACS Symp. Ser., # 240*, **1984**, 281-296.

[8] Ryan, K. *Chem. Ind.*, **1988**, 6 June, 359.

[9] Plueddemann, E.P., *Silane Coupling Agents*, Pienum Press, New York, 1982.

[10] Badley, R.D.; Ford, W.T.; McEnroe, F.J.; Assink, R.A. *Langmiur*, **1990**, *6*, 792.

[11] van Blaaderen, A.; Vrij, A. *J. Colloid Interface Sci.*, **1992**, *8*, 2921.

[12] Verhaegh, N.A.M.; van Blaaderen, A., *Langmuir*, **1994**, *10*, 1427.

[13] Tsubokawa, N.; Kimoto, T.; Koyama, K. *Colloid Polym. Sci.*, **1993**, *271*, 940; Sunkara, H.B.; Jethmalani, J.M.; Ford, W.T. *Chem. Mater.*, **1994**, *6*, 362.

[14] Pathmamanoharan, C. *Colloids and Surfaces*, **1988**, *50*, 1; Pathmamanoharan, C. *Colloids and Surfaces*, **1988**, *34*, 81.

[15] Auroy, P.; Auvray, L.; Leger, L. *J. Colloid. Interface Sci.*, **1992**, *150*, 187.

[16] Ketelson, H.A.; Brook, M.A.; Pelton, R.H. *Polym. Adv. Tech.*, **1995**, *6*, 335.

[17] Eaborn, C.; Bott, R.W. in *Organometallic Compounds of the Group IV Elements*, Vol. 1, MacDairmid, A. G. ed., Dekker, New York, 1968; Pawlenko, S. in *Organosilicon Chemistry*, Walter de Groyter & Co., New York, 1986.

[18] Bräuer, L.; Gruber, H.; Greber, G. *Angew. Makromol. Chem.*, **1990**, *180*, 209.

[19] Sandoval, J.E.; Pesek, J.J. *Anal. Chem.* **1991**, *63*, 2634.

[20] Le Déoré, C.; Révillon, A.; Hamaide, T.; Guyot, A. *Polymer*, **1993**, *34*, 3048.

[21] B.D. Karstedt, General Electric Co. Ger. Offen., DE 2307085 730823 1973. *Chem. Abs.* **1973**, *80*, 16134.

[22] See Chapter 6 of this thesis.

[23] Harzdorf, C. *Z. Anal. Chem.*, **1971**, *256*, 192; Smith, A.L.; Ed.; *Analysis of Silicones*, Wiley, New York, 1991.

[24] van Blaaderen, A.; van Geest, J.; Vrij, A. *J. Colloid Interface Sci.*, **1992**, *154*, 481.

[25] Jelinek, L., Dong, P.; Rojas-Pazos, C.; Taibi, H.; Kovats, E. S. *Langmuir*, **1992**, *8*, 2152.

[26] Lukevics, E., Russian *Chem. Rev.* **1977**, *46*, 264.

[27] Musolf, M.C.; Speier, J.L. *J. Org. Chem.* **1964**, *29*, 2519; Lewis, L.N. *Chem. Rev.*, **1993**, *93*, 2693; Speier, J. L. *Adv. Organomet. Chem.* **1979**, *17*, 407.

[28] The silica sample used to prepare Si-TES-PDMS was taken from a batch that contained two populations of particles. Such bimodel distributions were periodically obtained during the early stages of this study. The TEM micrograph of this sample is shown here for the purposes of illustrating the interesting migration behaviour of the smaller particles towards the periphery of the larger particle clusters having an ordered arrangement.

[29] Brinker, C.J.; Scherer, G.W. *Sol-Gel Science: The Physics and Chemistry of Sol-Gel Processing*; Academic Press, Inc.: San Diego, 1990.

[30] Belot, V.; Corriu, R. Leclercq, P.H.; Mutin, P.H.; Vioux, A. *Chem. Mater.* **1991**, *3*, 127.

Chapter 5

Hydridosilsesquioxane Modified Silica-Supported Platinum Nanoparticles

Abstract

Colloidal silica particles modified with hydrosilane (Si-H) groups reacted with Karstedt's catalyst, bis(1,3-divinyl,1,1,3,3-tetramethyldisiloxane)Pt^0, to give catalytically active, surface-bound platinum nanoparticles with an average diameter of 2 nm. A hydridosilsesquioxane ($HSiO_{3/2}$) layer grafted to the silica surface was believed to be critical in controlling the ultimate size of the supported platinum nanoparticles; unlike analogous platinum particles which form in solution from platinum compounds without a stabilizer, platinum nanoparticles enmeshed in the hydridosilsesquioxane layer do not undergo further deactivating aggregation. Silica particles, surface modified with Si-H groups (Me_2SiH) without the hydridosilsesquioxane structure, did not lead to the formation of well-defined platinum nanoparticles but rather to large aggregates of the platinum species. The silica-supported platinum nanoparticles were catalytically active in the

hydrosilation reaction; the catalytic activity was maintained after recovering and recycling the catalyst through at least three further hydrosilation experiments.

5.1 Introduction

Platinum catalysts, such as chloroplatinic acid[1] and Karstedt's catalyst,[2] are frequently used to carry out hydrosilation reactions in which a hydrosilane (R_3SiH) adds across an alkene or alkyne function (Scheme 5.1).[3]

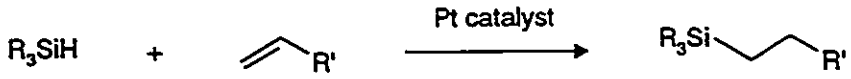

Scheme 5.1: Hydrosilation reaction catalyzed by a platinum.

In 1986, Lewis *et al.* provided evidence that platinum colloids[4] form during the hydrosilation reaction.[5] This work also showed the platinum colloids cause an acceleration of the hydrosilation reaction.[5,6] On the other hand, the platinum colloids that initially promote hydrosilation in high yields degenerate with time to give a catalytically inactive black precipitate.[7]

A variety of metal colloids have been prepared and characterized by prereacting platinum group metal compounds with hydrosilanes.[5,8,9] For example, the reaction between platinum metal compounds (i.e., $PtCl_2$, PtO_2, H_2PtCl_6, and Karstedt's catalyst) and dimethylethoxysilane, $Me_2(EtO)SiH$, gave rise to the evolution of hydrogen gas with a characteristic transition of solution

color from colorless to yellow or orange within 2 hours.[8a] Examination of the products by transmission electron microscopy (TEM) showed the presence of crystalline platinum particles having diameters which ranged from 1-5 nm. It has also been shown that the transition to the yellow colored solution during the hydrosilation reaction occurred simultaneously with the formation of platinum colloids having an average size of *ca.* 2 nm.[5] The chemical identity of the platinum particles formed during reduction by hydrosilane reagents, as determined by X-ray analysis and EXAFS, suggests they are composed of platinum and organosilane fragments.[8,10,11]

This communication reports a simple method for the preparation of platinum nanoparticles supported on inorganic oxide materials,[12] particularly silica modified with Si-H groups.[13,14] The supported platinum nanoparticles, derived from the reaction of Karstedt's catalyst with Si-H modified silica, are catalytically active towards hydrosilation reactions and offer the advantage that the platinum does not aggregate to form an inactive precipitate. Thus, a single sample of the supported catalyst could be recycled to carry out more than one hydrosilation reaction.

5.2 Results and Discussion

Colloidal silica particles were prepared using the Stöber method[15] (Si-OH, Scheme 5.2), which is based on the hydrolysis and condensation of $Si(OEt)_4$ in an aqueous ethanol medium containing ammonia.[13,16] The mean hydrodynamic diameter of the particles in acetone, measured by DLS, was 179 nm with a standard deviation of the particle size distribution of 10%.

Si-OH was modified with $HSi(OEt)_3$ according to a previously reported published method to give Si-TES (Scheme 5.2).[13] From DLS measurements, Si-TES was found to have an increased hydrodynamic diameter of 192 nm indicating a 6 nm silsesquioxane layer on the silica surface. The electrophoretic mobility in acetone of Si-TES decreased, relative to the untreated particles, from -4.79×10^{-8} $m^2V^{-1}s^{-1}$ to -3.70×10^{-8} $m^2V^{-1}s^{-1}$ providing further evidence that the silica surface was coated with TES. The presence of Si-H groups on Si-TES was confirmed by DRIFTS and ^{29}Si CP-MAS NMR spectroscopy.[17] The spectroscopic data of Si-TES revealed that the outer layer on the silica surface was composed of a cross-linked siloxane species bearing $HSiO_{3/2}$ units (Scheme 5.2) consistent with the structure reported for hydridosilsesquioxane gels.[18] The number of Si-H groups per nm^2 was estimated to be 6-8 by titration with *N*-bromosuccinimide.[13]

The silica-supported platinum nanoparticles were prepared by the addition of Karstedt's catalyst (see Scheme 5.2) to Si-TES dispersed in THF.[19] The presence of platinum attached to Si-TES was confirmed by elemental analysis[20] and X-ray microanalysis using transmission electron microscopy (TEM).[21] A typical TEM micrograph is shown in Figure 5.1 (Top photo) in which platinum nanoparticles are observed to be uniformly distributed and attached to the silica surface. The diameters of at least 100 supported platinum nanoparticles were measured to give an average diameter of 2 nm.

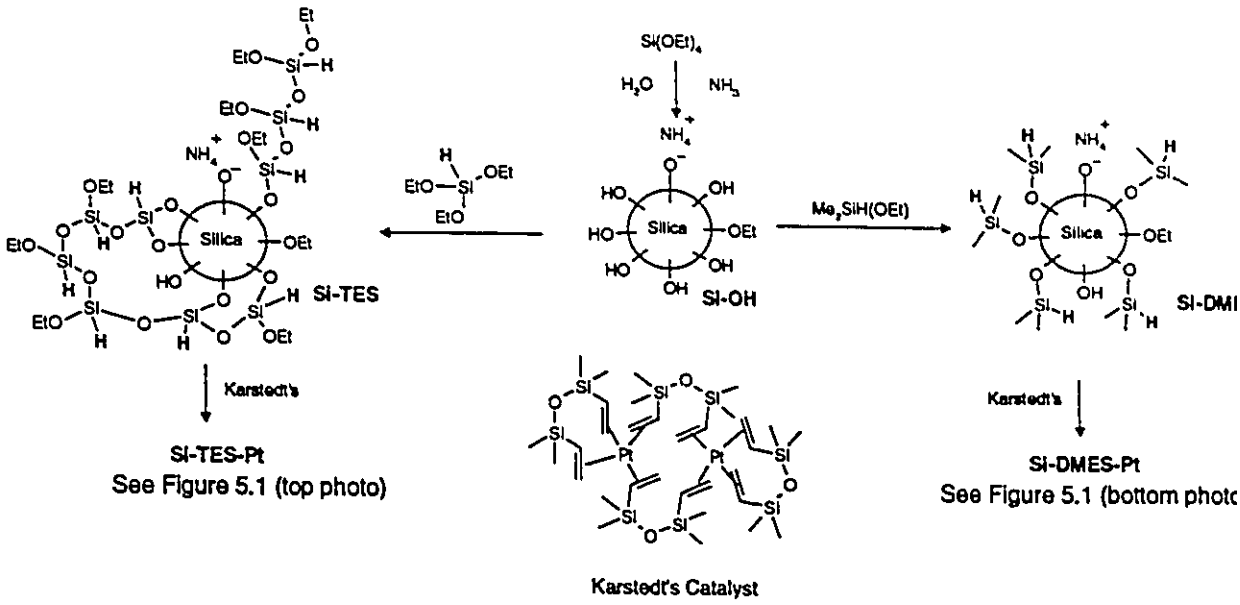

Scheme 5.2. Chemical modification of unmodified silica, Si-OH, with triethoxysilane (TES) to give Si-TES and dimethylethoxysilane (DMES) to give Si-DMES. The surface reaction of Si-TES and Si-DMES with Karstedt's catalyst leads to Si-TES-Pt (see Figure 5.1 (top photo)) and Si-DMES-Pt (see Figure 5.1 (bottom photo)), respectively.

Figure 5.1. **Top Photo:** TEM micrograph of silica-supported platinum nanoparticles (Si-TES-Pt). The average diameter of the supported platinum nanoparticles was 2 nm (Scale bar = 100 nm). **Bottom Photo:** TEM micrograph of Si-DMES particles which have been treated with Karstedt's catalyst (*i.e.*, Si-DMES-Pt) (Scale bar = 100 nm).

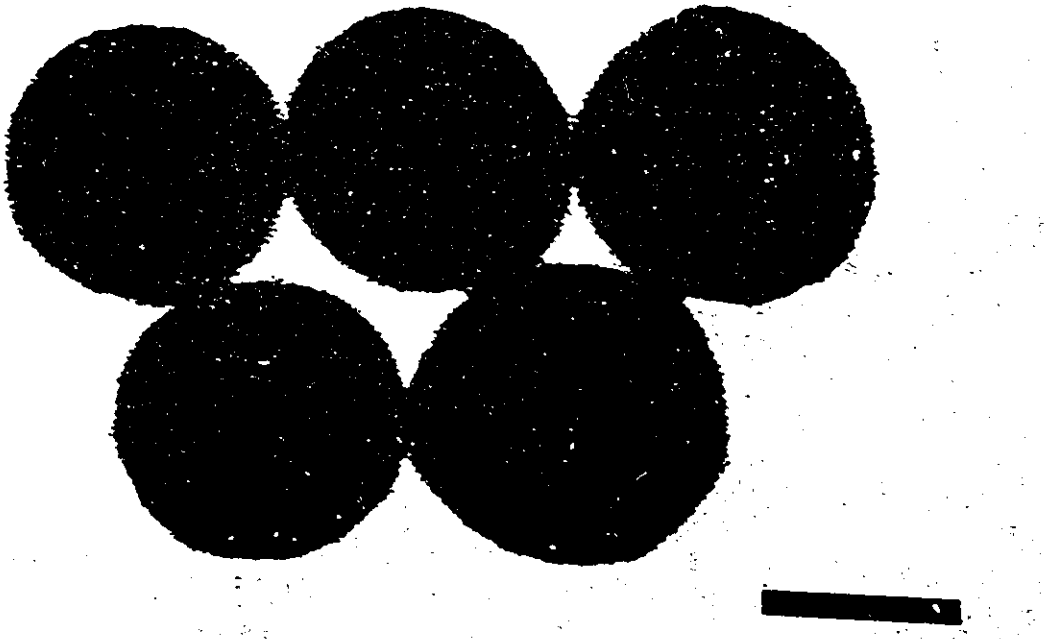

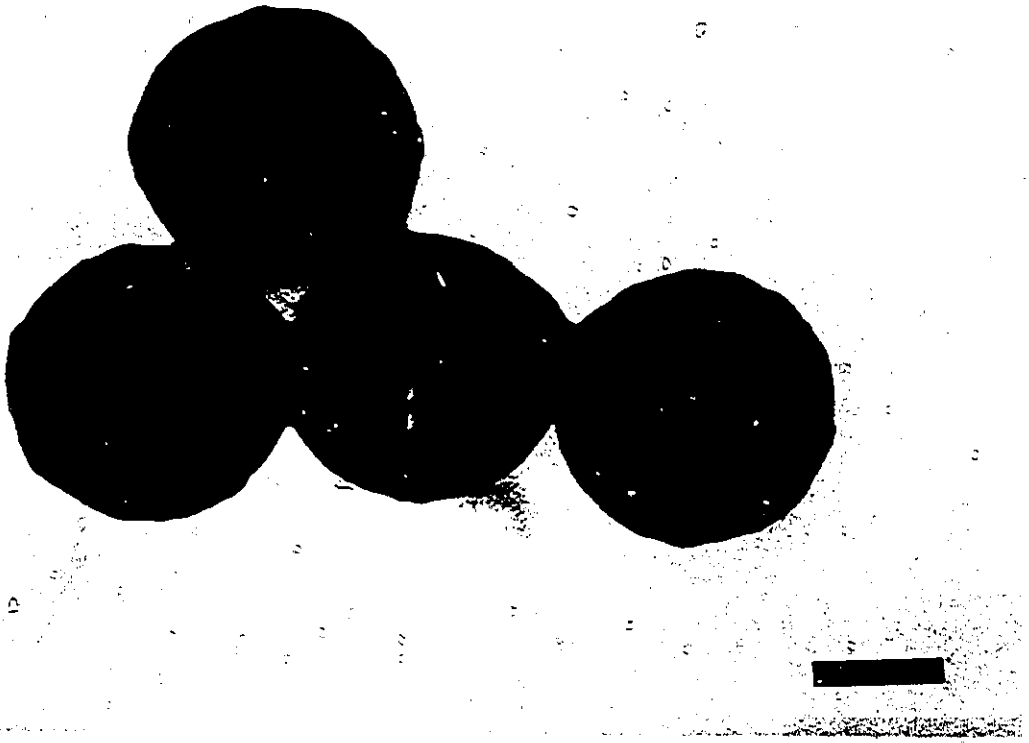

Thin sections of the platinum-silica samples,[22] probed by X-ray microanalysis, showed no platinum signals in the silica core indicating that most or most or all of the platinum resided on the silica surface.

The supported platinum nanoparticles were also imaged after silver staining; the platinum nanoparticles served as catalysts and nucleation sites for the reduction of silver ions (silver lactate) to metallic silver in the presence of hydroquinone (Figure 5.2 (top photo)).[2325] As shown in Figure 5.2a, the metallic silver precipitates grew selectively from the platinum nanoparticles. The x-ray spectrum of Si-TES-Pt stained with silver is shown in Figure 5.2 (bottom photo). The electroless deposition of metals including copper, nickel, and palladium on substrates has previously been shown to occur when metal colloids such as gold, palladium and platinum are used as catalysts.[26,27] See Appendix A5.1 for further work on silver reduction using Si-TES-Pt.

The role of the Si-H functional groups was illustrated by the following experiments: i) no supported platinum on silica was observed when Si-OH dispersions were treated with Karstedt's catalyst; ii) platinum nanoparticles were prepared in the absence of silica (see Figure 5.3) and subsequently added to Si-TES. [28] Platinum on the silica surface was not observed by TEM analysis or detected by X-ray microanalysis.

Figure 5.2. **Top Photo:** TEM photo of Si-TES-Pt after silver staining. **Bottom spectrum:** X-ray spectrum of silver stained Si-TES-Pt showing platinum and silver signals detected on silica (Scale bar = 100 nm). Copper signals is due to grid used to support the sample and sulfur signal arises from sulfate and sulfite solutions used in silver staining preparation method.

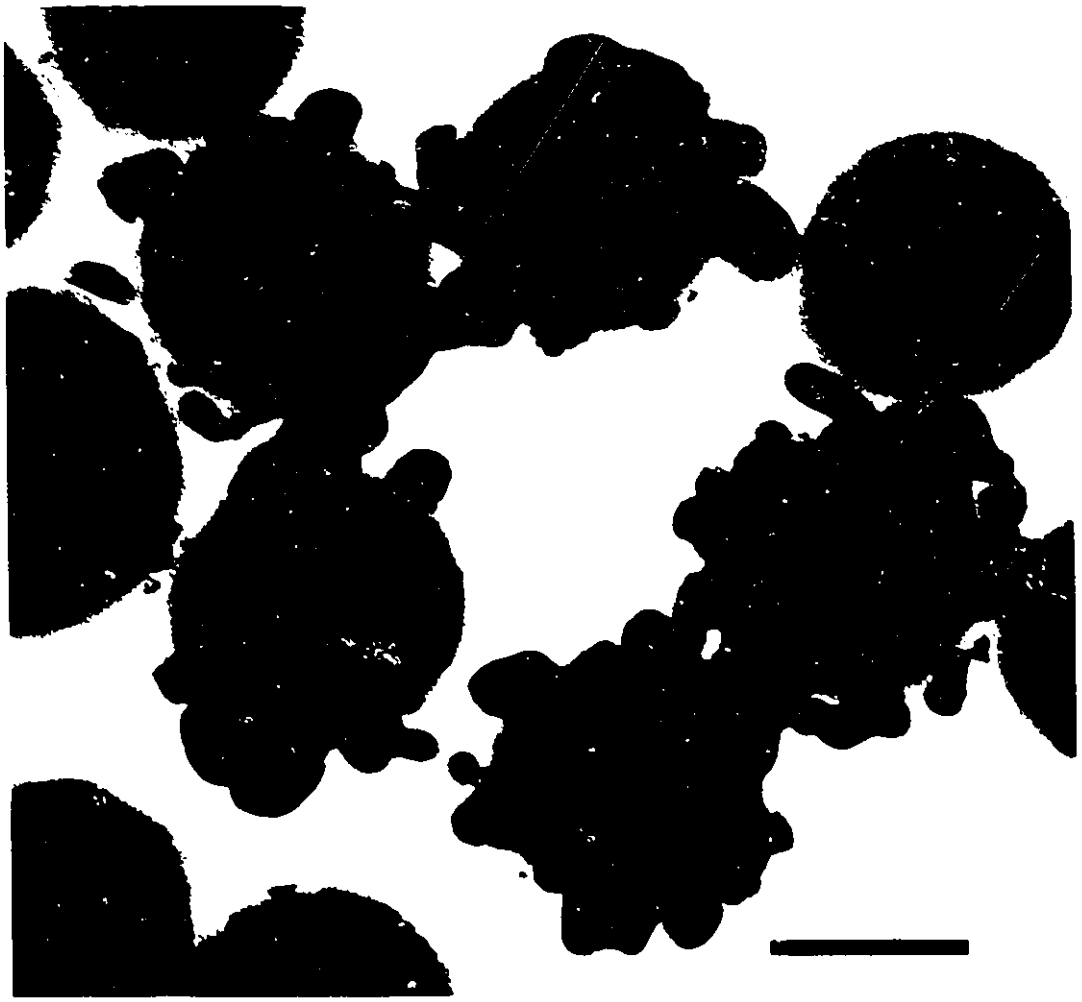

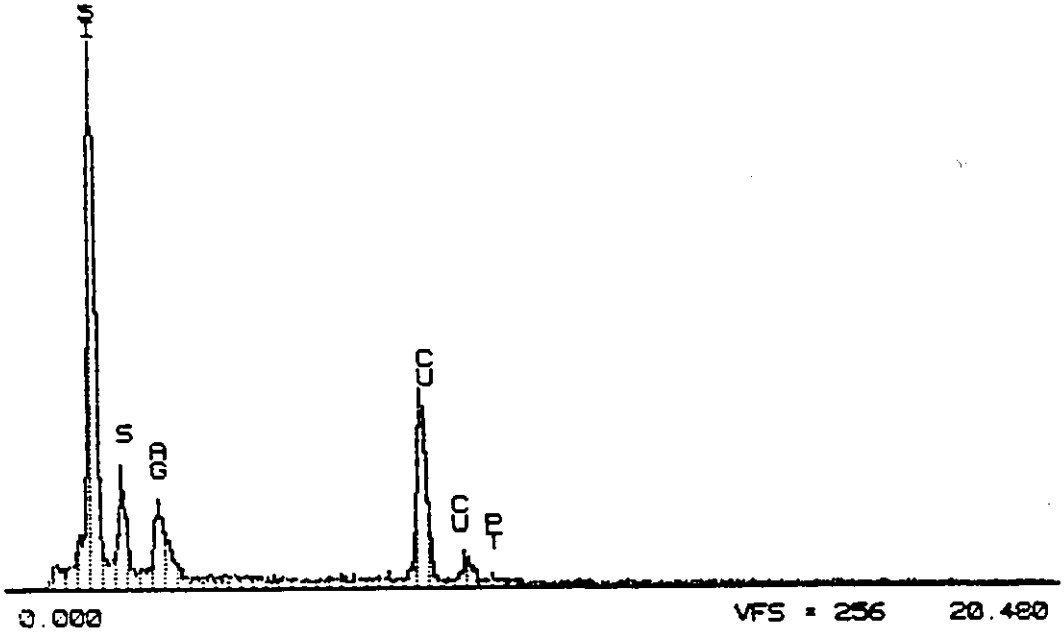
SI
S
AG
CU
CU
PT
0.000
VFS = 256
20.480

Figure 5.3 (opposite page 164). Top photo: TEM micrograph of platinum nanoparticles formed in the absence of Si-TES by reacting TES with Karstedt's catalyst in THF (Scale bar = 100 nm). Bottom bar graph: Particle size distribution of several hundred platinum nanoparticles imaged by TEM.

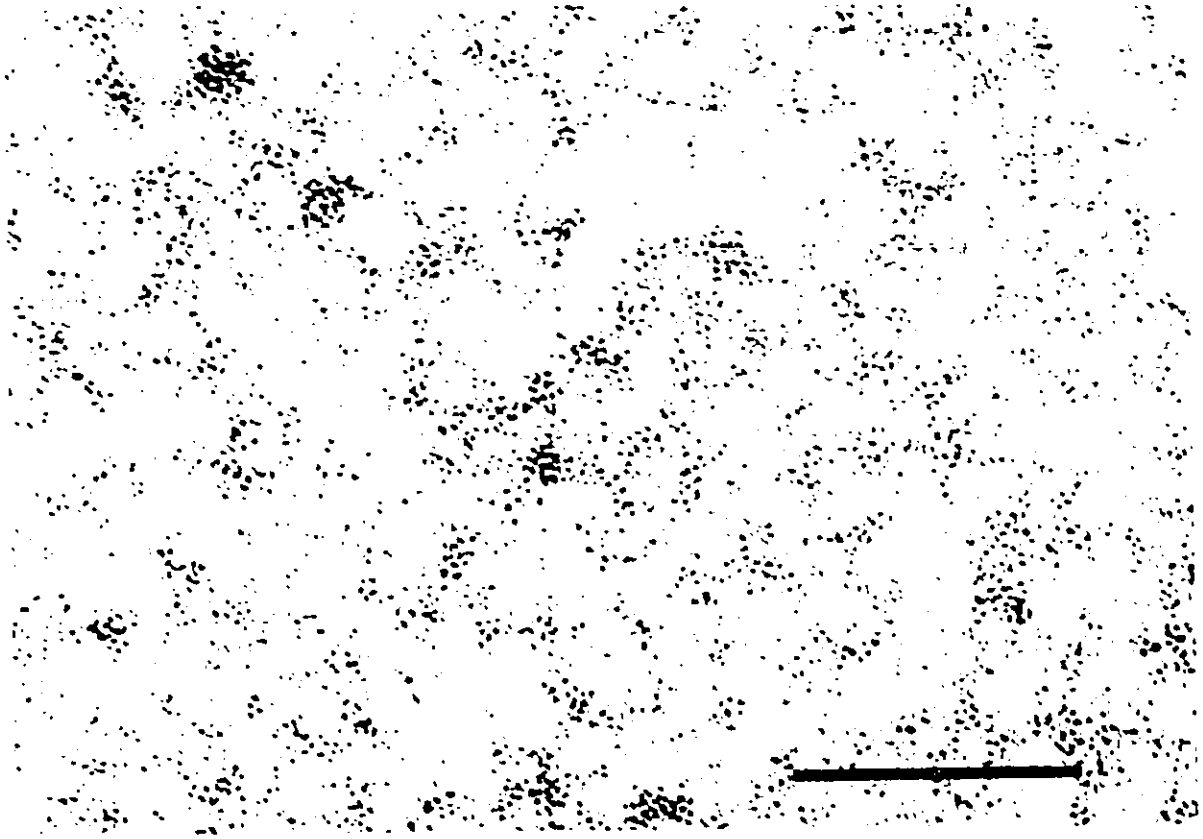

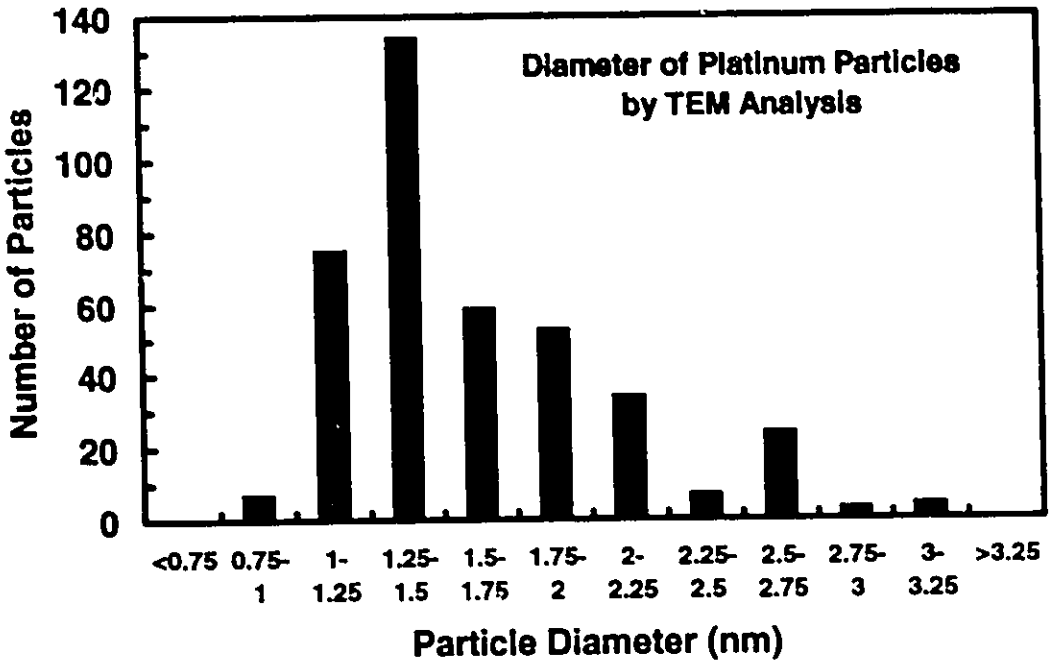
Diameter of Platinum Particles
by TEM Analysis
Number of Particles
140
120
100
80
60
40
20
0
<0.75
0.75-1
1-1.25
1.25-1.5
1.5-1.75
1.75-2
2-2.25
2.25-2.5
2.5-2.75
2.75-3
3-3.25
>3.25
Particle Diameter (nm)

To show that the method used to support the platinum nanoparticles was not an artifact of the Stöber silica surface, crystalline alumina (Figure 5.4) and silica gel (Figure 5.5) were modified using TES and Karstedt's catalyst under the same conditions used for Si-TES-Pt.[29] TEM analysis of the cleaned alumina and silica gel materials demonstrated that platinum nanoparticles having an average diameter of 3 nm were uniformly distributed on the Si-H-modified support materials. A few larger particles, 4-5 nm in diameter, were also observed as shown in Figures 5.4 and 5.5.

While the presence of Si-H groups is necessary for the formation of the supported platinum nanoparticles, they do not control the platinum nanoparticle size. Rather, the control of size appears to be provided by the hydridosilsesquioxane structure (on the Si-TES surface). To demonstrate this, identical Si-OH was modified with a silane $EtOSiHMe_2$ (DMES), which cannot form a network structure, but rather binds with a surface monolayer or less to give Si-DMES (Scheme 5.2).[13] Subsequent reaction of Si-DMES with Karstedt's catalyst led to the formation of platinum aggregates (see Figure 5.1 (Bottom photo)) on the silica surface.

Figure 5.4. TEM micrograph of alumina particles modified with TES which have been treated with Karstedt's catalyst (Scale bar = 50 nm).

The catalytic properties of Si-TES-Pt (Figure 5.1 (top photo)) were demonstrated by using them in a hydrosilation reaction with phenylacetylene and bis(trimethylsiloxy)methylsilane to give *E*-PhCH=CHSiMe($OSiMe_3$)$_2$ and H_2C=CHPh(SiMe($OSiMe_3$)$_2$).[30,31] A single catalyst sample was effective in 3 consecutive reactions with no indication of poisoning. Furthermore, TEM examination of Si-TES-Pt following three hydrosilation reactions showed no indication of platinum agglomeration. This behavior is in marked contrast to Karstedt's catalyst which initially promotes hydrosilation in high yields but quickly degenerates into almost completely inactive metal aggregates.

Figure 5.5. TEM micrograph of silica gel modified with TES after treatment with Karstedt's catalyst (Scale bar = 100 nm).

5.3 Conclusion

In summary, we have demonstrated that Si-H groups grafted to silica can be used to prepare supported nano-sized platinum particles that are catalytically active towards hydrosilation reactions. We speculate that the hydridosilsesquioxane network structure constrains the growth of the particles and prevents their aggregation.

The method described herein to prepare supported platinum particles may prove to be an attractive system to study the actual catalytic species involved in the hydrosilation reaction. The focus of future work will be to extend the preparation procedure to other metal compounds and to elucidate the structure of the platinum species and the platinum particle growth mechanism[32] in the presence of hydridosilsesquioxane modified silica. See Appendix A5.2.

Appendix A5.1

Figure A5.1-1. Selective reduction of silver from photographic waste solutions. Top photo: (a) The Si-TES-Pt particles were used to selectively reduce silver ions in photographic waste solutions. The TEM shown on the opposite page consists of Si-TES-Pt particles which were mixed with a photographic fixer waste solution (from color development). The image shows a "snapshot" after mixing the particles with the waste solution for 2 hours and cleaning them by centrifugation/redispersion cycles with water at pH=6.8. The micrograph shows that the silver in solution was selectively reduced on the Si-TES-Pt surface. Scale bar = 100 nm. Bottom spectrum: (b) X-ray microanalysis spectrum of Si-TES-Pt after reaction with silver waste solution. The particles were probed and silver was detected. The other signals, sodium and sulfur are from components in the waste solution. Copper is detected from the grid used to support the particles for the TEM analysis.

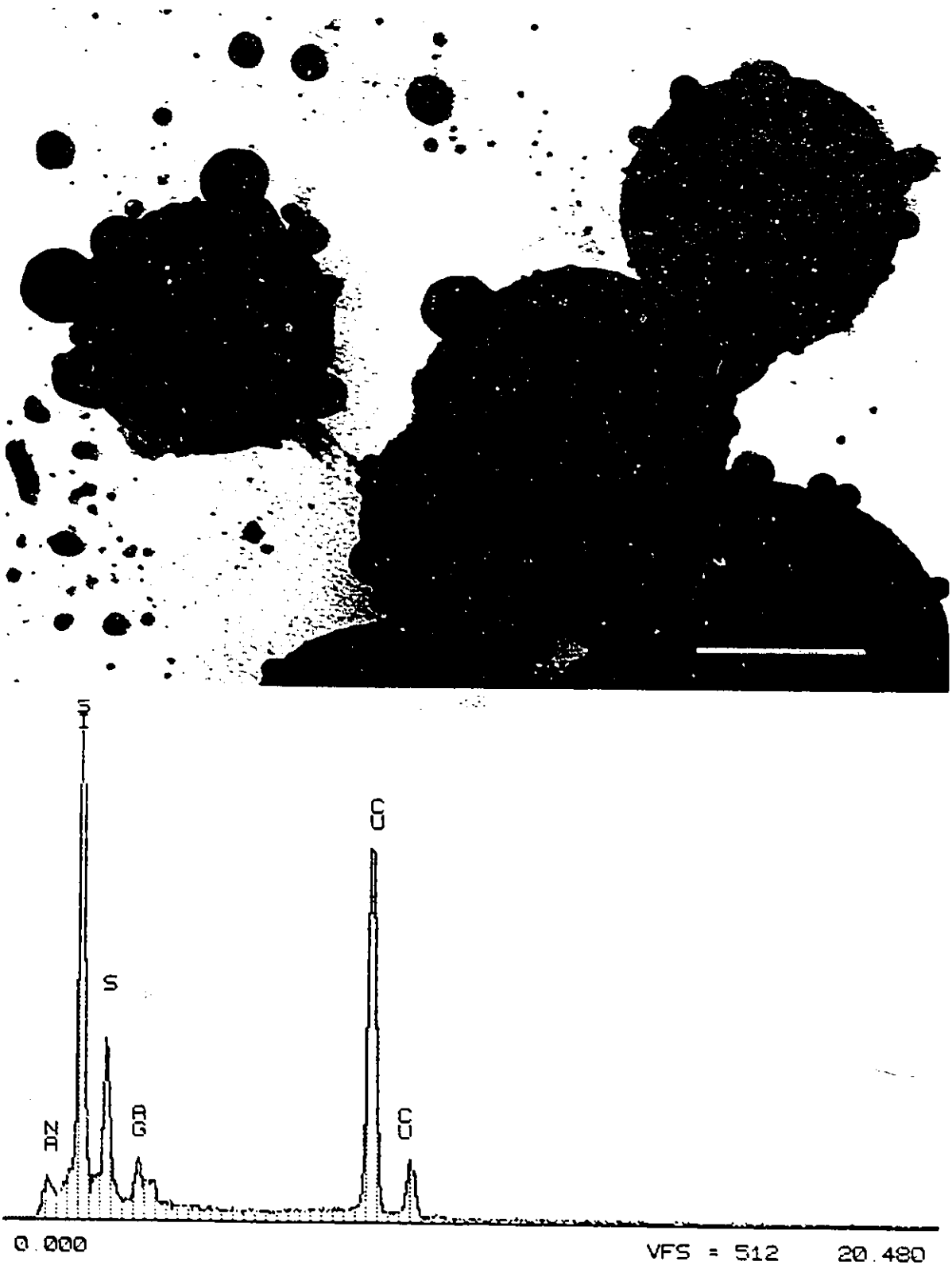
Si
S
Ag
Au
Cu
Cu
0.000
VFS = 512
20.480

Appendix A5.2

Figure A5.2-1. ^{29}Si CP - MAS solid state NMR: Top spectrum: (a) Si-TES; and Bottom spectrum: (b) Si-TES-Pt.

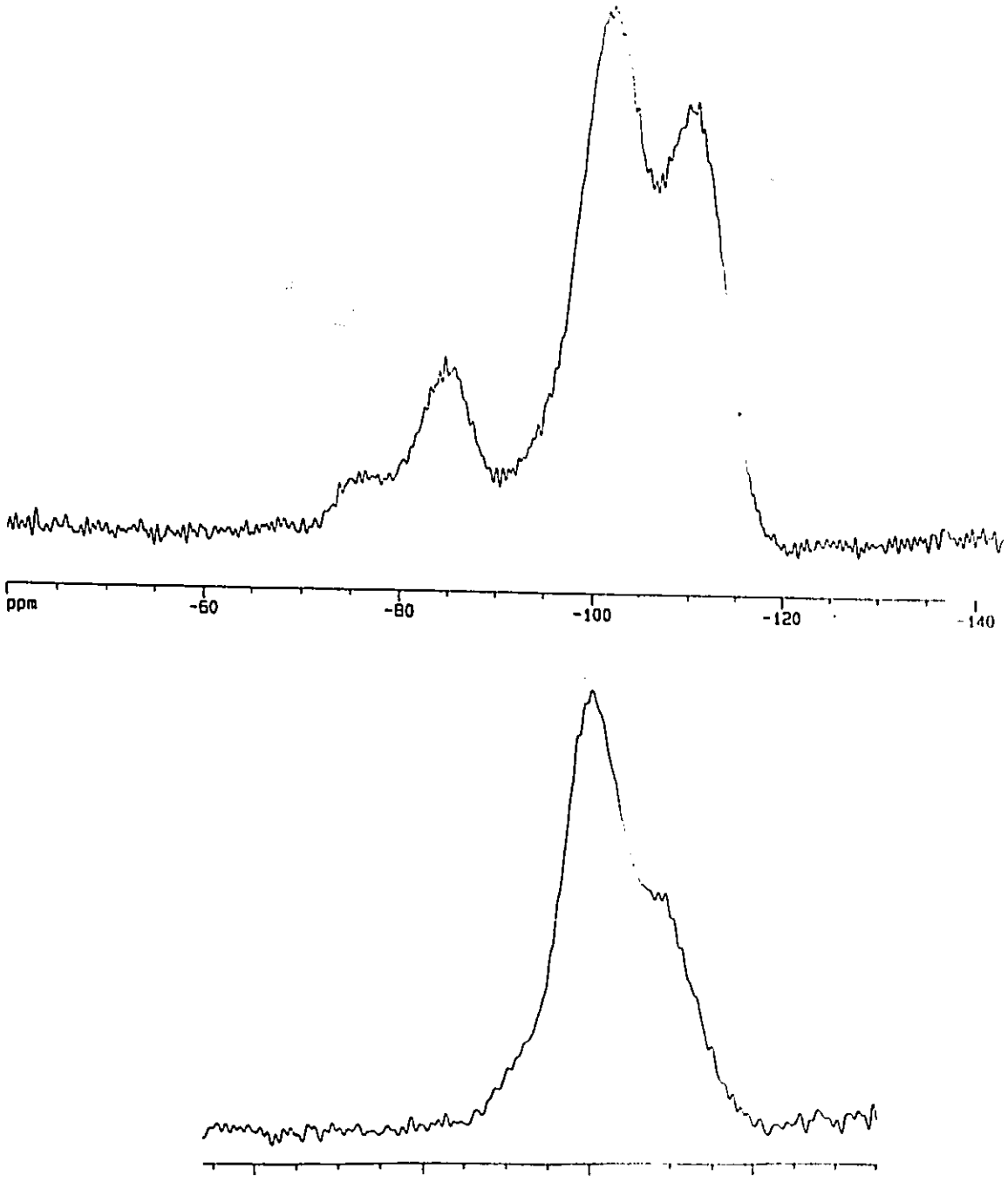

In Figure A5.2-1, the signal at -75.2 ppm was assigned to the $HSi(OH)(OSi)_2$ unit and the signal at -84.6 ppm corresponds to $HSiO_{3/2}$. Further details are given in Chapter 6. After reaction of Si-TES with Karstedt's catalyst to give Si-TES-Pt, the ^{29}Si spectrum shown in Figure 5.2b showed that the signals corresponding to the Si-H species disappeared. One possibility for the decrease in the Si-H signal is that the Karstedt's catalyst is being hydrosilylated onto the Si-TES surface. In this respect, the first step towards the Pt nano-particle growth could be illustrated as given in Scheme A5.1-1. The initial step towards the formation of the platinum nanoparticles may (*i.e.*, R_3Si-Pt-H) be due to a formal oxidative addition step of the Si-H bond. Most truly homogeneous hydrosilation catalysts are believed to react by a oxidative, insertion, and reductive elimination mechanisms.[33]

Scheme A5.1-1. Proposed genesis of platinum nanoparticle growth on silica surface.

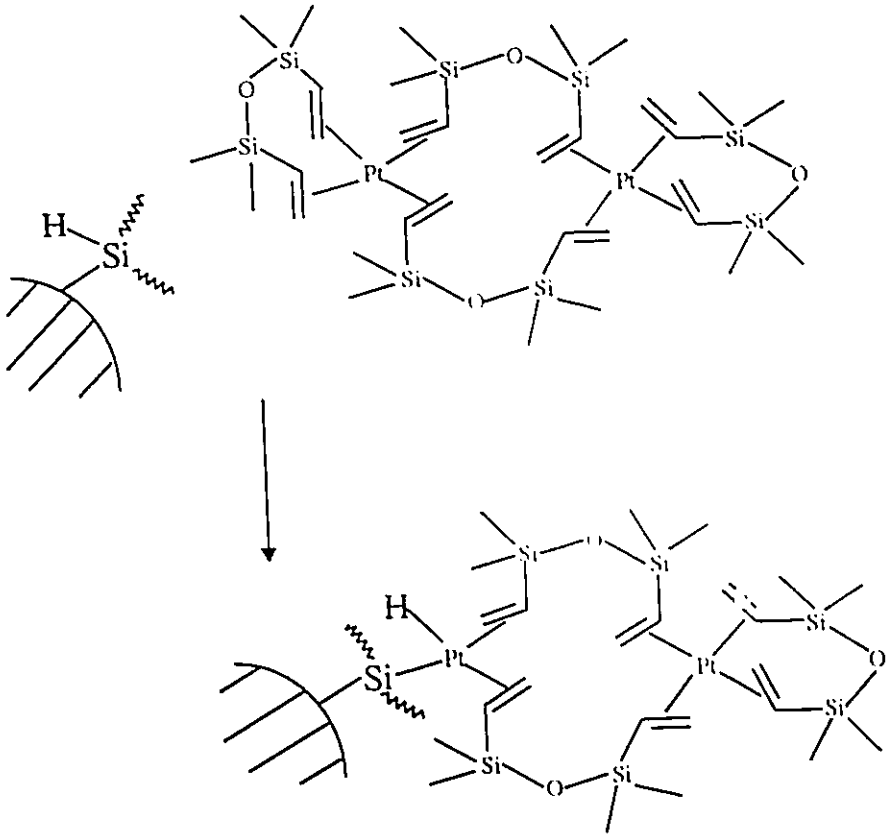

5.5 References

[1] (a) Saam, J.C.; Speier, J.L. *J. Am. Chem. Soc.* **1958**, *80*, 4104. (b) Speier, J.L. *Adv. Organomet. Chem.* **1979**, *17*, 407.

[2] (a) Karstedt, B.D. U.S. Patent 3 775 452 1973. (b) Chandra, G.; Lo, P.Y.; Hitchcock, P.B.; Lappert, M.F. *Organometallics* **1987**, *6*, 191. (c) Lewis, L.N.; Colborn, R.E.; Grade, H.; Bryant, Jr., G.L.; Sumpter, C.A.; Scott, R.A. *Organometallics* **1995**, *14*, 2202.

[3] (a) Lukevics, E.; Belyakova, Z.V.; Pomerantseva, M.G.; Voronkov, M.G. *Organomet. Chem. Rev.* **1977**, *5*, 1. (b) Parshall, G.W., Ittel, S.D., *Homogeneous Catalysis;* John Wiley: New York, 1992, p. 39.

[4] Although the term "platinum colloids" was used by the Lewis group, we have used the general term "nanoparticles" to describe the platinum particles prepared in this work. See Lewis, L. N. *Chem. Rev.* **1993**, *93*, 2693 for a detailed discussion on the distinctions and similarities between metal clusters and metal colloids and a complete review of the literature on platinum group metal colloids. The distinction between metal colloids and metal clusters has been discussed by Schmid (see Schmid, G. *Endeavour* **1990**, *14*, 172) where the size of metal clusters was defined as being less than or equal to 10 nm. Using this definition, metal colloids would be considered to be greater than 10 nm.

[5] Lewis, L.N.; Lewis, N. *J. Am. Chem. Soc.* **1986**, *108*, 7728.

[6] (a) Lewis, L.N. *J. Am. Chem. Soc.* **1990**, *112*, 5998. (b) Lewis, L. N.; Uriarte, R. J. *Organometallics* **1990**, *9*, 621.

[7] The absence or depletion of oxygen in the hydrosilation reaction environment has been attributed to the darkening color of the platinum mixture over time. This color change reflects the formation of larger size colloids whose catalytic activity is reduced. It has been proposed that oxygen prevents irreversible platinum colloid (derived from Karstedt's catalyst) aggregation. See reference 6a.

[8] (a) Lewis, L.N.; Lewis, N. *Chem. Mater.* **1989**, *1*, 106. (b) Lewis, L.N.; Uriarte, R.J.; Lewis, N. *J. Catal.* **1991**, *127*, 67. (c) Lewis, L.N.; Lewis, N.; Uriarte, R.J., *Homogeneous Transition Metal Catalyzed Reactions*; Advances in Chemistry Series 230; American Chemical Society: Washington, DC, 1992; p. 541.

[9] For other related studies reporting the reduction of metal salts using hydrosilanes, see: (a) Anderson, H.H. *J. Am. Chem. Soc.* **1958**, *80*, 5083. (b) Keinan, E.; Greenspoon, N. *J. Am. Chem. Soc.* **1986**, *108*, 7314. (c) Tour, J.M.; Pendalwar, S.L.; Cooper, J.P. *Chem. Mater.* **1990**, *2*, 647. (d) Tour, J.M.; Cooper, J.P.; Pendalwar, S.L. *J. Org. Chem.* 1990, 55, 3452. (e) Tour, J.M.; Pendalwar, S.L. *Tetrahedron Lett.* **1990**, *31*, 4719. (f) Nadkarni, D.V.; Fry, J.L. *J. Chem. Soc., Chem. Commun.* **1993**, 997. (g) Kini, A.D.; Nadkarni, D.V.; Fry, J.L. *Tetrahedron Lett.* **1994**, *35*, 1507. (h) Fry, J.L.; Nadkarni, D.V. U.S. Patent 5,281,440, 1994. (i) Reed-Mundell, J.J.; Nadkarni, D.V.; Junz, Jr., J.M.; Fry, C.W.; Fry, J.L. *Chem. Mater.* **1995**, *7*, 1655.

[10] The Lewis group has characterized the products formed during hydrosilation reactions. See, Lewis, L.N.; Stein, J.; Smith, K.A.; Messmer, R.P.; Legrand, D. G.; Scott, R. A. "Recent Mechanism Studies on Hydrosilylation", *Progress in Organosilicon Chemistry*, Chojnowski, J.; Marciniec, B.; Eds., Gordon and Breach: Basel, 1995, pp. 263-285.

[11] The term "platinum nanoparticles" used throughout this paper should not be regarded as meaning they are only composed of bulk platinum metal. Although we do not know the specific chemical identity of the supported metal species, work by the Lewis group (see reference 10)

suggests the platinum species formed during the hydrosilation reaction contains both platinum and silicon.

[12] Marzán, L. Liz; Philipse, A.P. *Colloids Surf.* **1994**, *90*, 95.

[13] Ketelson, H.A.; Brook, M.A.; Pelton, R. *Chem. Mater.* **1995**, *7*, 1376.

[14] For other Si-H modification procedures reported using silica gel as the substrate see (a) Bräuer, L.; Gruber, H.; Greber, G. *Angew. Makromol. Chem.* **1990**, *180*, 209. (b) Sandoval, J.E.; Pesek, J.J. *Anal. Chem.* **1989**, *61*, 2067. (c) Sandoval, J.E.; Pesek, J.J. U.S. Patent 5,017, 540, 1991. (d) Le Déoré, C.; Révillon, A.; Hamaide, T.; Guyot, A. *Polymer*, **1993**, *34*, 3048. (e) See also, references 9(g - i).

[15] Stöber, W.F.; Fink, A.; Bohn. E. *J. Colloid Interface Sci.* **1968**, *26*, 62.

[16] Ketelson, H.A.; Brook, M.A.; Pelton, R. *Polymers Adv. Tech.* **1995**, *6*, 335.

[17] ^{29}Si CP-MAS δ (ppm) : -75.2, -84.6, -101.9, -110.8. IR, cm^{-1}: 2251 s. Elemental analysis: 4.12%C , 1.45%H, 43.88%Si.

[18] (a) Pauthe, M.; Phalippou, J.; Corriu, R.; Leclercq, D.; Vioux, A. *J. Non-Cryst. Solids* **1989**, *113*, 21. (b) Belot, V.; Corriu, R.; Leclercq, D.; Mutin, P.H.; Vioux, A. *Chem. Mater.* **1991**, *3*, 127. (c) Tour, J.M.; Kafka, C.M. *Adv. Mater.* **1993**, *5*, 47. (d) Soraru, G.D.; D'Andrea, G.; Campostrini, R.; Babonneau, F. *J. Mater. Chem.* **1995**, *5*, 1363.

[19] To a suspension of Si-TES (0.1 g) dispersed in THF (10 mL) was added Karstedt's catalyst[19] (0.15 g, 3.1 mg Pt) under a dry atmosphere which after heating for 8 h at 60°C yielded a translucent yellow dispersion. The product, Si-TES-Pt, was cleaned with THF using 4 x centrifugation/redispersion and sonication cycles.

[20] Elemental analysis performed by Guelph Chemical Laboratories, Guelph, Ont., Canada showed 3.78%C, 1.27%H, 40.14%Si, 0.53%Pt.

[21] A JEOL 1200 EX TEM (80 kV) was used to examine and image all specimens. For TEM imaging of the silica particles in whole, a drop of the colloidal dispersion was put on a 200 mesh nickel grid with a support film and air dried.

[22] Slices of the silica particles, approximately 50 nm thick, were prepared by embedding the particles in epoxy resin and sectioning with an ultramicrotome.

[23] The silver enhancement experiments were carried out as follows. The whole mount particles were prepared as described above. The developer consisted of citrate buffer (5 parts of 2.3 M citric acid (BDH) and 2 parts of 1.6 M sodium citrate (BDH)) at pH 3.6, 17% gum arabic (Fluka), 0.6% hydroquinone (BDH), and 0.35% silver lactate (lactic acid, silver salt (Sigma)). A grid was incubated in the developer at room temperature for 15 min followed by incubation in Kodak rapid fix (diluted 1:4 with water) for 4 min at room temperature. Both incubation steps were performed in the dark. The grid was thoroughly washed with water before examining in the electron microscope.

[24] (a) James, T.H. *J. Am. Chem. Soc.* **1939**, *61*, 648. (b) Danscher, G.; Norgaard, J.R. *J. Histochem. Cytochem.* **1981**, *29*, 531. (c) Danscher, G.; Norgaard, J.R. *J. Histochem. Cytochem.* **1983**, *31*, 1394.

[25] Using the procedure described in reference 23 there was no detection by TEM analysis of silver growth directly from the silica surfaces bearing only Si-H groups. We note, however, that silver reduction (as evidenced by the formation of a black color) occurred during the addition of aqueous silver lactate to Si-TES. Examination of Si-TES samples by TEM, after being mixed with the silver solution for 30 min, showed that the silver was only dispersed in the interstitial spaces. See reference 9(i) for a method which is claimed to deposit ultrathin layers of silver on silica gel modified with Si-H groups.

[26] Niederprum, H. *Angew. Chem., Int. Ed. Engl.* **1974**, *14*, 614.

[27] Hamilton, J.F.; Baetzold, R.C. *Science* **1979**, *205*, 1213.

[28] Karstedt's catalyst (0.1 g, 0.82 mM Pt) was added to a THF solution (5 mL) containing triethoxysilane (0.2 mL, 1.1 mmol). Hydrogen gas evolution was immediately observed after adding the platinum catalyst to the solution which became yellow after 15 min of stirring. The particle size distribution was narrow with a mean diameter of 2 ± 1 nm based on TEM analysis by measuring 400 particles prepared on a carbon film.

[29] Aluminium oxide powder (0.2g, Johnson Matthey, <1 μm, alpha 99.99%) was dispersed into 75 mL acetone (99.5 wt%) by sonication and triethoxysilane (2.8 mL, 15 mmol) was added under a nitrogen atmosphere. The dispersion was refluxed under a positive nitrogen pressure for 36 h. ^{29}Si CP-MAS δ (ppm) : -75, -85, -102. After washing the alumina with THF 3 x centrifugation/redispersion cycles, the modified alumina was dispersed in THF (10 mL) to which Karstedt's catalyst (0.16 g, 3.2 mg Pt) was added.

[30] A typical experiment: To a solution consisting of bis(trimethylsiloxy)methylsilane (4.9 g, 22 mmol) and phenylacetylene (2.3 g, 22 mmol) was added Si-TES-Pt (0.3 g) dispersed in THF (5 mL). After heating at 60°C for 8 h, the solids were removed by centrifugation and the supernatant was analyzed by ^{1}H NMR spectroscopy. The solids were washed 3 x THF using centrifugation/redispersion cycles before use in a subsequent hydrosilation reaction.

[31] ^{1}H NMR analysis of the hydrosilation product mixture showed 61% of the E isomer, $PhCH{=}CHSiMe(OSiMe_3)_2$, obtained from the β addition, and 39% of the α product, $Ph(SiMe(OMe_3)_2)C{=}CH_2$. This was verified from the ratios of the vinyl signal areas obtained by integration of their respective ^{1}H NMR signals. β (*E*-isomer): ^{1}H NMR ($CDCl_3$) δ (ppm) 0.12 (s, 3H), 0.17 (s, 18H), 6.25 (d, 1H, J=19 Hz), 6.95 (d, 1H, J=19 Hz), 7.2-7.4 (m, 5H). α isomer: ^{1}H NMR ($CDCl_3$) δ (ppm) 0.05 (s, 3H), 0.19 (s, 18H), 5.69 (d, 1H, J=3 Hz), 5.90 (d, 1H, J=3 Hz), 7.2-7.4 (m, 5H).

[32] Whitesides and co-workers have studied the platinum catalyzed reaction of dialkyl(diolefin)platinum(II) complexes with dihydrogen in the presence of glass beads coated

with Pt(0). McCarthy, T.J.; Shih, Y.-S.; Whitesides, G.M. *Proc. Natl. Acad. Sci. USA* **1981**, *78*, 4649. More recently, work has appeared which describes in detail the mechanism of formation of Ir sols which may be generally applicable to the formation of metal nanoparticles. Lin, Y.; Finke, R.G. *J. Am. Chem. Soc.* **1994**, *116*, 8335.

[33] Harrod, J.F.; Chalk, A.J. "Hydrosilation Catalyzed by Group VIII Complexes"; in I. Wender and P. Oino, Eds., *Organic Synthesis via Metal Carbonyls*; Wiley - Interscience: New York, Vol. 2, 1977, pp. 673-704.

Chapter 6

Surface and Colloidal Properties of Hydrosilane Modified Silica Dispersions

Abstract

Triethoxysilane (TES), $HSi(OEt)_3$ was used to functionalize Stöber silica and the resulting particles were characterized in acetone and water by light scattering, disk centrifugal photosedimentometry, microelectrophoresis, transmission electron microscopy, and ^{29}Si CP-MAS and ^{1}H MAS NMR spectroscopy. Using 38 mM TES (polyTES38) and 75 mM TES (polyTES75) the thicknesses of the polyTES layer bound to the silica surfaces were 7.6 and 8.2 nm, respectively. Using an initial concentration of 150 mM TES, polyTES150 coagulated in acetone as reflected by broad particle size distributions. In the pH range of 5.0 to 9.0, the polyTES38 particle diameter increased from 191 to 200 nm indicating a dynamic polyTES layer existed in the interfacial region. ^{1}H MAS NMR spectra of polyTES38 showed narrowed ^{1}H line widths suggesting the presence of a mobile Si-H species on the silica surface in which the polyTES polymer bound to the surface was above its glass transition temperature. The

critical coagulation concentrations (c_c's) determined for SiOH and polyTES38 using CaI_2 were 10 and 11.5 mM, respectively. TEM analysis of SiOH and polyTES mixed with 11 mM CaI_2 showed the polyTES layer underwent phase separation.

6.1 Introduction

In the last decade there has been increasing interest in applying silane coupling agents to colloidal silica prepared according to the Stöber method.[1,2] The Stöber particles, formed *viz.* the base catalyzed hydrolysis and condensation of tetraethylorthosilicate in an aqueous mixture containing ethanol and ammonia, are colloidally stable, have a narrow size distribution and have a spherical geometry. These particle properties permit studies (electrokinetic, light scattering) of the particle surface properties following silane modification procedures which are difficult to do using the other silica materials which are less defined (*e.g.*, precipitated and fumed silica).

In a recent paper, we reported the preparation of hydrosilane (Si-H) modified silica particles using triethoxysilane (TES), $HSi(OCH_2CH_3)_3$.[2a] The TES reacted to form a hydrosilane polymer layer (the modified particles are subsequently referred to as "polyTES") on the silica with a hydrodynamic thickness of 13 nm. The treated silica particles were colloidally stable in acetone and THF. More recently, we have shown the polyTES particles can be used to immobilize 1-3 nm diameter Pt nanoparticles on the silica surface.[3] It was postulated that the Pt nanoparticles were immobilized by the presence of the polyTES layer and thus did not cluster to form macrosize Pt particles.

experiments confirmed that without silica or the polyTES surface layer on the silica surface, the Pt nanoparticles were not formed.

The general utility of Si-H modified colloidal silica as a support for nano-metal particles, in part, depends on maintaining the colloidal stability. Although our initial work indicated good stability of polyTES particles in acetone and THF, we did not know the mechanism(s) controlling the polyTES colloidal stability. We have therefore investigated and report herein the colloidal and surface properties of the polyTES particles. Information such as the polymer thickness, grafting density, and surface dynamics at the interface were obtained to provide a molecular picture of the TES polymer bound to the silica surface.

6.2 Experimental

Materials.

Acetone (Caledon, glass distilled and dried, water content from Karl Fisher titration is 0.3 wt%) and calcium iodide $CaI_2 \cdot (H_2O)_{6-8}$ were used as received. Triethoxysilane (TES) (Aldrich, 95%) and dimethylethoxysilane (DMES) (United Chemical Technologies, 98%) were vacuum distilled prior to use.

Particle Characterization.

Solid-state Nuclear Magnetic Resonance Spectroscopy: A Bruker ASX-200 spectrometer operating at 39.75 MHz for silicon was used to obtain ^{29}Si cross polarization (CP) / magic angle spinning (MAS) solid state spectra. Spectra were accumulated using 16K data points. The spinning frequency of the sample in a ziroconia rotor was 4 kHz, the sweep width was 8400 Hz and contact times were varied between 1-5 ms. The recycle time was 4.05 s and the acquisition pulse at 90° was 4.8 µsec. All spectra were acquired with high power ^{1}H decoupling during acquisition.

^{29}Si MAS experiments with ^{1}H high power decoupling (without CP) were performed using a recycle delay of 2 min and 4 µs pulse corresponding to a tip

angle of 90°. All other acquisition parameters were the same as described for the ^{29}Si CP-MAS experiments.

^{1}H MAS solid state spectra were performed on a Bruker ASX-200 spectrometer operating at 200.103 MHz. Spectra were accumulated using 16K data points. A spinning frequency of 6 kHz was employed and the sweep width was adjusted to 200 kHz. The recycle time was 4.0 s and the acquisition pulse was 4.8 µsec corresponding to a tip angle of 90°.

FT - IR Spectroscopy. A Bio-RAD spectrophotometer was used to record the spectra which were measured from 4000 to 400 cm^{-1} and the number of scans was typically 64 with a resolution of 8 cm^{-1}. The sample chamber was purged several times with dry nitrogen before sample analysis. Solid samples were analyzed by preparing KBr pellets. The empty chamber was used as the background file.

Intensity Light Scattering. Dust free silica dispersions were prepared by successively rinsing all glassware with acetone, Mill-Q water, a 2% HF solution followed by several washings using Milli-Q water. All the solvents and salt solutions used to prepare the particle dispersions were filtered through 0.2 µm Millipore filters. The core diameter of the modified particles was obtained by

intensity light scattering using the dissymmetry method.[4] A Brookhaven Instruments (Holtsville, NY) photon correlation spectrometer fitted with a Brookhaven Model BI - 9000AT digital correlator and a Lexel (Fremont, CA) Model 95 Ar ion laser operating at a power of 150 mW was used.

The dissymmetry method is based on the angular dependance of light scattered by large particles, *i.e.*, $d > (\lambda_0/n)/20$ where d corresponds to the particle diameter, λ_0 is the wavelength of light and n is the refractive index of the dispersion medium. Seebergh and Berg have recently applied the dissymmetry method to determine the core size of a monodisperse sample of "hairy" polystyrene latex particles.[5] The dissymmetry ratio, Z, is defined by

$$Z = \frac{I_\theta}{I_{(180-\theta)}} \qquad [6.1]$$

where I_θ is the total scattered light measured at angle θ.

Z is related to the shape factor, $P(\theta)$, which varies with the angle of observation and is related to Z as follows

$$\frac{I_\theta}{I_{(180-\theta)}} = \frac{P_\theta}{P_{(180-\theta)}} \qquad [6.2]$$

where

$$P_\theta = \left[\left(\frac{3}{x^3}\right)(\sin x - x\cos x)\right]^2 \qquad [6.3]$$

and x is given by

$$x = 2\pi\left[\frac{d_c}{\lambda_0 n}\right]\sin\left(\frac{\theta}{2}\right) \qquad [6.4]$$

The particle's radius of gyration, R_g, can be related to the core particle radius, R_c, since the Stöber silica particles are characterized by a spherical geometry and narrow size distributions. For a homogeneous sphere, $R_g^2=(3/5)R_c^2$. The core diameter is therefore $d_c=2R_c$.

In the present study, the core sizes for both unmodified and modified silica using 75 mM TES (polyTES75) at pH=7.5 were determined using four different particle number concentrations (particles/cm^3); 6.3x10^8, 12.6x10^8, 18.9x10^8, and 25.2x10^8. The angle pairs at 45° and 135°, and 55° and 125°, were used to obtain Z. The scattering from the solvent and the background intensity (dark counts) were subtracted from the total intensity. The core size was determined by plotting Z versus the particle number concentration.

Critical coagulation concentrations (c_c). c_c's for silica dispersions using CaI_2 solutions at pH=7.5 ± 0.2 were determined from plots of the stability ratio (W) as a function of salt concentration (c).[6] W is defined by the following expression which gives the ratio of rate constants for doublet formation:

$$W = \frac{k_f}{k_s} \qquad [6.5]$$

where k_s is the rate constant for the slow aggregation regime where not every particle collision will result in permanent contact and k_f is the Smoluchowski diffusion-limited fast aggregation constant given by the following equation:[7]

$$k_f = \frac{8k_BT}{3\eta} \qquad [6.6]$$

Here k_B is Boltzmann's constant, T is the temperature, and η refers to the viscosity of the continuous phase.

Experimental stability ratios (W) were calculated by obtaining k_s according to the following expression developed by Virden and Berg:[8]

$$k_s = \frac{1}{r_{H_0}(\alpha)N_0}\left[\frac{dr_H}{dt}\right]_{t=0} \qquad [6.7]$$

where r_{H_0} corresponds to the initial hydrodynamic radius at t=0, α is an optical factor, N_0 is the initial particle number concentration, and $\frac{dr_H}{dt}$ is the measured initial slope extrapolated to t=0. The silica particle concentration used in the kinetic experiments was 6.3×10^8 particles cm^{-3} and α was 0.35.

Disk Centrifugal Particle Sizing (DCP). Particle size distributions were examined in acetone and water using a BI-DCP disk centrifuge photosedimentometer (Brookhaven Instruments Corp.) at 25°C. The homogeneous method was used to analyze the dispersions.[2a] Particle dispersions having 4.3 g solids / L of either acetone or water were prepared. 15 mL of the dispersion was injected via syringe into the polycarbonate disk and run times between 10-20 min were typically needed to obtain constant baselines. The silica density used to calculate the particle sizes was 1.70 g cm^{-3}. Volume mean averages were using the BI-DCP software (version 5.02).

In a previous study for the SiOH particles it was shown that similar particles sizes between the DLS and DCP data can be obtained when silica

particle densities in the DCP experiments are in the range of 1.65-1.75 g cm^{-3}.[12] The density reported for the SiOH silica which was lower than those usually quoted for silica particles (*i.e.*, 2.0 g cm^{-3}) was believed to reflect the microporous nature of Stöber silica. In comparison, the TES particle diameters obtained from the DCP experiments were calculated to be the same as that obtained from the DLS measurements when a density of approximately 1.7 g cm^{-3} was used instead of 2.0 g cm^{-3}. These calculations suggest that the densities of the silica corona and the TES layers covering the particle surface are similar.

Microelectrophoresis. The electrophoretic mobilities for the silica samples in water and acetone were measured using a Coulter DELSA. Details of the experimental procedure have been published elsewhere.[9]

Syntheses.

The preparation, characterisation and surface modification of Stöber silica with TES has been described in a previous paper.[2a] A brief summary of the modification procedure is described below. The Stöber particles were prepared for modification by first washing them with absolute ethanol using 5 x centrifugation/redispersion cycles followed by 5 x centrifugation/redispersions using acetone. The organosilane was added to a clean and colloidally stable acetone/silica dispersion containing 0.5

g solid / 200 mL solvent. The hydrosilane concentrations used to modify the silica particles were 38, 75, and 150 mM, respectively. The mixture was stirred at 60°C under a stream of nitrogen for 36 h. The silica was subsequently cleaned free of unreacted silanes using 5 x centrifugation/redispersion cycles with acetone.

polyTES38 and 75.

IR (DRIFTS) v:Si-H 2251 cm^{-1} v strong; this peak was not observed in Si-OH. The Si-H peak is found at 2225 cm^{-1} for neat TES. ^{29}Si NMR (CP-MAS) δ(ppm): -75.2, -84.6, -101.9, -110.8. ^{1}H MAS δ(ppm): 4.0 (broad), 2.0, 1.0. ^{1}H MAS (w/ D_2O) δ(ppm): 4.4 (broad).[10]

6.3 Results

A 184.6±0.3 nm diameter sample of Stöber silica was divided into two samples; one was called polyTES38 and treated with a 38mM TES acetone solution whereas the other, polyTES75, was reacted with a 75mM TES acetone solution. The properties of these two polyTES samples are described in the following sections.

Elemental Analysis. The carbon, hydrogen and silicon wt % contents for the unmodified silica (SiOH) and polyTES samples are given in Table 6.1. The elemental analysis results showed both SiOH and SiTES samples contained substantial amounts of carbon and hydrogen. For example, SiOH contained 3.40% C, 1.07% H, and 45.86% Si. The detection of carbon in the SiOH sample was expected since it has been previously shown that several percent of the ethoxy groups remain attached to TEOS under base catalyzed conditions.[11] Quantitative ^{29}Si CP-MAS solid-state NMR results have indicated that the relative abundances of silicon species making up the Stöber particle (unmodified) composition are 4% Q_2, 38% Q_3 and 58% Q_4.[11a]

Table 6.1. Elemental analysis results for unmodified silica, SiOH, and TES modified silica using 38 and 75 mM TES.

	SiOH	polyTES38	polyTES75
Weight % C	3.40	4.36	4.55
C atoms per nm^2	-	121	145
Weight % H	1.07	1.37	1.42
H atoms per nm^2	-	362	437
Weight % Si	45.86	43.81	42.59
Si atoms per nm^2	-	60	73

Following treatment of the silica with TES, the elemental analysis results (Table 6.1) showed the carbon wt %'s for polyTES38 and polyTES75 were 4.36 and 4.55, respectively. This data for the polyTES samples indicated that not all the ethoxy groups of the TES coupling agent are lost upon surface treatment.

Light Scattering Properties. The influence of increasing the initial TES concentration on the final particle size was studied by DLS. The hydrodynamic particle diameters for the TES modified silica dispersions in acetone obtained at their respective initial TES concentration used to modify the particles are plotted

in Figure 6.1. The particle size results for the unmodified (SiOH) silica are also given in Figure 6.1.

The average particle diameter for SiOH dispersed in acetone was 184.6 ± 0.3 nm. After reaction with TES, the particle diameter (in acetone) was measured to be 199.9 ± 2.0nm and 200.9 ± 0.9 nm for polyTES38 and polyTES75, respectively. The thickness of the bound polymer on the silica surface can be calculated using the following expression:

$$\delta_p = \frac{1}{2}\left(d_{modified} - d_{SiOH}\right) \qquad [6.8]$$

where δ_p is the thickness of the bound polymer; $d_{modified}$ and d_{SiOH} correspond to the hydrodynamic diameters obtained by DLS for the TES modified and unmodified silica particles, respectively.

Intensity light scattering using polyTES75 in water at pH=7.5 was also performed based on the dissymmetry method (see Experimental section- 6.2). From the intensity light scattering experiment, the particle radius of gyration is obtained which can be related to the core particle radius assuming the polymer has a spherical geometry. The experiment showed the core diameter, D_c, for

polyTES75 was 186 ± 2nm which was within the experimental error of the hydrodynamic diameter, 184.6 ± 0.3nm, measured for SiOH.

Particles treated with 150 mM TES (polyTES150) had an average particle diameter obtained from DLS to be 230 nm. Figure 6.2 shows particle size distribution curves for SiOH, polyTES38, and polyTES150 obtained by disk centrifugal photosedimentometry (DCP) using acetone as the dispersion medium. Narrow particle size distribution curves with low polydispersities were observed for SiOH and polyTES38. By contrast, polyTES150 had a broad particle size distribution curve (see Figure 6.2) in which the average particle diameter was calculated to be 288 nm. Thus, treatment with 150 mM TES appeared to cause aggregation of the silica particles in acetone.

Figure 6.1. Influence of TES concentrations used to modify the silica particles on the hydrodynamic diameters, d_H, and the electrophoretic mobilities (dashed lines), μ_E. The measurements were performed after washing the silica particles with acetone to remove the unreacted TES. The silica particles were dispersed in acetone at 25 °C for the DLS and electrophoresis experiments. d_H is equal to 184.6±0.3 nm and μ_E is equal to -4.8±0.1 $m^2\ V^{-1}\ s^{-1}$ for unmodified silica, SiOH, in acetone; these values correspond to the plotted data where the TES concentration is equal to zero.

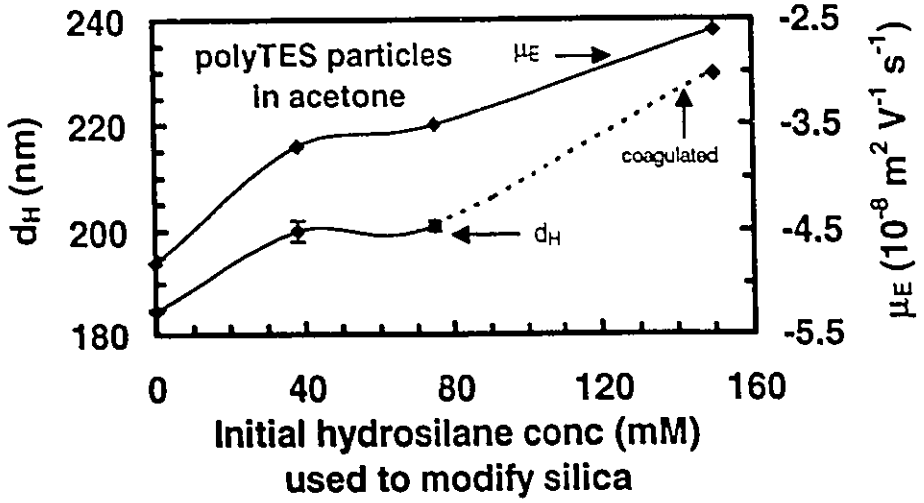

Figure 6.2. Volume-average particle size distribution curves obtained by disk centrifugal analysis for polyTES dispersions in acetone after modification with 38 and 150 mM TES concentrations. The particle sizes were calculated assuming a density of 1.7 g cm^{-3} for silica. The distribution curve for unmodified silica, SiOH, in acetone is also shown for comparison. The numbers below the captions for the distribution plots refer to the average particle size, d_{av}, of the dispersion.

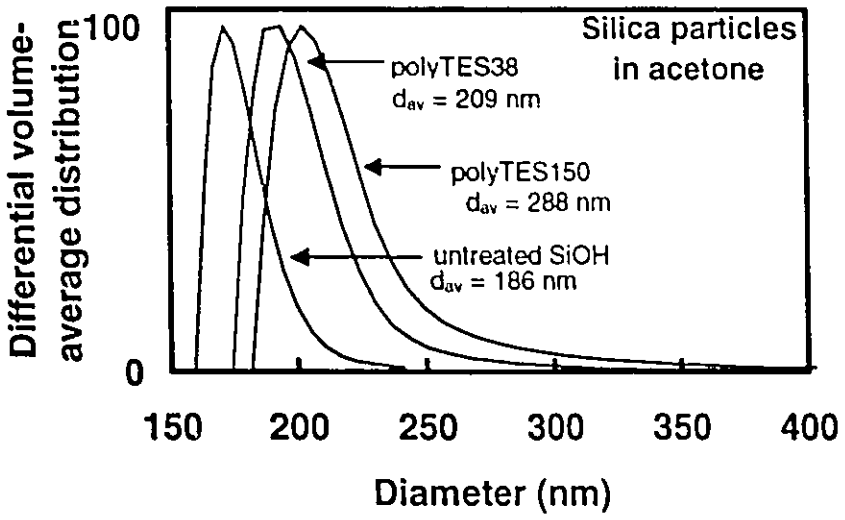

Figure 6.3 shows the effect of pH on the hydrodynamic particle diameters obtained by DLS for polyTES38 and SiOH. Also shown in Figure 6.3 are the hydrodynamic diameters of the untreated SiOH particle diameters as a function

of pH. The SiOH particle diameter measurements were within experimental error as the pH was raised from 4.6 to 8.2. By contrast, for polyTES38, the particle diameters increased from 190.7 ± 0.8 nm to 200.3 ± 1.1 nm when the pH changed from 5.0 to 9.0.

Electrokinetic Properties. The electrophoretic mobilities of the TES modified silica particles in acetone for polyTES using 38, 75, and 150 mM TES are shown in Figure 6.1. TES treatment decreased the electrophoretic mobility for all the treated silica samples. The electrokinetic properties of the untreated SiOH particles in acetone and acetone - water mixtures have been described in detail elsewhere.[12]

Electrophoretic mobility measurements were also carried out in aqueous solutions at pH 6.5 and 9.3. The mobility for SiOH at pH=6.5 was $-3.6 \pm 0.2 \times 10^{-8}$ $m^2\ V^{-1}\ s^{-1}$ whereas that for polyTES38 was $-2.7 \pm 0.1 \times 10^{-8}$ $m^2\ V^{-1}\ s^{-1}$.

Figure 6.3. Measurements of hydrodynamic diameters by dynamic light scattering for polyTES38 and SiOH silica dispersions as a function of pH.

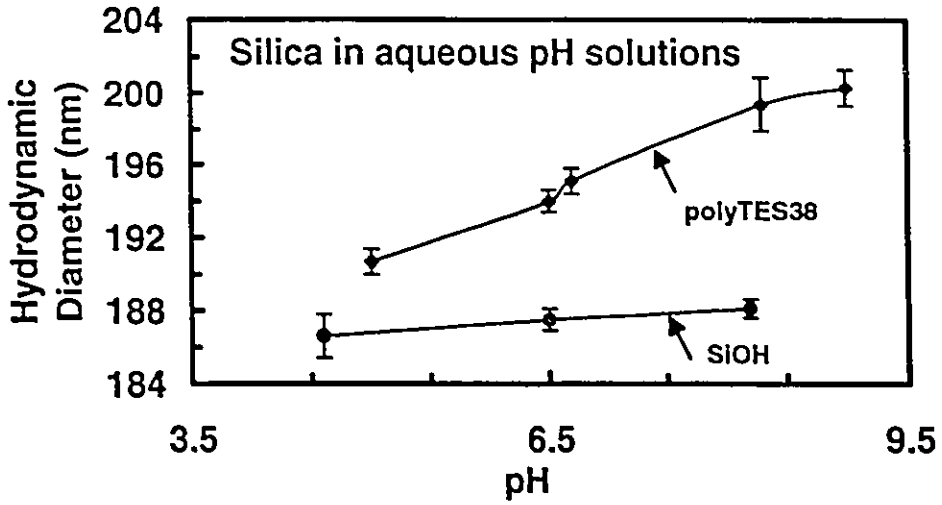

The lower mobility of the polyTES dispersions could reflect a lower concentration of surface silanols after the TES treatment. The trend was opposite at pH=9.3; the electrophoretic mobilities for SiOH and polyTES38 were $-4.4 \pm 0.1 \times 10^{-8}$ m^2 V^{-1} s^{-1} and $-4.6 \pm 0.2 \times 10^{-8}$ m^2 V^{-1} s^{-1}, respectively. The higher electrophoretic mobility of polyTES compared to SiOH at pH=9.3 may be due to the hydrolysis of the polyTES Si-H groups to give ionizable SiOH groups in alkaline conditions.[13]

Coagulation Studies. Stability of aqueous dispersions of SiOH and polyTES38 were measured as a function of CaI_2 and the results are shown in Figure 6.4. The kinetics were measured by DLS using the analysis of Virden and Berg.[8a] The critical coagulation concentrations (c_c) were taken at the intersection of the two aggregation regimes (slow *versus* fast). The c_c for SiOH was 10mM whereas the c_c for polyTES38 was 11.5mM. The ζ - potential obtained at the c_c for SiOH was -22mV compared with -19mV for the polyTES38 particles.

An interesting feature of the results shown in Figure 6.4 is that in the fast aggregation regime the stability ratios were not equal to 1. For example, Figure 6.4 shows for SiOH and polyTES38 that their stability ratio values displayed minima of 2.0 and 2.7, respectively. Previous work using polystyrene latices have reported similar findings which were explained by the presence of a "hairy layer" on the particle surface.[8b,14]. The polyTES layer on the silica surface could assume the same role. Similarly, a silicic acid surface gel layer has been proposed for silica.[12,15]

The effect of CaI_2 on the particle surface morphologies for SiOH and polyTES38 were investigated by TEM analysis. After mixing 11mM CaI_2 solution with the silica samples, TEM analysis showed the untreated SiOH and polyTES38 particles displayed different surface morphologies.

Figure 6.4. Stability ratios as a function of CaI_2 concentration at pH=7.5±0.2 obtained using DLS for unmodified silica, SiOH, and hydrosilane modified silica particles using polyTES38. The particle number concentration for all the dispersion samples was 6.3 x 10^8 particles cm^{-3}. The ζ-potentials were obtained for particle dispersions at their critical coagulation concentration (c_c) values and are displayed in the plot.

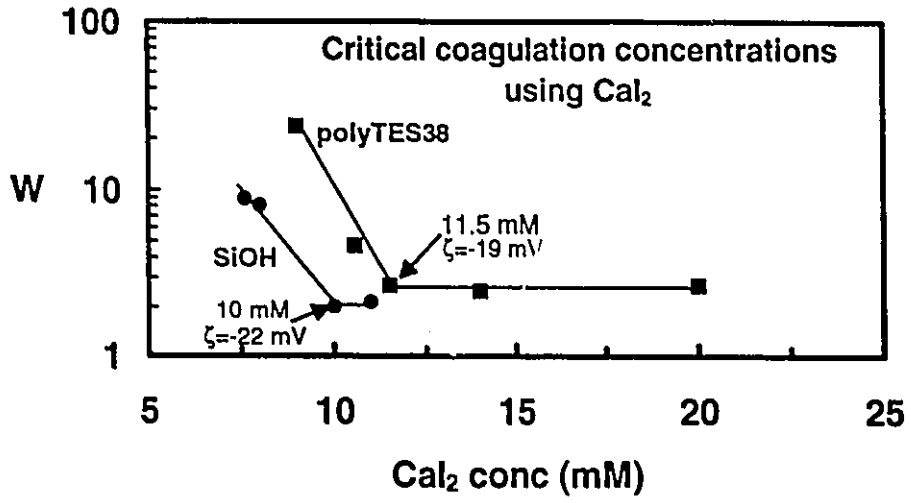

Figure 6.5 shows the polyTES38/Ca^{++} particle surfaces were covered with nanoscale size irregularities. By contrast, the surface irregularities observed for SiOH have been shown to be less pronounced (see also Chapter 2-Figure 6.2a).[16] The irregular surface morphology on the polyTES38 surface after

addition of Ca^{++} could be due to the collapse (phase separation) of the polyTES surface layer induced by specifically adsorbed Ca^{++} ions onto SiO^- sites.

Solid state NMR spectroscopy. In order to characterize TES in the interfacial layer, polyTES75 was examined by ^{29}Si CP-MAS and ^{1}H MAS solid state NMR spectroscopy. The ^{29}Si CP-MAS NMR spectrum of polyTES75 showed 4 distinct peaks. The chemical shift at -75.2 ppm was assigned to the $HSi^*(OH)(OSi)_2$ unit previously reported for hydrosilane modified silica samples.[17] The peak at -84.6 ppm has been assigned to the $HSi^*(OSi)_3$ unit, in agreement with other studies in which a shift of -85.0 ppm was observed for a soluble hydrosiloxane oligomer species represented by $HSiO_{3/2}$.[18] The ^{29}Si resonances at -101.9 and -110.8 ppm have been observed in previous studies using colloidal silica samples and were assigned to the Q_3 and Q_4 siloxane units, respectively.[2]

To obtain a quantitative estimate of the relative concentration of Si-H sites on the polyTES particle surface a ^{29}Si MAS spectrum was acquired with ^{1}H high power decoupling and no CP with a relaxation delay of 120 seconds. The ^{29}Si MAS experiment showed the Si-H sites made up a small percentage (<5%) of the total composition (mostly Q_3 and Q_4 sites) of the silica. Similar conclusions are supported by the fact that the hydrodynamic TES layer thickness occupies only

15% of the total particle volume. On the other hand, these results indicate that the polyTES layer should consist of at least 30% Si-H groups and 70% Q_3 and Q_4 groups.

The ^1H MAS solid state NMR spectrum (Figure 6.6a) for polyTES75 showed three distinct peaks. The broadest resonance at 4.0 ppm was assigned to the Si-H unit based on the Si-H chemical shift of 4.25 ppm observed in the liquid state ^1H NMR for neat TES ($(CH_3CH_2O)_3SiH$). The peak at 2.3 ppm was assigned to unreacted SiOH groups based on the 1.7-2.1 ppm chemical shift range assigned to isolated SiOH groups of silica gel by Bronnimann *et al.*[19] The other peak at 1.0 ppm was tentatively assigned to the methyl group of an unhydrolyzed ethoxy group. Bronnimann *et al.*[19] have observed peaks at 3.5 ppm and 3.0 ppm for silica gel at 25°C and assigned them to physisorbed water and to hydrogen-bonded SiOH groups, respectively, hence these species could also be contributing the ^1H NMR line shapes. After deuteration of polyTES75 by mixing with D_2O and drying the ^1H MAS spectrum (Figure 6.6b) of the silica sample showed only one broad resonance at 4.4 ppm. The D_2O exchange experiment led to the disappearance of the resonances at 2.3 ppm and 1.0 ppm, whereas the broad peak at 4.0 ppm narrowed in the non-deuterated polyTES75 spectrum (*c.f.* Figures 6.6a and 6.6b).

Figure 6.5. Transmission electron micrographs taken of SiTES38 particles after dispersing them in 11 mM CaI_2. Scale bar = 100 nm.

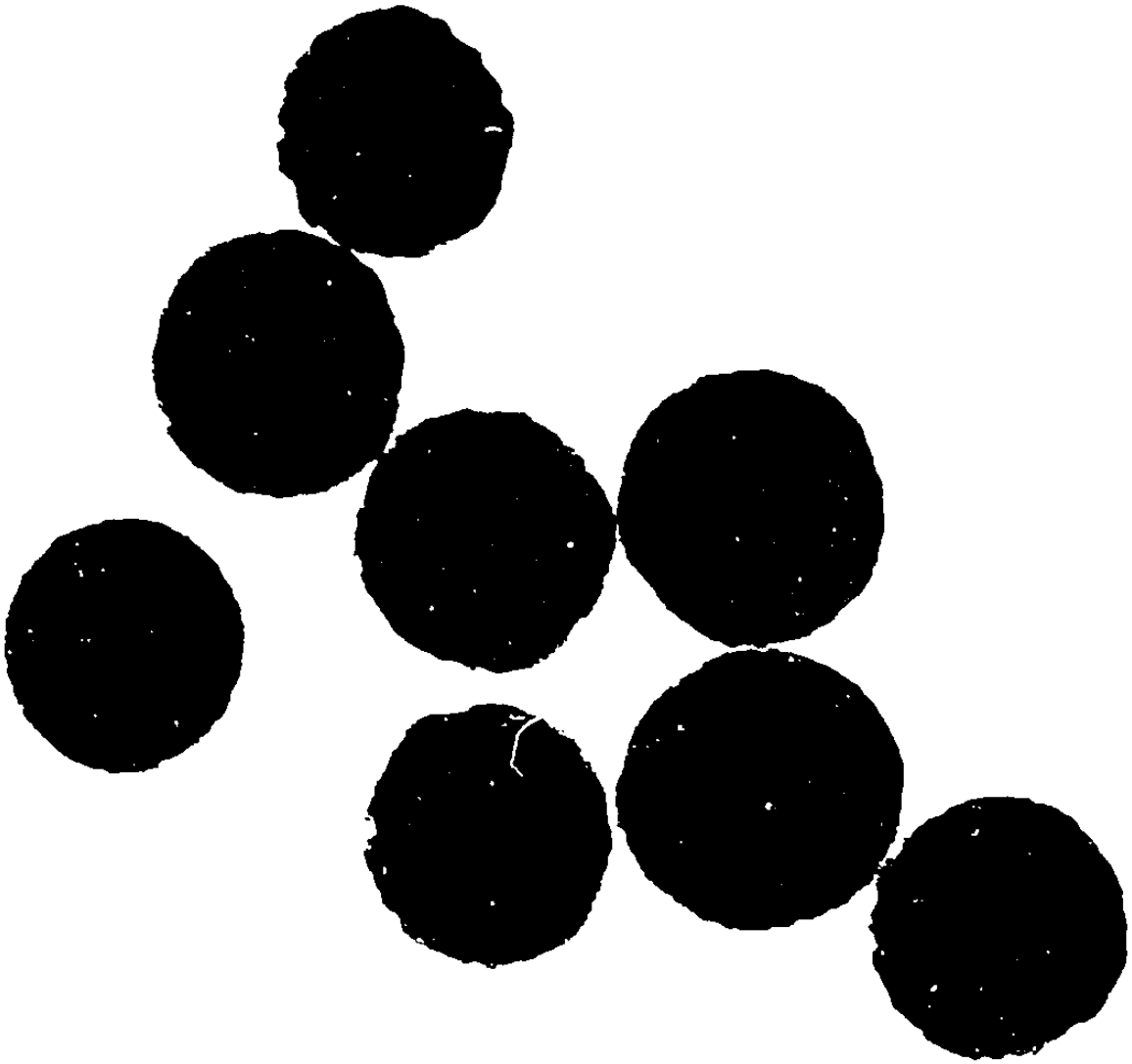

Figure 6.6. ^{1}H NMR MAS spectra of polyTES75 (a) nondeuterated (b) deuterated.

(a)

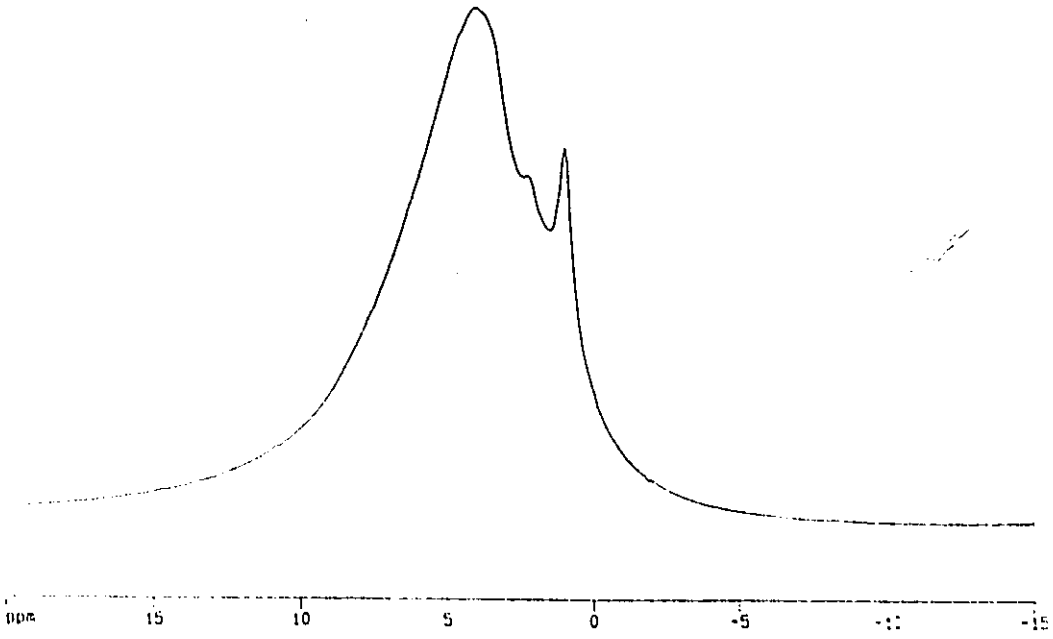

(b)

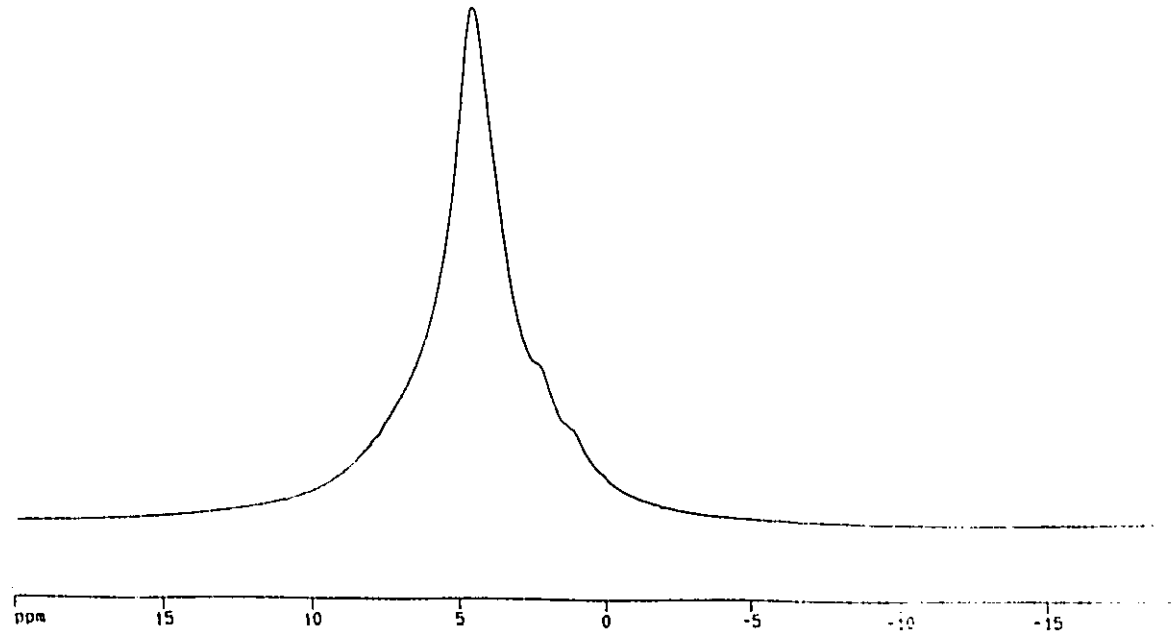

6.4 Discussion

Previous work has shown that TES is a reactive coupling agent which may be used to modify silica to incorporate Si-H groups on the surface.[2a] The current work has extended these results by characterizing the surface properties and colloidal stability of the TES modified particles. The issues relevant to the present work include the polyTES composition, microstructure, and chain motion at the silica interface.

The composition of the unmodified silica needs to be addressed before discussing the polyTES surface composition and properties. In order to characterize the chemical composition of the Stöber silica particles a mass balance approach (based on the elemental analysis data) was used. The elemental analysis data for the unmodified silica (Table 8.1) was 45.86 %Si, 3.40 %C, and 1.07 %H. The particle density was taken to be 1.7 g mL^{-1}, the untreated particle radius was 92.5 nm and the mass of 1 particle was calculated to be 5.6 x 10^{-12} mg. The particles were assumed to be composed of the following 4 species: SiO_2 (species 1); $Si_{2.5}OC_2H_5$ (species 2); $SiO_{2.5}H$ (species 3); and H_2O (species 4) and their elemental fractions are described by the following sets of equations.

Species 1 = SiO_2:

$$Si_{nt1} = \frac{AM_{Si}}{AM_{Si} + 2AM_O} \qquad [6.9]$$

$$O_{nt1} = 1 - Si_{nt1} \qquad [6.10]$$

where the subscript "*nt1*" refers to untreated silica of species 1 and "*AM*" corresponds to the atomic mass.

Species 2 = $SiO_{2.5}C_2H_5$:

$$Si_{nt2} = \frac{AM_{Si}}{AM_{Si} + 2.5AM_O + 2AM_C + 5AM_H} \qquad [6.11]$$

and similar equations may be written for the C_{nt2}, H_{nt2}, and O_{nt2} to give

$$Si_{nt2} + O_{nt2} + C_{nt2} + H_{nt2} = 1 \qquad [6.12]$$

Species 3 = $SiO_{2.5}H$:

$$Si_{nt3} = \frac{AM_{Si}}{AM_{Si} + 2.5AM_O + AM_H} \qquad [6.13]$$

and similar equations may be written for the C_{nt3}, H_{nt3}, and O_{nt3} to give

$$Si_{nt3} + O_{nt3} + C_{nt3} + H_{nt3} = 1 \qquad [6.14]$$

Species 4 = H_2O

$$Si_{nt4} = 0 \qquad [6.15]$$

$$H_{nt4} = \frac{2AM_H}{AM_O + 2AM_H} \qquad [6.16]$$

$$O_{nt4} = \frac{AM_O}{AM_O + 2AM_H} \qquad [6.17]$$

$$Si_{nt4} + H_{nt4} + O_{nt4} = 1 \qquad [6.18]$$

From the wt% of Si, C, H and O from the elemental analysis results, a mass balance can be carried out to determine the mass fraction of the species 1, 2, 3, and 4 (assumed to characterize the chemical composition of the untreated silica). The silicon, hydrogen and carbon balance for each of the four species is described by

$$\alpha Si_{nt1} + \beta Si_{nt2} + \gamma Si_{nt3} + \omega Si_{nt4} = 45.86\% \qquad [6.19]$$

$$\alpha H_{nt1} + \beta H_{nt2} + \gamma H_{nt3} + \omega H_{nt4} = 1.07\% \qquad [6.20]$$

$$\beta C_{nt2} = 3.40\% \qquad [6.21]$$

where α, β, γ, ω, correspond to the mass fractions of species 1, 2, 3, and 4.

Mathcad was used to determine when the mass fractions of species 1, 2, 3,and 4 converged according to

$$\alpha+\beta+\gamma+\omega=1 \qquad [6.22]$$

Unfortunately, the mathematical analysis showed the solve block would not converge based on the four species assumed to make up the silica chemical composition. On the other hand, assuming there are only three chemical species making up the chemical composition of the silica, that is SiO_2, $SiO_{2.5}C_2H_5$, and $SiO_{2.5}H$, only a poor convergence was obtained.(*i.e.*, $\alpha+\beta+\gamma+\omega=1.065$). The mass fractions in this case were 68.3% SiO_2, 13.8% $SiO_{2.5}C_2H_5$, and 24.5% $SiO_{2.5}H$. One of the difficulties in this mass balance analysis could be related to the presence of impurities (*e.g.*, water and ammonia species), trapped within the particle matrix pores.[20] Notwithstanding, the mass balance showed that the silica consisted of approximately 14% ethoxy groups which is consistent with previous reports using the Stöber silica which was characterized by both elemental analysis and ^{13}C CP-MAS solid-state NMR spectroscopy.[11,20]

The chemistry of alkoxysilanes bearing Si-H functional groups has been studied and the hydrolysis and condensation reactions are similar to those described for silane coupling agents except that the Si-H group is able to undergo a variety of reactions. For example, hydrosilanes undergo alcoholysis (see Scheme 6.1) *via* nucleophilic substitution, to generate alkoxysilanes and hydrogen gas and this is usually catalyzed by acid or base:

$$R_3SiH + R'OH \longrightarrow R_3SiOR' + H_2$$

Scheme 6.1. Alcoholysis of hydrosilanes (Si-H).

The surface treatment conditions used in this study simply involved refluxing the silica and TES in acetone, hence the chemical reactions were expected to be performed under neutral conditions. The acetone contained 0.31 wt % water content and this would correspond to approximately 4 H_2O monolayers on the silica surface assuming there were 7-8 SiOH groups per nm^2.[21] Under these conditions, the chemistry of the hydrolysis and condensation reactions of TES could be described by Scheme 6.2. Usually, alkoxysilane hydrolysis is acid or base catalyzed. For example, Scheme 6.3 shows the effect of acid catalysis on a TES molecule.

Hydrolysis

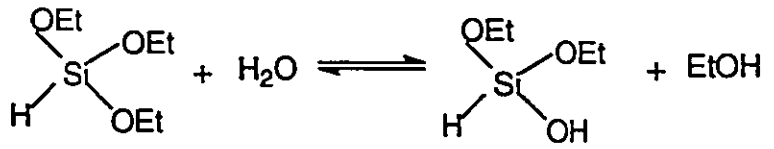

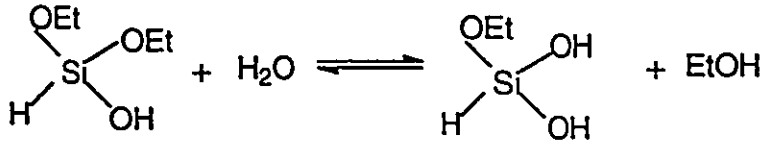

Condensation

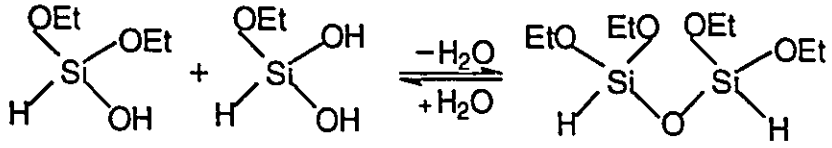

Scheme 6.2. Hydrolysis and condensation reaction chemistry of trialkoxysilane, TES, expected to occur under neutral conditions in the presence of water.

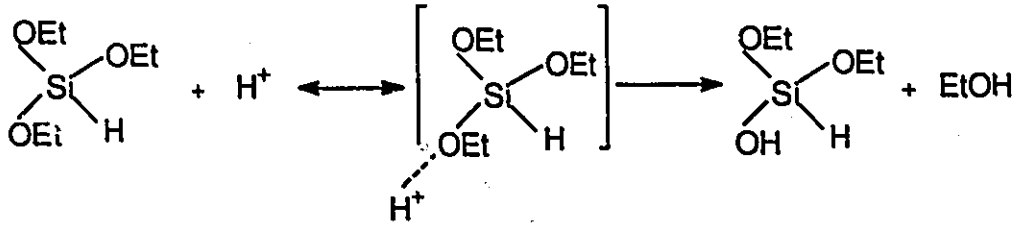

Scheme 6.3. The influence of acid catalysis on the hydrolysis and condensation reactions of TES. Acid catalysis will induce the ethoxy groups

(EtO-) to become better leaving groups. This will increase the lability of the ethoxy groups and lead to a higher degree of TES cross-linking (removal/loss of EtO-).

The lability of the TES alkoxy groups would be expected to be low and a low degree of cross-linking would be expected (see Scheme 6.3 for the influence of acid catalysis on the hydrolysis and condensation reactions with alkoxysilanes).[13] The net effect occurring under the neutral conditions is that the loss of ethoxy groups from the TES should occur at a very slow rate. The increased carbon content from the elemental analysis results (see Table 6.1) after the surface treatment with TES supports the presence of unhydrolyzed ethoxy groups from the starting material (*i.e.*, TES). A possible polyTES chemical structure would have either ethoxy or hydroxy groups (formed by hydrolysis of ethoxy of Si-H group) along the silsesquioxane polymer chain (see Scheme 6.4).

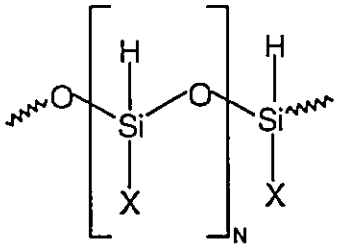

Scheme 6.4. Monomers proposed for polyTES on silica surface

where X = OH or OCH_2CH_3.

The elemental analysis data for silicon, carbon and hydrogen can be used to perform a mass balance for the untreated and treated particles. Taking silicon as an example, the following equation provides a mass balance for the silicon species before and after the surface treatment:

Core *polyTES surface* *Total*

$$MSi_{core} + \xi MSi_{modified} = Si_{total}(1+\xi)M \qquad [6.23]$$

where M is the mass of 1 particle before treatment with TES, ξ corresponds to the particle mass increase divided by M (see Eq. [6.25]), Si_{core} is the weight fraction of silicon for the untreated silica (Table 6.1), Si_{total} is that for the total Si content after treatment with TES (Table 6.1), and $Si_{modified}$ is that for silica modified with TES given by Eq. [6.24] where the polyTES75 particles were

assumed to have a surface composition of $SiO_2C_2H_6$ which corresponds to the chemical structure in Scheme 6.3 where X= -OCH_2CH_3.

$$Si_{modified} = \frac{Si_{am}}{Si_{am} + 2O_{am} + 2C_{am} + 6H_{am}} \qquad [6.24]$$

where the subscript "*am*" corresponds to the atomic mass of the element.

Similar equations may be written for both carbon and hydrogen using the data shown in Table 6.1

The particle mass increase per mass of 1 particle, following the modification with TES, can be calculated as

$$\xi = -\frac{(Si_{core} - Si_{total})}{(Si_{modified} - Si_{total})} \qquad [6.25]$$

From the elemental analysis data (Table 6.1) and using Eq. [6.25] to calculate ξ, the particle mass increase per mass of 1 particle for the silicon, carbon, and hydrogen data were calculated to be 0.29, 0.05, and 0.07, respectively. This calculation showed the mass balance for the silicon species is much too high compared with the more realistic values calculated for carbon and

hydrogen. The results for carbon and hydrogen indicated there was a 5%-7% total mass increase for polyTES75.

Assuming the best value is 0.05, the surface density of silicon, carbon and hydrogen atoms was calculated. As an example, the surface density of silicon atoms after TES treatment is given by

$$\sigma_{SI} = \frac{\xi M\% Si_{modified} N_A}{\pi r^2 Si_{am}} \qquad [6.26]$$

where ξ is the particle mass (for Si in this case) increase per 1 particle, M is mass of 1 particle, N_A is Avogadro's number, and r is the particle radius of the untreated silica.

σ_{SI} , σ_C , σ_H , were calculated to be 73 Si atoms nm^{-2}, 146 C atoms nm^{-2}, and 437 H atoms nm^{-2}, respectively, for polyTES75. Similarily, the σ_{SI} , σ_C , and σ_H corresponding to polyTES38 were 60 Si atoms nm^{-2}, 121 C atoms nm^{-2}, and 362 H atoms nm^{-2}, respectively.

Since the thickness, $\delta_{polyTES}$, of the polyTES surface layer is known from the DLS data, and the length of one repeat unit, $\delta_{monomer}$, can be considered to be 0.25 nm, the surface density of polyTES chains, σ_{chains}, attached to the surface can be calculated as

$$\sigma_{chains} = \frac{\sigma_{Si}}{\left(\frac{\delta_{polyTES}}{\delta_{monomer}}\right)} \qquad [6.27]$$

Assuming the chains are terminally attached and the polyTES chain length is equal to the hydrodynamic thickness, σ_{chains} was calculated to be 2.22 nm^{-2}. The area occupied per polyTES chain would be expected to occupy 0.45 nm^2. This latter value is similar to that which has been reported for closely packed alcohol chains grafted to a silica surface (*i.e.*, 0.22 nm^2).[20]

Information on the molecular motion of the TES layer bound to silica can be inferred from the ^1H MAS NMR experiments. The observation of relatively narrow line widths of the resonance's in the ^1H NMR MAS spectrum (Figure 6.1a) are uncharacteristic for solid silicate samples due to the strong ^1H-^1H magnetic dipolar interactions.[18] In the limit of the rigid lattice, the ^1H-^1H homonuclear dipolar interactions are in the range of 40 to 60 kHz, and are strongly distant dependent.[21] Highly crystalline materials will give rise to dipolar interactions of this magnitude. We can attribute the narrow ^1H line widths to two phenomena; 1) the low density of protons in the TES layer and 2) the motion of the protons in the TES layer. The relative importance of these two contributions to the observed ^1H line widths cannot be obtained from the current MAS

experiments. However, we can comment that the residual ^{1}H-^{1}H homonuclear dipolar interactions are less than 6 KHz (the MAS spinning frequency was 6 KHz in these experiments). The ^{1}H MAS spectrum in Figure 6.6a strongly suggests that a mobile species is bound to the silica surface. This conclusion is in agreement with previous studies using other trialkoxysilanes.[24] For example, a high degree of molecular motion of deuterated amino alkyl derivatized silicas was observed using ^{2}H solid-state NMR.[24a]

Further support for a dynamic TES adlayer came from the influence of pH on the hydrodynamic polyTES38 particle size. For example, raising the pH from 5 to 9 caused the hydrodynamic particle diameter to increase by 10 nm (see Figure 6.4). This behavior was believed to be caused by the repulsion between the high concentration of negatively charged silanol groups expected in this pH range between polyTES polymer segments (see Scheme 6.5) and also between the negatively charged polymer segments and the silica surface.

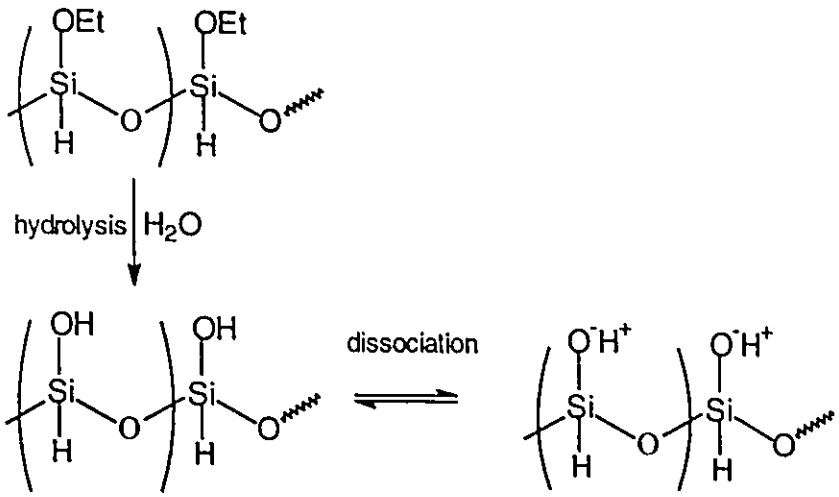

Scheme 6.5. Hydrolysis of ethoxy groups attached along polyTES segments bound to silica surface under aqueous conditions at 3.0 < pH < 7.0

From the above analysis of the surface composition and dynamics of the polyTES layer attached to the silica surface, we propose the tentative polyTES structure under aqueous conditions is as shown in Figure 6.7. Since water is a poor solvent for siloxanes/silsesquioxanes, the polyTES segments will be poorly solvated and tend to collapse under neutral conditions giving rise to macroscopic polyTES domains (Figure 6.7a). Under these conditions, electrostatic stabilization will dominate any steric effects (hence the polyTES particles will be stabilized by electrostatic repulsions). The similar c_c values between the untreated and polyTES silica particles supports this hypothesis (see Figure 6.4). With increases in the pH towards more alkaline conditions, the ethoxy and Si-H groups will be displaced by OH- and this will chemically transform the polyTES

chemical composition to have a structure resembling a polyelectrolyte. In the latter scenario, the electrostatic interaction of the charged groups along the polyTES segments and those with the silica surface silanols will be repulsive and cause the polyTES layer to expand and the polymer will behave as though it were above its glass transition temperature (see Figure 6.7b). The polyTES particles will be expected to behave more like an electrosterically stabilized system (see also Figure 6.3).

A more accurate description of the density profile and dynamic properties of the polyTES layer on the silica surface will require more advanced experimental techniques such as small-angle neutron scattering[25] and will be the focus for future studies.

Figure 6.7. Schematic representation of polyTES bound to silica particles under different pH conditions. Top: (a) At pH 3.0 < pH < 7, the polyTES layer will be poorly solvated leading to collapsed domains as represented in the cartoon. The polyTES particles (as represented in (a)) behave as an electrostatically stabilized system with most of the charged groups originating from the silica surface silanols (iso-electric point = 3.0 ± 0.5). Bottom: (b) At pH > 7, both the ethoxy and Si-H groups are displaced by OH- leading to an increase of ionizable silanol groups along the polyTES segments. In this case the polyTES layer would be expected to be better solvated and become expanded due partly to electrostatic repulsions between chain-chain and chain-particle SiO- groups. The polyTES layer resembles a polyelectrolyte.

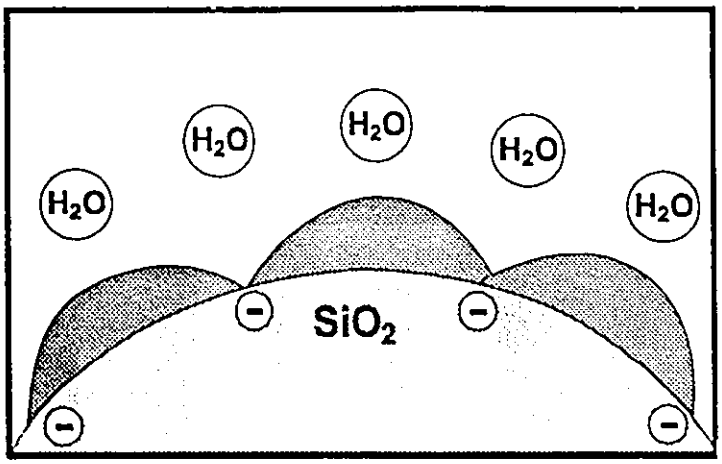
H2O
H2O
H2O
H2O
H2O
SiO2

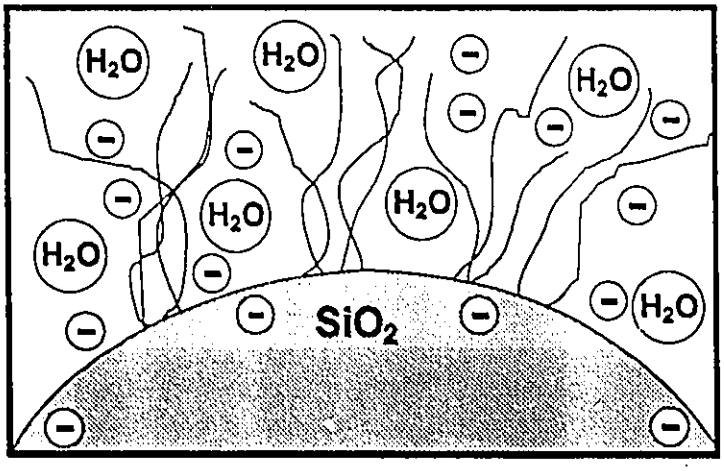
H2O
H2O
H2O
H2O
H2O
H2O
SiO2

6.5 Conclusions

1) The colloidal stability of polyTES dispersions modified with TES concentrations of 38 and 75 mM TES were similar as judged by their sensitivity to aqueous CaI_2 solutions and behavior as studied by electrophoresis and dynamic light scattering. By contrast, the polyTES dispersions aggregated when prepared with 150 mM TES.

2) A model based on elemental analysis and DLS data was given and it was proposed that the polyTES chains adopt two different configurations which depended on their exposure to acidic or alkaline aqueous pH environments.

3) ^1H MAS solid - state NMR and DLS experiments indicated the polyTES layer was not rigid but dynamic. Under aqueous conditions, at pH values less than 7, the polyTES layer was in a collapsed state due to the poor solvency of the polyTES segments. The polyTES particles were electrostatically stabilized and their colloidal behavior was similar to the untreated particles. For pH values greater than 7, the polyTES layer was expanded and resembled a polyelectrolyte.

6.6 References

[1] Stöber, W. F.; Fink, A.; Bohn, E. *J. Colloid Interface Sci.* **1968**, *26*, 62.

[2] (a) Ketelson, H.A.; Brook, M.A.; Pelton, R. *Chem. Mater.* **1995**, *7*, 1376. (b) van Blaaderen, A.; Vrij, A.. *J. Colloid Interface Sci.* **1993**, *156*, 1. (c) Badley, R.D.; Ford, W.T.; McEnroe, F.J.; Assink, R.A. *Langmuir*, **1990**, *6*, 792. (d) Goodwin, J.W.; Harbron, R.S.; Reynolds, P.A. *Colloid Polym. Sci.* **1990**, *268*, 766.(e) Philipse, A.P.; Vrij, A. *J. Colloid Interface Sci.* **1989**, *128*, 121. (f) van Helden, A.K.; Jansen, J.W.; Vrij, A. *J. Colloid Interface Sci.* **1981**, *81*, 354. (g) Ketelson, H.A.; Brook, M.A.; Pelton, R. *Polymers. Adv. Tech.*, **1995**, *6*, 335

[3] Ketelson, H.A.; Brook, M.A.; Pelton, R. *Chem. Mater.* in press.

[4] Kratochvil, P. Classical Light Scattering from Polymer Solutions, Elsevier, Amsterdam, 1987.

[5] Seebergh, J.E.; Berg, J.C. *Colloids Surf.* **1995**, *100*, 139.

[6] (a) Reerink, H.; Overbeek, J.T.G. *Discuss. Faraday Soc.*, **1954**, *18*, 74. (b) Ottewill, R.H.; Shaw, J.N. *Discuss. Faraday Soc.*, **1966**, *42*, 154.

[7] Overbeek, J.T.G., in "Kinetics of Flocculation", H.R. Kruyt, Ed., p.278. Elsevier, Amsterdam, 1952.

[8] (a) Virden, J.W.; Berg, J.C. *J. Colloid Interface Sci.* **1992**, *149*, 528; (b) Einarson, M.B.; Berg, J.C. *J. Colloid Interface Sci.* **1993**, *155*, 165.

[9] Pelton, R.; Miller, P.; McPhee, W.; Rajaram, S. *Colloids Surf.* **1993**, *80*, 181.

[10] A dry polyTES sample (200 mg) was mixed with D_2O for about 30 minutes and then centrifuged to isolate the deuterated material. This material was quickly

dried under a bunsen burner flame and used to perform the ^{1}H MAS solid-state NMR experiment.

[11] (a) Badley, R.D.; Ford, W.T.; McEnroe, F.J.; Assink, R.A. *Langmuir* **1990**, *6*, 792. (b) van Blaaderen, A. Ph.D. Thesis - Chapter 2; Utrecht University, The Netherlands, 1992.

[12] (a) Ketelson, H.A.; Pelton, R.; Brook, M.A. *Langmuir* **1996**, *12*, 1134. (b) Ketelson, H.A.; Pelton, R.; Brook, M. *J. Colloid Interface Sci.* **1996**, *179*, 600.

[13] Lukevics, E.; Dzintara, M. *J. Organomet. Chem.* **1985**, *295*, 265.

[14] Seebergh, J.E.; Berg, J.C. *Colloids Surfaces*, **1995**, *100*, 139.

[15] Vigil, G.; Zenghe, X.; Steinberg, S.; Israelachvili, J. *J. Colloid Interface Sci.* **1994**, *165*, 367.

[16] Although nanoscale sized surface irregularities have been observed by TEM analysis of unmodified Stöber silica particles, see van Helden, A.K.; Jansen, J.W.; Vrij, A. *J. Colloid Interface Sci.* **1986**, *114*, 471, the polyTES surface irregularities are more pronounced in the presence of CaI_2 and the effect was confirmed by observing approximately 100 particles.

[17] Sandoval, J.E.; Pesek, J.J. *Anal. Chem.* **1991**, *63*, 2634.

[18] (a) Engelhardt, G.; Jancke, H.; Lippmaa, E.; Samoson, A. *J. Organomet. Chem.* **1981**, *210*, 295. (b) Horn, H.G.; Marsmann, H.C. *Makromol. Chem.* **1972**, *162*, 255.

[19] Bronnimann, C.E.; Chuang, I.S.; Hawkins, B.L.; Maciel, G.E. *J. Am. Chem. Soc.* **1987**, *109*, 1562. Bronnimann, C.E.; Zeigler, R.C.; Maciel, G.E. *J. Am. Chem. Soc.* **1988**, *110*, 2023.

[20] Jelinek, L.; Dong, P.; Rojas-Pazos, C.; Taibi, H.; Kovats, E.S. *Langmuir* **1992**, *8*, 2152.

[21] See Chapter 2.

[22] D.H. Napper, "Polymeric Stabilization of Colloidal Dispersions," Academic Press, London, 1983.

[23] Abragam, A. *Principles of Nuclear Magnetism.* Oxford University Press: 1961; Ch. 4.

[24] (a) Kang, H-J.; Blum, F.D. *J. Phys. Chem.* **1991**, *95*, 9391. (b) Kelusky, E.C.; Fyfe, C.A. *J. Am.Chem. Soc.* **1986**, *108*, 1746.

[25] (a) Barnett, K.G.; Cosgrove, T.; Vincent, B.; Sissons. D.S.; Cohen-Stuart, M. *Macromolecules* **1981**, *14*, 1018; (b) Auroy, P.; Auvray, L.; Leger, L. *Macromolecules* **1991**, *24*, 2523.

Chapter 7

Sterically Stabilized Silica Colloids: Radical Grafting of Poly(methyl methacrylate) and Hydrosilylative Grafting of Silicones to Functionalized Silica

Abstract

Colloidal silica sols having a narrow dispersity, prepared by the ammonia catalyzed hydrolysis of $Si(OEt)_4$, were functionalized by reaction with vinyltrimethoxysilane (H_2C=$CHSi(OMe)_3$) or methacryloxypropyltrimethoxysilane (H_2C=$CMeCO_2(CH_2)_3Si(OMe)_3$. The electrostatically stabilized colloids were stable in acetone and DMF. Radical polymerization of methyl methacrylate in the presence of either type of functionalized particle led to particles with surface grafted poly(methyl methacrylate). The efficiency of polymer grafting was shown to be related to the nature of the functional groups. The PMMA-modified, sterically stabilized particles were colloidally stable in solvents ranging from acetone to toluene but unstable in water or hexane. The vinyl functionalized silica was alternatively reacted with $HSiMe_2$-terminated silicones in a platinum catalyzed hydrosilylation. The resultant sterically stabilized particles were stable

in hexane. It was thus possible to convert the unmodified silica to organo-functionalized silica and finally to polymer-grafted silica while maintaining colloidal stability. During the course of these modifications, the mechanism for colloidal stability changed from electrostatic to steric stabilization.

7.1 Introduction

Colloidal dispersions in non-aqueous media of low dielectric constant are increasingly attracting attention.[1,2,3] Under such solvency conditions, colloidal stability can be achieved by the attachment to the colloid surface of a "steric barrier" composed of solvent swollen polymers.[4]

We have an interest in the preparation of well-defined sterically stabilized systems in non-aqueous media which can be used to develop the critical parameters required for colloidal stability. In particular, we wish to explore methods which allow the attachment of steric layers of known length/surface density and surface orientation (tails *versus* loops, etc.) utilizing a variety of chemical processes.

Of the reported studies on sterically stabilized, non-aqueous latex systems, only a few fulfill the requirements for a model system. Colloidal silica, prepared by the ammonia catalyzed hydrolysis of tetraethyl orthosilicate (TEOS) in a process developed by Stöber, constitutes such a system.[5] The main advantage of Stöber silica is the flexible control of the particle size; monodisperse silica spheres can be easily grown to diameters ranging between 10 nm and 1 μm.[6]

In order to transfer colloidal silica to non-aqueous solvents, several types of surface modification reactions have been employed. van Blaaderen and Vrij have used methacryloxypropyltrimethoxysilane (MPS) to disperse Stöber silica in weakly polar organic solvents.[7] Pathmamanoharan has modified silica using a poly(stearic acid) derivative and poly(isobutene) which allowed the particles to be dispersed in non-polar solvents.[8] Poly(methyl methacrylate) (PMMA) modified silica has been prepared from high surface area amorphous silica bearing surface vinyl or initiating groups that were used to carry out radical grafting with methyl methacrylate.[9] The silica employed in these cases was difficult to study from a colloidal perspective since the surface was highly irregular. PMMA-silica composite films have been prepared from modified Stöber silica; the colloidal properties of these materials was not described.[10]

Silica has also been sterically stabilized by poly(dimethylsiloxanes) (PDMS). Edwards *et al.*[11] and Auroy *et al.*[12] have grafted PDMS chains to unmodified Stöber silica by condensation routes in order to transfer the particles to low dielectric constant solvents. In the Auroy study, it was claimed that long PDMS chains had been grafted by their ends to the particle surface and that the particles could be transferred to low dielectric solvents. We and others[13] have been unable to reproduce these results; in our hands, the particles were observed to coagulate in the presence of solvents such as hexane.

The aim of this study was to prepare well-defined, sterically stabilized, non-aqueous colloidal dispersions and to examine their colloidal stability. Herein we report the preparation and characterization of colloidal particles having organic polymer sheaths (PMMA or PDMS) as steric stabilizers grafted to the particle surface. To do so, colloidal silica was modified with either vinyltrimethoxysilane (VTM) or MPS and then subjected tc the radical grafting of PMMA (Scheme 7.1A).

We further describe in this paper an alternative approach for obtaining PDMS coated silica dispersions using a hydrosilylation reaction between vinyl modified silica and a silane hydrogen (SiH) difunctional terminated PDMS polymer in the presence of a transition-metal catalyst to form Si-C linkages (Scheme 7.1B).[14]

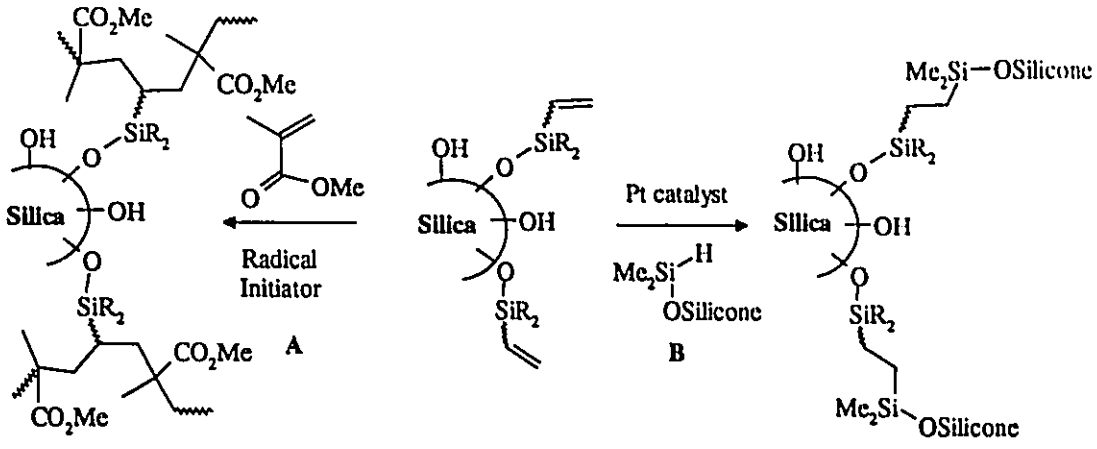

Scheme 7.1. Silicone grafting via: A) radical coupling, B) the hydrosilation reaction.

7.2 Experimental

General Procedures.

The glassware used for the silica synthesis and surface modifications was cleaned by rinsing several times with acetone, Milli Q water and finally with a 2% HF solution. The colloidal silica synthesis was carried out under sonication using a Branson Model 450 sonifier probe. A Lauda Series RMS-6 Refrigerating Circulator bath was used to control reaction temperatures. A Beckman L7-55 Ultra Centrifuge with a type 60Ti rotor was used to carry out all the sedimentation / redispersion cycles on the unmodified and modified silica samples. The sedimented silica samples were redispersed using a Branson model 5200 ultrasonic bath.

Instrumentation and Analytical Procedures.

Solid-state ^{13}C and ^{29}Si Nuclear Magnetic Resonance Spectroscopy: A Bruker-100 spectrometer operating at 25.2 MHz for carbon was used to obtain ^{13}C cross polarization (CP) / magic angle spinning (MAS) solid state spectra. Direct polarization ^{29}Si spectra were obtained using a Bruker AM 500 spectrometer equipped with a solid state accessory operating at 99.3 MHz for silicon.

Electron Microscopy: The transmission electron micrographs (TEM) of the colloids were acquired using a JEOL JEM-1200EX microscope. Carbon coated Formvar grids were used as sample grids.

Elemental analyses: Combustion analyses (CH) of the unmodified and modified silica products were performed by Guelph Chemical Laboratories Ltd., Guelph, Ontario, Canada.

Dynamic light scattering (DLS): DLS experiments were performed at 25°C and the colloid samples were prepared for analysis by filtering the dispersions through Millipore filters several times to remove dust particles. The DLS apparatus used a fixed angle helium-neon laser (Nicomp Model 370 submicrometer particle sizer, Pacific Scientific). Samples were diluted manually to achieve an optimum signal output. Data for all the samples was collected for 60 min. Nicomp software version 3.70 was used to record the intensity averaged particle diameters based on Gaussian analysis.

Moving Boundary Electrophoresis: The electrophoretic mobilities of the unmodified and modified particles were measured using the U-tube method as described by Burton.[15] A glass U-tube was constructed in which each of the tubes having a diameter of 1.5 cm was 18.7 cm in length (vertically measured from the top of U-tube to stopcock base). See Appendix A7.1 for a diagram of

the glass apparatus. The delivery funnel contained a volume of 250 mL. The boundary layers were formed by first adding approximately 25 mL of acetone (called the zone boundary) to the U-tube vessel after which the colloidal solution (called the moving boundary) was introduced into the U-tube by careful manipulation of the stopcock in order to obtain a uniform and distinct moving boundary layer below the zone boundary. Two Pt electrodes were connected to a power supply and inserted at the top of the U-tubes through a septum and they were immersed into the zone boundary at the same depth. Each run was conducted for 3 h between 23±1°C and measurements of the boundary position were taken every 30 min.

Materials.

Toluene (Caledon, reagent grade), dimethylformamide (DMF) (Aldrich-Sigma, 99.9+%, HPLC grade), methanol (Caledon, reagent grade), chloroform (BDH, reagent grade), diethyl ether (BDH), hexane (Fisher Scientific, HPLC grade), acetone (Caledon, glass distilled), sodium iodide (Fisher Scientific), calcium iodide hydrate, $CaI_2 \cdot 4\text{-}6\ H_2O$ (Aldrich, 98%), tetrabutylammonium bromide (Aldrich, 99%), ammonia in ethanol (2.0 M, Aldrich), hydrogen-terminated poly(dimethylsiloxane) (PDMS-H, United Chemicals, Mw=62 700), 2,2'-azobis(2,4-dimethylvaleronitrile) (ADVN, Nalco Canada), and Karstedt's Pt catalyst[16] (2-3 wt% Pt concentration in xylene, $[(Pt)_2(H_2C{=}CH\text{-}$

$SiMe_2OSiMe_2CH=CH_2)_4$], United Chemicals) were used as received. Benzene (BDH, reagent grade) was washed with sulfuric acid and distilled from Na under a nitrogen atmosphere. Methyl methacrylate (Aldrich, 99%) was purified by vacuum distillation and stored under a nitrogen atmosphere. Tetraethyl orthosilicate (Aldrich, 99.999+%), vinyltrimethoxysilane (VTM) (Aldrich, 98%), 3-methacryloxypropyltrimethoxysilane (MPS) (Aldrich, 97%) were distilled in vacuo prior to use.

Colloidal Systems Nomenclature.

The colloidal dispersions are named according to the following rationale where the colloidal silica is called *Six* with ***x*** being the batch number. *SG* refers to a seeded growth preparation, and *OH* (unmodified silica), *VTM* (vinyltrimethoxysilane modified), *MPS* (methacryloxypropyltrimethoxysilane modified), *PMMA* (poly(methyl methacrylate) modified), and *PDMS* (poly(dimethylsiloxane) modified silica) are used to designate the type of surface modification performed on the silica surface. For example, *Si1SGOH* refers to unmodified colloidal silica (batch #1) prepared using the seeded growth approach and *Si1SGVTM / PMMA* refers to PMMA modified colloidal silica having VTM surface groups prepared from batch #1.

Preparation of Stöber Silica.

Si1SGOH: H_2O (10.8 mL, 600 mmol), NH_3 (2.0 M in ethanol, 112 mL, 5.17 mmol) and absolute ethanol (70 mL) were mixed in a glass vessel inserted in a 30°C water bath fitted with a submerged magnetic stirrer. The mixture was stirred for 30 min to allow the liquids to come to thermal equilibrium. Tetraethoxysilane (TEOS, 7.1 mL, 32 mmol) was quickly added. A sonicating probe was inserted through a specially fitted hole through the top of the vessel and positioned 5 cm below the liquid level. The mixture turned cloudy after approximately 10 min and was left stirring with sonication for 10 h. At that time, TEOS (14.2 mL, 64 mmol) and H_2O (2.3 mL, 128 mmol) were added to the alcosol mixture. Following a further 10 h mixing period, a second addition of TEOS (14.2 mL, 64 mmol) and water (2.3 mL, 128 mmol) were added to the dispersion. Centrifugation and redispersion cycles, 3 x EtOH followed by 3 x acetone, were employed to clean the products of unreacted material. The sedimented silica solids were redispersed using a Branson model 5200 ultrasonic bath.

Si1SGOH: ^{29}Si NMR (MAS) δ -102.92, -109.72, -95.5

Si2SGOH and Si3SGOH: The same procedures were used as described above except H_2O (6.4 mL, 355 mmol), NH_3 (2.0 M in ethanol, 76 mL, 152 mmol), absolute ethanol (109 mL), and TEOS (9 mL, 40 mmol) were mixed together to prepare Si2OH (denoted as the seed mixture). To prepare the seeded growth

samples, TEOS (18 mL, 80 mmol) and water (2.91 mL, 161 mmol) were added to the seed mixture and stirred under sonication for a further 10 h. This procedure was repeated once more to give a milky white dispersion.

Modified Colloidal Silica.

SixSGVTM or SixSGMPS: The particles were prepared for modification by transferring them to DMF using 3 x centrifugation / redispersion cycles. To a clean and colloidally stable DMF/silica dispersion containing about 2 g solid / 200 mL solvent was added 15 mmol of either MPS or VTM. The mixture was stirred under reflux and a stream of nitrogen under positive pressure for 36 h. The silica was subsequently cleaned free of unreacted silane coupling agent using centrifugation/redispersion cycles, 5 x DMF.

SixSGVTM: ^{13}C NMR (CP-MAS) δ = 129.31, 60.56, 51.41, 24.59.

SixSGMPS: ^{13}C NMR (CP-MAS) δ = 166.5, 136.2, 124.5, 60.48, 17.79, 51.5, 33.34, 17.34, 9.2.

Graft Polymerization using Modified Silica.

SixSG VTM / MMA or SixSG MPS / MMA: After cleaning the modified particles with DMF, methyl methacrylate (MMA, 7.5 g, 75 mmol) and freshly distilled benzene (20 mL) was added to the particles. The dispersion was sonicated for 10 min after which ADVN (0.06 g, 0.24 mmol) was charged into the reaction

vessel. After purging the dispersion with nitrogen for 30 min, the reaction mixture was mixed using a magnetic stirrer under a nitrogen atmosphere at 40°C for 8 h. In order to free the particles from unreacted PMMA, they were sedimented by centrifugation at 7000 rpm for 55 min. The product was washed with toluene and chloroform using 6 x centrifugation / redispersion cycles at the same speed. The particles were sonicated each time in fresh solvent to ensure they would be efficiently washed. Methanol was added to the supernatant to confirm the absence of ungrafted PMMA.

SIxSG VTM / MMA: ^{13}C NMR (CP-MAS) δ 177.70, 165.70, 60.56, 51.31, 44.98, 17.62.

SIxSG MPS / MMA: ^{13}C NMR (CP-MAS) δ 177.11, 60.48, 51.48, 45.09, 17.26.

Grafting of PDMS to Vinyl Modified Silica.

Si3SG VTM / PDMS: Vinyl modified spheres (*ca.* 1 g) were transferred to acetone (100 mL) and added to PDMS-H (Mw=62 700, 10 g) dissolved in hexane (100 mL). Karstedt's catalyst (100 µL) was charged into the reaction vessel. The mixture was stirred under an open atmosphere for 10 h at 80°C. The silica was cleaned of unreacted PDMS with fresh hexane using the same procedure as described for the PMMA modified particles.

Si3SG VTM / PDMS: ^{29}Si NMR (MAS) δ -110.97, -101.25, -91.74, -22.34.

7.3 Results and Discussion

Preparation and Characterization of Colloidal Silica Particles

Colloidal silica sols were prepared by the ammonia catalyzed hydrolysis of $Si(OEt)_4$. The properties of the silica sols are summarized in Table 7.1. The average diameter of the particles obtained by DLS measurements was 350 nm for Si1SGOH, 181 nm for Si2SGOH and 171 nm for Si3SGOH. The transmission electron micrographs (TEM's) of the particles, shown in Figure 7.1, provide further evidence that the particles had a narrow dispersity with spherical surfaces; the larger particles, Si1SGOH, were better in both respects than the smaller ones, Si2SGOH.

The silica particles were electrostatically stabilized by the presence of negative surface charges resulting from the dissociation of the surface silanol groups and any residual silanolate / ammonium ion pairs.[17] The transfer of the unmodified silica to toluene or THF caused the loss of colloidal stability as shown by particle coagulation. It was determined for Si2SGOH that the moving boundary layer was observed to slowly migrate towards the anode. The boundary layer movement was inferred to be due to a migration of negatively charged particles.

Table 7.1. Diameters of Colloidal Silica Particles Before and After Chemical Modification According to Dynamic Light Scattering.

System	Solvent	Diameter nm (st. dev. %)[a]
Si1SGOH	acetone	350.0 (10)
Si1SGVTM	acetone	354.0 (12)
Si1SGMPS	acetone	360.0 (9)
Si2SGOH	acetone	181.0 (16)
Si2SGVTM	acetone	185.1 (18)
Si2SGMPS	acetone	190.9 (19)
Si2SG VTM / MMA	acetone	212.5 (18)
Si2SG VTM / MMA	toluene	204.9 (15)
Si2SG VTM / MMA	chloroform	225.0 (12)
Si2SG MPS / MMA	acetone	197.9 (19)
Si2SG MPS / MMA	toluene	212.1 (15)
Si2SG MPS / MMA	chloroform	237.0 (14)
Si3SGOH	acetone	170.5 (14)
Si3SGVTM	acetone	172.7 (16)
Si3SG VTM / PDMS	hexane	230.8 (17)

a The intensity averaged particle diameters were measured based on a Gaussian analysis. The standard deviations are reported as the breadth of the particle size distribution based on a Gaussian fit.

Figure 7.1. TEM's of A) Si1SGOH (Scale bar = 1.0 μm), B) Si1SGOH (higher magnification, Scale bar = 500 nm), C) Si2SGOH (Scale bar = 500 nm).

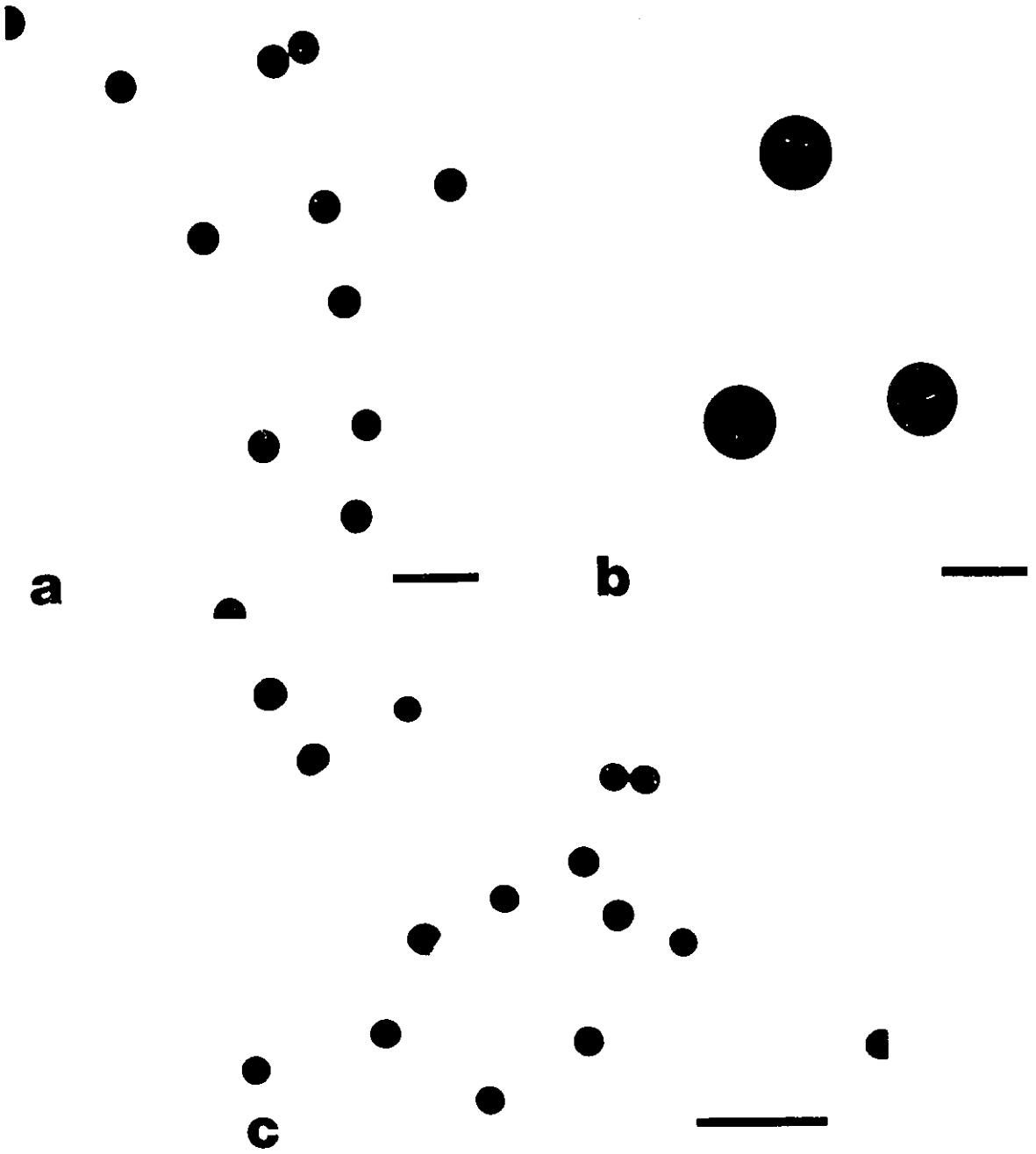
a
b
c

VTM and MPS Modified Particles

The silica colloids were chemically modified by refluxing a silica / DMF dispersion with either VTM or MPS.

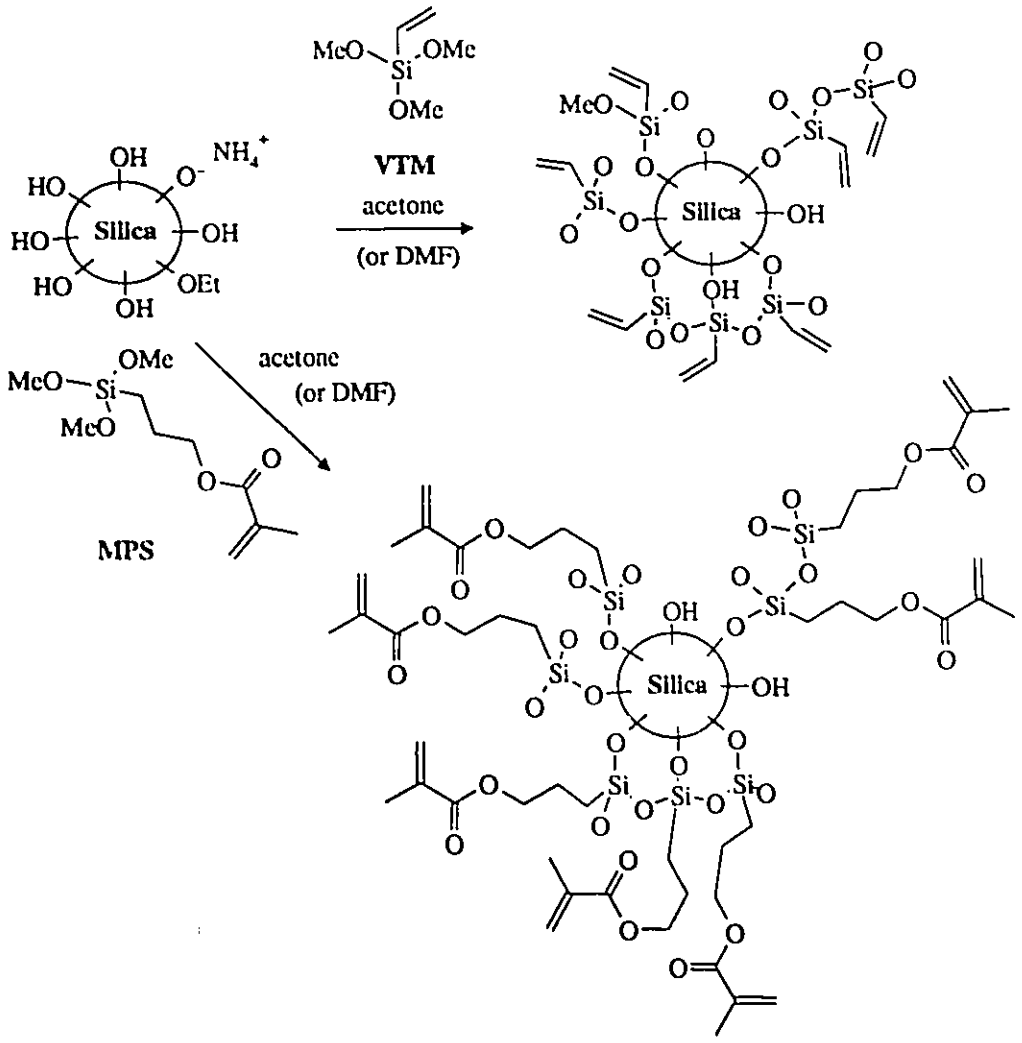

Scheme 7.2. Functional group modification of colloidal silica using VTM and MPS coupling agents.

These coupling agents may graft to the surface directly as monomeric units or oligomerize in solution prior to grafting, as shown in Scheme 7.2.[18] Table 7.1 shows the diameters obtained by DLS for the modified particles. A comparison of the sizes between the unmodified and modified particles reveals that the hydrodynamic diameter was observed to increase by 4 nm and 10 nm for Si1SGVTM and Si1SGMPS, respectively. For Si2SGVTM and Si2SGMPS, the diameter increased by 4 nm and 9 nm, respectively. These measurements support the proposition that the organosilane is present as oligomers grafted to the surface or a surface gel.

The results obtained from the elemental analysis of the modified samples are given in Table 7.2; increased carbon contents were obtained for both the VTM (1.6 wt % for Si2SGVTM) and MPS (1.9 wt% for Si2SGMPS) functionalized samples. The specific surface area of the Si2SGVTM 181 nm (diameter) silica sol was 16.6 m^2 / g, assuming spherical particles with a density of 2000 kg/m^3.[19] Using the weight percentage of carbon obtained for the modified particles, surface coverage values of 57 and 48 carbon atoms / nm^2 for Si2SGMPS and Si2SGVTM, respectively, were calculated. Philipse and Vrij[7] have also modified colloidal silica using MPS and a value of about 70 carbon atoms / nm^2 was calculated in that case.

The transfer of the VTM or MPS particles to toluene or chloroform led to particle coagulation. However, the particles were observed to be colloidally stable in acetone, DMF, acetonitrile and THF. In contrast to the stability results reported for the unmodified particles,[17] we found no apparent changes in the stability behavior of the VTM and MPS particles in highly polar solvents over time. The addition of acetone solutions of NaI or CaI_2 led to coagulation of both types of particles. The mobility measurements obtained for the modified particles indicate that the VTM and MPS particles are negatively charged. These data demonstrated that the modified particles, like the Stöber silica, were electrostatically stabilized.[20]

Table 7.2. Elemental Analysis of Colloidal Silica Particles Before and After Chemical Modification.

System	C(%)	H(%)
Si2SGOH	3.33	1.36
Si2SGVTM	4.93	1.40
Si2SG VTM / MMA	6.93	1.60
Si2SGMPS	5.21	1.47
Si2SG MPS / MMA	7.96	1.84
Si2VTM	4.56	1.20
Si2 VTM / MMA	9.00	1.89
Si2MPS	4.97	1.34
Si2 MPS / MMA	12.67	2.24

PMMA Grafted Silica Dispersions

The radical grafting reactions performed using the VTM and MPS functionalized spheres are shown in Scheme 7.3 and Scheme 7.4, respectively. The vinyl functionalized silica particles, in the presence of MMA and a radical initiator, were reacted in benzene. The ungrafted PMMA was separated from the particles by repeated sedimentation and resuspension in fresh solvent.

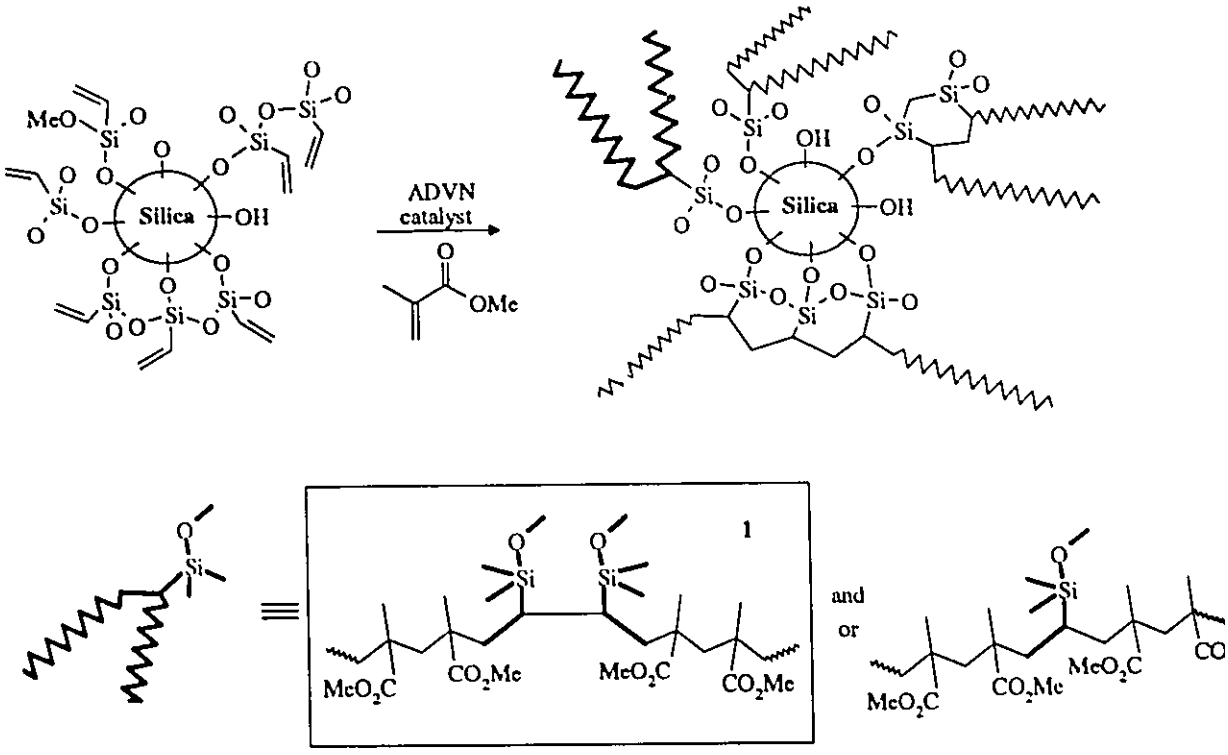

Scheme 7.3. Copolymerisation reactions of MMA onto vinyl functionalized colloidal silica.

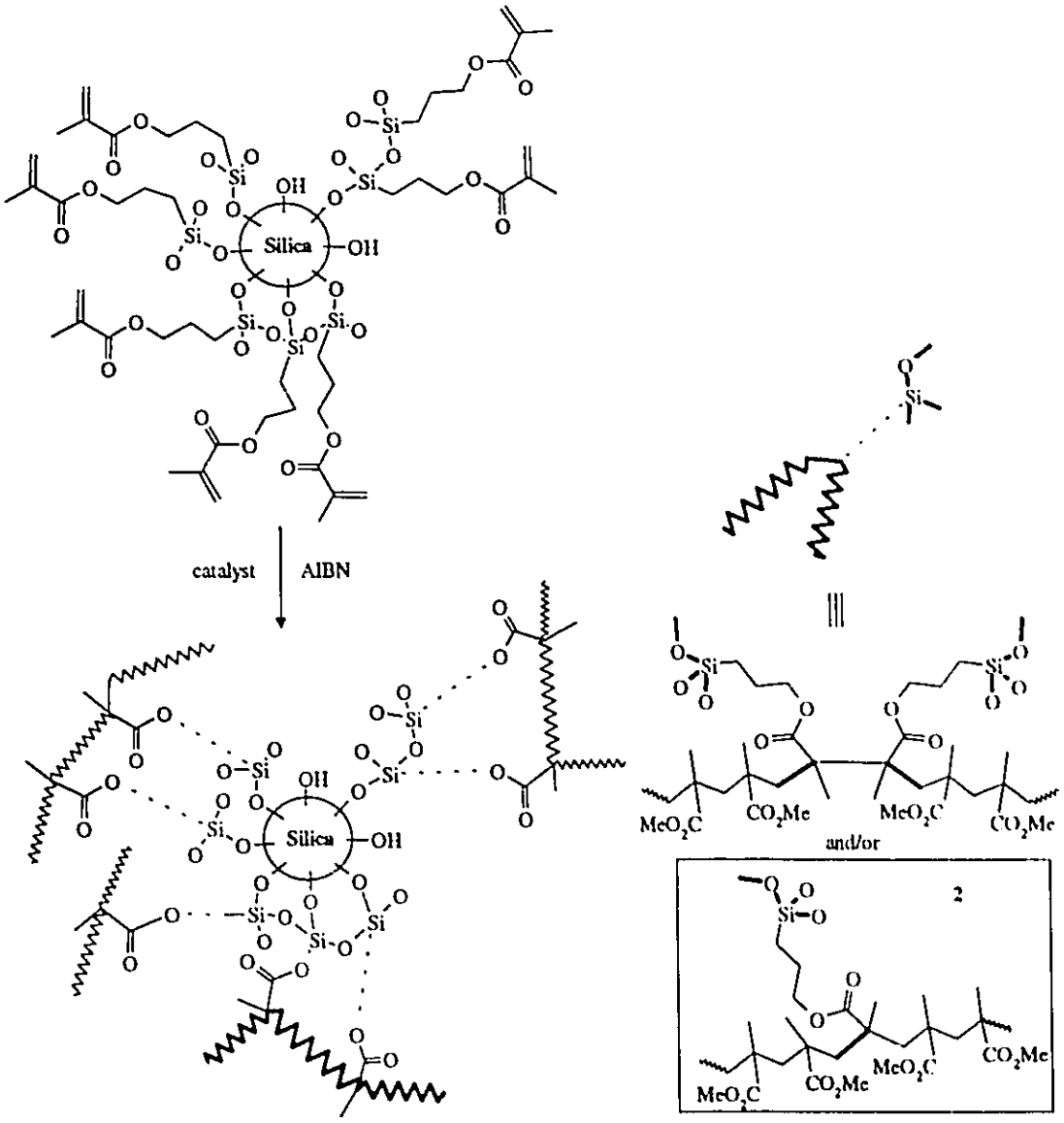

Scheme 7.4. Copolymerisation reactions of MMA onto vinyl functionalized colloidal silica.

The elemental analysis results given in Table 7.2 indicate increased carbon contents were observed for both Si2SG VTM / MMA and Si2SG MPS / MMA as compared to their respective vinyl-modified precursor particles. Assuming the % C difference between the PMMA-grafted and precursor vinyl functionalized spheres corresponds to PMMA grafted to the particle surface, a simple calculation indicates there were 83 and 60 additional carbon atoms / nm^2 on the surfaces of Si2SG MPS / MMA and Si2SG VTM / MMA, respectively. Since each MMA monomer has 5 carbon atoms, we estimate that there are about 16 monomer units / nm^2 for the MPS particles and 12 monomer units / nm^2 for the VTM functionalized spheres.

The difference between PMMA particles formed from the two different precursor particles is a manifestation of the distinct radical activities of vinylsilanes and methacryloxypropylsilanes.[21] Vinylsilanes react to form relatively stable radicals which undergo termination by combination **1** (Scheme 7.3).[22] In contrast, the MPS group behaves essentially like a methacrylate monomer and polymerization with MMA will lead to a graft copolymer **2** (Scheme 7.4). Thus, in the former case, particularly given the proximity of vinyl groups on the surface, lower degrees of conversion are expected for MMA copolymerization. These differences in radical behaviour account for the lower surface coverage of PMMA on an VTM functionalized particle than on an MPS functionalized particle.

The sizes of the PMMA grafted spheres were characterized using DLS and the results shown in Table 7.1 indicate that an increase in diameter for all samples was observed by comparison with the precursor vinyl functionalized particles. The influence of different solvents on the diameter of the particles is also given in Table 7.1. For Si2SG MPS/MMA, the differences in diameter from the precursor MPS particles were found to be 7 nm, 21 nm and 46 nm in acetone, toluene and chloroform, respectively; the corresponding differences for Si2SG VTM / MMA were determined to be 17 nm, 20 nm and 40 nm, respectively. We attribute the differences in particle size to different hydrodynamic thicknesses of the surface polymer layer which is a function of the swelling efficiency of PMMA by the different solvents.

The colloidal stability of the vinyl functionalized particles following the grafting reaction was first assessed by dispersing them in several solvents ranging from water to hexane. In the presence of water, methanol or hexane the particles coagulated, whereas in acetone, chloroform or toluene the particles remained colloidally stable. The addition of CaI_2 or NaI solutions in acetone or Bu_4NBr in $CHCl_3$ led to no change in colloidal stability. The TEM of the Si2SG MPS/MMA grafted particles, dried from toluene, shows an absence of particle clustering (Figure 7.2). The data from the TEM, elemental analyses, solvency and salt effect studies are consistent with steric stabilization for these particles.

To ensure that the PMMA was chemically bonded to the particle surface, the radical grafting reaction was also performed on unmodified silica instead of the vinyl modified particles. In this case, the "modified" particles were observed to coagulate in the presence of chloroform or toluene. This difference in behavior between vinyl- and unmodified silica allowed us to conclude that the PMMA was indeed grafted to the silica surface in the former case.

PDMS Grafted Silica Dispersions

The hydrosilylation[14] of VTM silica spheres with hydrogen-terminated PDMS having a molecular weight of 62 700 was carried out in acetone/hexane in the presence of Karstedt's catalyst (Scheme 7.5).[23] This reaction occurs under mild conditions, with very small amounts of catalyst, and gives the product silane both in high yields, typically > 95%, and with high regioselectivity (only one regioisomer observed).

Figure 7.2. TEM of PMMA grafted onto MPS silica (Si1SG MPS / MMA) at two different magnifications. (Scale bar = 5 μm).

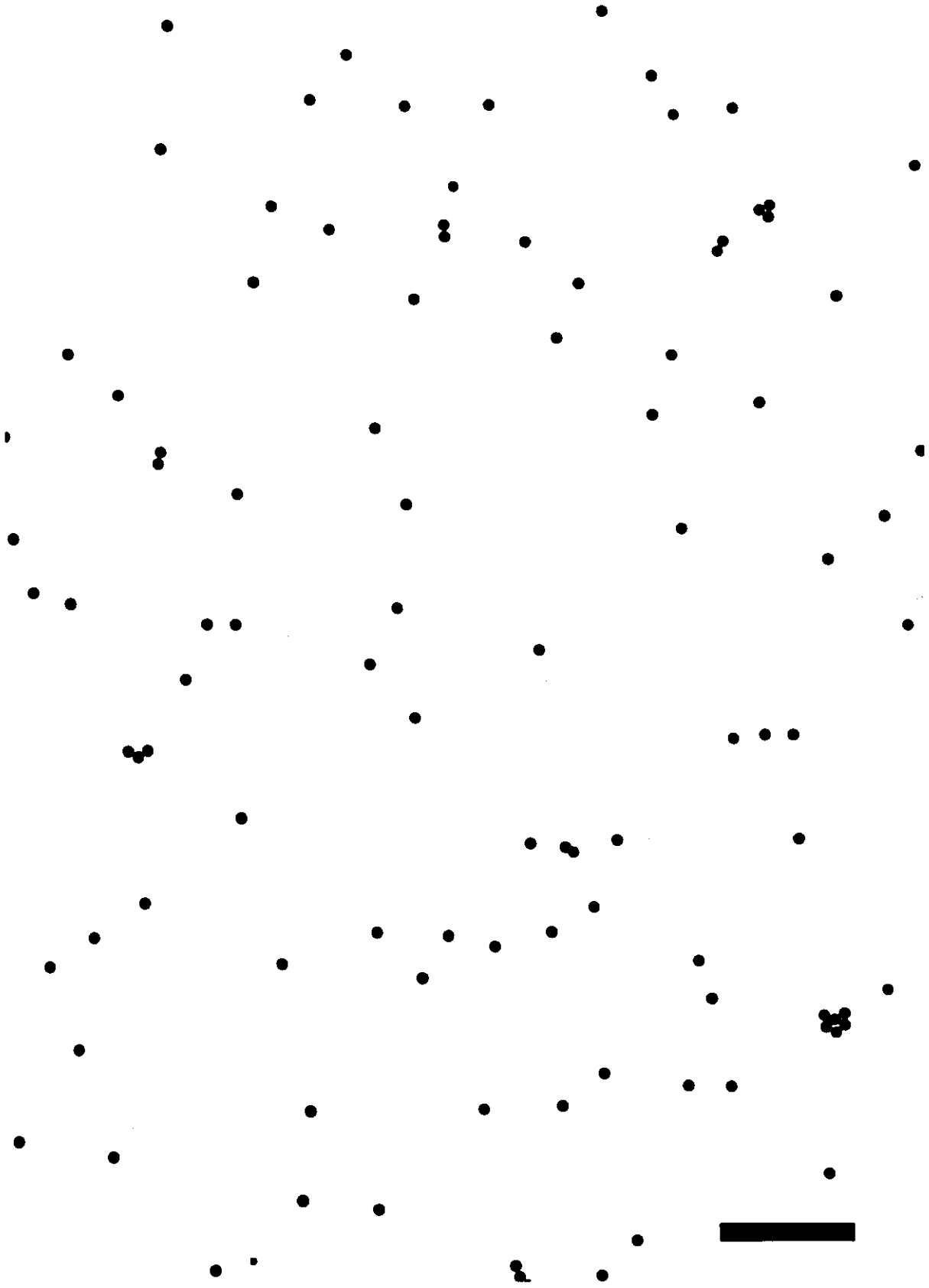

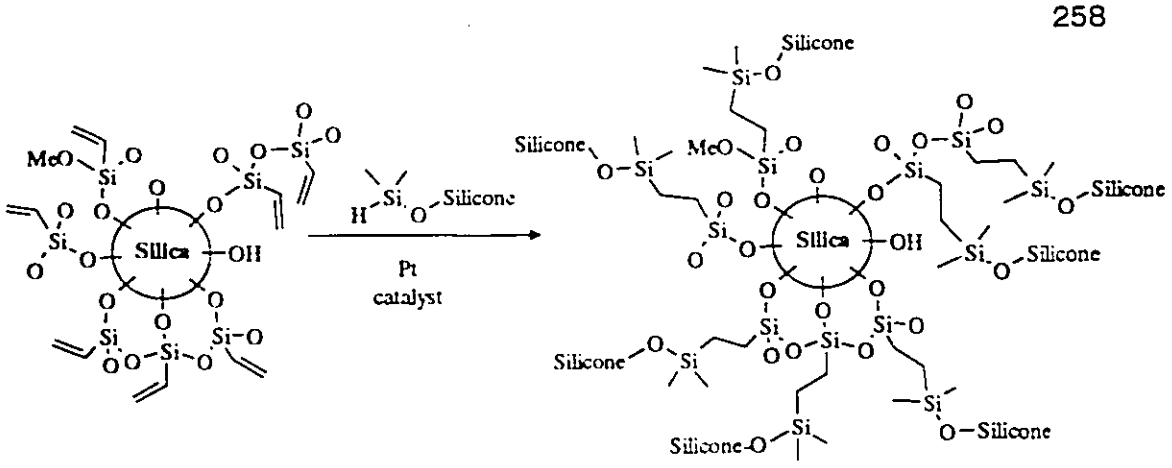

Scheme 7.5. Hydrosilylation reaction using VTM silica particles and $HSiMe_2$ terminated PDMS to prepare sterically stabilized non-aqueous silica dispersions.

The ^{29}Si NMR resonance of the product particles at -22 ppm was consistent with the presence of silicone on the particle surface. The other peaks at -110, -102 and -93 ppm corresponded to the $Si(OSi)_4$ (Q_4), $Si(OSi)_3OH$ (Q3) and $Si(OSi)_2(OH)_2$ (Q_2) environments, respectively, in colloidal silica.[19,23]

Table 7.1 shows that the diameters of the PDMS-silica spheres were 231 nm in heptane compared to 173 nm for the VTM modified particles. The TEM of the PDMS particles dried from heptane was similar to that shown in Figure 4.4 (Chapter 4).

The PDMS silica dispersions were colloidally stable in chloroform, toluene and hexane whereas coagulation was observed in ethanol and acetone. If unmodified particles were used in place of the VTM functionalized particles to carry out the grafting reaction, the particles were found to be only stable in polar solvents such as acetone, ethanol, DMF and water. On the basis of these data, the colloidal stability of the particles arises from steric stabilization.

Synthetic Flexibility

Some further comments should be made on the hydrosilation reaction. This reaction can be facilitated by radical initiators or transition metal catalysts. Because of the importance of this reaction to the silicone industry, a great deal is known about the reaction mechanism and the types of reagents susceptible to the reaction. In essence, the regiochemistry and stereochemistry of addition of a silane R_3SiH to an alkene or alkyne can be completely controlled by the reaction conditions (Scheme 7.6). Not only does the reaction occur in high yield, typically > 90%, but occurs under mild conditions and is simple to perform. In principle, therefore, using this technology it is possible to functionalize silica particles in a wide variety of ways to make novel colloidal materials both for the study of steric stabilization and for the exploitation of the properties that these interesting materials possess.

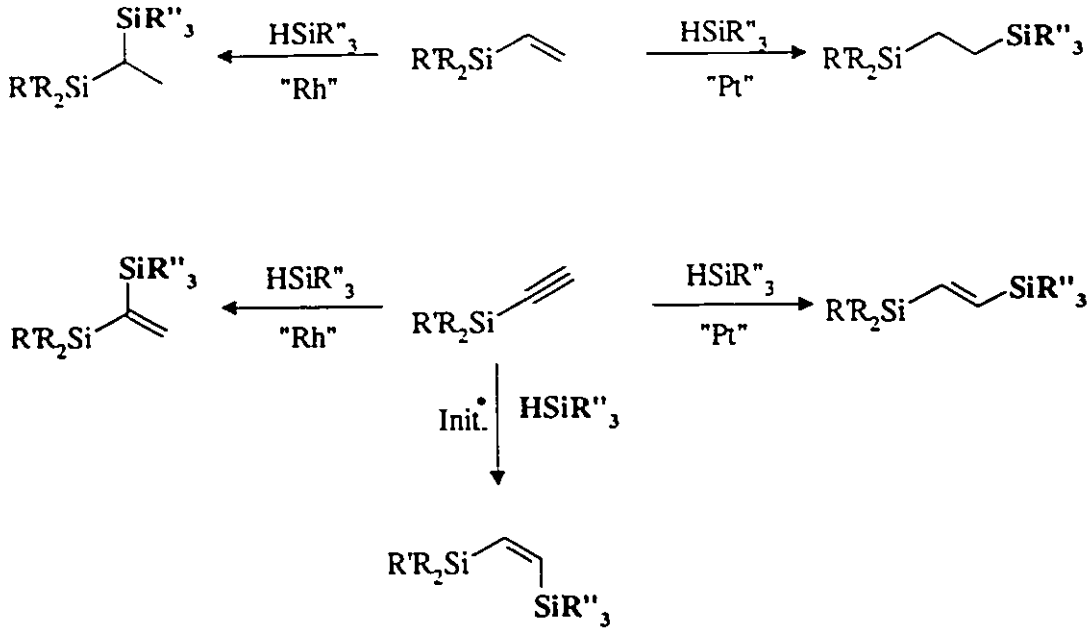

Scheme 7.6. Typical hydrosilation reactions.

7.4 Conclusion

In the work described above, we have prepared well-defined colloidal silica particles that are stable in water and very polar organic solvents such as acetone / water and ethanol / water. Synthetic modification leads to vinylsilyl and methacryloxypropylsilyl functionalized particles that are stable in less polar solvents, acetone and DMF. In both cases, the particles bear surface negative charges and are electrostatically stabilized. These functionalized particles can be converted to sterically stabilized particles in two distinct ways. First, the radical polymerization with methyl methacrylate leads to colloids stable in toluene and chloroform. Second, hydrosilation by hydrogen-terminated silicones of the vinyl-functionalized particles leads to colloids that are stable in hexane. The latter synthetic route provides a high degree of flexibility in the preparation of sterically stabilized colloids that may bear a wide variety of organofunctional moieties. Thus, by the judicious choice of conditions, the nature of the colloidal particles can be changed from electrostatic to steric stabilization and, furthermore, colloidal stability can be maintained as the solvent is changed from water to hexane.

Appendix A7.1. Schematic diagram of the moving boundary electrophoresis apparatus which was built in order to obtain the electrophoretic mobilities of the silica dispersions.

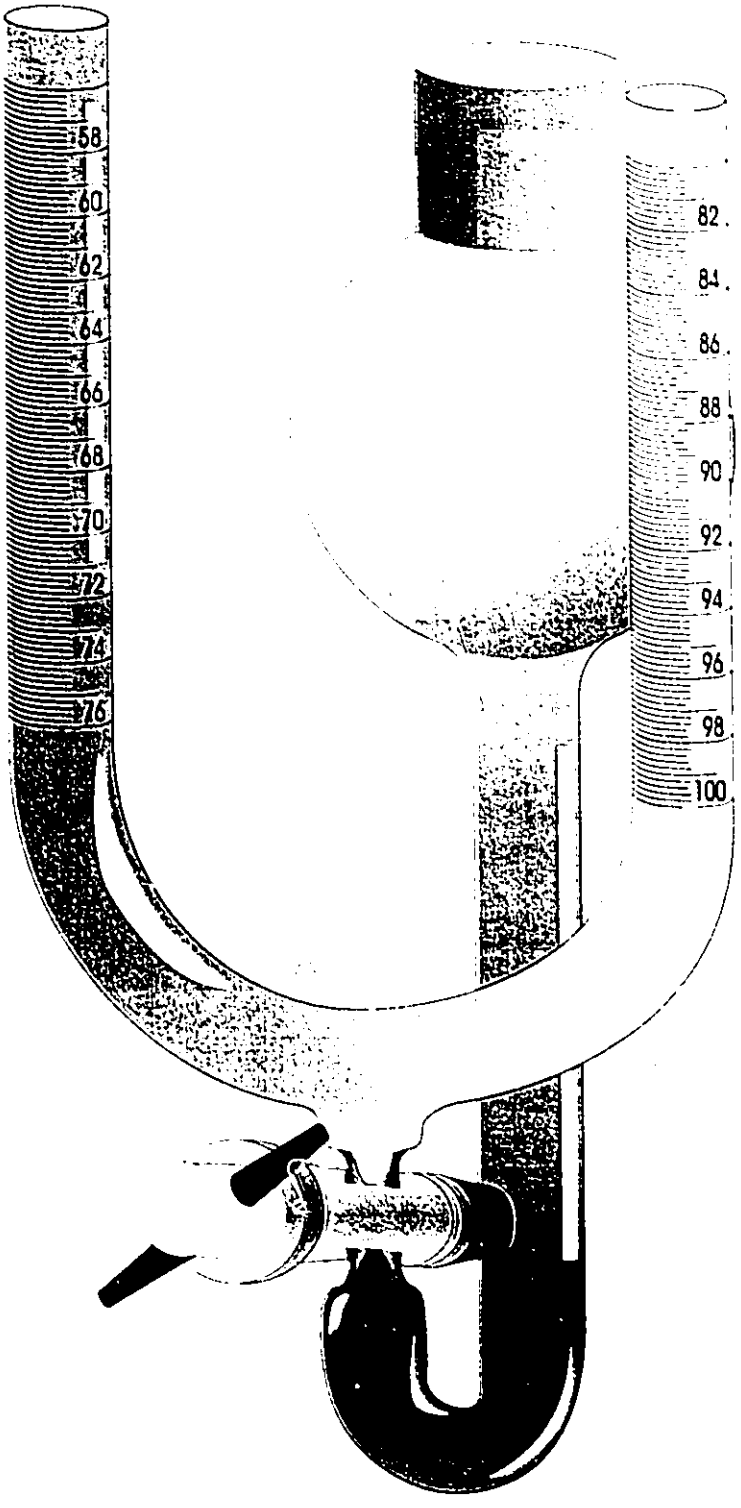

7.5 References

[1] Lyklema, J. *Adv. Colloid Interface Sci.* **1968**, *2*, 65.

[2] Kitahara, A. *Adv. Colloid Interface Sci.* **1992**, *38*, 1.

[3] van der Hoeven, Ph.C.; Lyklema, J. *Adv. Colloid Interface Sci.* **1992**, *42*, 205.

[4] Napper, D. *Polymeric Stabilization of Colloidal Dispersions*; Academic Press: London, 1983.

[5] Stöber, W.; Fink, A.; Bohn, E. *J.Colloid Interface Sci.* **1968**, *26*, 62.

[6] Bogush, G.H.; Tracy, M.A.; Zukoski IV, C.F. *J. Non-Cryst. Solids* **1988**, *104*, 95.

[7] Philipse, A.P.; Vrij, A.J. *J. Colloid Interface Sci.* **1989**, *128*, 121.

[8] (a) Pathmamanoharan, C. *Colloids and Surfaces*, **1988**, *50*, 1. (b) Pathmamanoharan, C. *Colloids and Surfaces* **1988**, *34*, 81.

[9] Tsubokawa, N.; Kimoto, T.; Koyama, K. *Colloid Polym. Sci.* **1993**, *271*, 940.

[10] Sunkara, H.B.; Jethmalani, H.M.; Ford, W.T. *Chem. Mater.*, **1995**, *7*, 291.

[11] Edwards, J.; Lenon, S.; Toussaint,A.F.; Vincent, B. ACS Symp. Ser., # 240, 281-296 (1984).

[12] Auroy, P.; Auvray, L.; Leger, L. *J. Colloid. Interface Sci.* **1992**, *150*, 187.

[13] Personal communication, M. Duits, Twente, The Netherlands.

[14] (a) Musolf, M.C.; Speier, J.L. *J. Org. Chem.*, **1964**, *29*, 2519. (b) J.L. Speier, *Adv. Organomet. Chem.*, **1979**, *17*, 407.

[15] Burton, E.F. *Physical Properties of Colloidal Solutions*; Longmans: Green and Co., London, 1938.

[16] B.D. Karstedt, U.S. Patent 3,775,452, 1973.

[17] Iler, R.K. *The Chemistry of Silica*; Wiley; New York, 1979.

[18] Plueddemann, E.P. *Silane Coupling Agents*; Plenum Press, New York, 1982.

[19] Badley, R.D.; Ford, W.T.; McEnroe, F.J.; Assink, R.A. **1990**, *Langmuir*, **6**, 792.

[20] See Chapter's 2 and 3 in this thesis.

[21] (a) Pelton, R.; Osterroth, A.; Brook, M.A. *J. Colloid Interface Sci.*, **1991**, *147*, 523. (b) Pelton, R.; Osterroth, A.; Brook, M.A. *J. Colloid Interface Sci.*, **1990**, *137*, 120.

[22] Brook, M.A.; Stefanac, T. to be published.

[23] (a) Lewis, L.; Lewis, N. *J. Am. Chem. Soc.*, **1986**, *108*, 7228. (b) Lewis, L. *J. Am. Chem. Soc.* **1990**, *112*, 5998.

[24] van Blaaderen, A.; Vrij, A. *J. Colloid Interface Sci.*, **1993**, *156*, 1.

Chapter 8

The Preparation of Cationic Silica

Abstract

Several cationic silica materials were prepared (by reacting pyridine, 4-dimethylaminopyridine (DMAP), and tetramethylethylenediamine (TMEDA)) with silica modified with (3-chloropropyl)trimethoxysilane) (Cl-PTMS) and characterized by ^{13}C CP-MAS NMR, elemental analysis, and microelectrophoresis experiments. The iso-electric point (iep) of silica **1** *after chemical modification with Cl-PTMS* **2** *was 2.8. Quaternization of* **2** *with pyridine to give* **3** *led to a shift in the iep to 6.5. The electrophoretic mobilities for* **3** *measured at pH's 4.8 and 6 were 2.8 x 10^{-8} m^2V^1 s^{-1} and 0.8 x 10^{-8} m^2V^1 s^{-1}, respectively.* **3** *was flocculated with a cationic copolymer, at solution pH's of 3 and 5 indicating the net charge on the silica surface was positive. On the other hand, no flocculation occurred using* **3** *at pH 7.2 in the presence of an anionic copolymer. The reaction of* **3** *with chlorotrimethylsilane (Cl-TMS) was also performed to give* **4** *and it was found that the iep could be further shifted to 8. The electrophoretic mobilities for* **4** *dispersed in solutions of pH 5.6, 7.0, and 9.1 were 2.0 x 10^{-8} m^2V^1 s^{-1}, 0.96 x 10^{-8} m^2V^1 s^{-1}, and -2.4 x 10^{-8} m^2V^1 s^{-}*

*^{1}, respectively. Cationic silica **5** was prepared by mixing **3** with both pyridine and Cl-TMS to give a colloidally stable non-aqueous dispersion. The electrophoretic mobilities of **5** in cyclohexane and ethanol were 0.2 x 10^{-8} m^2V^1 s^{-1} and 1.0 x 10^{-8} m^2V^1 s^{-1}, respectively.* DMAP *was reacted with **3** to give **6** which was determined to have an iep of 7.7. Methylation of **6** with methyl iodide **7** shifted the iep to 8.2. An alternative route to prepare cationic silica involved first reacting **2** with TMEDA **8** followed by methylation using iodomethane **9**. The iep's for **8** and **9** were 5.5 and 6.9, respectively.*

8.1 Introduction

Cationic silica support materials have found widespread applications in separation processes such as chromatography and ultrafiltration, and also as phase transfer catalysts.[12] Cationic groups have been introduced on silica by surface treatment with cationic polyelectrolytes and molecules hearing quaternary ammonium or phosphonium groups.[3,4,5,6] Organosilicon-substituted quaternary ammonium salts have also been prepared and supported on solids to study their anti-microbial activity.[7]

Due to the growing interest in anchoring cationic groups to mineral support materials we report herein the preparation of quaternized silica obtained by reacting a variety of amine compounds with chloropropyl modified silica (*e.g.*, see Scheme 8.1).[8] The electrophoretic mobilities as a function of pH for the silica supported ammonium salt materials were studied to characterize their iso-electric points.

$$(RO)_3Si{-}(CH_2)_3{-}Cl + R'_3N \longrightarrow (RO)_3Si{-}(CH_2)_3{-}NR'_3{}^{+}Cl^{-}$$

Scheme 8.1. Preparation of organosilane - substituted amine salts by nucleophilic displacement of -Cl^- from chloropropyltrialkoxysilane.

8.2 Experimental

Instrumentation.

Solid-state Nuclear Magnetic Resonance Spectroscopy. A Bruker ASX-200 spectrometer operating at 50.32 MHz for carbon was used to obtain ^{13}C cross polarization (CP) / magic angle spinning (MAS) solid state spectra. Spectra were accumulated using 16K data points. The spinning frequency was 4 kHz, the sweep width was 18050 Hz, the recycle time was 4.0 s and the acquisition pulse at 90° was 4.3 µsec. The contact time was 1 msec. All spectra were acquired with high power ^{1}H decoupling during acquisition.

Dynamic light scattering (DLS). See Chapter 2-Experimental 2.2.

Microelectrophoresis. See Chapter 2-Experimental 2.2.

Elemental Analysis. Analysis for C, H, Si, Cl, and N was performed by Guelph Chemical Laboratories (Guelph, Ontario, Canada).

Materials.

Hydrophilic precipitated silica **1**, was obtained from GM Hubor (Zeofree 80: specific surface area = 140 m^2 / g; average particle diameter = 4-6 μm; %Si = 45.74; %H = 0.74)[9]. Stöber silica particles were prepared as described previously in Chapter 2-Experimental 2.2. A cationic (5%) copolymer, Percol-455, composed of quaternary acrylate and acrylamide groups was used from Allied Colloids. An anionic copolymer, Organopol, composed of sodium acrylate and acrylamide was used from Allied Colloids.

Chemicals.

(3-chloropropyl)trimethoxysilane (Gelest, 97%), chlorotrimethylsilane (Aldrich, redistilled, 99+%), pyridine (Py, Aldrich, 99.8%), iodomethane (Aldrich, 99.5%), 4-Dimethylaminopyridine (DMAP, Aldrich, 99%), N, N, N', N'-tetramethylethylenediamine (TMEDA, Aldrich, 99%), acetone (Caledon, glass distilled, 99.5%), diethyl ether (BDH), toluene (Caledon, reagent grade).

Tetrahydrofuran (Caledon, reagent grade) was distilled from Na / benzophenone under a nitrogen atmosphere. Dichloromethane (Caledon, reagent grade) was distilled from phosphorous pentoxide (P_2O_5).

Relative Turbidity Analysis. A photometric dispersion analyzer (Rank Brothers, UK) was used to measure the turbidity of the silica / polymer samples. The samples were prepared for analysis by mixing (400 rpm) 200 ppm of the polymer with a 5 wt% aqueous silica dispersion (Milli-Q water) at room temperature. Details of the experimental details using the instrument can be found elsewhere.[10]

Synthesis.

All of the treated silica products were washed by centrifugation / redispersion cycles and then dried at 120°C overnight before further modification reactions or characterization.

3-Chloropropyl-Functionalized Silica **2.** **1** (10 g) was dispersed in water by sonication. After 15 min, the pH of the dispersion was adjusted to 4 (using acetic acid) and the reaction was left to stir at room temperature for 24 h. The particles were isolated by centrifugation and redispersed in a 10 wt% ethanol:water (pH=4) mixture. **1** (5 g) was dispersed in the ethanol:water mixture (300 mL) to which (3-chioropropyl)trimethoxysilane (6g, 6.5 mL, 30 mmol) was added. The dispersion was left stirring for 10 h at 23 ± 2 °C. The silica was cleaned free of the excess silane by washing with ethanol (3x) followed by acetone (2x). The modified silica sample was dried at 120°C for 24 h.

^{13}C NMR (CP-MAS) δ(ppm): 60.0; 50.0; 30.0; 26.1; 10.0.

Elemental analysis: %C = 0.69; %H = 0.73; %Si = 42.22; %Cl = 0.67.

Pyridinium-Functionalized Silica **3.** **2** (0.5 g) was dispersed in pyridine (50 mL) and heated at 100°C for 24 h. After cooling to room temperature, the

silica was washed with diethyl ether (3x), followed by ethanol (2x) and acetone (2x). The silica was dried at 120°C for 24 h.

^{13}C NMR (CP-MAS) δ(ppm): 147.2; 139.0; 125.4; 65.0; 45.0; 25.0.

Elemental analysis: %C = 1.87, %H = 0.75, %N = 0.25.

Pyridinium-Functionalized Silica Modified With Chlorotrimethylsilane **4**. **3** (0.1 g) dried at 120°C, was dispersed in freshly distilled dichloromethane (10 mL) to which was added triethylamine (1.0 mL, 7.2 mmol). Under a positive nitrogen pressure, chlorotrimethylsilane (0.9 mL, 9 mmol) was added dropwise and the mixture was stirred at room temperature for 24 h. The solids were washed with dimethylformamide (3x), followed by ethanol (2x) and acetone (2x) and dried at 120°C for 24 h.

Pyridinium-Functionalized Hydrophobic Silica **5**. **2** (0.5 g) was placed in a round bottom flask and heated in an oven at 120°C. Under a positive pressure of nitrogen, pyridine (50 mL) was added to the silica and the dispersion was sonicated for a 5 minutes. Chlorotrimethylsilane (5.8 mL, 46 mmol) was added dropwise and the mixture was stirred for a further 15 min followed by heating at 100°C for 24 h. After cooling to room temperature, the silica was washed with dimethylformamide (3x), followed by ethanol (2x) and acetone (2x). The silica was dried at 120°C for 24 h.

4-Dimethylaminopyridinium-Functionalized Silica **6**. **2** (0.2 g) dried at 120°C, was dispersed by sonication in a toluene solution containing DMAP (62 mg, 0.5 mmol). The suspension was refluxed for 10 h. After cooling to room temperature, the silica was washed with toluene (2x), followed by ethanol (2x) and acetone (2x). The silica was dried at 120°C for 24 h.

Methylation of 4-Trimethylammoniumpyridinium-Functionalized Silica **7**. **6** (0.1g) was dispersed by sonication in THF (5 mL) and iodomethane (0.5 mL, 1.1 g, 8 mmol) was added to the silica suspension and stirred at room temperature in a reaction vessel protected from light for 10 h. The silica was washed with THF (3x), followed by ethanol (2x) and acetone (2x). The silica was dried at 120°C for 24 h.

(2-dimethylamino)ethyl(4-dimethylammonium)-Functionalized Silica **8**. **2** (0.5 g) dried at 120°C, was dispersed by sonication in TMEDA (50 mL). Under a positive nitrogen pressure, the dispersion was refluxed for 72 h. The solids were washed with diethyl ether (3x), followed by acetone (4x) and dried at 120°C.

^{13}C NMR (CP-MAS) δ(ppm): 44.7; 36.1.

Elemental analysis: %C = 3.31, %H = 0.98, %N = 1.09.

Pentamethyldiammonium-Functionalized Silica **9**. **8** (50 mg) dried at 120°C, was dispersed in THF (3.0 mL) to which was added iodomethane (1.0mL, 16 mmol). The dispersion was stirred at room temperature for 10 h. The solids were washed with diethyl ether (3x), followed by acetone (4x) and dried at 120°C for 24 h.

8.3 Results and Discussion

A well-defined silica system (*i.e.*, Stöber silica) modified with (3-chloropropyl)trimethoxysilane (Cl-PTMS) (see Scheme 8.2) was characterized before carrying out further reactions with the precipitated silica **1**. All the quaternized silica's in this study were prepared starting from chloropropyl modified precipitated silica **2**.

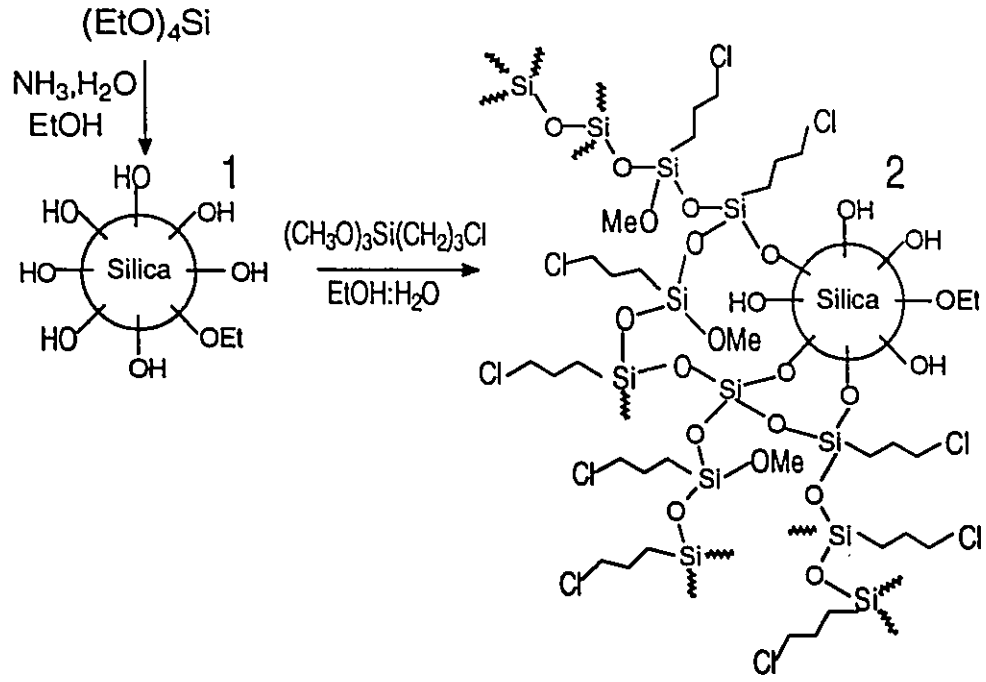

Scheme 8.2. Preparation of chloropropyl modified silica by treating Stöber silica with Cl-PTMS. .

The ^{13}C CP-MAS NMR spectrum of Stöber silica modified with Cl-PTMS showed weak resonance signals at approximately 7. 26, and 45 ppm. Based on the ^{13}C solution spectrum of the starting silane coupling agent, these peaks were assigned to the α, β, and γ carbons of the propyl chain (relative to silicon), respectively. The carbons of the methoxy groups in the starting silane resonate at 50 ppm. However, the spectrum of the silica showed no direct evidence for their presence on the surface in large concentrations. This observation is consistent with the chemistry of trialkoxysilanes in aqueous media where hydrolysis of alkoxy groups readily occurs in the presence of acid catalysis.[11]

Dynamic light scattering (DLS) measurements showed the average hydrodynamic particle diameter, d_H, for the unmodified Stöber silica was 193.4 ± 0.4 nm. Following treatment of the silica with Cl-PTMS (see Scheme 8.2) the d_H was measured to be 197.9 ± 0.4 nm. The DLS data indicated the silane reacted with the silica surface to give a 2.2 nm thick surface multi - layer. Due to the network structure of silsesquioxanes and the fact that oligomerization of Cl -PTMS occurs in solution prior to contact with the silica surface, monolayers are rarely obtained with silane coupling agents.

Precipitated silica **1** was subsequently used in the study to carry out the quaternization reactions. Elemental analysis results of **1** showed 0.73% hydrogen and 45.74% silicon. Carbon was not detected within the detection limit of 0.01%. The *iep* occurred at 2.8 which is consistent with other values reported for silica.

Figure 8.1. Electrophoretic mobilities as a function of aqueous pH solutions for silica particles modified with (3-chloropropyl)trimethoxysilane ($Si(CH_2)_3Cl$) **2** and for **2** treated with pyridine ($SiPy^+Cl^-$) **3**. **4** was prepared by treating **3** with chlorotrimethylsilane (ClTMS). SiOH + Py corresponds to **1** (unmodified silica) mixed with pyridine (control).

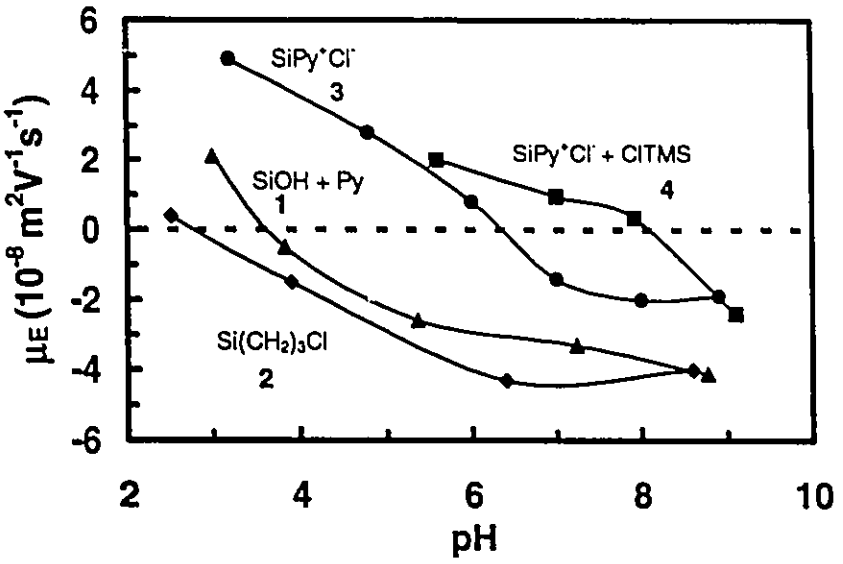

Following treatment of **1** with (3-chloropropyl)trimethoxysilane to give **2** (under the same conditions performed with the Stöber silica), both carbon (0.69%) and chlorine (0.67%) were detected by elemental analysis. The ^{13}C NMR results were the same as that reported for Stöber silica modified with (3-chloropropyl) trimethoxysilane. The *iep* of **2** was determined to be 2.8 as shown in Figure 8.1. **2** was reacted with pyridine to quaternize the supported 3-chloropropyl groups to give **3** (see Scheme 8.3). Figure 8.1 shows that the *iep* for **3** was shifted to 6.5 in relative to the *iep* of 2.8 observed for **2**.

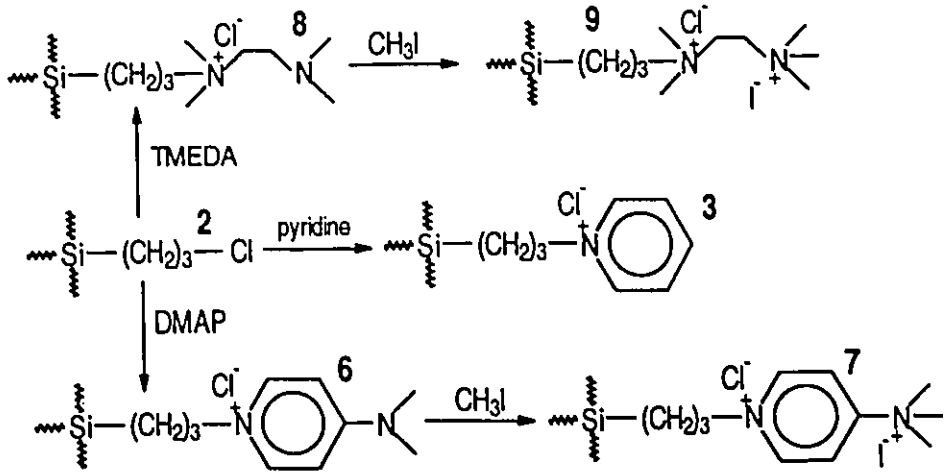

Scheme 8.3. Preparation of cationic functionalized silica's starting from chloropropyl modified silica **2** (see Scheme 8.2). DMAP = 4-dimethylaminopyridine; TMEDA=N,N,N',N' - tetramethylethylenediamine.

A preliminary flocculation study was carried out using **3** with two commercial polymer flocculants. **3** was mixed with an anionic copolymer (Organopol) in aqueous solutions adjusted to pH values of 3, 4.5 and 8.7. The relative turbidity values of the solutions as a function of time were subsequently measured. Figure 8.2 shows the relative turbidity values of the polymer/silica mixtures at a few pH values measured after mixing for 2 minutes. Flocculation of **3** occurred when the solution pH was adjusted to 3 and 4.5, but no change in stability was observed at pH 8.7 due to the net negative charge of the particles.

The flocculation behavior observed for **3** in the presence of Organopol can be explained by the attraction of the negatively charged polymer chains to the positively charged silica at pH's below the *iep* of 6.5. By contrast, above the iep for **3**, the surface is negatively charged (i.e., negative mobility values) and will repel the anionic polymer from binding to the solids hence no flocculation (see Figure 8.2) can occur. **3** was also mixed with a cationic flocculant (Percol-445) at pH 7.2 and the relative turbidity experiment showed the polymer was ineffective towards inducing flocculation. This experiment indicated that the pyridinium groups were still present on **3** above its iep to repel the cationic polymer and hence suppress flocculation.

Figure 8.2. Flocculation of cationic silica ($SiPy^+Cl^-$) **3** and **1** using commercial polymeric flocculants, CPAM (5% cationic) and APAM (anionic), in aqueous solutions of varying pH values. The relative turbidities of the solutions were measured as a function of time and the turbidities recorded after 5 min of adding the polymer are given in this plot. The arrow inset within the graph is a qualitative guide to interpret the flocculation efficiency of the polymers with the silica. Strong flocculation indicates the mixture became opaque due to flocculation.

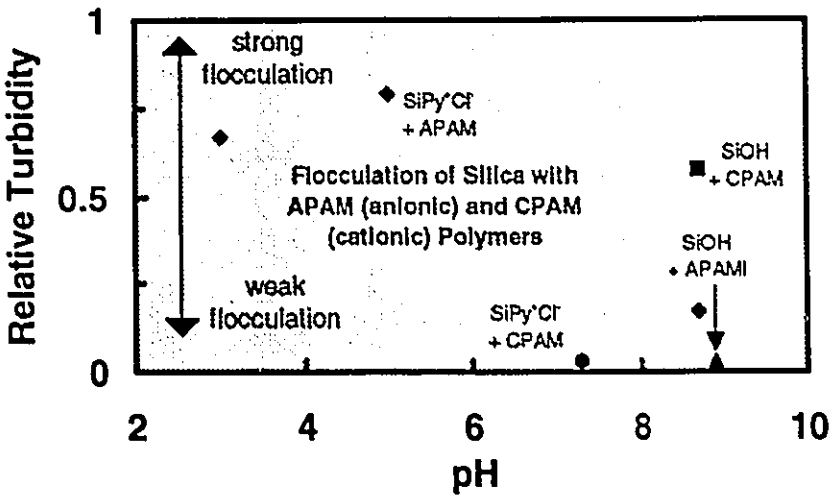

A control reaction was also performed using **1** mixed with pyridine to show that the reaction between the supported 3-chloropropyl groups and pyridine was responsible for the iep shift to 6.5 (see Figure 8.1). The electrophoretic data for the silica obtained from this control reaction are plotted in Figure 8.1 (SiOH + py). The results show that the *iep* was shifted

only to 3.4 (*e.g.*, the mobility values were negative for pH the values ranging from 3.8 to 8.8).

3 was further reacted with chlorotrimethylsilane (ClTMS), giving **4**, to decrease the number of untreated silanol groups remaining on the silica surface. The electrophoretic mobilities for **4** dispersed in solutions of 5.6, 7.0, and 9.1 were 2.0 x 10^{-8} m^2V^{-1} s^{-1}, 0.S6 x 10^{-8} m^2V^{-1} s^{-1}, and -2.4 x 10^{-8} m^2V^{-1} s^{-1}, respectively (see Figure 8.1). From these results, the iep shifted towards a pH of 8. The particle stability of **4** was checked in a variety of organic solvents ranging in polarity. Coagulation occurred in cyclohexane, hexane, and dichloromethane whereas stable dispersions were observed using DMF, acetone, and ethanol.

It was found that mixing chlorotrimethylsilane with pyridine under reflux in the presence of **3** gave a hydrophobic silica powder **5**. The contact angle measured from a drop of water on a film of this powder cast on a glass slide was 115°. The mobilities of **5** in cyclohexane and ethanol were 0.2 x 10^{-8} m^2 V^{-1} s^{-1} and 1.0 x 10^{-8} m^2 V^{-1} s^{-1}, respectively.

The reaction between **2** and DMAP was carried out (Scheme 8.3) and the electrophoretic mobilities as a function of pH for **6** are shown in Figure

8.3. Positive mobilities ranging from 3.6 x 10^{-8} $m^2V^{-1}s^{-1}$ to 0.2 x 10^{-8} $m^2V^{-1}s^{-1}$, respectively were observed, when the pH ranged from 3.8 to 7.5, respectively. Above pH 7.5 the mobilities were negative as indicated by the observed iep of 7.7. Using pyridine to quaternize the silica the iep was only shifted to 6.5 (see Figure 8.1). Thus, the stronger nucleophilic character of DMAP was more effective at quaternizing the chloropropyl groups. DMAP has dimethylamino groups which should also be available for reaction on the silica surface. Therefore, **6** was methylated with iodomethane to give **7** (Scheme 8.3). The electrophoretic mobility curve as a function of pH for **7** is given in Figure 8.3 and shows that the methylation reaction shifted the iep to 8.2.

Figure 8.3. Plots of electrophoretic mobilities versus pH for chloropropyl derivatized silica **2** reacted with DMAP **6**. **6** was methylated using iodomethane to give **7** and the mobility curve is represented as SiDMAP$^+$ + CH_3I.

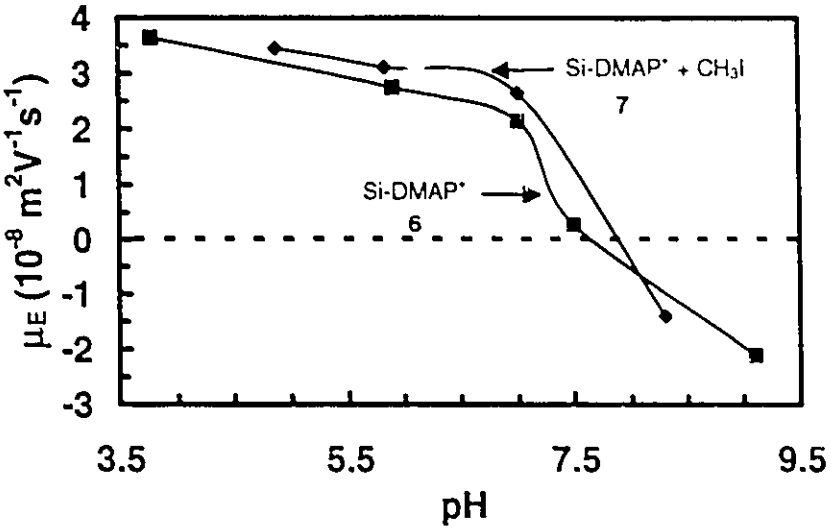

An alternate route towards a cationic functionalized silica system was tried by reacting TMEDA with **2** to give **8** (Scheme 8.3). Figure 8.4 shows the influence of pH on the electrophoretic mobilities of **6** where positive mobility values ranged from 3.6 x 10^{-8} $m^2V^{-1}s^{-1}$ to 0 as the pH increased from 3.3 to 5.5 (which correpsonds to the iep). To improve the pH range under which the silica would be positively charged, **8** was methylated with iodomethane **9**

(Scheme 8.3). Figure 8.4 shows the iep was shifted to 6.9 after the methylation reaction.

Figure 8.4. Plots of electrophoretic mobilities versus pH for chloropropyl derivatized silica **2** reacted with TMEDA **8**. **8** was methylated using iodomethane to give **9** and the mobility curve is represented as SiTMEDA$^+$ + CH_3I. SiOH + TMEDA corresponds to **1** mixed with TMEDA (control).

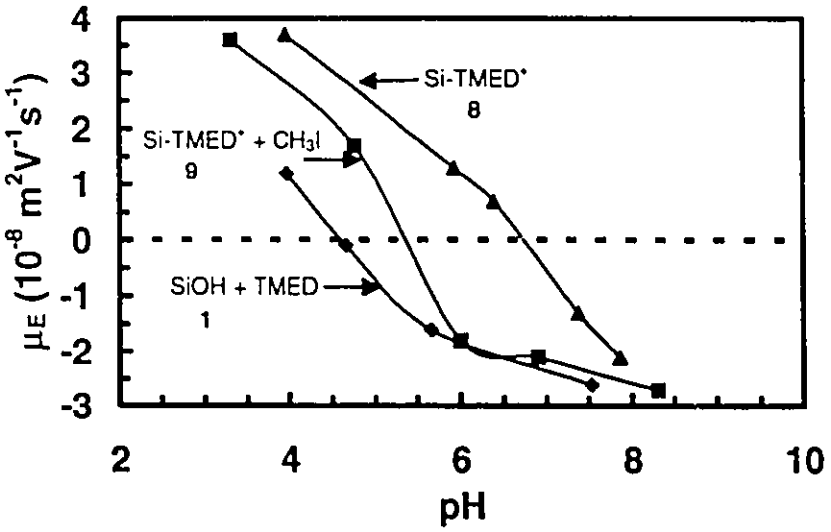

A summary list of the iep results obtained for the cationic silica materials is provided in Table 8.1.

Table 8.1. Summary of iso-electric points for cationic silica products.

Silica Sample	iso-electric point pH
2	2.8
3	6.5
1 + Py	3.4
4	8.0
6	7.7
7	8.2
8	5.5
9	6.9

8.4 Conclusions

(1) A series of cationic silica particles were prepared and their iep values were determined by microelectrophoresis experiments. The treatment of **2** with 4-dimethylaminopyridine **6** followed by methylation **7** was found to be the most effective route towards cationic silica having an *iep* of 8.2.

(2) The cationic silica material **3** was used in a flocculation study with negatively and positively charged polymers. Flocculation only occurred in the presence of the **3** and the anionic polymer.

8.5 References

[1] Sherrington, D.C. In "*Polymer - Supported Reactions in Organic Synthesis*"; Hodge, P.; Sherrington, D.C. Ed.; Wiley: New York, 1980.

[2] Majors, R.E. *J. Chromatog. Sci.* **1977**, *15*, 334.

[3] Popping, B.; Deratani, A.; Sebville, B.; Desbois, V.; Lamarche, J.M.; Foissy, A. *Colloids Surf.* **1992**, *64*, 125.

[4] Neumann, R.; Miller, H. *J. Chem. Soc., Chem. Comm.* **1995**, 2277.

[5] Clark, J.H.; Tavener, S.J.; Barlow, S.J. *J. Mater. Chem.* **1995**, *5*, 827.

[6] Tundo, P.; Venturello, P.; Angeletti, E. *J. Am. Chem. Soc.* **1982**, *104*, 6547.

[7] Speier, J.L.; Roth, C.A.; Ryan, J.W. *J. Org. Chem.* **1971**, *36*, 3120. Speier, J.L.; J.R. Malek *J. Colloid Interface Sci.* **1982**, *89*, 68.

[8] Deschler, U.; Kleinschmit, P.; Panster, P. *Angew. Chem. Int. Ed. Engl.* **1986**, *25*, 236.

[9] The carbon and nitrogen content were also analysed by elemental analysis but they were not detected by elemental analysis (Detection limit=0.01%)

[10] Gregory, J. *J. Colloid Interface Sci.* **1985**, *105*, 357.

[11] Plueddemann, E.P. *Silane Coupling Agents*; Pelnum Press: New York, 1982.